The role of alpha-synuclein oligomers in Parkinson's disease pathophysiology and biology

Rosalind F. Roberts

Wolfson College

Department of Physiology, Anatomy and Genetics

University of Oxford

Hilary Term 2015

A thesis submitted towards the degree of Doctor of Philosophy

The role of alpha-synuclein oligomers in Parkinson's disease pathophysiology and biology

A thesis submitted for the degree of Doctor of Philosophy, Hilary Term 2015

Rosalind Roberts, Wolfson College, University of Oxford

Accumulating evidence links oligomeric species of the protein alpha-synuclein to the neuronal death associated with Parkinson's disease. However, the direct detection of alpha-synuclein oligomers in post-mortem brain has been challenging and this has limited our understanding of their structure, distribution and effects in Parkinson's disease.

The work presented in this thesis addresses two aspects of the role of alpha-synuclein oligomers in Parkinson's disease. Firstly, I describe the development of a novel technique, the alpha-synuclein proximity ligation assay (AS-PLA), which specifically detected alpha-synuclein oligomers *in vitro* and in post-mortem brain tissue. In a blinded study with post-mortem brain tissue from eight Parkinson's disease patients and eight controls, AS-PLA revealed widespread, previously unrecognised pathology in the form of extensive diffuse deposition of alpha-synuclein oligomers. Furthermore, AS-PLA preferentially detected early-stage, loosely compacted Parkinson's disease lesions such as pale bodies, whereas Lewy bodies, considered heavily compacted late lesions were only very exceptionally stained. The oligomeric species detected by AS-PLA displayed a unique, intermediate proteinase K resistance profile, suggesting the detection of a conformer that is different from both physiological pre-synaptic alpha-synuclein (proteinase K sensitive) and highly aggregated alpha-synuclein within Lewy bodies (proteinase K resistant). In addition, AS-PLA revealed the age-dependent accumulation of alpha-synuclein oligomers in the *substantia nigra* of a BAC transgenic mouse model of Parkinson's disease that overexpresses human wild-type alpha-synuclein, *SNCA*-OVX.

Secondly, the detection of early pathology in Parkinson's disease brain tissue using AS-PLA suggests that oligomeric species of alpha-synuclein could represent a potential target for therapeutic intervention. Therefore, I undertook a screen to identify compounds that can prevent the formation of alpha-synuclein oligomers *in vitro*. Using bimolecular fluorescence complementation constructs, I identified nine compounds capable of reducing the fluorescence indicative of the formation of alpha-synuclein oligomers. Two of these compounds showed dose-dependent activity. Future work will confirm the hits *in vitro* before studying whether Parkinson's-like phenotypes in the *SNCA*-OVX mice can be ameliorated or reversed by treatment with the compounds.

This thesis is dedicated to the memory of

Paul Robertson,

an exceptional neuroscientist and a dear friend.

Acknowledgements

First and foremost, I would like to thank my supervisors, Dr Javier Alegre-Abarrategui and Professor Richard Wade-Martins for their support and encouragement over the past four years. Thanks to Javier for believing in me, for his passion for the project and for sharing his vast knowledge of neuroanatomy and neuropathology, something I never anticipated learning but which I have enjoyed immensely. The guidance of Richard, particularly over the last 6 months, has been invaluable and I have really appreciated his clear insights into my work and his ability to help me focus on 'the bigger picture'. I would also like to thank Dr Angela Russell and Dr Graham Wynne for their helpful collaboration for the screening. This work would not have been possible without funding from The Cure Parkinson's Trust.

So many people have helped to make the Wade-Martins lab an intellectually stimulating, but more importantly fun, place to work. Brent Ryan has been an incredibly helpful sounding board for ideas for the project and it's been great to be able to do that with someone who actually pronounces their Rs (even if you are a Meader). I'd also like to thank Milena Cioroch for her animal expertise and for care-free happy dancing together and Elizabeth Hartfield for her help in the lab, the made-up jokes, the cheese and all the other fun we've had outside of the lab. To my past and present office buddies: Alastair Kerr for keeping it real, Anna Popplestone for hugs and cawfay, James Groves for support and flippancy when I needed it, Ana Silva for procrastinatory chats and Michele Lufino for mindfulness and screening tips. To Max Sloan, Ben Hunn, Heike Wobst, Hugo Fernandes and Matt Thomas for intense or ridiculous (or both) conversations while making tea and Tara Caffrey for all of her wise Canadian goodness.

To Paul. There isn't a day that goes by when I don't think about and miss you. I always imagined you having your own group, where you could make your ambitious (sometimes wacky?) ideas reality and I can't quite believe this will never happen. It fills me with such sadness that we aren't sharing the process of completing our DPhils together, but I feel privileged to have met you and will carry your enthusiasm for rigorous science and the memory of your incredible laugh with me always.

My coffee (and WINE) buddies, Ellie Grant, Aisling O'Loughlin and Laura Corrigan (and honorary member Gabe Aughey) have provided immense support over the past few years. Special love to Ellie for helping me to learn that a PhD inevitably involves worrying (a bit).

Charlotte, Tim, Manu and Tim gave me such a lovely welcome to Oxford and I've never felt more instantly at home than I did at Aston Street. Thanks for all the East Oxford love, for TPS times (thanks also to Rachel for her keen interest in my research into neurodegenerative disease) and to Charlotte and Tim for the ever joyful little Lawrie. To the Denmark/Argyle Street crew for making a fun, hug-filled home where I didn't have to think about work: Jenny, for her calmness, encouragement, serious discussions

and zany moments and for all the delicious food. Pri for sage advice and her vast knowledge of 80s and 90s trivia (actually, just trivia), Beth for fun at Bossaphonik and singing our hearts out on our cycles into work and Jo for throwing (and making us throw!) some amazing parties.

My life in Oxford has involved a lot of ringing, so I'd like to thank my darling OUS for making it so fun and for letting me be Master for a year. In particular, thanks to Emma Stanford for learning how to hug and letting me cut her hair, Simon Bond for making me care about striking and generally being awesome, Hannah Guggiari for getting me started on the road to ringing the 41 (we will do it!!), Rachel Prior for over-excited times and to Wilf Lewis, Chris Griggs, and Nick Hartley for their friendship.

So many lovely people outside of Oxford have been there for me over the past few years: Gemma, all the chats and voicemails have made up for our limited gangle time together, and the doctor gang, Kristina, Lizzle, Rhi and Jonny have provided much needed weekends away. Quaker Camp, and especially Jessie and Charlie, has given me an endless circle of love and I am so privileged to know my friend and Friend Roger Cann and thank him for letting me share my work with his PDUK group, which was such a valuable and humbling experience. I'd also like to thank Bristol Area Meeting Weekly Committee for their funding support that allowed me to write up in Oxford.

Finally, I would like to thank my wonderful family for all their love and Roberts-ness. To Grandma(ma), for the crosswords and letters, and Auntie Jennie for all the walks and visits. To my brothers Seth, Daniel and Kenneth for their sense of humour (which must be great, because I modelled mine on it) and for not letting me get down on myself. To my parents, Dave and Carole for keeping me going, for always being there for me (usually with advice that turns out to be right) and for their incredible strength and love.

Declaration

I hereby declare that this thesis is the product of my own work and that where others have contributed every effort has been made to acknowledge the contribution. This work has not been submitted for any other degree.

This thesis contains 36,000 words.

Publications and conference presentations

Publications

Roberts R, Wade-Martins R, Alegre-Abarrategui J. (2015). Direct visualization of alpha-synuclein oligomers reveals previously undetected pathology in Parkinson's disease brain. *Brain*. First published online: 2 March 2015. (http://dx.doi.org/10.1093/brain/awv040)

Ryan B, Roberts R, Hester S, Sloan M, Charles P, Thomas B, Wade-Martins R. (2015). Bioenergetic dysfunction and oxidative stress mediate alpha-synuclein-dependent neurodegeneration in a BAC-transgenic model of Parkinson's disease. Manuscript in preparation.

Conference presentations

Roberts R, Wade-Martins R, Alegre-Abarrategui J. (2014). Silent pathological oligomeric alpha-synuclein revealed in Parkinson's disease brain. Oral presentation. *Society for Neuroscience Annual Conference*. Washington DC, US.

Roberts R, Wade-Martins R, Alegre-Abarrategui J. (2014). Novel pathology is uncovered by the specific detection of alpha-synuclein oligomers in Parkinson's disease. Poster presentation. *Parkinson's UK Research Conference.* York, UK.

Roberts R, Wade-Martins R, Alegre-Abarrategui J (2013). A novel method to detect alpha-synuclein oligomers in Parkinson's disease brain. Poster presentation. *5th Conference on Advances in molecular mechanisms underlying neurological disorders.* University of Bath, UK.

Contents

List of figures

Chapter 1

Chapter 3

Chapter 4

Chapter 5

List of tables

Chapter 1

Chapter 2

Abbreviations

A-beta	Amyloid beta
AAV	Adeno-associated virus
ABC	Avidin-biotin complex
AD	Alzheimer's disease
ADom	Autosomal-dominant
ANOVA	Analysis of variance
AP-1	Activation protein 1
AR	Autosomal-recessive
AS-IF	Alpha-synuclein immunofluorescence
AS-IHC	Alpha-synuclein immunohistochemistry
AS-PLA	Alpha-synuclein proximity ligation assay
ATP13A2	ATPase type 13A2
BAC	Bacterial artificial chromosome
BCA	Bicinchoninic acid
BiFC	Bimolecular fluorescence complementation
BSA	Bovine serum albumin
CMV	Cytomegalovirus
CNS	Central nervous system
DAB	3,3'-Diaminobenzidine
DAPI	4',6-diamidino-2-phenylindole
DBS	Deep brain stimulation
DLB	Dementia with Lewy bodies

DMEM	Dulbecco’s Modified Eagle Medium
DMNV	Dorsal motor nucleus of the vagus
DMSO	Dimethyl sulfoxide
dNTP	Deoxynucleotide triphosphate
EDTA	Ethylenediaminetetraacetic acid
eGFP	Enhanced green fluorescent protein
ELISA	Enzyme linked immunosorbent assay
ER	Endoplasmic reticulum
FBXO7	F-box only protein 7
FKBP	FK506 binding protein
FLIM	Fluorescence lifetime imaging microscopy
FRB	FK506-rapamycin binding
FRET	Förster resonance energy transfer
GBA	Glucocerebrosidase
GCH1	GTP cyclohydrolase 1
GCI	Glial cytoplasmic inclusion
GFP	Green fluorescent protein
GPi	Globus pallidus internus
GRP78	78 kDa glucose regulated protein
GWAS	Genome-wide association study
HEK	Human embryonic kidney
HEPES	4-(2-Hydroxyethyl)piperazine-1-ethanesulfonic acid
HNE	4-hydroxy-2-nonenal

HRP	Horseradish peroxidase
IF	Immunofluorescence
IHC	Immunohistochemistry
iLBD	Incidental Lewy body disease
iPSC	Induced pluripotent stem cell
KO	Knock-out
LB	Lewy body
L-DOPA	L-3,4-dihydroxyphenylalanine
LN	Lewy neurite
LRRK2	Leucine-rich repeat kinase 2
MAPT	Microtubule-associated protein tau
MPP+	1-methyl-4-phenylpyridinium
MPPP	1-methyl-4-phenyl-4-propionoxypiperidine
MPTP	1-methyl-4-phenyl-1,2,3,6-tetrahydropyridine
MSA	Multiple system atrophy
mTOR	Mammalian target of rapamycin
NAC	Non-amyloid-beta component
NACP	Non-amyloid-beta component precursor
PAGE	Polyacrylamide gel electrophoresis
PB	Pale body
PBS	Phosphate buffered saline
PCA	Protein complementation assay
PCR	Polymerase chain reaction

PD	Parkinson’s disease
PDD	Parkinson’s disease with dementia
PFA	Paraformaldehyde
PLA	Proximity ligation assay
PLA2G6	Phospholipase A2, group VI
PINK1	PTEN-induced putative kinase 1
PK	Proteinase K
PK-PET	Proteinase K - paraffin embedded tissue
PPI	Protein-protein interaction inhibitor
PRKN	Parkin
PSP	Progressive supranuclear palsy
PVDF	Polyvinylidene fluoride
RBD	Rapid eye movement behaviour disorder
RIPA	Radio-immunoprecipitation assay
SDS	Sodium dodecyl sulphate
SDS-PAGE	Sodium dodecyl sulphate polyacrylamide gel electrophoresis
SEM	Standard error of the mean
SNARE	Soluble *N*-ethylmaleimide-sensitive factor attachment protein receptor
SN	Substantia nigra
SNc	Substantia nigra pars compacta
SNCA	Alpha-synuclein
SNP	Single nucleotide polymorphism
SPR	Sepiapterin reductase

STN	Subthalamic nucleus
TAE	Tris/acetic acid/EDTA
TBE	Tris/borate/EDTA
TBS	Tris-buffered saline
TBS-T	Tris-buffered saline + 0.1% Tween
WB	Western blotting
WT	Wild-type
YFP	Yellow fluorescent protein

1. Introduction

1.1 Parkinson's disease

1.1.1 Introduction

Parkinson's disease (PD), first described as the 'shaking palsy' by James Parkinson in 1817, is a neurodegenerative disorder characterised by progressive neuronal loss in nuclei throughout the brain, notably the heavy loss of dopaminergic neurons in the *substantia nigra pars compacta* (SNc). The loss of cells from the SNc results in the cardinal motor symptoms of PD. In the general population the incidence of PD is approximately 0.3%, which rises to 1-2% in those aged over 65 and approximately 5% in the over 80s (de Rijk *et al.*, 1997, Samii *et al.*, 2004). Ageing is an important risk factor for PD, and the lack of a cure or disease modifying treatment means PD will become an increasing societal burden as the population ages.

1.1.2 Clinical and pathological features

Clinically, PD is characterised by a triad of motor symptoms: resting tremor, rigidity and bradykinesia. Another common motor symptom is postural instability, which presents in the later stages of the disease and is associated with an increased risk of falls. The onset of motor symptoms occurs when approximately 70% of dopaminergic neurons in the lateral ventral tier of the SNc and 50% of those in the caudal region of the SNc have degenerated (Fearnley and Lees, 1991). The resulting loss of dopaminergic innervation to the striatum leads to over-inhibited motor pathways that cause the difficulty in initiating movement and bradykinesia observed in PD patients. Therefore, dopamine replacement therapies such as L-3,4-dihydroxyphenylalanine (L-DOPA) are used to treat the motor symptoms. A clinical diagnosis of PD is given following presentation with at least two of the motor symptoms and responsiveness to L-DOPA (D'Costa *et al.*, 1995).

Although clinical diagnosis is relatively reliable, PD can only be definitively

diagnosed upon post-mortem examination (Calne *et al.*, 1992, Hughes *et al.*, 2002). Neuropathologically, PD is defined by the loss of dopaminergic neurons in the SNc and the presence of eosinophilic inclusion bodies, known as Lewy bodies (LBs) in surviving neurons in regions where degeneration has occurred. The identification of alpha-synuclein as a major component of LBs (Spillantini *et al.*, 1997, Wakabayashi *et al.*, 1997, Baba *et al.*, 1998) eventually led to the classification of PD and other diseases that also feature alpha-synuclein rich inclusions, such as dementia with Lewy bodies (DLB) and multiple system atrophy (MSA), as alpha-synucleinopathies (Spillantini and Goedert, 2000). The role of LBs in PD will be discussed in more detail in section 1.2.1.

Many other neuroanatomical regions apart from the nigrostriatal system are affected in PD including the olfactory bulb, dorsal motor nucleus of the vagus (DMNV), raphe nuclei, locus coeruleus, and peripheral autonomic system. The presence of LB pathology, often accompanied by overt neuron loss, in these regions accounts for the presence of the non-motor symptoms of PD (Dickson *et al.*, 2009). Several non-motor symptoms including olfactory dysfunction (hyposmia or anosmia), constipation, rapid eye movement behaviour disorder (RBD) and depression often precede the development of the motor symptoms (Wolters, 2009, Meissner, 2012). Dementia occurs later in the disease, as pathology progresses to cortical regions, and up to 40% of PD patients develop dementia over the course of the disease (Cummings, 1988).

1.1.3 Aetiology

1.1.3.1 Environmental causes of PD

Idiopathic PD is primarily a disease of ageing, with an increase in risk concomitant with age (Hindle, 2010). However, the processes associated with ageing that lead to PD are not well understood. Thus, the identification of environmental factors that lead to the development of PD, or increased risk of developing PD, have provided insights into the disease process. Several toxins have been linked to PD in humans. The first of these was 1-methyl-4-phenyl-1,2,3,6-tetrahydropyridine (MPTP), an unwanted by-product of the synthesis of the opioid 1-methyl-4-phenyl-4-propionoxypiperidine (MPPP). Injection of MPPP contaminated with MPTP caused a rapid-onset

Parkinsonism that closely resembled PD, was responsive to L-DOPA (Langston *et al.*, 1983) and resulted from the preferential loss of dopaminergic SNc neurons, although this occurred without the development of LB pathology (Di Monte, 2003).

Long-term exposure to pesticides such as rotenone and paraquat has been associated with an increased risk of developing PD in epidemiological studies (Liou *et al.*, 1997, Tanner *et al.*, 2011). Animal models of PD have been developed by administration of these chemicals to rodents (Betarbet *et al.*, 2000, Manning-Bog *et al.*, 2002). However, such toxins only target dopaminergic neurons and the models do not fully recapitulate PD, as only the motor symptoms are mimicked (Di Monte *et al.*, 2002). Rotenone, paraquat and the metabolite of MPTP, 1-methyl-4-phenylpyridinium (MPP+), are all potent mitochondrial complex I inhibitors, suggesting that mitochondrial dysfunction is an important process in the pathogenesis of PD.

Other environmental factors that have been associated with an increased risk of PD include exposure to heavy metals such as manganese and copper (Gorell *et al.*, 1997, Logroscino *et al.*, 2008) and head injuries (Goldman *et al.*, 2006, Harris *et al.*, 2013). The risk of PD following a head injury is increased if the trauma is severe or if head injuries have previously been sustained suggesting neuroinflammation may play a role in the disease (Goldman *et al.*, 2006, Harris *et al.*, 2013).

1.1.3.2 Genetic causes of PD

Until the identification of mutations in the gene encoding alpha-synuclein in families with PD, it was thought that PD had no genetic component. The identification of the A53T mutation in an Italian kindred and three unrelated families of Greek origin in 1997 (Polymeropoulos *et al.*, 1997) heralded the beginning of an explosion in interest in the genetics of PD. To date 18 genomic loci associated with PD, known as PARK loci, have been identified (Table 1.1). PARK loci have been identified in a variety of ways, from pedigree linkage analysis or candidate gene approaches to genome wide association studies (GWAS) and range from monogenic causative genes for PD to risk genes. However, the involvement of several of the PARK genes in PD has not been

Designation	Locus	Gene	Disorder	Inheritance	Status	Method of identification
PARK 1/4	4q21-22	*SNCA*	EOPD	ADom	C	Linkage analysis
PARK 2	6q25.2-q27	*PRKN*	EOPD	AR	C	Linkage analysis
PARK 3	2p13	U	Classical PD	ADom	UC – possible risk factor	Linkage analysis
PARK 5	4p13	*UCHL1*	Classical PD	ADom	UC	Candidate gene approach
PARK 6	1p35-p36	*PINK1*	EOPD	AR	C	Linkage analysis
PARK 7	1p36	*DJ-1*	EOPD	AR	C	Linkage analysis
PARK 8	12q12	*LRRK2*	Classical PD	ADom	C	Linkage analysis
PARK 9	1p36	*ATP 13A2*	Atypical PD	AR	C	Linkage analysis
PARK 10	1p32	U	Classical PD	Risk factor	C	Linkage analysis
PARK 11	2q36-27	U	Late-onset PD	ADom	UC	Linkage analysis
PARK 12	Xq21–q25	U	Classical PD	Risk factor	C	Linkage analysis
PARK 13	2p12	*HTRA2*	Classical PD	ADom/risk factor	UC	Candidate gene approach
PARK 14	22q13.1	*PLA2 G6*	EO atypical PD	AR	C	Linkage analysis
PARK 15	22q12 –q13	*FBX07*	EO atypical PD	AR	C	Linkage analysis
PARK 16	1q32	U	Classical PD	Risk factor	C	GWAS
PARK 17	16q11.2	*VPS35*	Classical PD	ADom	C	Exome sequencing
PARK 18	3q27.1	*EIF4G1*	Classical PD	ADom	UC	Linkage analysis

Table 1.1. Genetic loci associated with Parkinson's disease. ADom: Autosomal-dominant; AR: Autosomal-recessive; C: confirmed; UC: unconfirmed, U: unknown. *SNCA*, alpha-synuclein; *PRKN*, parkin; *UCHL1*, ubiquitin carboxy-terminal hydrolase L1; *PINK1*, PTEN-induced putative kinase 1; *LRRK2*, leucine-rich repeat kinase 2; *PLA2G6*, phospholipase A2; *FBXO7*, F-box only protein 7. Adapted from Klein and Westenberger (2012).

confirmed since their initial reporting.

Six genes are associated with monogenic forms of PD, each with varying characteristics of disease onset, symptoms and pathology. Monogenic forms of PD are very rare, accounting for 3-5 % of cases (Klein and Westenberger, 2012) but can inform studies to understand the underlying pathogenesis of PD. Three point mutations in the gene encoding alpha-synuclein (*SNCA,* PARK1/4), which cause autosomal dominant PD, have been identified. A53T was initially described in Italian and Greek families, but has since been described in further Greek families (Athanassiadou *et al.*, 1999) as well as families in Korea (Ki *et al.*, 2007) and Sweden (Puschmann *et al.*, 2009). The point mutations A30P (Kruger *et al.*, 1998) and E46K (Zarranz *et al.*, 2004) have each been described in one family. Recently, two independent studies described sporadic patients with the H50Q mutation in alpha-synuclein, one of which had family history (Appel-Cresswell *et al.*, 2013, Proukakis *et al.*, 2013), and two familial cases exhibiting features of PD and MSA were found to harbour a G51D mutation in alpha-synuclein (Lesage *et al.*, 2013). In addition, duplication or triplication of the alpha-synuclein locus has been described in several PD families (Singleton *et al.*, 2003, Chartier-Harlin *et al.*, 2004, Ibanez *et al.*, 2004, Kara *et al.*, 2014) and in a handful of sporadic cases (Ahn *et al.*, 2008). A gene dosage effect of alpha-synuclein has been suggested due to the observation that patients with a triplication have an earlier onset, more severe and faster progressing disease (Chartier-Harlin *et al.*, 2004).

Mutations in *LRRK2* (PARK8) also cause PD with an autosomal dominant inheritance pattern, although with incomplete penetrance. Several missense mutations in LRRK2, including R1441C/G/H, Y1699C, G2019S and I2020T, have been shown to be pathogenic (Zimprich *et al.*, 2004, Zimprich *et al.*, 2004, Gilks *et al.*, 2005, Nichols *et al.*, 2005). These mutations cluster in the GTPase and kinase domains of the protein and have been reported to result in changes to enzymatic activity (West *et al.*, 2005, Jaleel *et al.*, 2007, West *et al.*, 2007). The G2019S mutation, localised to the kinase domain, has been shown to increase LRRK2 kinase activity, suggesting that a pathological cascade may be initiated by the upregulated phosphorylation of LRRK2 targets. Therefore, inhibitors of LRRK2 kinase activity are viewed as a potential

PD therapy. Interestingly, G2019S has been found in patients with familial PD (5%, (Nichols *et al.*, 2005)) and in patients with no known family history of PD (1-2%, (Gilks *et al.*, 2005)) and the similarity of clinical presentation in patients with LRRK2 mutations to sporadic patients suggests that investigation of LRRK2 mutations could provide important insights into the sporadic disease (Healy *et al.*, 2008).

In addition, *Parkin* (PARK2), *PINK1* (PARK6), *DJ-1* (PARK7) and *ATP13A2* (PARK9) have been confirmed to cause autosomal-recessive forms of PD (Klein and Westenberger, 2012). PINK1 is a kinase that acts in a common pathway with Parkin, an E3 ubiquitin ligase, for mitochondrial maintenance. Together, PINK1 and Parkin regulate processes such as mitophagy, mitochondrial fission and fusion and mitochondrial transport (Scarffe *et al.*, 2014), which are crucial for neuronal health. Similarly, DJ-1 is upregulated during oxidative stress and may maintain mitochondrial function under conditions of oxidative stress (McCoy and Cookson, 2011). ATP13A2 is a transmembrane lysosomal P5-type ATPase, with an unclear physiological role, although it has been shown that PD-linked mutations result in impaired lysosomal function (Dehay *et al.*, 2012).

GWAS have identified several moderate genetic risk factors for sporadic PD, including common single nucleotide polymorphisms (SNPs) in *SNCA, LRRK2* and *MAPT*, which encodes microtubule associated protein tau (Satake *et al.*, 2009, Simon-Sanchez *et al.*, 2009, Edwards *et al.*, 2010). A recent meta-analysis of previous GWAS confirmed these susceptibility factors and identified six further loci conferring susceptibility (Nalls *et al.*, 2014), including the gene coding for GTP cyclohydrolase 1 (*GCH1*), which was also identified as a risk factor for PD in a study utilising a candidate gene approach (Mencacci *et al.*, 2014).

Furthermore, variations in *GBA*, which encodes the lysosomal enzyme beta-glucocerebrosidase (GBA), are also associated with an increased risk of developing PD (Do *et al.*, 2011, Nalls *et al.*, 2014). The link between GBA and PD has long been suspected, as patients suffering from Gaucher's disease, which is caused by homozygous mutations in GBA, were often observed to co-present with Parkinsonism

(Neudorfer *et al.*, 1996, Tayebi *et al.*, 2003). The association of GBA with PD was confirmed in 2004, following the observation that carriers of mutant GBA, including the parent of a child with Gaucher's disease, were predisposed to the development of PD (Goker-Alpan *et al.*, 2004).

Despite the identification of many environmental and genetic factors that contribute to the development of PD, individually they cannot account for all cases of PD. It is likely that PD is triggered by a complex interplay of genetic and environmental factors, each contributing a relatively small individual component of risk, which become more important with ageing, itself contributing the largest non-genetic risk for sporadic PD (Hindle, 2010).

1.1.4 Treatment

Treatment options for PD currently focus on alleviating the motor symptoms by replacing dopamine in the striatum that is lacking due to the degeneration of SNc neurons. L-DOPA, which is a dopamine pre-cursor converted to dopamine by the enzyme DOPA decarboxylase, is the gold-standard treatment for PD. L-DOPA is administered with a peripheral DOPA decarboxylase inhibitor to prevent hyperdopaminergia in areas outside the brain, which would cause side effects that include nausea and vomiting. Although L-DOPA is effective at providing relief from PD motor symptoms for a number of years, its use over long periods of time results in dyskinesias due to the decreasing ability of the brain to buffer synaptic dopamine levels (Jankovic, 2006). Treatment with dopamine receptor agonists, such as ropinirole, early in the disease is a strategy to prevent L-DOPA induced dyskinesias. However, motor symptoms do not respond as well to dopamine agonists as to L-DOPA treatment and patients generally have to transition to L-DOPA treatment within five years (Rascol *et al.*, 2000).

Patients who are refractory to medication targeting the motor symptoms can benefit from surgical intervention. Deep brain stimulation (DBS) involves the insertion of electrodes into the subthalamic nucleus (STN) or global pallidus internus (GPi), which

are thought to be over-active in PD (Breit *et al.*, 2004). Stimulation by the electrodes can be activated by the patient when required and the activity of the STN or GPi modulated to compensate for the lack of SNc input to the basal ganglia. DBS results in fewer side-effects than dopaminergic replacement treatment, can provide longer relief and most importantly unlike its precursor, lesioning, is reversible and adjustable.

An experimental approach to replace dopamine in the striatum was the grafting of foetal ventral midbrain tissue into the putamen of PD patients. Although initially reported to improve symptoms and slow disease progression (Lindvall *et al.*, 1994, Kefalopoulou *et al.*, 2014), in double-blind studies no difference was observed between the graft and control group (Freed *et al.*, 2001, Olanow *et al.*, 2003). Furthermore, in some patients the graft exacerbated dyskinesias, most likely due to contaminating serotonergic neurons present in the graft (Politis *et al.*, 2010). Post-mortem analyses demonstrated that the grafted neurons had integrated into the basal ganglia circuit (Mendez *et al.*, 2008), although in several cases LB pathology was observed in a small number of the grafted neurons, suggesting that the grafted neurons are not resistant to the pathological milieu and providing credence to the hypothesis that pathogenic forms of alpha-synuclein can spread between neurons in a prion-like manner (Kordower *et al.*, 2008, Li *et al.*, 2008).

Much attention has been paid in recent years to the potential use of human stem cells for cell replacement therapy. Although promising results have been obtained by grafting neural stem cells or neurons derived from induced pluripotent stem cells (iPSCs) in animal models of PD (Redmond *et al.*, 2007, Wernig *et al.*, 2008, Cai *et al.*, 2010, Hargus *et al.*, 2010), the totipotent nature of stem cells can result in the formation of teratomas (Yamashita *et al.*, 2011). Although iPSC-derived neurons are particularly attractive for cell therapy due to the reduction in rejection likelihood, the presence of contaminating undifferentiated iPSCs render these therapies risky, despite the reporting of techniques for removing undifferentiated iPSCs from transplant material (Wernig *et al.*, 2008, Hargus *et al.*, 2010). Furthermore, the reprogramming process for the production of iPSCs may result in genetic modifications that could cause cancer (Blasco *et al.*, 2011).

An alternative approach to cell replacement therapy is to promote the survival of the neurons that remain. Glial derived neurotrophic factor (GDNF) has shown protective effects for dopaminergic neurons both *in vitro* and in animal models of PD and therefore intrastriatal infusion of GDNF was considered to be a potential option for protective therapy for PD (Kirik *et al.*, 2004). Open label trials found an improvement in symptoms in PD patients (Gill *et al.*, 2003, Slevin *et al.*, 2005) but this was not replicated in double-blind placebo-controlled trial (Lang *et al.*, 2006). Worryingly, 3/17 patients in the blind trial treated with GDNF produced neutralising anti-GDNF antibodies. However, it is thought that the reason for the lack of success of the blinded clinical trial was the variability in the delivery technique (Patel and Gill, 2007), and therefore a new trial in the UK is currently being undertaken to test whether a more reliable delivery technique can ensure a positive effect of GDNF.

The therapeutic avenues described thus far focus on the relief of the motor symptoms, while there are few treatments that can ameliorate the non-motor symptoms. The non-motor symptoms, including gait dysfunction, autonomic disturbances and cognitive decline, are often overlooked, despite the fact they can be more disabling than the motor symptoms (Zesiewicz *et al.*, 2010).

To develop a therapy that encompasses all of the symptoms, approaches must move from focusing on the relief of particular symptoms to identifying disease modifying treatments that target the underlying pathophysiological processes. For example, current targets include enhancers of autophagy (Hochfeld *et al.*, 2013), inhibitors of alpha-synuclein aggregation (Rohn, 2012) and LRRK2 kinase inhibitors (Chan *et al.*, 2013). Treatments that target aberrant molecular processes, in tandem with identifying PD patients at a much earlier stage, will ensure a cure can be delivered.

1.2 Parkinson's disease pathology

1.2.1 Lewy bodies

The pathological hallmark of PD was first described by Friedrich Lewy in 1912 (Lewy, 1912) but the intraneuronal inclusions found in PD brains only became eponymously known as Lewy bodies (LBs) in 1919 in the thesis of Konstantin Trétiakoff, a Russian neuropathologist (Rodrigues e Silva *et al.*, 2010). LBs appear in the brainstem as eosinophilic spherical bodies, consisting of a dense core surrounded by a clearer halo, while cortical LBs can be difficult to identify with haematoxylin and eosin due to the lack of the distinctive core and halo structure (Shults, 2006). Ultrastructurally, filamentous and granular material is found in the dense core, which is surrounded by radially oriented filaments (Roy and Wolman, 1969).

A proteomics study of LBs isolated by laser capture microdissection identified approximately 300 proteins present in the inclusions (Leverenz *et al.*, 2007), while a mass spectrometry study identified approximately 40 proteins specifically enriched in LBs (Xia *et al.*, 2008). However, the major component is alpha-synuclein: antibodies raised against purified LBs are specific against alpha-synuclein (Baba *et al.*, 1998). Antibodies directed against alpha-synuclein allow the visualisation of significantly more LBs with immunohistochemistry compared to ubiquitin antibody detection, the previous standard for identifying LBs (Spillantini *et al.*, 1998). Alpha-synuclein mediated detection of LBs is preferable to ubiquitin staining as LBs are not the only type of inclusion rich in ubiquitin (Gomez-Tortosa *et al.*, 2000). Notably, the alpha-synuclein fibrils that are found in LBs have an amyloid-like cross-beta structure consisting of beta-strands running perpendicular to the fibre axis (Vilar *et al.*, 2008). Other components of LBs include ubiquitin (Lowe *et al.*, 1988), various chaperones such as Hsp70 (Auluck *et al.*, 2002, McLean *et al.*, 2002), cytoskeletal components such as neurofilaments (Galvin *et al.*, 1999), tubulin (Galloway *et al.*, 1988), tau (Arima *et al.*, 1999) and gelsolin (Welander *et al.*, 2011), mitochondria (Roy and Wolman, 1969) and proteins involved in autophagy such as LC3 (Alvarez-Erviti *et al.*, 2010), LAMP1 (Chu *et al.*, 2009), p62 (Kuusisto *et al.*, 2003) and LRRK2 (Alegre-Abarrategui *et al.*,

2008). The incorporation of molecules such as heat shock proteins, ubiquitin and p62 into LBs may represent attempts by the cellular protein quality control and degradation machinery to remove alpha-synuclein aggregates or could be due to a general build-up of degradation substrates due to proteasomal and autophagic impairment (McNaught *et al.*, 2002, Kuusisto *et al.*, 2003). Whether each component of LBs plays a functional role in their formation or is incorporated during the compaction process remains to be seen.

The identification of possible precursors to LBs has provided strong evidence that alpha-synuclein aggregates are progressively compacted to form LBs (Wakabayashi *et al.*, 1997, Arima *et al.*, 1998, Gomez-Tortosa *et al.*, 2000, Kuusisto *et al.*, 2003). Delineating the relationships between the morphologically distinct pathological alpha-synuclein stained structures has provided an insight into the sequence of events that leads to LB formation. Pale bodies (PBs) are weakly or non-eosinophilic structures that are comprised ultrastructurally of disorganised fibrils and vacuoles (Gibb *et al.*, 1991). PBs have long been thought to be pre-cursors to LBs, due to the correlation between the abundance of PBs and LBs and the presence of larger numbers of PBs than LBs in cases with short duration of disease or that are non-symptomatic (Dale *et al.*, 1992). More recently, 'cloud-like' and punctate perikaryal alpha-synuclein staining and perikaryal threads have been described (Arima *et al.*, 1998, Gomez-Tortosa *et al.*, 2000, Kuusisto *et al.*, 2003). These structures were identified in the brains of PD patients alongside PBs and LBs and add to the previously recognised complement of alpha-synuclein pathology. They are thought to be early accumulations of alpha-synuclein, in part due to their diffuse appearance, but also because none of them were stained by ubiquitin in contrast to many PBs and LBs. The punctate perikaryal alpha-synuclein staining described by Kuusisto *et al* (2003) was also shown to be negative for p62, which is also a marker for PBs and LBs.

Lewy neurites (LNs), which are neuritic inclusions that stain positive for alpha-synuclein (Braak *et al.*, 1999), have been shown to share the same layered structure as LBs (Kanazawa *et al.*, 2008). However, they are thought to precede LBs, as they appear in PD patient brains in regions yet to develop LBs (Braak *et al.*, 2003). Further studies

have identified precursors to LNs, termed pale neurites (Kanazawa *et al.*, 2012), hinting at a similar compaction process occurring in neuritic lesions as in perikaryal lesions. The presence of such structures, in addition to extrasomal LBs, which are thought to be localised in neuronal processes (Kuusisto *et al.*, 2003), suggest the pathological process of alpha-synuclein compaction may begin in axons and be intimately linked to the mislocalisation of alpha-synuclein from synapses to cell body.

1.2.2 Sites of pathology

PD is frequently defined by the selective loss of dopaminergic neurons from the nigrostriatal system. However, this inadequately describes the extent of pathology throughout the brain in PD patients and neglects the pathology underlying symptoms apart from the cardinal motor signs of PD. Indeed, when Lewy first studied the pathology in PD brains, he described the presence of LBs in the nucleus basalis of Meynert and the DMNV and was not convinced that the SNc was the main site of pathology (Lewy, 1912, Shults, 2006, Rodrigues e Silva *et al.*, 2010). Components of the medullary autonomic system, which includes the DMNV, the reticular formation and intermediate reticular zone, and the gain setting system, formed of the lower raphe nuclei, magnocellular reticular nuclei and the coeruleus-subcoeruleus complex are affected by LB pathology (Del Tredici *et al.*, 2002). In particular, the DMNV and the locus coeruleus are particularly prone to heavy LB load. Lesions in these areas may account for autonomic dysfunction observed in PD patients. Parts of the limbic system, such as the hippocampus, amygdala and cingulate cortex are also subject to extensive pathology, while neocortical areas, including the prefrontal cortex are affected in late-stage cases and lesions in these locations are associated with cognitive impairment (Apaydin *et al.*, 2002).

Furthermore, pathology is not restricted to the CNS and components of the peripheral and enteric nervous systems are also affected. Alpha-synuclein aggregates have been found in the cardiac sympathetic nervous system (Orimo *et al.*, 2008), in cutaneous autonomic nerves (Wang *et al.*, 2013) and the pharyngeal motor nerves (Mu *et al.*, 2013) and are associated with orthostatic hypotension, autonomic dysfunction and

dysphagia, respectively. There has been particular interest in gastrointestinal alpha-synuclein pathology, which has been identified in archived biopsies from PD patients up to 8 years preceding their diagnosis (Shannon *et al.*, 2012, Hilton *et al.*, 2013) suggesting it may represent very early pathology. However, in post-mortem studies, no gut pathology has been identified in the absence of brain pathology to date (Braak *et al.*, 2006).

1.2.3 Braak hypothesis of pathological progression

The progressive nature of LB pathology through the PD brain has lent itself to a staging system. Braak and colleagues have proposed that pathology begins in the DMNV and the olfactory bulb and progresses caudorostrally from the DMNV in a stereotypic manner that can be split into six stages, shown in Figure 1.1 (Braak *et al.*, 2002, Del Tredici *et al.*, 2002, Braak *et al.*, 2003). In stage I, LB pathology is confined to the DMNV and intermediate reticular zone of the medulla, or the olfactory bulb, with involvement of further medullary and pontine nuclei, including the locus coeruleus, beginning in stage II. Stage III is thought to be coincident with the onset of motor symptoms as pathology extends to the midbrain, including the SNc. Regions of the basal forebrain, such as the basal nucleus of Meynert are also affected at stage III, before pathology is found in limbic structures such as the amygdala, hippocampus and transentorhinal cortex at stage IV. Finally, areas of the basal ganglia, further limbic structures such as the anterior cingulate cortex, and the neocortex become involved at stages V and VI, while pathology in regions affected earlier worsens leading to, for example, almost complete denuding of the SNc and locus coeruleus (Braak *et al.*, 2003).

This scheme was intended purely to describe the progression of pathology through the brain and not to provide clinico-pathological correlation. For example, in a study of 226 subjects with alpha-synuclein pathology, approximately 55% of cases classified as Braak stage V and VI, i.e. with extensive alpha-synuclein pathology in areas including the neocortex, did not show the motor symptoms of PD or dementia (Parkkinen *et al.*, 2008), raising interesting questions about the relationship between LBs and

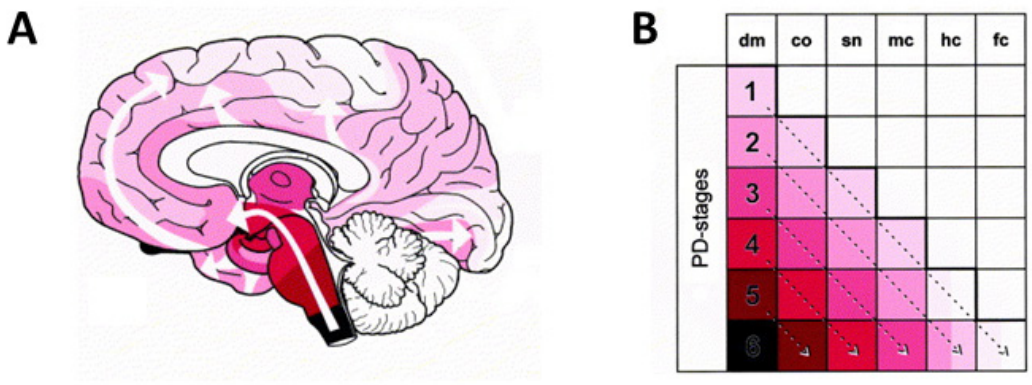

Figure 1.1. The Braak hypothesis of Parkinson's disease neuropathological progression. **A** Schematic of the proposed caudo-rostral progression of alpha-synuclein pathology through the PD brain, beginning in the medulla and ascending through the brainstem to affect limbic and cortical regions. **B** Table of regions affected at each Braak stage. dm: dorsal motor nucleus of the vagus; co: locus coeruleus; sn: substantia nigra; mc: anteromedial temporal mesocortex (i.e. transentorhinal cortex). hc: high order sensory association areas and prefrontal fields. fc: first order sensory association areas, premotor areas and primary sensory and motor fields. Hc and fc are components of the neocortex. Images are from Braak *et al* (2003) and are used with permission from the publisher.

symptomatic signs of disease.

The Braak hypothesis, although widely accepted, remains controversial. Several studies have reported that most PD cases display the proposed order of pathology (Parkkinen *et al.*, 2008, Dickson *et al.*, 2010, Kingsbury *et al.*, 2010), while others have found that up to 50% of incidental or PD cases do not adhere to the scheme of pathological progression proposed by Braak (Kalaitzakis *et al.*, 2008, Zaccai *et al.*, 2008). The criteria for selecting incidental LB disease (iLBD) cases in the study of Braak *et al* (2003) have been questioned (Kalaitzakis *et al.*, 2008). iLBD cases are neurologically normal subjects in whom LBs are identified post-mortem, leading to the postulation that iLBD represents a pre-symptomatic phase of PD (Braak *et al.*, 2003, Dickson *et al.*, 2008). The iLBD cohort studied in Braak *et al* (2003) were selected for the presence of LB pathology in the DMNV (Del Tredici *et al.*, 2002), even though pathology in several regions has been identified in iLBD cases and can be present in areas such as the amygdala in the absence of any pathology in the DMNV (Markesbery *et al.*, 2009). Therefore, the DMNV may not be the start site for PD pathology and there may be other areas affected by pathology at the pre-symptomatic Braak stages I and II that were not identified in their study.

Furthermore, cases of dementia with LBs (DLB) were excluded from the study by Braak and colleagues. There is significant clinical and pathological overlap between PD and DLB and the possibility that PD and DLB are part of the same disease spectrum is well acknowledged (McKeith, 2000). The incidence of dementia in PD patients is high (Cummings, 1988) and clinically the distinction between PD with dementia (PDD) and DLB is arbitrarily implemented, based on the ‘one year rule’ whereby if dementia symptoms appear within one year of presentation with parkinsonian symptoms, DLB is diagnosed. If dementia presents any later, the disease is classified as PDD (McKeith *et al.*, 2005). A neuropathological staging system for DLB has been proposed (McKeith *et al.*, 2005), although, as with Braak staging for PD, many cases are unclassifiable using this system (Fujimi *et al.*, 2008, Leverenz *et al.*, 2008). A unified staging scheme has been proposed (Beach *et al.*, 2009) that classifies the sub-type of LB disease by the area (olfactory, brainstem, limbic or neocortical) in which LB pathology is predominant.

This scheme allows for the heterogeneity of pathology within PD or DLB patients and could provide insights into the overlap between PD and DLB, the clinical outcome of pathological differences, and perhaps how pathology progresses within the different sub-types.

1.3 Alpha-synuclein

1.3.1 Introduction

Alpha-synuclein was initially isolated from the electric organ of the fish *Torpedo californica* in a screen to identify synaptic proteins and gained its name due to its localisation in the nucleus and pre-synaptic terminals (Maroteaux *et al.*, 1988)1988. Subsequently, a fragment of the protein was isolated from neuritic plaques in AD tissue, and therefore was referred to as the non-amyloid beta component (NAC), while the full-length protein was known as the non-amyloid beta component precursor (NACP) (Ueda *et al.*, 1993). Although further studies did not confirm the presence of alpha-synuclein in amyloid plaques in AD brain (Bayer *et al.*, 1999, Culvenor *et al.*, 1999), the identification of mutations in the gene coding for alpha-synuclein in families with PD and the demonstration that alpha-synuclein was a major component of LBs cemented its association with neurodegeneration (Polymeropoulos *et al.*, 1997, Spillantini *et al.*, 1997). The exact role of alpha-synuclein physiologically and pathophysiologically has been subject to intense investigation since these discoveries.

1.3.2 Structure

Alpha-synuclein is a small acidic protein, consisting of 140 amino acids in its full length form, that is highly expressed in the central nervous system but also present in a number of other tissues including the pancreas, heart, kidney and skeletal muscle (Ueda *et al.*, 1993). The gene consists of seven exons, five of which are protein coding, and four different isoforms can be produced by alternative splicing of exons 3 and 5. The domain organisation is conserved within the synuclein family, which also includes beta- and gamma-synuclein, and consists of three structurally distinct regions shown in Figure 1.2 (Jakes *et al.*, 1994, Lavedan, 1998). In the N-terminal

half of alpha-synuclein are seven imperfect 11 amino acid repeats with the consensus sequence KTKEGV, four of which are found in the N-terminal domain and form amphipathic alpha-helices in the presence of lipids (Davidson *et al.*, 1998, Ulmer *et al.*, 2005). The point mutations that cause familial PD all localise to the region of helices. The hydrophobic core of alpha-synuclein is known as the NAC domain and displays amyloidogenic properties that make this region responsible for the protein's propensity to aggregate (Giasson *et al.*, 2001). The acidic carboxy-terminal is unstructured and contains several amino acids that can be subject to modification by phosphorylation, including tyrosines 125, 133 and 136 and serine 129 (Recchia *et al.*, 2004).

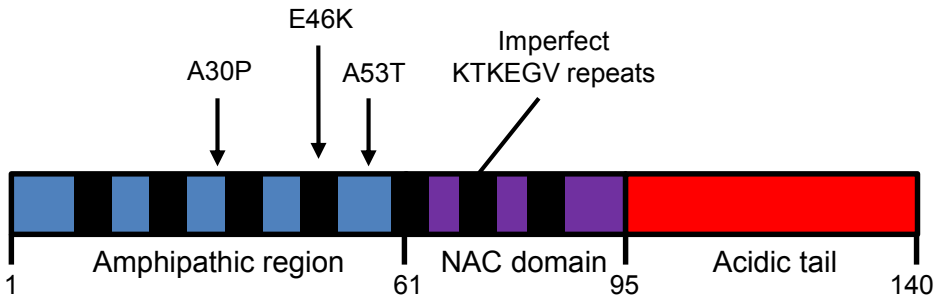

Figure 1.2. Alpha-synuclein structure. The primary structure of alpha-synuclein, with each of the three domains and familial mutations indicated. The black bars represent the imperfect KTKEGV repeats.

In terms of secondary and tertiary structure, alpha-synuclein has long been considered a natively unfolded monomer that acquires alpha-helical secondary structure upon interaction with acidic phospholipids (Weinreb *et al.*, 1996). Recently it has been proposed that the physiological form of alpha-synuclein is a helically-folded tetramer (Bartels *et al.*, 2011, Wang *et al.*, 2011). Although the presence of a tetrameric form of alpha-synuclein was reported in several cell lines and neuronal and non-neuronal tissues (Bartels *et al.*, 2011), this has not been replicated in independent laboratories (Fauvet *et al.*, 2012, Burre *et al.*, 2013) which has been suggested to be due to the inherent instability of the tetrameric form of alpha-synuclein outside of the cellular environment (Dettmer *et al.*, 2013, Luth *et al.*, 2015). The conformation of physiological alpha-synuclein remains a contentious issue but understanding the identity of the

native form, or whether there are multiple native conformers in equilibrium in the cell, is important to inform the development of potential anti-aggregation therapies for PD.

1.3.3 Physiological function of alpha-synuclein

Despite almost two decades of intense investigation, the exact functional role of alpha-synuclein is unknown, although promising avenues have been revealed. The pre-synaptic enrichment of alpha-synuclein and its localisation to synaptic membranes and vesicles suggested a role in the regulation of synaptic function (Iwai *et al.*, 1995, Kahle *et al.*, 2000, Fortin, 2004). The functional relevance of this localisation to neuronal plasticity was first recognised when alpha-synuclein was observed to be upregulated in nuclei associated with song learning in the male zebra finch at crucial periods in the development of this behaviour (George *et al.*, 1995). Alpha-synuclein knock-out (KO) animals have been utilised to further investigate this connection. Several strains of alpha-synuclein KO mice have been generated, all of which were viable and showed no overt dysfunctional phenotype but had subtle, although differing, vesicle release phenotypes. In one study, there was no change in dopamine release and reuptake in the nigrostriatal system in response to a single electrical stimulus, but increased release of dopamine was observed following paired stimuli, suggesting that alpha-synuclein is an activity dependent negative regulator of dopamine neurotransmission (Abeliovich *et al.*, 2000). This was replicated in an independent study (Yavich *et al.*, 2004) and both proposed the effects were due to decreased inhibition of the refilling of the synaptic vesicle readily releasable pool as a result of the lack of alpha-synuclein. In contrast, Cabin *et al* (2002) found the reserve pool of synaptic vesicles was depleted in the hippocampus of alpha-synuclein KO mice following a prolonged train of stimulations and concluded that alpha-synuclein was required for genesis and/or maintenance of the synaptic vesicles in the reserve pool (Cabin *et al.*, 2002). The observations of Cabin *et al* (2002) are supported by studies in cultured rat hippocampal neurons in which alpha-synuclein was targeted with RNAi, which resulted in fewer synaptic vesicles in the reserve pool (Murphy *et al.*, 2000). A recent study *in vitro* using synaptic vesicle mimics supports this paradigm, as alpha-synuclein was demonstrated to promote clustering of the vesicles and may therefore have a similar role in the reserve pool *in vivo* (Diao *et al*., 2013). The exact pathway by which alpha-synuclein

exerts such effects is unknown, but it is possible the ability of alpha-synuclein to promote curvature of membranes may be involved (Ulmer *et al.*, 2005, Mizuno *et al.*, 2012).

The subtle changes to synaptic vesicle release observed in alpha-synuclein KO animals may be due to redundancy between the members of the synuclein family. In double KOs of alpha- and gamma- synuclein or alpha- and beta- synuclein, expression levels of the remaining synuclein are increased (Chandra *et al.*, 2004, Robertson *et al.*, 2004). Mice null for all three members of the synuclein family displayed hyperactivity and increased evoked dopamine release in the dorsal striatum (Anwar *et al.*, 2011), while in another study triple KO mice displayed age dependent neuronal dysfunction and reduced SNARE complex formation (Burre *et al.*, 2010). Although inconsistent results have been obtained through the use of KO animals to study the function of alpha-synuclein, it is clear that alpha-synuclein is important for neuronal function. It is also worth noting that alpha-synuclein has been shown to play key roles in the function of other tissues, for example in regulating the release of insulin from pancreatic beta cells (Geng *et al.*, 2011).

Given its interactions with a wide array of proteins, it has been postulated that alpha-synuclein may function as a signalling molecule. For example, 14-3-3 has been identified as an interactor of alpha-synuclein, and the 40% homology between the amino-terminal of alpha-synuclein and 14-3-3 suggests they may share a similar chaperone function, particularly as they share many interacting partners (Ostrerova *et al.*, 1999). Interactions with cytoskeletal components, including tau (Jensen *et al.*, 1999) and tubulin (Payton *et al.*, 2001), have also been reported. An interaction with actin showed that alpha-synuclein may be able to influence cytoskeletal dynamics by preventing the polymerisation of actin and promoting its depolymerisation (Sousa *et al.*, 2009). A putative role in lipid signalling has also been reported for alpha-synuclein. Alpha-synuclein has been shown to influence membrane fluidity (Sharon *et al.*, 2003) and bind the fatty acid oleic acid, suggesting it may be involved in transport of fatty acids between membrane and cytosolic compartments (Sharon *et al.*, 2001). Alpha-synuclein has also been shown to play a regulatory role in the phosphatidylinositol

signalling pathway (Narayanan *et al.*, 2005). More recently, alpha-synuclein and poly-unsaturated fatty acids have been shown to interact to stimulate clathrin-mediated endocytosis (Ben Gedalya *et al.*, 2009). The plethora of functions for alpha-synuclein implicated in these studies suggests alpha-synuclein is a promiscuous protein with a complex variety of interplaying roles within cells.

1.3.4 Relationship to Parkinson's disease

Alpha-synuclein has been linked to both familial and sporadic forms of PD. As discussed in section 1.1.3, rare familial forms of PD have been shown to result from point mutations in, or multiplications of, the gene coding for alpha-synuclein (Polymeropoulos *et al.*, 1997, Kruger *et al.*, 1998, Singleton *et al.*, 2003, Farrer *et al.*, 2004, Zarranz *et al.*, 2004, Appel-Cresswell *et al.*, 2013, Lesage *et al.*, 2013, Proukakis *et al.*, 2013). Triplications of the alpha-synuclein locus were demonstrated to result in the expected two-fold increase in alpha-synuclein mRNA and protein levels, which is particularly interesting given the increased disease severity and earlier age of onset in cases with the locus triplication (Farrer *et al.*, 2004, Miller *et al.*, 2004). Cases with triplications of the alpha-synuclein locus show complete penetrance, such that all subjects developed a PD phenotype, while only approximately 70% of those with alpha-synuclein duplications presented with PD and penetrance has been reported to be as low as 33% in one kindred (Nishioka *et al.*, 2006, Elia *et al.*, 2013). These observations suggest an alpha-synuclein dosage effect, whereby alpha-synuclein levels are directly linked to the onset of disease.

The clear relationship between alpha-synuclein expression levels and PD in the familial multiplication cases raised the question of the relevance of alpha-synuclein expression levels in idiopathic PD. In sporadic patients, increased levels of alpha-synuclein mRNA in the SNc have been reported (Rockenstein *et al.*, 2001, Chiba-Falek *et al.*, 2006), while others have demonstrated a decrease (Neystat *et al.*, 1999, Kingsbury *et al.*, 2004, Dachsel *et al.*, 2007). Conflicting results were obtained in other regions of the brain, including the cortex where in some studies no change in transcript expression levels between patients and controls was observed (Neystat *et al.*, 1999, Chiba-Falek

et al., 2006) while others reported decreased levels in patients (Kingsbury *et al.*, 2004, Dachsel *et al.*, 2007). All of these studies were conducted in post-mortem human tissue in PD patients that necessarily, especially in the SNc, would have displayed advanced PD-related pathological changes. The association between alpha-synuclein expression levels and disease in the multiplication kindreds suggest that they may be an initiating factor and thus it may not be prudent to study sporadic cases for this information at such a late stage. In light of this, it is interesting to note that alpha-synuclein protein levels increase in normal human individuals and rhesus monkeys with age in nigral neurons, which is associated with a decrease in tyrosine hydroxylase levels (Chu and Kordower, 2007).

In addition, a risk allele for PD has been identified that has provided a potential basis for increased alpha-synuclein expression in some sporadic patients. Variability in the dinucleotide sequence repeat REP1 that lies in the alpha-synuclein gene promoter has been repeatedly associated with PD (Farrer *et al.*, 2001, Pals *et al.*, 2004, Maraganore *et al.*, 2006). REP1 alleles linked to PD were subsequently shown to result in increased alpha-synuclein protein levels in the blood, compared to a 'protective' allele (Fuchs *et al.*, 2008).

GWAS uncovered further susceptibility loci associated with sporadic PD that included SNPs at the alpha-synuclein locus. The association of common SNPs in the alpha-synuclein locus has been confirmed several times, in different populations, confirming the strong link between risk of PD and variation in alpha-synuclein (Satake *et al.*, 2009, Simon-Sanchez *et al.*, 2009, Edwards *et al.*, 2010, Mata *et al.*, 2011, Nalls *et al.*, 2014). A PD associated SNP in the 3' untranslated region of the alpha-synuclein gene has also been associated with increased alpha-synuclein mRNA levels in post-mortem brain tissue (Fuchs *et al.*, 2008), further linking sporadic forms of the disease with increased alpha-synuclein expression levels.

At the cellular level, alpha-synuclein is linked to both sporadic and familial forms of PD as a major component of the proteinaceous inclusions, LBs, the presence of which is considered a requirement for the pathological diagnosis of PD (Spillantini *et al.*, 1997).

The aggregation of alpha-synuclein, therefore, is thought to be the key process in the pathogenesis of PD.

1.3.5 Aggregation

Given the proposed central role of alpha-synuclein aggregation in PD (Volles and Lansbury, 2003) and the interest in modifying the aggregation process as a therapeutic avenue, it is important to understand the key molecular events underpinning the formation of aggregates (Figure 1.3).

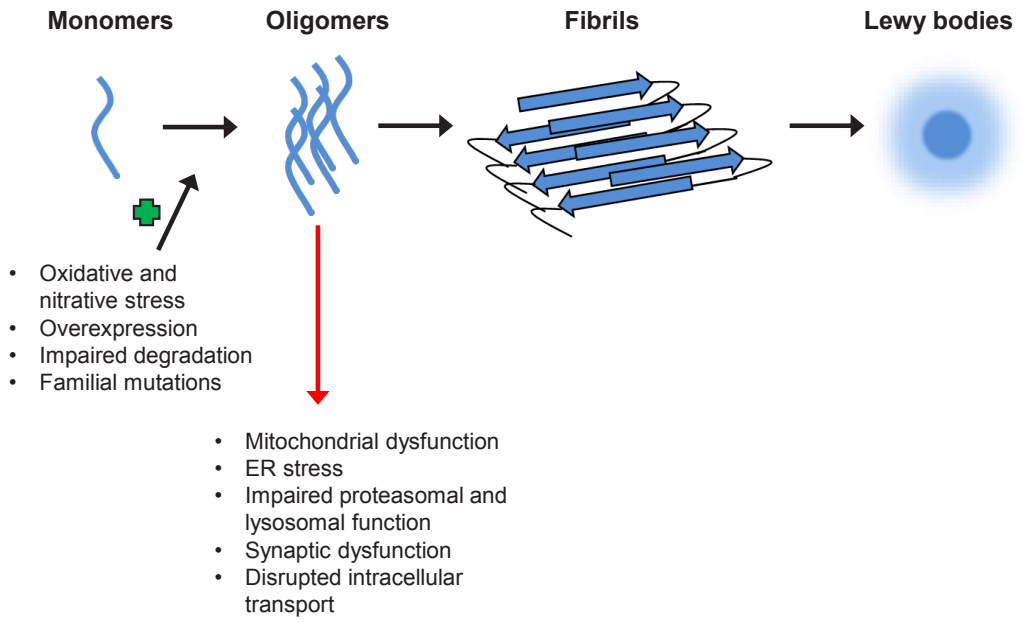

Figure 1.3. Alpha-synuclein aggregation. The process of alpha-synuclein aggregation from monomers via oligomers and fibrils that become compacted to form Lewy bodies. Processes that promote alpha-synuclein are indicated with a green positive sign, while the detrimental effects of oligomers are indicated with a red arrow.

Biophysical studies have demonstrated a nucleation-dependent mechanism for alpha-synuclein aggregation, which is characterised by an initial lag phase in aggregate formation following by an exponential growth phase and final plateau (Uversky and Eliezer, 2009). In the process of forming fibrils with the cross-beta structure of amyloid, alpha-synuclein aggregates are known to proceed through a variety of structurally diverse intermediates termed oligomers or protofibrils. The nomenclature for such

species is currently unclear: although ‘protofibrils’ has often been used to refer to oligomeric species that have some aspect of fibril structure or properties, such as proteinase K resistance (for example, (Nasstrom *et al.*, 2011)), in contrast to small, amorphous oligomers, there is no convention and frequently the two terms are used interchangeably (for example, (Danzer *et al.*, 2007)). Therefore, in this thesis I will refer to all oligomeric forms of alpha-synuclein as ‘oligomers’, unless referring to a study in which the term ‘protofibril’ was explicitly used to provide a useful distinction between oligomeric species.

Alpha-synuclein aggregation is influenced by the protein structure itself. Natively unfolded proteins, such as alpha-synuclein, have been shown to be particularly prone to aggregation as unwanted contacts are more likely to occur in a highly dynamic, unstructured protein (Uversky, 2008). The beta-sheet structure of alpha-synuclein amyloid comprises five beta-sheets made up of residues from 30-110 of the protein (Vilar *et al.*, 2008), while the N- and C-termini remain in solution. Residual structure, involving residues that form key components of the beta-sheets of fibrils, has been shown in soluble, monomeric alpha-synuclein (Esteban-Martin *et al.*, 2013). All of these interactions involve the NAC domain, which is required for aggregation. In particular, an 11 amino acid sequence (amino acids 71-82) of the NAC domain is key and beta-synuclein, which lacks this sequence, is resistant to fibrillisation (Uversky *et al.*, 2002). Although the contacts described by Esteban-Martin *et al* are transient, a partially folded monomeric structure that increases the propensity of alpha-synuclein to form fibrils was induced with heating or with a decrease in pH, suggesting that under conditions of stress such contacts will inevitably lead to fibrillisation (Uversky *et al.*, 2001).

It has been proposed that distinct intramolecular interactions between the N- and C-termini exist in physiological alpha-synuclein that reduce its aggregation ability and if the autoinhibition is released, aggregation ensues, possibly due to the formation of the aforementioned fibril-like contacts (Bertoncini *et al.*, 2005). This model provides an explanation for the increased propensity of C-terminally truncated alpha-synuclein to aggregate (Crowther *et al.*, 1998).

Over-expression of alpha-synuclein is known to induce its aggregation due to the resultant higher concentration of amyloidogenic intermediates (Uversky, 2008, Zhang *et al.*, 2008, Uversky and Eliezer, 2009) and the effects of molecular crowding (Shtilerman *et al.*, 2002, Munishkina *et al.*, 2009). The inhibition of degradation mechanisms for alpha-synuclein, such as the ubiquitin proteasome system and autophagy (Bennett *et al.*, 1999, Webb *et al.*, 2003, Vogiatzi *et al.*, 2008, Ebrahimi-Fakhari *et al.*, 2011), are likely to have the same net result as overexpression of the protein. Induction of dysfunction in proteasome or autophagic function has therefore been used to generate models of PD, which develop alpha-synuclein inclusions (McNaught *et al.*, 2004, Friedman *et al.*, 2012). In the SNc of PD patients, decreased 20S proteasomal activity has been observed (McNaught *et al.*, 2003), while the number of lysosomes and lysosomal proteins such as LAMP-1, LAMP-2a and cathepsin D were decreased, suggesting impaired autophagic function (Anglade *et al.*, 1997, Chu *et al.*, 2009, Alvarez-Erviti *et al.*, 2010). Interestingly, alpha-synuclein itself has been shown to inhibit both proteasomal and autophagic processes, suggesting a vicious cycle could occur if either system is impaired or alpha-synuclein begins to aggregate (Snyder *et al.*, 2003, Winslow *et al.*, 2010). The presence of both deleterious events (increased alpha-synuclein levels combined with impairment in degradation pathways) in the ageing brain has been proposed to distinguish those who develop PD from those who remain neurologically normal despite increased alpha-synuclein expression levels with age (Chu and Kordower, 2007).

Familial mutations in alpha-synuclein have also been demonstrated to affect the aggregation properties of the protein. A53T, E46K and H50Q mutated alpha-synuclein showed accelerated fibril formation compared to wild-type whereas alpha-synuclein with the A30P or G51D mutations formed fibrils more slowly, despite consuming monomeric protein at the same rate, which was due to the preferential formation of oligomers (Conway *et al.*, 2000, Fredenburg *et al.*, 2007, Ghosh *et al.*, 2013, Fares *et al.*, 2014, Porcari *et al.*, 2015). Further investigations demonstrated the formation of annular, pore-like protofibrils by A30P alpha-synuclein, whereas A53T alpha-synuclein formed annular and tubular protofibrils (Lashuel *et al.*, 2002). Wild type alpha-synuclein was also capable of forming annular protofibrils, albeit at a slower

rate (Lashuel *et al.*, 2002) and recent structural studies have shown the formation of a 'wreath-like' oligomer that can permeabilize membranes (Giehm *et al.*, 2011). A cellular study corroborated the *in vitro* findings in which cells expressing A30P alpha-synuclein harboured fewer inclusions compared to wild type, whereas most (approximately 80%) of E46K expressing cells displayed inclusions (Lazaro *et al.*, 2014).

Phosphorylation of alpha-synuclein at serine 129 is a key pathological marker of PD and serine 129 phosphorylated alpha-synuclein is present in LBs (Fujiwara *et al.*, 2002) and smaller aggregates revealed in PD brain (Saito *et al.*, 2003). *In vitro* studies have also shown that the phosphorylation of alpha-synuclein at serine 129 promotes fibril formation (Fujiwara *et al.*, 2002). It is possible, however, that hyperphosphorylation of alpha-synuclein is a secondary phenomenon resulting from fibrillogenesis, and is not a prerequisite for inclusion formation. In *Drosophila,* phosphorylation of alpha-synuclein at serine 129 increased levels of soluble oligomers, which was associated with increased neurotoxicity (Chen *et al.*, 2009). In contrast, the expression of a mutant that abolishes phosphorylation (S129A) in a AAV-mediated alpha-synuclein expression model of PD led to increased neurodegeneration and aggregate formation compared with expression of wild type alpha-synuclein or the phosphorylation mimic mutant, S129D (Azeredo da Silveira *et al.*, 2008). Therefore, the relationship of this post-translational modification to aggregation remains unclear.

Post-translational modifications by pathogenic mediators such as oxidative and nitrative stress can impact alpha-synuclein aggregation. Oxidising and nitrating agents such as peroxynitrite induce covalent cross-links between tyrosine residues in alpha-synuclein to form *o*,*o'*-dityrosine linkages and subsequently stable oligomers (Souza *et al.*, 2000). Oligomers formed in this way *in vitro* do not form fibrils, suggesting that in PD brain dityrosine linkages may induce the formation of off-pathway oligomers (Yamin *et al.*, 2003). Oxidative agents such as copper and hydrogen peroxide induce alpha-synuclein oligomers in a process that does not require tyrosine residues and therefore results in aggregation via a mechanism that does not involve the formation of dityrosine linkages (Paik *et al.*, 2000, Norris *et al.*, 2003). One such dityrosine independent mechanism is the oxidation of methionine residues, which has been demonstrated

to result in the formation of alpha-synuclein oligomers (Leong *et al.*, 2009, Nakaso *et al.*, 2013, Carmo-Goncalves *et al.*, 2014). Antibodies against nitrated/oxidised alpha-synuclein have revealed extensive pathology in PD brain, indicating such modifications may play an important part in alpha-synuclein aggregation *in vivo* (Duda *et al.*, 2000, Giasson *et al.*, 2000, Duda *et al*., 2002).

A dysfunctional and reciprocal relationship has been described between GBA and alpha-synuclein. In a multi-system study, Mazzulli *et al* (2011) demonstrated that functional loss of GBA resulted in impaired degradation and accumulation of alpha-synuclein, as well as the GBA substrate glucosylceramide, which was able to stabilise alpha-synuclein oligomers *in vitro* (Mazzulli *et al.*, 2011). Alpha-synuclein was also able to inhibit the activity of normal GBA and thus initiated a positive feedback loop of impaired lysosomal activity, leading to further alpha-synuclein accumulation, which in turn led to further lysosomal dysfunction (Dehay *et al.*, 2013).

1.3.6 Alpha-synuclein oligomers and neurodegeneration

The presence of fibrillar alpha-synuclein in LBs brought attention to the potential involvement of aggregated alpha-synuclein in PD. However, several lines of evidence suggest LBs may be the 'innocent bystanders' in PD pathogenesis (Caughey and Lansbury, 2003). LBs have been found post-mortem in neurologically normal individuals at the surprisingly high rate of approximately 10% in those over 60 (Parkkinen *et al.*, 2005, Frigerio *et al.*, 2011). The LB load in patients has been shown to correlate poorly with the severity of symptoms such as cognitive impairment and dementia (Colosimo *et al.*, 2003, Parkkinen *et al.*, 2008). Furthermore, PD patients carrying familial mutations in the *parkin* gene*,* and some of those with the LRRK2 G2019S mutation, show neuronal degeneration in the absence of LB formation (Cookson *et al.*, 2008). Therefore the formation of LBs may not be linked to overt neuronal dysfunction *per se* and could suggest aggregates are not required for the disease process. Alternatively, these observations could point to an aggregated species of alpha-synuclein that is a precursor to LBs and is not as readily detectable in histological sections as the disease causative species. Indeed, evidence suggests

oligomeric forms of alpha-synuclein are key mediators in PD pathogenesis and LBs act as a sink for the toxic species, sequestering them away from the cellular machinery (Bucciantini *et al.*, 2002, Muchowski, 2002, Soto and Estrada, 2008).

Oligomeric species of alpha-synuclein have been isolated from diseased brain (Sharon *et al.*, 2003, Tofaris *et al.*, 2003) and are found in degenerating brain regions of animal models of PD generated by the over-expression of alpha-synuclein (Kahle *et al.*, 2001, Giasson *et al.*, 2002, Periquet *et al.*, 2007, Janezic *et al.*, 2013). *In vitro* formed alpha-synuclein oligomers ectopically applied to cell cultures or formed due to over-expression of alpha-synuclein induce cell death (Chen *et al.*, 2007, Danzer *et al.*, 2007, Tetzlaff *et al.*, 2008, Nasstrom *et al.*, 2011), which has been recapitulated *in vivo* in two studies. Firstly, expression of alpha-synuclein mutants rationally designed to reduce fibril propensity and increase oligomer formation was toxic to immortalised cell lines, primary cultures of rat neurons and dopaminergic neurons of *C. elegans* and *Drosophila* (Karpinar *et al.*, 2009). Similar results were obtained by Winner *et al* (2011) as expression of alpha-synuclein mutated to form conformationally trapped oligomers, which do not fibrillise, in the rat SNc induces neurodegeneration of dopaminergic neurons. Alpha-synuclein 30-110 that forms fibrils at a fast rate, in contrast, did not display toxicity (Winner *et al.*, 2011). Secondly, alpha-synuclein bimolecular fluorescence constructs, which have been shown to form oligomers (Outeiro *et al.*, 2008), were also shown to induce nigral degeneration upon injection of adeno-associated virus (AAV) particles containing the constructs into the rat SNc (Dimant *et al.*, 2013). The study of Winner *et al* raises interesting insights into the possible presence and the potential for increased toxicity of 'off-pathway' oligomers, which do not form fibrils, *in vivo.* Off-pathway species, which have also been reported to form *in vitro* (Conway *et al.*, 2001, Nasstrom *et al.*, 2011), may bypass the cellular protective mechanisms of LBs and thus result in more cellular damage. These studies suggest the formation of oligomers represent a toxic gain of function for alpha-synuclein.

The mechanism of alpha-synuclein oligomer-induced neurodegeneration may involve the disruption of a variety of cellular processes implicated in PD. The high energy demands of neurons render them particularly sensitive to mitochondrial dysfunction

(Keane *et al.*, 2011). Decreased mitochondrial complex I activity has been reported in PD brain, which was accompanied by an accumulation of alpha-synuclein in the mitochondria (Devi *et al.*, 2008) and alpha-synuclein oligomers have been shown to mediate impairment of complex I in a transgenic mouse model of PD (Chinta *et al.*, 2010). Non-pathogenic alpha-synuclein has also been shown to associate with mitochondrial membranes (Li *et al.*, 2007) and may regulate mitochondrial fusion regulation (Kamp *et al.*, 2010), although small oligomeric forms of alpha-synuclein lead to pathogenic mitochondrial fragmentation (Nakamura *et al.*, 2011). Physiological alpha-synuclein in rat brain inhibits complex I activity (Liu *et al.*, 2009) demonstrating pathology in this case may be associated with an over-active physiological function, as opposed to a toxic gain of function. Alpha-synuclein has been shown to localise to the mitochondria associated endoplasmic reticulum membrane, an interaction which is reduced for alpha-synuclein with familial PD point mutations (Guardia-Laguarta *et al.*, 2014). The effect of oligomers on this interaction was not reported but may be significant given the influence of alpha-synuclein oligomers on other aspects of mitochondrial function.

ER accumulation of oligomers has been demonstrated in a transgenic mouse overexpressing A53T alpha-synuclein and in PD brain tissue, resulting in chronic ER stress and impaired ER protein quality control (Colla *et al.*, 2012). The unfolded protein response, which is activated by ER stress, should remove misfolded proteins from the ER for degradation by the ubiquitin proteasome system but deficits in its function were observed in the A53T alpha-synuclein transgenic animals studied (Colla *et al.*, 2012). In addition, proteasomal activity can be inhibited by alpha-synuclein oligomers (Snyder *et al.*, 2003, Lindersson *et al.*, 2004, Chen *et al.*, 2006, Emmanouilidou *et al.*, 2010), suggesting an additional mechanism for failure of clearance of the oligomers from the ER.

Synaptic dysfunction is thought to occur at the early stages of PD (Schulz-Schaeffer, 2010) and oligomeric species of alpha-synuclein have been implicated in several pathways that could result in such an outcome. Firstly, alpha-synuclein oligomers bind synaptobrevin, a component of the SNARE complex required for synaptic vesicle

fusion, and prevent the formation of the SNARE complex (Choi *et al.*, 2013). *In vivo,* the result would be decreased neurotransmitter release and ensuing dysfunction. The trafficking of synaptic vesicles may also be negatively impacted by alpha-synuclein oligomers, which have been shown to decrease axonal transport by decreasing microtubule stability and impairing the interaction between kinesin and microtubules (Prots *et al.*, 2013), as well as inhibiting tubulin polymerisation (Chen *et al.*, 2007). Golgi fragmentation has also been observed as a result of oligomers formed by over-expression of alpha-synuclein in COS-7 cells (Gosavi *et al.*, 2002). Alpha-synuclein oligomers may therefore decrease the pool of synaptic vesicles available as well as inhibiting their fusion to the membrane. Pore-like oligomers could also rupture synaptic vesicles, again leading to decreased neurotransmitter release, as well as permeabilising cell membranes, which could result in Ca^{2+} influx and excitotoxicity (Danzer *et al.*, 2007).

Recent work suggests that alpha-synuclein may be able to self-propagate between neurons in the brain, in a prion-like manner. As in prion diseases, the ability of the molecule to self-interact and induce aggregation in another molecule is key, and appears to be a feature of alpha-synuclein, demonstrated by the ability of alpha-synuclein aggregates to seed inclusions *in vitro* (Luk *et al.*, 2009, Hansen *et al.*, 2011) and *in vivo* (Luk *et al.*, 2012, Masuda-Suzukake *et al.*, 2013, Rey *et al.*, 2013). Alpha-synuclein oligomers display properties, including solubility and seeding ability, which make them likely candidates for mediation of the spread of pathology. Oligomer-like preparations produced by sonicating alpha-synuclein fibrils, known as pre-formed fibrils (PFFs), have been shown to propagate through non-transgenic mouse brain (Luk *et al.*, 2012), while oligomers assembled from monomeric alpha-synuclein have also been described to have similar effects (Rey *et al.*, 2013). In another study, injection of sarkosyl-insoluble alpha-synuclein isolated from the brains of DLB patients or fibrils produced *in vitro* mediated spread of alpha-synuclein pathology in the brain of non-transgenic mice (Masuda-Suzukake *et al.*, 2013). On the other hand, HNE-induced alpha-synuclein oligomers did not succeed in seeding inclusions *in vivo* (Fagerqvist *et al.*, 2013) suggesting it is specific conformationally distinct alpha-synuclein oligomer(s) capable of spreading pathology.

Alpha-synuclein oligomers clearly affect many cellular processes, suggesting a central role in the multi-factorial causes of degeneration in PD. However, more investigation is required to fully understand the underlying processes.

1.4 Aims of thesis

The overall aim of this thesis is to investigate the role of alpha-synuclein oligomers in PD. This will be achieved by addressing three specific aims:

1) To develop a novel technique for the detection of alpha-synuclein oligomers utilising proximity ligation assay technology and to perform *in vitro* validation of the alpha-synuclein proximity ligation assay (AS-PLA).

2) To study oligomeric pathology in PD post-mortem tissue using AS-PLA.

3) To perform an *in vitro* screen to identify molecules that can prevent the formation of alpha-synuclein oligomers.

2. Materials and Methods

2.1 Cell culture

HEK293 cells were maintained in high glucose Dulbecco's modified Eagle's medium (DMEM, obtained from PAA) supplemented with 10% fetal bovine serum, 1% penicillin/streptomycin and 1% L-glutamine (all obtained from Life Technologies). BE(2)M17 cells were maintained in OptiMEM supplemented with 10% fetal bovine serum and 1% penicillin/streptomycin (all obtained from Life Technologies). All cells were grown at 37°C with 5% CO_2, except where indicated.

2.2 Transfection

HEK293 cells were seeded on poly-L-lysine coated coverslips in 24 well plates at a density of $2x10^5$ cells per well or in 6 well plates at a density of 10^6 cells per well and transfected 24 hours later. A suitable amount of DNA per well was transfected in serum-free media (OptiMEM) using Lipofectamine 2000 and Plus reagents (Life Technologies). The transfection complexes were replaced with standard HEK293 media 4 hours following transfection.

2.3 Protein extraction

2.3.1 Standard protein extraction

Cellular media was aspirated and cells were washed twice and scraped in 1x PBS then pelleted by centrifugation for 10 minutes at 300 x g at 4°C. The pellet was snap frozen then resuspended and lysed in RIPA buffer (1% NP-40, 0.1% sodium dodecyl sulphate (SDS), 0.5% sodium deoxycholate, 150mM NaCl, 50mM Tris pH 8) with 1 protease inhibitor cocktail tablet (Roche) added per 50ml, followed by sonication. The lysate was centrifuged at 650 x g for 10 minutes at 4°C and the supernatant was retained and stored at -80°C.

2.3.2 Native protein extraction

Cellular media was aspirated and cells were washed twice and scraped in 1x PBS then pelleted by centrifugation for 10 minutes at 300 x g at 4°C. The pellet was snap frozen then resuspended in 35 µL solubilization buffer (50mM NaCl, 50mM imidazole, 2mM 6-aminohexanoic acid, 1mM EDTA, pH 7), and solubilized with 8 µL digitonin (20% stock in water). Following 15 minutes centrifugation at 100,000 x g, the supernatant was retained and stored at -80°C (Wittig and Schagger, 2005).

2.3.3 Alpha-synuclein sequential extraction

Sequential extraction was performed as previously described with minor modifications (Tofaris *et al.*, 2003). Briefly, 100mg of tissue was homogenised in 3 volumes of TBS+ (50mM Tris HCL pH 7.4, 175mM NaCl, 5mM EDTA, plus complete protease inhibitor tablet [Roche]). The homogenate was centrifuged for 5 minutes at 1,000 x g at 4°C then the supernatant was ultracentrifuged for 30 minutes at 120,000 x g at 4°C. The resulting supernatant was the TBS+ soluble fraction. The pellet was rinsed twice in TBS+ then resuspended in TBS+ with 1% Triton X-100 and centrifuged for 20 minutes at 120,000 x g at 4°C. The resulting supernatant was the Triton soluble fraction. The pellet was resuspended in RIPA buffer (50mM Tris-HCl pH 7.4, 175mM NaCl, 5mM EDTA, 1% NP40, 0.5% sodium deoxycholate, 0.1% SDS plus complete protease inhibitor tablet [Roche]) and centrifuged for 20 minutes at 120,000 x g at 4°C. The pellet was washed 3 times with TBS+, then resuspended in 8M urea/5% SDS for the urea soluble fraction.

2.3.4 Protein quantification

Protein concentration in cell lysates and tissue homogenates was quantified using the bicinchoninic acid (BCA) assay. Bovine serum albumin (BSA) solutions of increasing concentrations ranging from 0-2000 µg/ml were used as protein standards. Samples were diluted in order to fall into this concentration range. 10 µl of samples were added, in triplicate, to 100 µl of a 1:50 solution of copper sulphate: BCA (Sigma) and incubated at 37 °C for 30 minutes. Following incubation, absorbance at 562 nm was measured

using a Synergy HT microplate reader (Biotek).

2.4 Protein separation and western blotting

10 µg of protein from cell lysates and tissue homogenates or 0.1 µg of recombinant protein was suspended in Laemmli buffer (60 mM Tris pH 6.8, 2% SDS, 10% glycerol, 5% β-mercaptoethanol, 0.01% bromophenol blue) and heated to 95°C for 10 minutes for sodium dodecyl sulphate polyacrylamide gel electrophoresis (SDS-PAGE), or suspended in SDS-free sample buffer (60 mM Tris pH 6.8, 10% glycerol, 0.01% bromophenol blue) for non-denaturing PAGE. Proteins were separated, alongside Spectra Multicolor Broad Range Protein Ladder (Thermo Scientific) to determine target protein weight, on 10% SDS-polyacrylamide or non-denaturing polyacrylamide gels, except in Figures 1.11 and 1.14B where proteins were separated on a pre-cast BioRad Criterion TGX 4-15% gradient gel. Following transfer of proteins to polyvinylidene fluoride (PVDF) membranes (Millipore) and blocking in 3% (w/v) powdered skim milk in 1x Tris-buffered saline/0.1% Tween 20 (TBS-T), membranes were incubated overnight at 4 °C in primary antibody (Table 2.1) diluted in 1% (w/v) powdered skim milk in TBS-T. Following washing 3 times in TBS-T, the membrane was incubated with horseradish peroxidase-conjugated secondary antibody (Bio-Rad) diluted 1:5000 in 1% (w/v) powdered skim milk in TBS-T for 1 hour at room temperature. The membrane was washed again in TBS-T and the signal visualised with ECL reagent (Millipore) and exposure in the BioRad GelDoc.

Antibody	Host species	Dilution	Supplier and catalogue number
Alpha-synuclein syn211	Mouse (monoclonal)	WB - 1:2000 IF - 1:1000 IHC - 1:1000	Abcam, ab80627
A-beta 4G8	Mouse (monoclonal)	WB - 1:500 IF - 1:500 IHC - 1:500	Covance, SIG-39200-1000
Phosphorylated tau AT8	Mouse (monoclonal)	IHC - 1:200	Fisher, MN1020
FKBP12	Rabbit (monoclonal)	IF - 1:50	Stratech (Epitomics), 3201-S
mTOR	Mouse (monoclonal)	IF - 1:50	Cell Signaling Technology, 4517

Table 2.1. Antibodies used for western blotting (WB), immunofluorescence (IF) and immunohistochemistry (IHC).

2.5 Immunofluorescence

Cells cultured in 24-well plates on poly-L-lysine coated glass coverslips were fixed in 4% paraformaldehyde for 15 minutes at room temperature, washed with PBS then permeabilized with IF block solution (0.1% Triton X-100, 10% normal goat serum in TBS) for 1 hour at room temperature. Coverslips were washed in TBS + 0.1% Triton X-100 and primary antibodies (Table 2.1) were diluted in IF block solution and incubated overnight at 4°C with gentle shaking. Cells were then washed 4 times in IF wash solution (TBS + 0.1% Triton X-100) and AlexaFluor IgG secondary antibody (goat anti-mouse Alexa 488, 594 or 647; goat anti-rabbit Alexa 488, all at 1:500, Invitrogen) was applied for 1 hour at room temperature with gentle rocking and protected from light. Cells were counterstained using the fluorescent nuclear stain diluted in 4,6-diamidino-2-phenylindole (DAPI) diluted 1:2000. Coverslips were mounted using FluorSave (Merck) and imaged using fluorescent microscopy (Nikon Eclipse TE200-U).

2.6 Immunohistochemistry

Paraffin embedded tissue was dewaxed and rehydrated by immersion in the following: xylenes for 2 minutes, histoclear for 2 minutes, 100% ethanol for 2 minutes, 95% ethanol for 2x2 minutes, 70% ethanol for 2 minutes and dH2O for 3x2 minutes. Tissue was incubated in 10% H_2O_2 in PBS for 1 hour at room temperature in the dark to quench endogenous peroxidases. Antigens were retrieved by microwave heating with citrate buffer, pH 6 with 10 minutes total heating, or where indicated by incubating the sections with 80% formic acid for 5 minutes. The sections were washed in running tap water for 5 minutes following antigen retrieval. Tissue was then blocked in 10% normal goat serum in TBS + 0.1% Triton-X100 for 1 hour at room temperature. Primary antibodies (Table 2.1) were incubated with the tissue overnight at 4°C, followed by washing and incubation with biotinylated goat anti-mouse IgG secondary antibody (1:200, Jackson Immunoresearch) for 1 hour at room temperature. After washing, VectaStain ABC reagent (Vector Labs) was added for 1 hour at room temperature, then sections were incubated with 3,3′-diaminobenzidine (DAB, Sigma) and H_2O_2 for

3 minutes. The tissue sections were then counterstained using haematoxylin (Vector Labs) and dehydrated in graded alcohols and xylenes (dH_2O for 3x2 minutes, 70% ethanol for 2 minutes, 95% ethanol for 2x2 minutes, 100% ethanol for 2 minutes and xylenes for 2 minutes) before mounting with DPX mounting reagent.

2.7 Alpha-synuclein proximity ligation assay

Alpha-synuclein proximity ligation assay experiments were carried out using Duolink kits supplied by Olink Bioscience according to the manufacturer's instructions.

2.7.1 Generation of AS-PLA probes

We chose an alpha-synuclein antibody for the AS-PLA probes that has previously been shown to display blocking activity (syn211 (El-Agnaf *et al.*, 2006)). The probes were prepared using the Duolink Probemaker kit by incubating 20µg of antibody (mouse anti-alpha-synuclein 211, 1 mg/ml, no BSA or azide, Abcam) with the Probemaker activated oligonucleotide (Minus or Plus) and conjugation buffer and leaving overnight at room temperature. The conjugates were incubated with Probemaker stop solution for 30 minutes at room temperature, then suspended in Probemaker storage buffer and stored at 4 °C.

2.7.2 Fluorescent AS-PLA

Cells in culture grown on poly-L-lysine coated glass coverslips were fixed in 4% paraformaldehyde in preparation for fluorescent AS-PLA. Following washing with PBS, the coverslips were incubated in a humidity chamber in Duolink block solution at 37 °C for 1 hour, followed by the probes diluted at 1:750 in Duolink PLA diluent for 1 hour at 37 °C, then overnight at 4 °C. Samples were washed 5 times in TBS + 0.05% Tween20 then incubated with Duolink ligation solutions and ligase for 1 hour at 37°C. Following washing 5 times in TBS + 0.05% Tween20, the samples were incubated with Duolink amplification reagents, which also included the fluorescently tagged detection oligonucleotide, and polymerase for 2.5 hours at 37 °C. Samples were then washed 5 times in the dark with wash buffer B (0.2 M Tris, 0.1 M NaCl) and counterstained and

mounted as for immunofluorescence. The number of AS-PLA puncta and the area of AS-PLA signal was analysed in ImageJ using the Analyze Particles function.

2.7.3 Brightfield AS-PLA

Paraffin embedded tissue was dewaxed and rehydrated by immersion in the following: xylenes for 2 minutes, histoclear for 2 minutes, 100% ethanol for 2 minutes, 95% ethanol for 2x2 minutes, 70% ethanol for 2 minutes and dH2O for 3x2 minutes. Tissue was incubated in 10% H_2O_2 in PBS for 1 hour at room temperature in the dark to quench endogenous peroxidases. Antigens were retrieved by microwave heating with citrate buffer, pH6 with 10 minutes total heating, or where indicated by incubating the sections with 80% formic acid for 5 minutes. The sections were washed in running tap water for 5 minutes following antigen retrieval. Following incubation in Duolink block solution at 37 °C for 1 hour, the sections were incubated with the AS-PLA probes diluted in Duolink PLA diluent (1:100 for human tissue, 1:500 for mouse tissue) for 1 hour at 37°C, then overnight at 4°C. Following 5 washes in TBS + 0.05% Tween20, samples were incubated with Duolink ligation solutions and ligase for 1 hour at 37°C, before washing 5 times in TBS + 0.05% Tween20 and incubation with Duolink amplification reagents and polymerase for 2.5 hours at 37°C. Samples were washed 5 times in TBS + 0.05% Tween20 and then incubated with a Duolink detection solution, which included a horseradish peroxidase (HRP) tagged detection oligonucleotide, for 1 hour at room temperature followed by washing 5 times in TBS + 0.05% Tween20 and incubation with a Duolink NovaRED substrate solution, which contained H_2O_2, for 20 minutes at room temperature. The samples were washed 5 times with MQ H_2O following this step. The tissue sections were then counterstained using haematoxylin and dehydrated in graded alcohols and xylene, (dH_2O for 3x2 minutes, 70% ethanol for 2 minutes, 95% ethanol for 2x2 minutes, 100% ethanol for 2 minutes and xylenes for 2 minutes), before mounting with DPX mounting reagent. Brightfield AS-PLA signal was analysed semi-quantitatively, as described in section 2.15.

2.8 Alpha-synuclein bimolecular fluorescence complementation assay

Professor Tiago Outeiro (University of Göttingen, Germany) kindly provided the alpha-synuclein bimolecular fluorescence complementation (BiFC) constructs. For assays in 24 well plates, 0.25 µg of each construct per well was transfected into HEK293 cells and 1 µg of each construct per well was used for 6 well plates, according to the protocol described in section 2.2. Following incubation at 37°C for 4 hours after transfection, the cells were transferred to 30°C in 25mM HEPES to allow the GFP chromophore to mature. Cells were imaged, fixed for immunofluorescence and AS-PLA or harvested for western blotting 48 hours following transfection.

2.9 Generation of FKBP-alpha-synuclein and FRB-alpha-synuclein constructs

2.9.1 DNA mini-preps

E. coli colonies containing the desired plasmid were inoculated into 1.5 ml lysogeny broth per sample and incubated at 37°C with shaking at 225 rpm overnight. The next day, cultures were centrifuged at 1,900 x g for 10 minutes, the supernatant aspirated and the pellet resupended in 70 µl STET resuspension buffer (8% sucrose, 5% Triton X-100, 50 mM EDTA and 50 mM Tris.Cl at pH8). The cells were lysed with 200 µl alkaline SDS buffer (1% SDS, 0.2 M NaOH) and neutralised with 150 µl 7.5 M ammonium acetate. After 5 minutes incubation on ice, the samples were centrifuged at 12,500 x g for 20 minutes at 4°C and the supernatant was transferred to a clean tube. 250 µl isopropanol was added and the DNA was pelleted by centrifugation at 7,500 x g for 8 minutes. The supernatant was aspirated and 200 µl 70% ethanol was added followed by centrifugation at 7,500 x g for 8 minutes, which washed the DNA pellet. The DNA pellet was left to air dry for 15 minutes and was then resuspended in 50 µl TE buffer containing 5 µg/ml RNase A.

2.9.2 DNA maxi-preps

To obtain larger amounts of plasmid DNA, 1.5 ml lysogeny broth starter cultures were prepared by incubating cultures at 37°C with shaking at 225 rpm for 8 hours. The resulting cultures were diluted in 250 ml lysogeny broth and grown overnight at 37°C

with shaking at 225 rpm. The DNA was extracted using a QIAGEN plasmid Maxiprep Column Kit. The kit was used according to the manufacturer's protocol with the following exception: to avoid a second centrifugation step to remove excess debris, the supernatant of centrifuged neutralised samples was filtered through a double layer of Kimwipes.

2.9.3 Electrocompetent cells

1.5 ml bacterial cultures were grown overnight at 37°C with shaking at 225 rpm then diluted in 100 ml LB. The diluted cultures were grown until the optical density at 600 nm (OD600) reached 0.3 - 0.5, when they were incubated on ice for 20-40 minutes. The bacteria were pelleted by centrifugation at 4,500 x g for 15 minutes at 4°C and washed three times with 100 ml ice-cold autoclaved 10% glycerol by centrifugation at 6,750 x g for 15 minutes at 4°C. After the final wash the supernatant was discarded and the pellet was resuspended in the residual 10% glycerol from the last wash step. The cells were divided into 50 µl aliquots and snap-frozen on dry ice then stored at - 80°C.

2.9.4 Electroporation of electrocompetent cells

DNA transfer to bacteria was achieved by electroporation using a Gene Pulser System (Bio-Rad). 50 µl of electrocompetent cells were electroporated using the following settings:

Voltage (V): 1800

Capacitance (µF): 25

Resistance (Ω): 200

The electroporated cells were incubated with 450 µl SOC medium (Invitrogen) for 1 hour at 37°C with shaking at 225 rpm and then plated on lysogeny broth agar plates supplemented with ampicillin.

2.9.5 Preparation of long PCR fragments for subcloning

Long DNA fragments for subcloning were prepared by PCR amplification. Primers

contained a short (18-26 bp) sequence complementary to the target DNA fragment to be amplified and a long (30-72 bp) sequence containing restriction enzyme sites to allow for various combinations of open reading frames to be subcloned. Primer sequences are listed below.

Primer name	Forward primer	Reverse primer
SNCA long	TTTTTTCTTAAGGGCGCGCCCTC-GAGCGCCACCATGGATGTAT-TCATGAAAGGAC	TTTTTTCCGCGGACACCAGTAC-CAGCCTTAGGCTTCAGGTTCG-TAGTCTTG
FKBP long	TTTTTTCTTAAGGTTGAGGGTG-GTGGTACTGGTGTTGCCACCAT-GGGCGCCGGCGGCGCCGGCG-GCGGCGCCGGAGTGCAGGTG-GAAACC	TTTTTTCCGCGGTTAACTCGAG-CCGCCGGCGCCGCCGGCGC-CGCCGCCAGGCGCGCCTTC-CAGTTTTAGAAGCTCCACATC
FRB long	TTTTTTCTTAAGGTTGAGGGTG-GTGGTACTGGTGTTGCCACCAT-GGGCGCCGGCGGCGCCGGCG-GCGGCGCCATGTGGCATGAAGG-CCTGG	TTTTTTCCGCGGTTAACTCGAGC-CGCCGGCGCCGCCGGCGCCGC-CGCCAGGCGCGCCCTTTGAGAT-TCGTCGGAACAC

Table 2.2. Sequences of long primers used to generate PCR products for subcloning.

FKBP and FRB were obtained from plasmids kindly provided by Professor Carolyn Bertozzi (University of California, Berkeley; Addgene plasmids 20211 and 20228) (Czlapinski *et al.*, 2008) and alpha-synuclein from the BiFC constructs.

PCR master mixes were prepared for each primer pair using a BIO-X-ACT Long DNA polymerase kit (Bioline) according to the following protocol for each 60 µl PCR reaction:

	Volume (µl)
10x buffer	6
50mM $MgCl_2$	2.1
8mM dNTPs	3.74
Template DNA	0.1
1 µM primer mix	12
Bio-X-ACT poly-merase	0.6
MQ H_2O	35.46

Table 2.3. PCR components for long PCR reactions.

The samples were run on a DNA Engine Tetrad 2 Peltier Thermal Cycler (Bio-Rad) using the PCR programme below.

1. 94 °C for 10 min
2. 94 °C for 10 sec
3. 55 °C for 30 sec
4. 68 °C for 2.5 min
5. Go to step 2. Repeat for 34 cycles
6. 68 °C for 5 min
7. 15 °C forever

Following DNA amplification, 10 µl PCR product was added to 2 µl 6x loading dye and was separated by gel electrophoresis on a 1% agarose gel containing ethidium bromide (1 g agarose in 100 ml 1X TBE buffer, 6 µl ethidium bromide) alongside a Gene Ruler 1 kb Plus DNA ladder (Thermo Scientific) at 95 mA for 35 minutes.

PCR products from three wells (60 µl each) were pooled and purified using a Qiagen PCR Purification Kit following the manufacturer's instructions. Each sample was eluted in 20 µl elution buffer and 1 µl of pooled purified PCR product was then re-run on a 1% agarose gel. The product was then ligated into pGEM-T (Promega) by incubating overnight at 16 °C with the following mixture:

	Volume (µl)
PCR product	3.5
pGEM-T	0.5
2x ligation buffer	5
Ligase	1

Table 2.4. Components for ligation reactions.

2.9.6 Standard PCR amplification

PCR amplification was utilised to confirm the formation of new junctions during the cloning process. Primer sequences are shown below.

Primer name	Forward primer	Reverse primer	Product size (bp)
T7 and pUC/ M13	TAATACGACTCA CTATAGGG	CAGGAAACAGCTATGAC	SNCA: 695 FKBP: 660 FRB: 628
FKBP pcD-NA4	GCTCGTTTAGTG AACCGTCAG	GATGGCTGGCA ACTAGAAGG	773
FRB pcDNA4 whole	GCTCGTTTAGTG AACCGTCAG	ACAATGCGATGC AATTTCC	658
FRB pcDNA4 5' junction	GCTCGTTTAGTG AACCGTCAG	GGCCCCGTTCC ATCATAG	268
FRB pcDNA4 3' junction	TGTCAAGGACC TCCTCCAAG	ACAATGCGATG CAATTTCC	244
SNCA pcD-NA4	ATCCACGCTGTT TTGACCTC	CAACAGATGGC TGGCAACTA	694
FKBP-SNCA whole	GCTCGTTTAGT GAACCGTCAG	CAACAGATGGCT GGCAACTA	1119
FKBP-SNCA 5' junction	GCTCGTTTAGT GAACCGTCAG	ACCACTCCCTCC TTGGTTTT	697
FKBP-SNCA 3' junction	GGGTCAGAGAG CCAAACTGA	ACCACTCCCTCC TTGGTTTT	311
FRB-SNCA whole	GCTCGTTTAGT GAACCGTCAG	CAACAGATGGCT GGCAACTA	1038
FRB-SNCA 5' junction	GCTCGTTTAGT GAACCGTCAG	ACCACTCCCTCC TTGGTTTT	616
FRB-SNCA 3' junction	TGTCAAGGACC TCCTCCAAG	ACCACTCCCTCC TTGGTTTT	257

Table 2.5. Primer sequences targeting newly formed junctions following subcloning steps.

PCR master mixes were prepared for each primer pair using an AmpliTaq Gold DNA Polymerase kit (Invitrogen) for each 20 µl PCR reaction according to the following:

	Volume (µl)
10x buffer	2
25mM $MgCl_2$	2
8mM dNTPs	0.5
Taq polymerase	0.1
1 µM primer mix	9.9
MQ H_2O	5.5

Table 2.6. Components of a standard PCR reaction.

For each well of a 96-well plate, 20 µl of mastermix and 0.6 µl of template DNA were added. Samples were run on a DNA Engine Tetrad 2 Peltier Thermal Cycler (Biorad) using the PCR programme below.

1. 95 °C for 10 min
2. 95 °C for 20 sec
3. 58 °C for 30 sec
4. 72 °C for 40 sec
5. Go to step 2. Repeat for 29 cycles
6. 72 °C for 5 min
7. 15 °C forever

Following DNA amplification, 10 µl PCR product was separated by gel electrophoresis on a 1% agarose gel containing ethidium bromide (1 g agarose in 100 ml 1X TBE buffer, 6 µl ethidium bromide) alongside a Gene Ruler 1 kb Plus DNA ladder (Thermo Scientific) at 95 mA for 35 minutes.

2.9.7 Restriction enzyme digestion

Restriction enzyme digests of the constructs were carried out to confirm the presence of the desired components. Digests were set up using as follows for each 15 µl reaction:

	Volume (µl)
10x buffer	1.5
20x BSA	0.75
Restriction enzyme	0.375
DNA	1
MQ H_2O	11.375

Table 2.7. Components for restriction enzyme digestions.

All solutions were bought from New England Biolabs (NEB) and the appropriate buffer mix was chosen for each enzyme reaction. The samples were incubated for 3 hours at 37 °C. Restriction enzyme products were analysed using gel electrophoresis on 1%

agarose TBE gels.

2.9.8 Sequencing

Following ligation into the pGEM-T cloning vector, the coding and flanking regions of FKBP, FRB and alpha-synuclein were sequenced to confirm that no mutations had been introduced in the PCR cloning process. The region to be sequenced was amplified by PCR using the BIO-X-ACT Long DNA polymerase kit (Bioline) and primers targeting the T7 promoter (forward) and pUC/M13 site (reverse) of pGEM-T. PCR master mixes were prepared for each 60 µl reaction as below:

	Volume (µl)
10x buffer	6
50mM $MgCl_2$	2.1
8mM dNTPs	3.74
Template DNA	0.1
1 µM primer mix	12
Bio-X-ACT poly-merase	0.6
MQ H_2O	35.46

Table 2.8. Components of PCR to amplify regions for sequencing.

Samples were amplified using a DNA Engine Tetrad 2 Peltier Thermal Cycler (Biorad) set to the programme below:

1. 95 °C for 15 min
2. 95 °C for 30 sec
3. 54 °C for 30 sec
4. 68 °C for 2 min
5. Go to step 2. Repeat for 34 cycles
6. 68 °C for 5 min
7. 15 °C forever.

To confirm successful amplification, 10 µl of each PCR product was run on a 1% agarose gel. Primers and dNTPs were removed using an ExoSAP reaction, which was

added directly to each 50 µl PCR product sample:

	Volume (µl)
10x SAP buffer	2.5
SAP enzyme	2.5
EXO I	0.25
MQ H_2O	2.25

Table 2.9. Components for ExoSAP reactions.

The samples were incubated at 37°C for 30 minutes then 80°C for 15 minutes. The sequencing reaction mix was then assembled:

	Volume (µl)
BigDye	0.5
5x sequencing buffer	1.75
10 µM primer mix	1
Template DNA	5
MQ H_2O	1.75

Table 2.10. Components for BigDye sequencing reactions.

Samples were then run on a DNA Engine Tetrad 2 Peltier Thermal Cycler (Biorad) using the PCR programme below.

1. 96 °C for 1 min
2. 96 °C for 10 sec
3. 50 °C for 5 sec
4. 60 °C for 4 min
5. Go to step 2. Repeat for 29 cycles
6. 15 °C forever

Samples were precipitated by adding 2 µl of each of 125 mM EDTA and 3 M NaAc to each well and washed by adding 50 µl 100% ethanol followed by a 30 minute spin (3000 x g) at 4°C and then 70% ethanol followed by a 15 minute spin (1650 x g) at 4 °C. Samples were left to dry and sequencing was carried out on a Applied Biosystems 3700 DNA Analyzer sequencing platform (Department of Zoology, University of Oxford).

Sequence results were analysed using the Vector NTI software (Life Technologies).

2.9.9 Preparative restriction enzyme digestion

To subclone the inserts generated by long armed PCR from pGEM-T into the mammalian expression vector pcDNA4/TO/myc-HisB and to produce the fusion constructs of FKBP or FRB and alpha-synuclein, preparative restriction enzyme digestions were undertaken. 1 µg of the plasmid to act as the vector and 3 µg of the plasmid containing the insert were both digested with 1 µl of each of the relevant restriction enzymes in a total volume of 50 µl at 37 °C for 3 hours.

Following digestion, the vector preparation was treated with 1.5 µl of calf intestinal alkaline phosphatase to prevent re-annealing and incubated for 10 minutes at 37 °C, 10 minutes at 50 °C and 5 minutes at 80 °C.

The products of each digestion were separated by gel electrophoresis on a 1% agarose TAE gel containing ethidium bromide (1 g agarose in 100 ml 1X TAE buffer, 6 µl ethidium bromide) alongside a Gene Ruler 1 kb Plus DNA ladder (Thermo Scientific) at 85 mA for 1 hour. The required bands were identified by UV exposure, cut out and the DNA purified from the gel using the GeneClean kit (MP Biomedicals) according to the manufacturer's instructions. The purified DNA was checked by running 1 µl on a 1% agarose TBE gel and the vector and insert were ligated overnight at 16 °C using the pGEM-T ligation reagents (Promega) according to the protocol below:

	Volume (µl)
Vector	1
Insert	3
2x ligation buffer	5
Ligase	1

Table 2.11. Components for ligation reactions to complete subcloning.

2.10 FKBP-FRB-rapamycin assay

25 ng each of FKBP-alpha-synuclein and FRB-alpha-synuclein constructs were transfected into HEK293 cells, as described in section 2.2. After 4 hours at 37°C following transfection, the transfection reagents were replaced with normal HEK293 media supplemented with 400nM rapamycin for the + rapamycin condition. Cells were fixed for AS-PLA analysis 1 hour following transfection.

2.11 Preparation and analysis of alpha-synuclein oligomers, A-beta oligomers and alpha-synuclein fibrils

Oligomers were produced as previously described (Nasstrom *et al.*, 2011) by incubating recombinant human alpha-synuclein (r-Peptide) or A-beta (Tocris Bioscience) at 1 mg/ml (70 μM and 220 μM, respectively) with a 30:1 molar excess of the aldehyde 4-hydroxy-2-nonenal (HNE) at 37°C for 18 hours. Following incubation, unbound aldehyde was removed with an Amicon 3 kDa cut-off ultra-centrifugal unit (Millipore).

To produce alpha-synuclein fibrils, 2 mg/ml (140 μM) recombinant human alpha-synuclein (r-Peptide) in assembly buffer (50 mM Tris pH 7.4, 100 mM NaCl) was shaken at 37 °C with constant agitation (1,000 rpm) for 5 days.

To attempt to purify alpha-synuclein fibrils, ultracentrifugation and filtration methods were used. Ultracentrifugation was undertaken as previously described (Volpicelli-Daley *et al.*, 2014). The fibril solution was ultracentrifuged at 100,000 x g for 1 hour at 20 °C. The supernatant was removed and the pellet containing the fibrils was resuspended in 1x PBS. For filtration, the solution was diluted 20-fold before centrifugation at 14,000 x g for 10 minutes at 4 °C in an equilibrated Amicon 100 kDa cut-off ultra-centrifugal unit (Millipore). The eluate was removed and the remaining solution centrifuged at 14,000 x g for 10 minutes at 4 °C twice more. The remaining purified solution was retained.

Western blot analysis was carried out as described in section 2.4. For immunofluorescence analysis, 0.5 µg of protein was spotted onto poly-D-lysine coated coverslips and fixed for 30 minutes at room temperature in 4% paraformaldehyde. Immunofluorescence and fluorescent AS-PLA protocols were then carried out as described in section 2.6 and 2.7.2, respectively.

2.12 Electron microscopy

Electron microscopy imaging was performed by Dr Errin Johnson (Dunn School of Pathology, University of Oxford). 10 µl of 50 µM protein sample was applied to carbon formvar copper grids, which had been glow discharged immediately prior to use, and incubated for 2 minutes. Grids were blotted using filter paper and transferred to a droplet of 2% aqueous uranyl acetate for 60 seconds, then blotted and transferred to a droplet of filtered milli-Q water for 60 seconds, blotted and dried. Grids were imaged in a FEI Tecnai 12 transmission electron microscope operated at 120 kV and digital images were captured using a Gatan US1000 ccd camera.

2.13 Human tissue

Tissue samples from Parkinson's patients and controls and associated clinical and neuropathological data were supplied by the Parkinson's UK Tissue Bank, funded by Parkinson's UK, a charity registered in England and Wales (258197) and in Scotland (SC037554). Sections from eight patients and eight age and gender matched controls were paraffin embedded and supplied at 5 µm thick. We studied sections at the level of the third oculomotor nerve in the midbrain, of the inferior olive in the medulla and the anterior cingulate cortex.

Tissue samples from patients with dementia with Lewy bodies, multiple system atrophy, progressive supranuclear palsy and Alzheimer's disease were supplied by the Oxford Brain Bank, supported by the Medical Research Council (MRC), Brains for Dementia Research (BDR) and the NIHR Oxford Biomedical Research Centre. The regions studied were: anterior cingulate cortex for dementia with Lewy bodies sections,

substantia nigra for multiple system atrophy and progressive supranuclear palsy sections and hippocampus for Alzheimer's disease sections. Sections from 2 patients per disease were paraffin embedded and supplied at 5 µm thick.

2.14 Mouse tissue

Mice were deeply anaesthetised by intraperitoneal injection of 140mg/kg pentobarbitone and perfused with 30 ml 0.2 M phosphate buffer followed by 35 ml 4% paraformaldehyde (PFA) in 2 M phosphate buffer. Brains were removed and placed in 4% PFA at 4 °C for 1 week to fix fully. Brains were washed in 1X PBS before transfer to 70% ethanol.

Fixed brains were paraffin-embedded using a Leica tissue processing machine. The following steps were taken during the embedding process under vacuum conditions: 70% ethanol for 45 minutes, 90% ethanol for 45 minutes, 100% ethanol for 30 minutes, 100% ethanol for 3x45 minutes, histoclear (Fisher) for 3x30 minutes, molten embedding wax (Fisher) at 60 - 65 °C for 30 minutes, molten embedding wax (Fisher) at 60 - 65 °C for 2x45 minutes. Paraffin blocks were microtome sectioned at 5 µm and mounted on slides by Richard Stillion (Dunn School of Pathology, University of Oxford).

2.15 Neuropathological analysis

2.15.1 Human tissue

For the quantification of AS-PLA staining, two independent assessors (RFR and Dr Javier Alegre-Abarrategui) analysed the blinded slides at 20x magnification. Pre-defined neuroanatomical areas in each region were studied.

Area	1	2	3	4	5	6
Medulla	Pyramid (corticospinal tract)	Inferior olivary nucleus	Raphe	Reticular formation	Intermediate reticular zone	Remaining tegmentum
Midbrain	Crus cerebri	Substantia nigra	Red nucleus	Reticular formation	Superior colliculi	Peri-aqueductal grey
Cingulate gyrus	Cingulate cortex	White matter	Corpus callosum			

Table 2.12. Neuroanatomical regions included in AS-PLA analysis of human tissue.

Within each area, the heaviness of staining in blinded sections was scored semi-quantitatively on a scale between 0 and 5 against pre-defined scoring standard plates (Figure 4.10) and the highest diffuse score that filled a whole field of view in each area was recorded. The average of two assessors' scores was taken; no significant difference between the assessors' scores was found (Mann-Whitney test, $p>0.05$). The number of Parkinson's disease lesions stained by AS-PLA was counted. Sections stained using alpha-synuclein immunohistochemistry were also analysed and the number of Parkinson's disease lesions stained was counted.

2.15.2 Mouse tissue

Sagittal sections of brain tissue from *SNCA*-OVX, hWT *SNCA* and *SNCA*-KO mice aged 3 months or 24 months were stained using AS-PLA. The neuroanatomical regions analysed were: substantia nigra, pons, striatum, hippocampus and cortex. The blinded slides were analysed at 20x magnification. Within each area, the heaviness of staining was scored semi -quantitatively, as for the human tissue, on a scale between 0 and 5 against pre-defined scoring standard plates (Figure 4.10) and the highest diffuse score that filled a whole field of view in each area was recorded.

2.16 Proteinase K assay

Paraffin embedded sections were treated as for immunohistochemistry or AS-PLA as described in section 2.7 and section 2.8, respectively, except following antigen

retrieval, sections were treated with 50 µg/ml proteinase K in 10mM Tris HCl pH 7.8, 100mM NaCl and 0.1% NP-40 (all from Sigma) at 37°C for the indicated times and then washed in tap water for 5 minutes.

2.17 BiFC miniaturisation for compound screen

In order to allow screening of compounds for the prevention of alpha-synuclein oligomerisation, the BiFC assay was miniaturised for use in 96 well plates.

2.17.1 Optimisation

For transfection in 96 well plates HEK293 cells were seeded and transfected in the same step, in contrast to the general transfection protocol described in section 2.2. Two transfection protocols, LF and JAA, were tested. The transfection complexes were prepared with serum free media (OptiMEM), Lipofectamine 2000 and Plus reagent (all from Life Technologies). 1500 ng total DNA (i.e. 750 ng of each BiFC construct) was utilised for each well. HEK293 cells were prepared for seeding in complete media. For the protocol LF, the transfection complexes were plated then HEK293 cells were directly added to the wells. For JAA, the cells to be seeded, still in suspension, and the transfection complexes were mixed and plated together. For both protocols, no change of media was required and the cells were maintained at 37 °C for 4 hours after transfection, then transferred to 30°C in 25mM HEPES to allow the GFP chromophore to mature.

2.17.2 Final protocol

For the screen, we utilised Venus BiFC constructs (kindly provided by Professor Tiago Outeiro, University of Göttingen, Germany) as opposed to the eGFP BiFC constructs described in earlier sections. 1500 ng total DNA (i.e. 750 ng of each BiFC construct) was utilised for each well. HEK293 cells, at a density of 50,000 cells per well, were prepared for seeding in complete media. The cells to be seeded, still in suspension, and the transfection complexes were mixed and plated together. No change of media was required and the cells were maintained at 37 °C until analysis.

2.17.3 Positive control

As a positive control for decreased BiFC fluorescence, the Venus BiFC constructs were transfected at a ratio of 99:1 (VN:VC) as opposed to 1:1. The transfection protocol was carried out as described in section 2.17.2 and the total amount of DNA transfected was the same, but 1485 ng of VN and 15 ng of VC were transfected for a ratio of 99:1.

2.18 Analysis of BiFC fluorescence

One image per well at 4x magnification was acquired using the EVOS FL Auto automated fluorescent microscope (Life Technologies). The resulting images of Venus BiFC fluorescence were analysed using Cell Profiler software (Carpenter *et al.*, 2006), which quantified the number of fluorescent cells and their fluorescence intensity.

2.19 Compound treatment

288 compounds were provided as 10 mM stocks dissolved in dimethyl sulfoxide (DMSO) by Dr Angela Russell (Departments of Chemistry and Pharmacology, University of Oxford). For the initial screen, compounds were prepared at 20 μM in 50 μl HEK293 media and were added to the plates before the cell and transfection mixture. For untreated wells, the same volume of HEK293 media was added and for DMSO control wells, 0.1% DMSO in 50 μl HEK293 media was used. For dose response curve analysis, the same approach was utilised but 50 μM compound was prepared initially and the other concentrations were prepared by further dilution of the 50 μM stock in HEK293 media. The transfection protocol was undertaken as described in section 2.17.2.

3. Validation of the alpha-synuclein proximity ligation assay

3.1 Introduction

The aetiology of PD is not fully understood, and although increasing evidence has indicated a key role for alpha-synuclein oligomers in the pathogenesis of PD, the mechanism by which they cause disease is not known. One of the limiting factors contributing to our lack of understanding of how alpha-synuclein oligomers are involved in PD is the absence of a technique for their detection *in situ*.

3.1.1 Detecting alpha-synuclein oligomers

Previously, approaches for the detection of alpha-synuclein oligomers have involved the development of antibodies specific to oligomeric conformations of alpha-synuclein. However, oligomers formed *in vitro* have been used as the immunogen and therefore the variety of species detected by such antibodies may be limited. Furthermore, several of these antibodies also detect oligomers composed of the aggregated molecules of other amyloidogenic proteins, including A-beta, prion protein and lysozyme (Kayed *et al.*, 2003, Zhang *et al.*, 2011). The A11 antibody, for example, binds the beta-sheet edge in pre-fibrillar oligomers, suggesting this is a common motif in pathogenic oligomers (Kayed *et al.*, 2003). A shortcoming of the broad specificity of A11 is that it results in the detection of non-pathogenic proteins that contain the beta-sheet edge motif, such as IgG (Yoshiike *et al.*, 2008).

Conformational antibodies specific to alpha-synuclein oligomers have been developed and used for enzyme linked immunosorbent assays (ELISAs). For example, an ELISA utilising the FILA-1 antibody demonstrated higher levels of alpha-synuclein oligomers in the brains of patients with DLB compared with control cases or patients with AD (Paleologou *et al.*, 2009), while an antibody raised against 4-hydroxy-2-nonenal (HNE)-induced alpha-synuclein oligomers, mAb38F, showed increased levels of oligomers in

aged Thy1-*SNCA*[A30P] transgenic mice (Fagerqvist *et al.*, 2013). A sandwich ELISA, using the same blocking antibody against alpha-synuclein for capture and detection, has been used to demonstrate that alpha-synuclein oligomer levels in blood plasma and cerebrospinal fluid (CSF) are higher in PD patients compared with controls (El-Agnaf *et al.*, 2006, Tokuda *et al.*, 2010). Although ELISAs are useful for quantifying the levels of oligomers in tissue, as well as in biological fluids, it is not possible to obtain high resolution localisation information using this technique.

The limitations of the techniques described led to the exploration of a different approach. The formation of alpha-synuclein oligomers requires interactions between molecules of alpha-synuclein. The aggregation of alpha-synuclein is thought to proceed via a nucleation-dependent mechanism, meaning that a seed of interacting molecules allows further aggregation to coalesce around it. Indeed, it has been shown that alpha-synuclein dimerisation is rate-limiting for the formation of alpha-synuclein oligomers (Krishnan *et al.*, 2003, Roostaee *et al.*, 2013). Therefore, I hypothesised that a method for the detection of protein-protein interactions would be ideal for the specific detection of alpha-synuclein oligomers.

3.1.2 Studying protein-protein interactions

In vitro, known protein-protein interactions and their effects can be studied using tagging methods such as F*ö*rster resonance energy transfer (FRET) and protein complementation assays (PCA).

In the case of FRET, the proteins of interest are tagged with fluorescent proteins, one of which acts as the donor fluorophore and the other as the acceptor fluorophore. The donor has an emission spectrum that corresponds to the excitation spectrum of the acceptor and thus, excitation of the donor can result in excitation of the acceptor. Energy transfer between the fluorophores is distance dependent and therefore the acceptor will only fluoresce if the donor is within approximately 10 nm, i.e. the tagged proteins are interacting. Additionally, the fluorescence lifetimes of a donor fluorophore decrease proportionally to its proximity to the acceptor fluorophore, and this can be

measured using fluorescence lifetime imaging microscopy (FLIM). This approach was previously used to identify novel conformations of alpha-synuclein oligomers within cells (Klucken *et al.*, 2006). A variation of FRET allows the detection of endogenous protein interactions by tagging antibodies raised against the proteins of interest with the relevant overlapping fluorophores (Konig *et al.*, 2006). However, this approach has only been adapted to study alpha-synuclein oligomers in solution thus far (Bidinosti *et al.*, 2012). Furthermore, the lack of amplification of signal due to the use of only one antibody means it cannot be used to detect low abundance protein interactions.

In PCA, proteins of interest are tagged with inactive halves of reporter proteins that only become fully functional when the tagged proteins interact. Different split reporter genes can be used for this technique such as dihydrofolate reductase (Remy *et al.*, 2007), luciferase (Remy and Michnick, 2006) and fluorescent proteins (Shyu *et al.*, 2006), which allows the user to manipulate the read-out. For example, a fluorescent protein based PCA, bimolecular fluorescent complementation (BiFC) utilises non-fluorescent halves of green fluorescent protein (GFP) to tag each protein of interest, thereby allowing conditional reconstitution of the fluorophore upon their interaction. Alpha-synuclein BiFC constructs form oligomers, which are toxic to cells in culture (Outeiro *et al.*, 2008) and AAV-induced overexpression of the BiFC constructs in rat SNc leads to neurodegeneration (Dimant *et al.*, 2013), demonstrating the toxicity of alpha-synuclein oligomers.

Both PCA and FRET provide a simple read-out for protein interactions. However, they also require the over-expression of tagged proteins and therefore may not necessarily be representative of protein interactions taking place under physiological conditions.

3.1.3 Proximity ligation assays

Proximity ligation assays (PLAs) were initially developed for the sensitive detection of proteins and were subsequently adapted for the detection of protein-protein interactions (Gullberg *et al.*, 2004, Soderberg *et al.*, 2006). PLA probes are generated from antibodies raised against the protein(s) of interest, one for each of the proteins involved

in the putative interaction. The antibodies are conjugated to short oligonucleotides to form the probes. If both probes bind interacting molecules of the proteins of interest, the oligonucleotides are sufficiently close to allow the binding of complementary connector oligonucleotides, which are then ligated to form a circular DNA template for rolling circle amplification. Finally, the product of the amplification reaction is detected by oligonucleotides labelled with a fluorescent chromophore or horseradish peroxidase (HRP), producing punctate signal (Figure 3.1).

The ligation step ensures the generation of PLA signal is only possible upon dual recognition of the two interacting proteins, an innovation that reduces background noise compared to the analogous immuno-PCR. The amplification step provides increased sensitivity and allows for the detection of low abundance protein interactions. Furthermore, endogenous protein interactions can be studied, as the use of antibodies for detection means there is no need to tag the proteins of interest.

PLAs have previously been used to detect disease relevant protein interactions with high sensitivity, such as those between the various components of the transcription factor activator protein 1 (AP-1) in breast cancer (Baan *et al.*, 2010) and between 78 kDa glucose-regulated protein (GRP78) and AKT1 during endoplasmic reticulum (ER) stress (Yung *et al.*, 2011). Larger structures such as prostasomes, associated with prostate cancer (Tavoosidana *et al.*, 2011) can be detected with PLA, as well as viruses including avian influenza viruses (Schlingemann *et al.*, 2010) and the foot and mouth virus (Nordengrahn *et al.*, 2008). Amyloid-beta protofibrils have previously been detected in homogenised brain samples from transgenic mice using PLA (Kamali-Moghaddam *et al.*, 2010).

The advantages of PLAs for the sensitive and specific detection of protein interactions led me to develop a new PLA to detect endogenous alpha-synuclein oligomers *in situ.* In this chapter, I describe the *in vitro* validation of the alpha-synuclein proximity ligation assay (AS-PLA) and demonstrate its specific detection of alpha-synuclein oligomers.

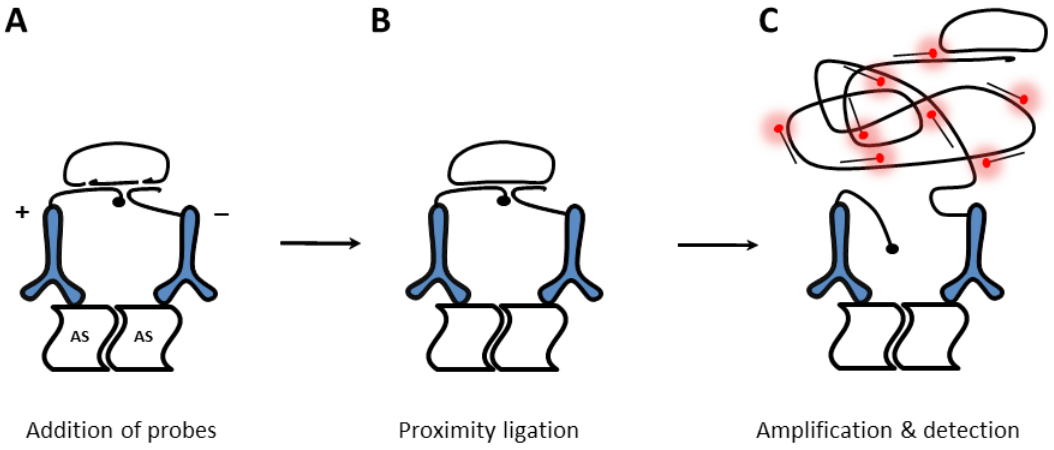

Figure 3.1. Alpha-synuclein proximity ligation assay (AS-PLA). AS-PLA probes consist of an alpha-synuclein antibody conjugated to one of two short oligonucleotides to form + and - probes. When both + and – AS-PLA proximity probes are brought close enough together by each binding one of the contiguous alpha-synuclein monomers in a dimer or oligomer, complementary linear connector oligonucleotides can bind to the probe oligonucleotides (**A**). The circular DNA structure produced by the connector oligonucleotides is ligated (**B**) and forms a valid substrate for rolling circle amplification (RCA). The DNA product of the amplification reaction is detected by fluorescently-labelled or horseradish peroxidase-tagged oligonucleotides (**C**).

3.1.4 Aims of the chapter

1. To demonstrate that AS-PLA detects spontaneously formed oligomers produced by alpha-synuclein BiFC constructs.
2. To generate inducible alpha-synuclein oligomerisation constructs and investigate whether the resulting oligomers are detected by AS-PLA.
3. To study whether AS-PLA detects oligomers formed *in vitro.*

3.2 Results

AS-PLA signal is conditionally produced by the dual recognition of interacting molecules of alpha-synuclein by the AS-PLA probes. To ensure that no spurious signals were produced by more than one AS-PLA probe binding to a single molecule of alpha-synuclein, the same alpha-synuclein antibody (syn211, Abcam) was used to produce both probes. Syn211 has previously been shown to display blocking activity on its epitope (El-Agnaf *et al.*, 2006) and thus should prevent more than one probe binding per alpha-synuclein molecule, allowing AS-PLA to recognise only alpha-synuclein molecules that are interacting (i.e. oligomers) and not monomers.

3.2.1 Spontaneously formed alpha-synuclein oligomers are detected by AS-PLA

In order to demonstrate that AS-PLA specifically detects alpha-synuclein oligomers, several *in vitro* oligomerisation assays were employed. First, spontaneous alpha-synuclein oligomerisation in cell culture was studied using a BiFC assay. BiFC constructs (kindly provided by Professor Tiago Outeiro, University of Göttingen, Germany) consist of alpha-synuclein fused to non-fluorescent halves of GFP. When the alpha-synuclein molecules self-interact, the two halves of GFP are able to form a fully folded molecule of functional GFP and thus produce fluorescence, providing a read-out for alpha-synuclein self-interaction (Figure 3.2Ai).

The constructs were transfected into HEK293 cells and their expression was verified by western blot (Figure 3.2Aii) and fluorescence microscopy. In HEK293 cells transfected with both constructs, green fluorescence indicative of alpha-synuclein self-interaction was observed (Figure 3.2Aiii). Although the minimum oligomeric unit required for fluorescence to be observed is a dimer, native extraction of proteins followed by SDS-PAGE showed that higher order oligomers were formed, including trimers (Figure 3.2Bi). Higher molecular weight smears were detected by native PAGE, confirming previous observations (Outeiro *et al.*, 2008) (Figure 3.2Bii).

BiFC signal in transfected HEK293 cells co-localised with punctate AS-PLA signal (arrows, Figure 3.3A). In untransfected cells (arrowhead), no AS-PLA signal was observed suggesting that the presence of alpha-synuclein oligomers is a pre-requisite for the generation of AS-PLA signal. Furthermore, in BE(2)M17 neuroblastoma cells, which endogenously express high levels of non-oligomeric alpha-synuclein as detected by alpha-synuclein immunofluorescence (AS-IF, Figure 3.3Bi), no AS-PLA signal was observed (Figure 3.3Bii), suggesting AS-PLA signal is not produced as an artefact due to the presence of non-oligomeric alpha-synuclein.

3.2.2 Generation of FKBP- and FRB-alpha-synuclein inducible oligomerisation constructs

Next, a system for the inducible formation of alpha-synuclein oligomers was developed by exploiting the ternary complex formed between FK506 binding protein (FKBP), the FK506-rapamycin binding (FRB) domain of the mammalian target of rapamycin (mTOR) and rapamycin (Muthuswamy *et al.*, 1999, Gruber *et al.*, 2006). Fusion proteins of alpha-synuclein and FKBP or FRB were generated that allowed the conditional induction of interactions between alpha-synuclein monomers in the presence of rapamycin (Figure 3.4A).

A cloning strategy was chosen that would allow the generation of constructs with alpha-synuclein located at the N-terminal or C-terminal relative to FKBP or FRB, with or without a linker. The linker was rich in glycine and alanine residues to produce a flexible linker that would allow proper folding of both proteins (Chen *et al.*, 2013) and

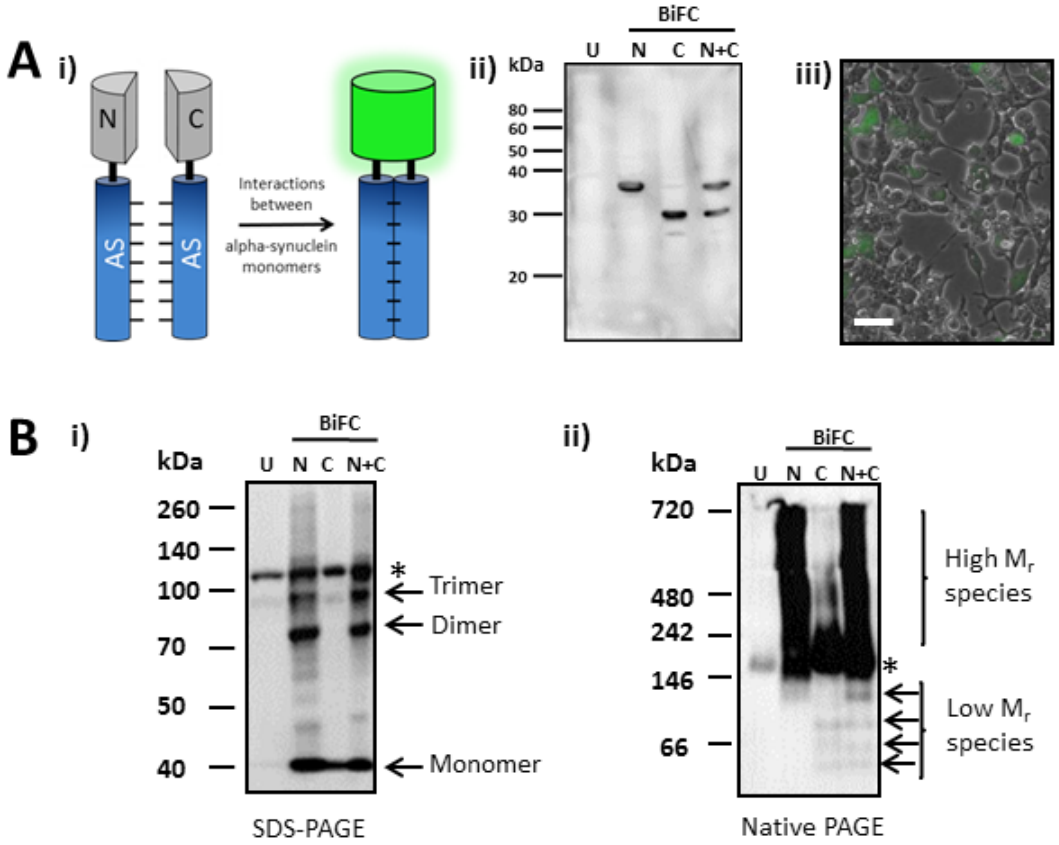

Figure 3.2. Bimolecular fluorescence complementation (BiFC) constructs formed alpha-synuclein oligomers. A i) In order to visualize the formation of alpha-synuclein oligomers, non-fluorescent halves of GFP were fused to alpha-synuclein. When alpha-synuclein monomers interact, the fluorophore of GFP is reconstituted and fluorescence is observed. The constructs were transfected into HEK293 cells and expression was confirmed by western blot (**ii**). When both constructs were transfected, fluorescence indicative of alpha-synuclein self-interaction was observed (**iii**). Scale bar: 50 µm. N=3. **B** Lysates from transfected HEK293 cells were ultracentrifuged and proteins in the resulting supernatant were resolved on non-reducing denaturing SDS-PAGE (**i**) or non-denaturing PAGE (**ii**), before transfer to PVDF membrane that was probed with anti-alpha-synuclein antibody 211 (syn211). A variety of oligomeric species was observed. Lanes for all blots: U – Untransfected; N – GFP N-terminal-alpha-syn; C - alpha-syn-GFP C-terminal; N+C - GN-alpha-syn + alpha-syn-GC. * indicates non-specific bands. N=3.

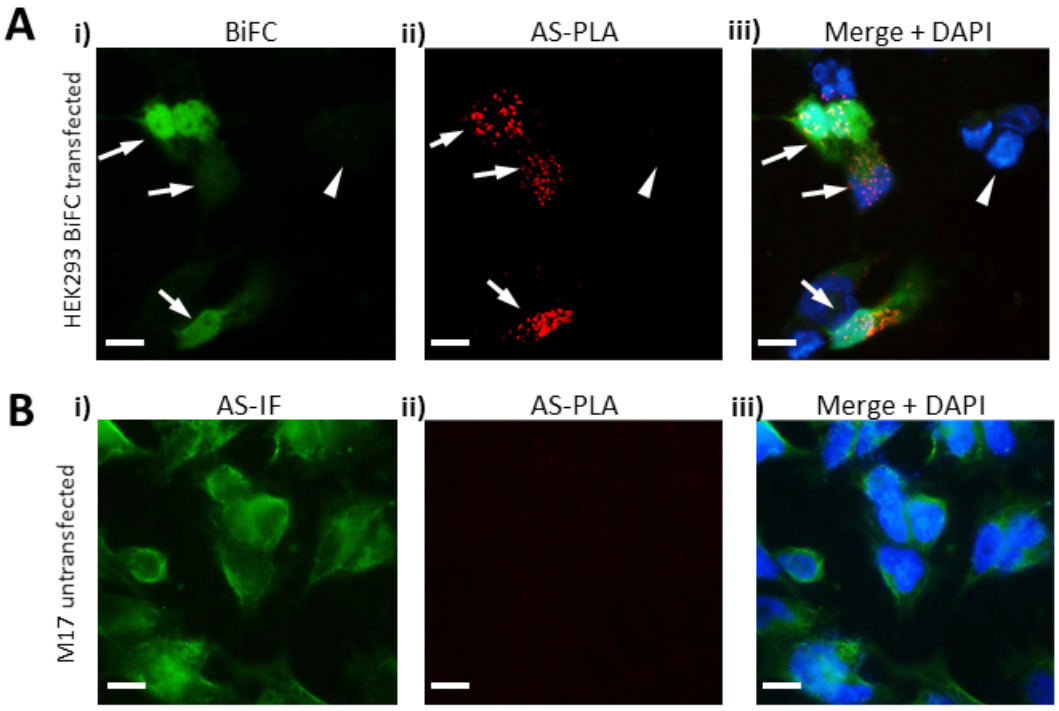

Figure 3.3. AS-PLA specifically recognised spontaneous BiFC formed alpha-synuclein oligomers. **A** HEK293 cells were transfected with alpha-synuclein BiFC constructs. GFP fluorescence indicated that alpha-synuclein oligomerisation has occurred (**i**, arrows). Each fluorescent red dot of AS-PLA signal represents a single oligomeric event (**ii**). BiFC and AS-PLA signal co-localised, as shown in the image of the merged channels plus DAPI (**iii**). Arrowheads indicate untransfected cells which act as an internal negative control for AS-PLA. N=3. **B** BE(2) M17 cells, which endogenously express robust levels of alpha-synuclein as demonstrated by green immunofluorescence (AS-IF, green, **ii**), do not contain AS-PLA-detectable alpha-synuclein oligomers. The merged channels plus DAPI are shown in (**iii**). Scale bars: 10 μm. N=3.

was flanked by KasI restriction sites to allow its removal. The restriction enzyme sites exploited first were those that resulted in the production of constructs with alpha-synuclein positioned C-terminal to FKBP or FRB with a linker between the two open reading frames. Long-armed primers that included the *de novo* restriction enzyme sites and the linker were used to amplify, by PCR, FKBP or FRB from myc-tagged constructs (kindly provided by Professor Carolyn Bertozzi, University of California, Berkeley; Addgene plasmids 20211 and 20228; (Czlapinski *et al.*, 2008)) and alpha-synuclein from each BiFC construct containing the N-terminal portion (GN) or C-terminal portion (GC) of GFP (Figure 3.4B). The PCR products were confirmed by agarose gel electrophoresis (Figure 3.4C) and purified by Qiagen PCR column purification (Figure 3.4D). The purified products were subsequently ligated into the cloning vector pGEM-T (Promega) and the presence of the insert in resulting colonies was confirmed, following preparation of mini-preps of their DNA, with PCR using primers targeting the T7 promoter (forward) and pUC/M13 site (reverse) in the pGEM-T vector backbone (Figure 3.4E). Clones containing the correct insert were sequenced and one clone with the correct sequence, indicated by an asterisk in Figure 3.4E, was used for further cloning steps. Although pGEMT SNCA and pGEMT FRB clones with the correct sequence were identified (2/9 and 1/6, respectively), none of the pGEMT FKBP sequences were without mutations. However, one clone was identified that only had mutations in a small region at the 5' end (Figure 3.4E, red asterisk). To obtain a clone with no mutations, the short mutated region was replaced with a synthesised DNA fragment (GeneArt, Life Technologies).

In order to allow the replacement of the mutated 5' end of the FKBP construct, an AscI restriction site unique to the synthesised DNA fragment ('GeneArt') was included. To insert the synthesised DNA fragment into pcDNA4/TO/myc-His B (Life Technologies), hereafter referred to as pcDNA4, both were subject to restriction digest with AflII and SacII, recognition sites of which were present in the multiple cloning site of pcDNA4 and at flanking ends of the synthesised fragment (Figure 3.5A). Positive clones were confirmed by restriction digestion with AscI, which was unique to the insert (Figure 3.5B).

To produce the full length FKBP construct, the unmutated segment of the original FKBP construct was excised from pGEMT FKBP using KasI and AscI and ligated into pcDNA4 FKBPGeneArt (Figure 3.5C). Clones were confirmed as positive for the full insert using PCR (Figure 3.5D) and by restriction digestion with AvrII alone or AvrII and XhoI (Figure 3.5E).

pcDNA4 FRB was generated by subcloning FRB from pGEMT FRB into pcDNA4 with AflII and SacII (Figure 3.6A) and confirmed the positive clones using junction PCRs (Figure 3.6B) and restriction digestion with NspI (Figure 3.6C).

A construct containing alpha-synuclein alone was also generated. Alpha-synuclein was subcloned from pGEMT into pcDNA4 using AflII and SacII restriction sites (Figure 3.7A) and its insertion was confirmed using PCR (Figure 3.7B) and restriction digestion with XhoI (Figure 3.7C).

The final inducible oligomerisation constructs were generated by subcloning the alpha-synuclein coding sequence from pGEMT SNCA into pcDNA4 FKBP or pcDNA4 FRB using XhoI and SacII restriction sites, thus producing FKBP-a-syn and FRB-a-syn (Figure 3.8A). The final vectors were confirmed by PCR using 3 primer pairs targeting different regions of the insert (Figure 3.8B, primers indicated in Figure 3.8A) and restriction digests (Figure 3.8C).

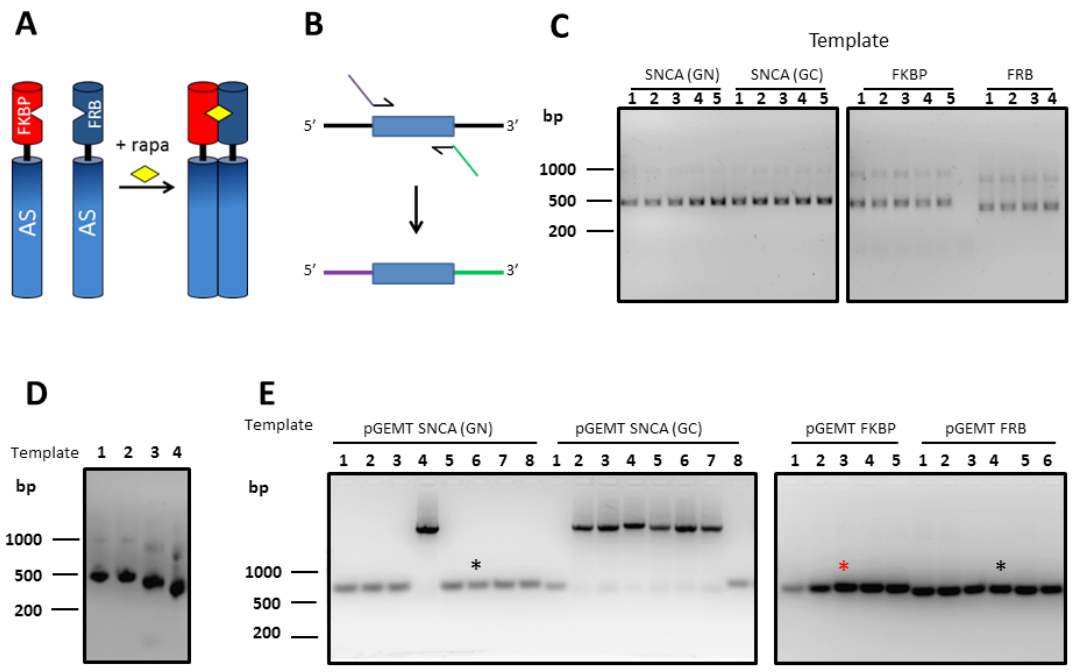

Figure 3.4. Generation of long PCR fragments containing open reading frames required for the formation of inducible alpha-synuclein oligomer constructs. A Interactions between alpha-synuclein molecules fused to FKBP or FRB are induced in the presence of rapamycin through the formation of a ternary complex. **B** Long-armed primers were used for PCR to generate inserts containing FKBP, FRB or alpha-synuclein open reading frames flanked by linkers for preparation of fusion proteins and restriction enzyme sites to facilitate cloning. **C** PCR products of each amplification were analysed using agarose gel electrophoresis: alpha-synuclein from either BiFC construct (SNCA GN or GC, expected size 485 bp), FKBP (expected size 450 bp), and FRB (expected size 418 bp). **D** PCR products from C were pooled and purified then analysed using agarose gel electrophoresis. Lane 1: SNCA (GN), 2: SNCA (GC), 3: FKBP, 4: FRB. **E** PCR products were ligated into the cloning vector pGEMT and inserts confirmed by PCR using primers targeting the T7 and pUC/M13 sites of the pGEMT vector backbone. PCR products were analysed using agarose gel electrophoresis. Clones containing the correct insert (SNCA – 695 bp, FKBP – 660 bp, FRB – 628 bp) were sequenced and clones chosen for maxi-prep are indicated by an asterisk. All FKBP clones were mutated, but we chose one with mutations in the 5' region that could be easily be replaced for further cloning, indicated with red asterisk.

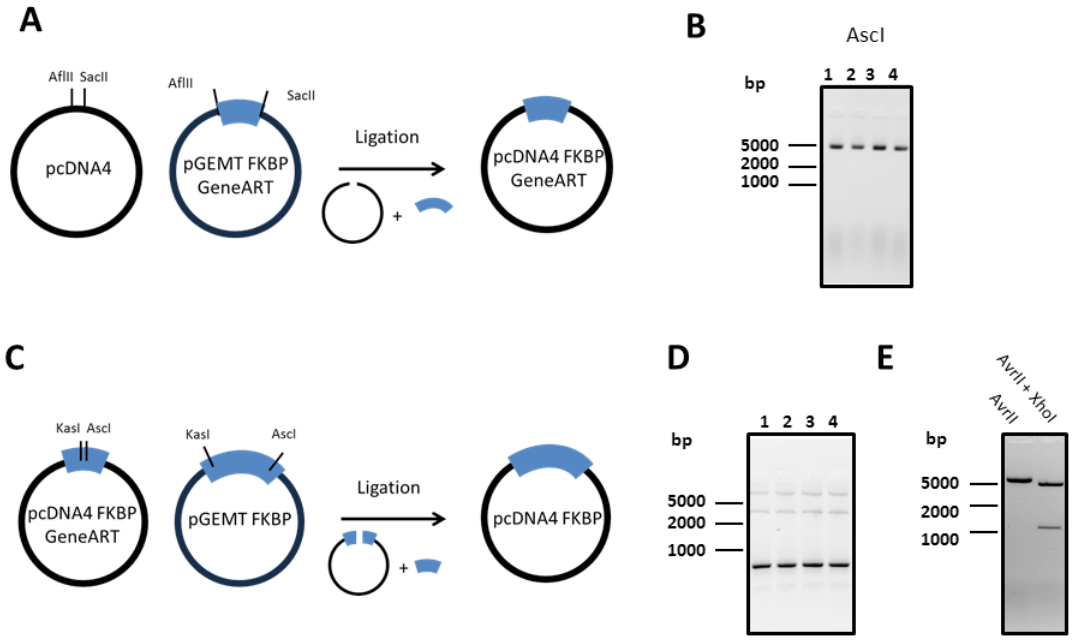

Figure 3.5. Generation of pcDNA4 FKBP. **A** To prepare a FKBP insert without mutation, the corresponding small fragment was synthesised (GeneArt, Life Technologies). The synthesised fragment (blue, GeneArt) was subcloned into pcDNA4 using the AflII and SacII restriction sites to generate pcDNA4 FKBP GeneArt. **B** Successful insertion in four colonies was confirmed by restriction digestion with AscI, which was unique to the insert, and agarose gel electrophoresis. **C** Full length FKBP was generated by subcloning the unmutated segment of FKBP from pGEMT using KasI and AscI restriction sites into pcDNA4 FKBP GeneArt. **D** The presence of the insert was confirmed in four colonies using PCR and agarose gel electrophoresis (expected product size: 773 bp) and (**E**) by restriction digestion with AvrII (5500bp) or AvrII and XhoI (1137 bp and 4369 bp) followed by agarose gel electrophoresis.

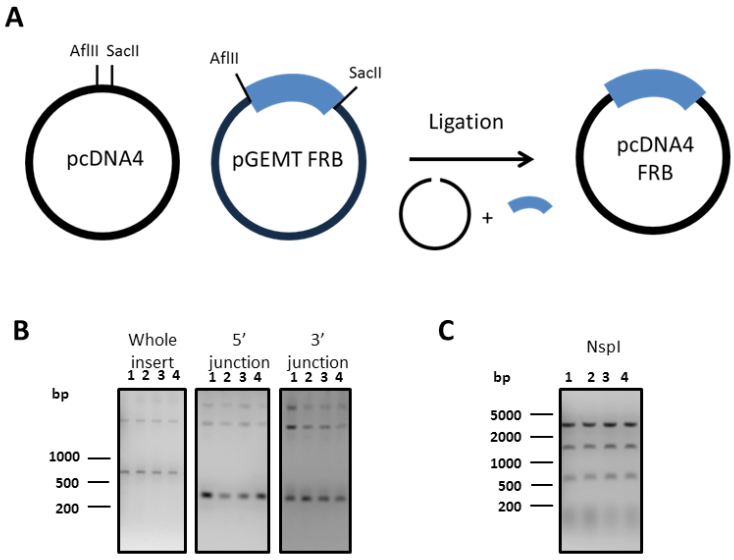

Figure 3.6. Generation of pcDNA4 FRB. A FRB was subcloned into pcDNA4 using AflII and SacII restriction sites. **B** The presence of the insert in four colonies was confirmed using PCR amplification of the whole insert, the 5' or 3' junction (expected product sizes: 658 bp, 268 bp and 244 bp, respectively) and (**C**) by digestion with NspI (2858 bp, 1328 bp, 575 bp, 561 bp, 72 bp, 25 bp), followed by agarose gel electrophoresis.

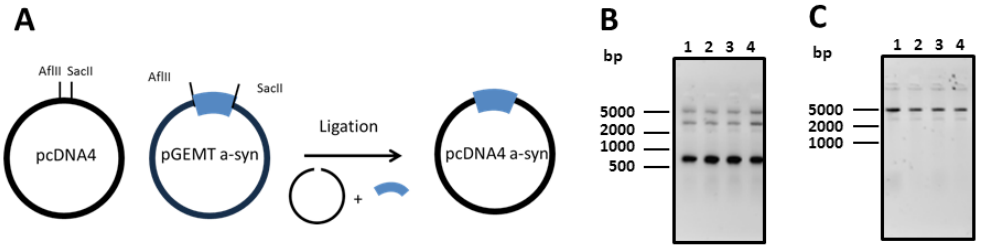

Figure 3.7. Generation of pcDNA4 a-syn. A Alpha-synuclein coding sequence was subcloned into pcDNA4 as an AflII SacII fragment. **B** The presence of the insert was confirmed in four colonies using PCR (expected product size: 694 bp) and (**C**) by restriction digestion with XhoI (5528 bp), followed by agarose gel electrophoresis.

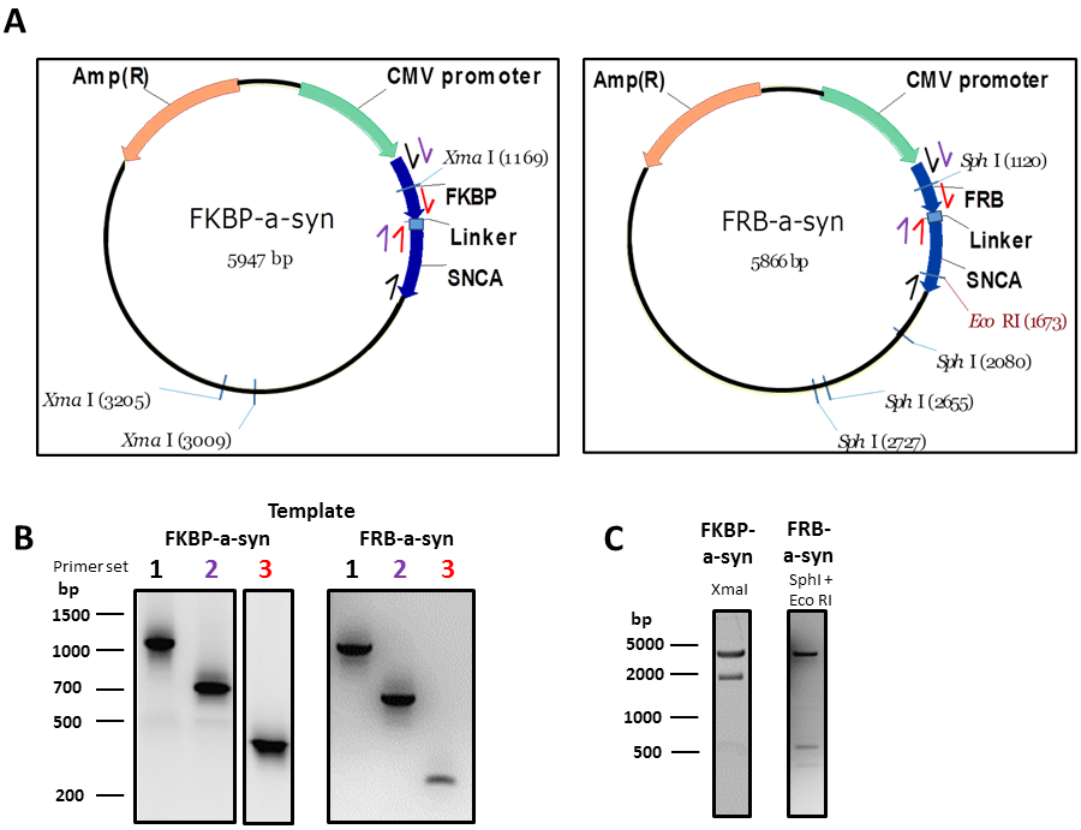

Figure 3.8. Generation of FKBP-a-syn and FRB-a-syn. **A** Vector maps of the final oligomerisation constructs, FKBP-a-syn and FRB-a-syn. Alpha-synuclein was subcloned into either pcDNA4 FKBP or pcDNA4 FRB using XhoI and SacII restriction sites. Primer pairs used for construct confirmation are indicated on each map as coloured arrows. Products of junction PCRs with 3 different primers across the coding region were analysed using agarose gel electrophoresis and are shown in **B** (expected product sizes: FKBP-a-syn (1) 1119 bp, (2) 697 bp and (3) 311 bp; FRB-a-syn (1) 1038 bp, (2) 616 bp and (3) 257 bp) and analysis of restriction digestions with the indicated enzymes using agarose gel electrophoresis are shown in **C** (XmaI: 3911 bp, 1840 bp, 196 bp; SphI + EcoRI: 4259 bp, 575 bp, 553 bp, 407 bp, 72 bp). Together, these confirmed the presence of the correct inserts in the FKBP-a-syn and FRB-a-syn constructs.

3.2.3 AS-PLA specifically recognises inducible oligomerisation constructs

The FKBP-a-syn and FRB-a-syn constructs were transfected into HEK293 cells and their expression confirmed using western blotting (Figure 3.9A) and immunofluorescence (Figure 3.9B). In untransfected cells, no bands were observed by western blotting using an alpha-synuclein antibody (syn211, Figure 3.9) and no immunofluorescence signal was present following immunostaining with the antibodies syn211 and FKBP12 (Figure 3.9Bi+ii). A robust immunofluorescence signal was observed in cells co-transfected with both constructs using the alpha-synuclein and FKBP antibodies (Figure 3.9Bi+ii). An antibody that targeted the FRB domain of mTOR specifically was not available and therefore an mTOR antibody was used with a large epitope that encompassed the FRB domain. However, no difference was observed in the fluorescent signal between untransfected and transfected cells using this antibody, suggesting that only endogenous mTOR and not ectopic expression of the FRB domain was detected using this antibody (Figure 3.9Biii).

As higher levels of the fusion protein were expressed from the FKBP-a-syn construct compared with the FRB-a-syn construct at various time points after transfection (24 hours: Figure 3.9A, 1 hour and 4 hours: Figure 3.10Ai), subsequent transfections with the constructs were undertaken at a ratio of 1:10 (FKBP-a-syn:FRB-a-syn) and it was found that this ratio produced a more equivalent expression of the two constructs by western blot (Figure 3.10Aii).

Co-transfected HEK293 cells treated with rapamycin for 1 or 4 hours that had been fixed were stained using AS-PLA. The ternary complex is formed rapidly, in as little as 15-30 minutes (Muthuswamy *et al.*, 1999, Luik *et al.*, 2008). Accordingly, at our early time-point of 1 hour, when the expression of the constructs was relatively low (Figure 3.10Aii), AS-PLA signal, which was negligible without rapamycin, increased significantly in the presence of rapamycin (Figure 3.10B). However, this was not the case at 4 hours post-transfection, when AS-PLA signal was observed both with and without rapamycin. This is most likely due to the high levels of the constructs found from 4 hours post-transfection onwards (Figure 3.10Bii), resulting in spontaneous interactions forming

alpha-synuclein oligomers independently of rapamycin that can be recognised by AS-PLA.

It was demonstrated that the propensity of the constructs to self-interact at high expression levels was due to alpha-synuclein, and its tendency to aggregate when over-expressed (Zhang *et al.*, 2008), and not the fusion tags by expressing untagged alpha-synuclein under the control of the same promoter (Figure 3.10Ci). As expected, no AS-PLA signal was present in cells expressing alpha-synuclein alone with or without rapamycin after 1 hour's treatment, but after 4 hours abundant AS-PLA signal was observed in both conditions, similarly to expression of both full constructs. When the FKBP and FRB constructs were transfected independently, no AS-PLA signal was observed at either time point (Figure 3.10Cii+iii). Therefore, after short incubation periods with rapamycin under conditions of low construct expression, the formation of alpha-synuclein oligomers is being driven by the induction of the ternary complex.

In further experiments the short incubation period with rapamycin was utilised and it was confirmed that in cells positive for expression of alpha-synuclein as indicated by AS-IF, AS-PLA signal was significantly greater in co-transfected HEK293 cells treated with rapamycin compared with untreated cells (Figure 3.11A), both in terms of the number of puncta (Figure 3.11Bi) and their total area (Figure 3.11Bii). This paradigm again demonstrates the specificity of AS-PLA for alpha-synuclein oligomers compared with non-oligomeric forms of alpha-synuclein.

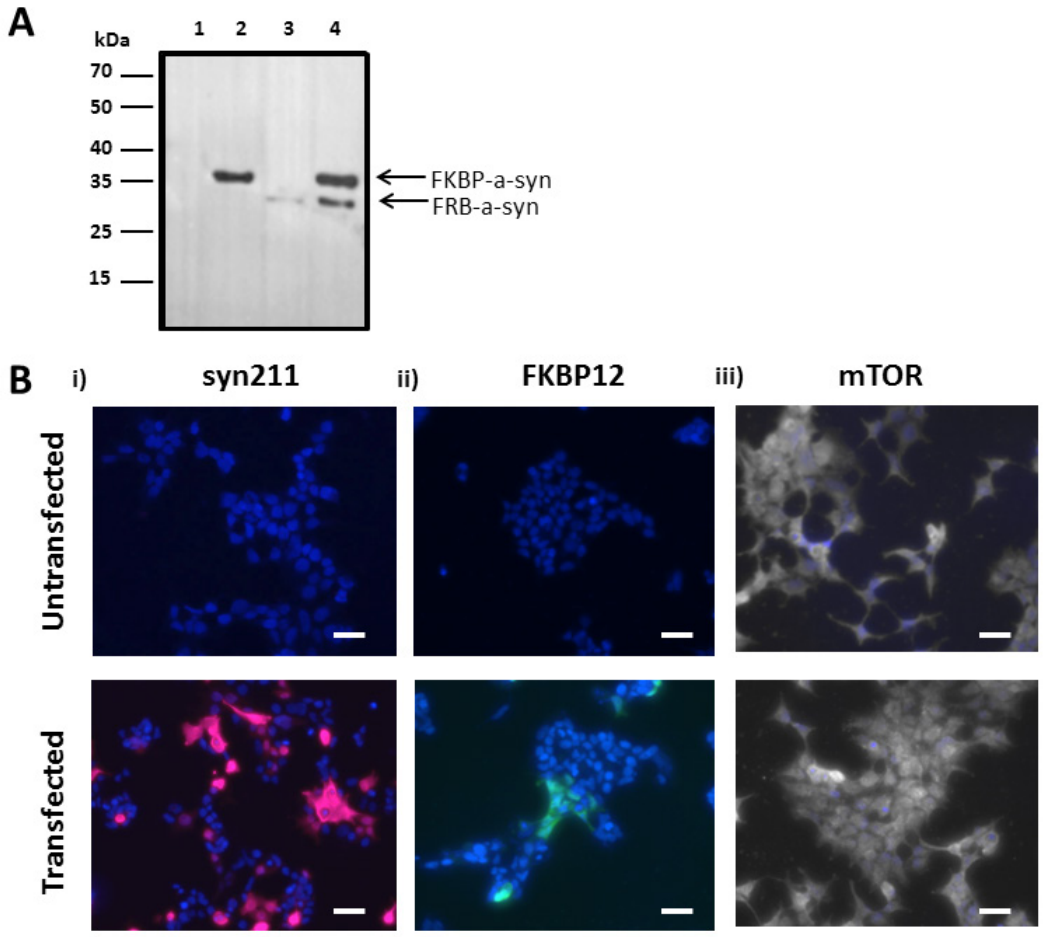

Figure 3.9. Expression of FKBP a-syn and FRB-a-syn in HEK293 cells. **A** The constructs were transfected into HEK293 cells and expression was demonstrated by western blot, probed with anti-a-syn syn211 antibody (Abcam). Lane 1: Untransfected. Lane 2: FKBP-a-syn. Lane 3: FRB-a-syn. Lane 4: FKBP-a-syn and FRB-a-syn. N=3. **B** Expression was also confirmed using immunofluorescence for alpha-synuclein (**i**, syn211, red) and FKBP (**ii**, FKBP12, green) antibodies in HEK293 cells co-transfected with both constructs. We were unable to obtain an antibody specific to the FRB domain of mTOR. No difference between untransfected and transfected cells could be observed with an mTOR antibody (white) suggesting that it cannot detect ectopically expressed FRB domain (**iii**). Nuclear staining with DAPI (blue). Scale bars 35 µm. N=3.

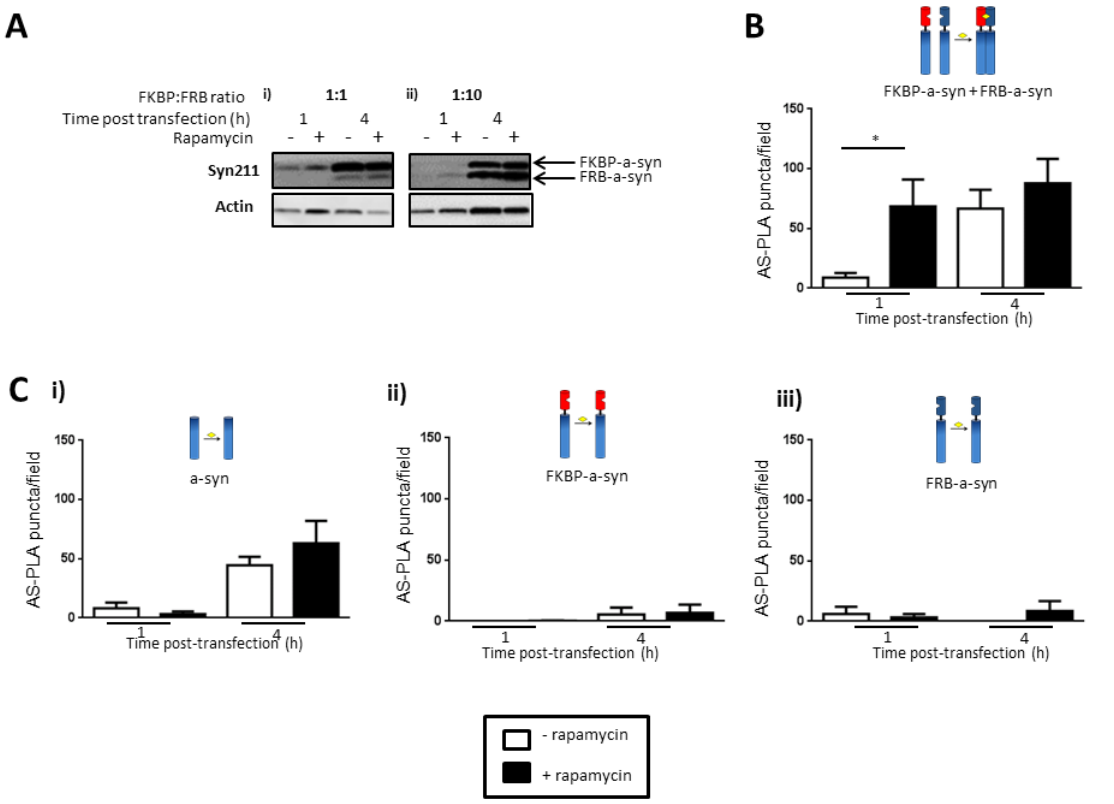

Figure 3.10. Oligomerisation of FKBP a-syn and FRB-a-syn was driven by rapamycin after short treatments. **A** When the oligomerisation constructs are co-transfected into HEK293 cells at an equal ratio, much higher protein expression of FKBP-a-syn is observed by western blot compared with FRB-a-syn (**i**). Adjustment of the ratio to 1:10 (FKBP-a-syn:FRB-a-syn) results in approximately equivalent expression of both constructs (**ii**). **B** HEK293 co-transfected with the constructs at a ratio of 1:10 and treated with rapamycin for the indicated times were fixed and stained with AS-PLA. Punctate AS-PLA signal from 10 fields of view per condition was quantified using ImageJ. After 1 hour of treatment with rapamycin, a significant increase in AS-PLA signal was observed but no difference was observed after 4 hours' treatment. **C** Rapamycin treatment of 1 hour does not induce the formation of alpha-synuclein oligomers when alpha-synuclein (**i**), FKBP-a-syn (**ii**) or FRB-a-syn (**iii**) are transfected into HEK293 cells. At higher expression levels of alpha-synuclein, 4 hours after transfection, AS-PLA detects oligomer formation (**i**). N=1. Error bars: +SEM. *=p<0.05. Student's *t* test.

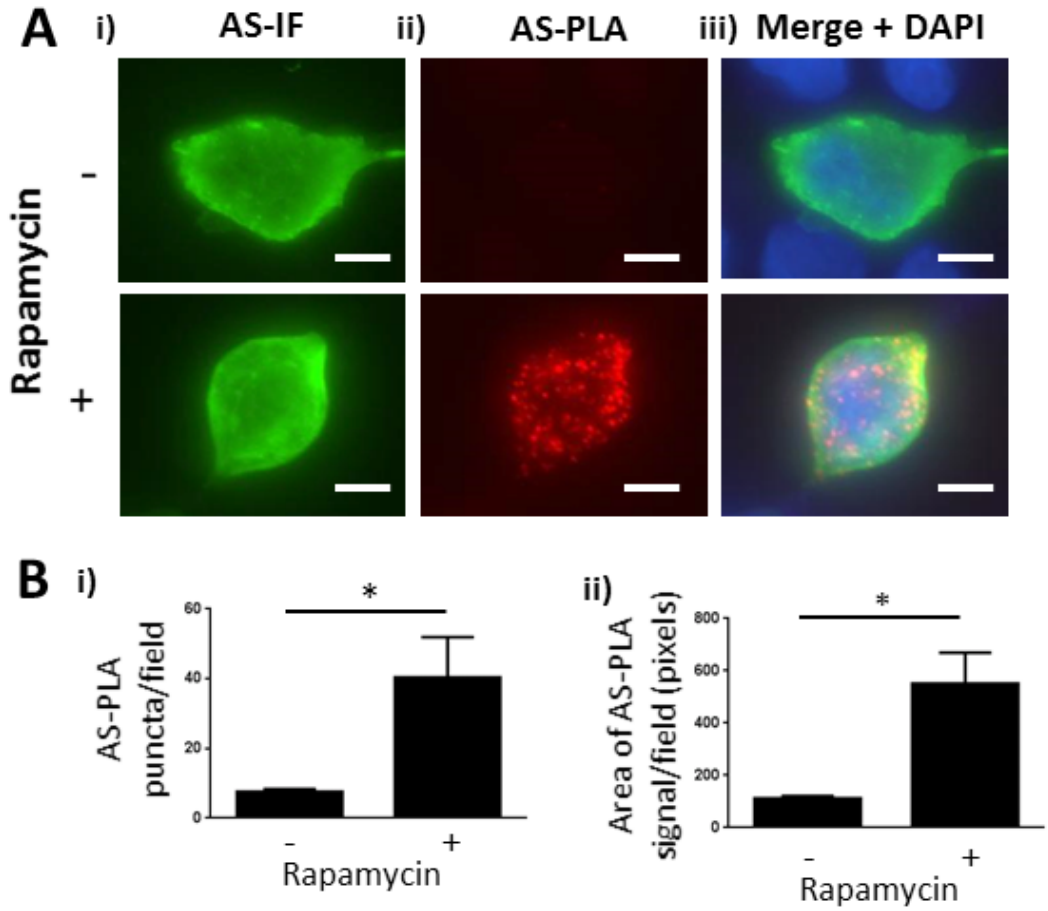

Figure 3.11. Inducible alpha-synuclein oligomers but not alpha-synuclein monomers were detected by AS-PLA. **A** HEK293 cells co-transfected with FKBP-a-syn and FRB-a-syn were treated with rapamycin for 1 hour post-transfection. Immunofluorescence (AS-IF, green, **i**) demonstrated equivalent expression of the constructs in both treatment conditions. AS-PLA signal (red) increases in the presence of rapamycin, suggesting AS-PLA detects inducibly-formed oligomers in this system. Scale bars: 10 µm. **B** Quantification of AS-PLA signal by **i**) number of puncta or **ii**) total area of the puncta. N=3. Error bars: +SEM. *=p<0.05. Student's *t* test.

3.2.4 In vitro formed alpha-synuclein oligomers are detected by AS-PLA

To ensure that the generation of AS-PLA signal was not affected by the tags on the BiFC and FKBP-FRB constructs, alpha-synuclein oligomers were produced *in vitro* by incubating monomeric, recombinant alpha-synuclein with the aldehyde HNE for 18 hours at 37°C (Nasstrom *et al.*, 2011). Oligomers of a variety of different sizes were produced, as shown by the range of bands revealed by western blotting, compared with the single band for monomeric alpha-synuclein when recombinant alpha-synuclein was run (Figure 3.12Ai). Electron microscopy analysis revealed well-structured chains of oligomers of different sizes (Figure 3.12Cii), which contrasted with the amorphous structures of recombinant monomeric alpha-synuclein (Figure 3.12Ci).

To further determine whether AS-PLA was specific for alpha-synuclein oligomers, alpha-synuclein fibrils were produced by constant shaking at 1000 rpm for 5 days at 37°C. Alpha-synuclein fibrils produced a much higher molecular weight smear by western blot analysis compared with alpha-synuclein oligomers (Figure 3.12Ai), although there were also contaminating monomers and oligomers present. The fibrils were shown to have an amyloid-like fibril structure by EM and smaller, oligomer-like species were also present (Figure 3.12Biii). It was attempted to purify the fibrillar species in the mixture using ultracentrifugation as previously described (Volpicelli-Daley *et al.*, 2014) and by filtration with a 100 kDa cut-off ultra-centrifugal unit (Millipore). However, neither of these methods was able to separate alpha-synuclein monomers and oligomeric species from the fibrils, as shown by western blotting (Figure 3.12Aii+iii).

A-beta oligomers were produced using the same procedure as alpha-synuclein oligomers to demonstrate that oligomers of other proteins were not detected by AS-PLA. Similarly to the alpha-synuclein oligomers, A-beta oligomers of multiple sizes appeared on western blots (Figure 3.12B) but were observed as slightly less well-defined chains by electron microscopy (Figure 3.12Civ).

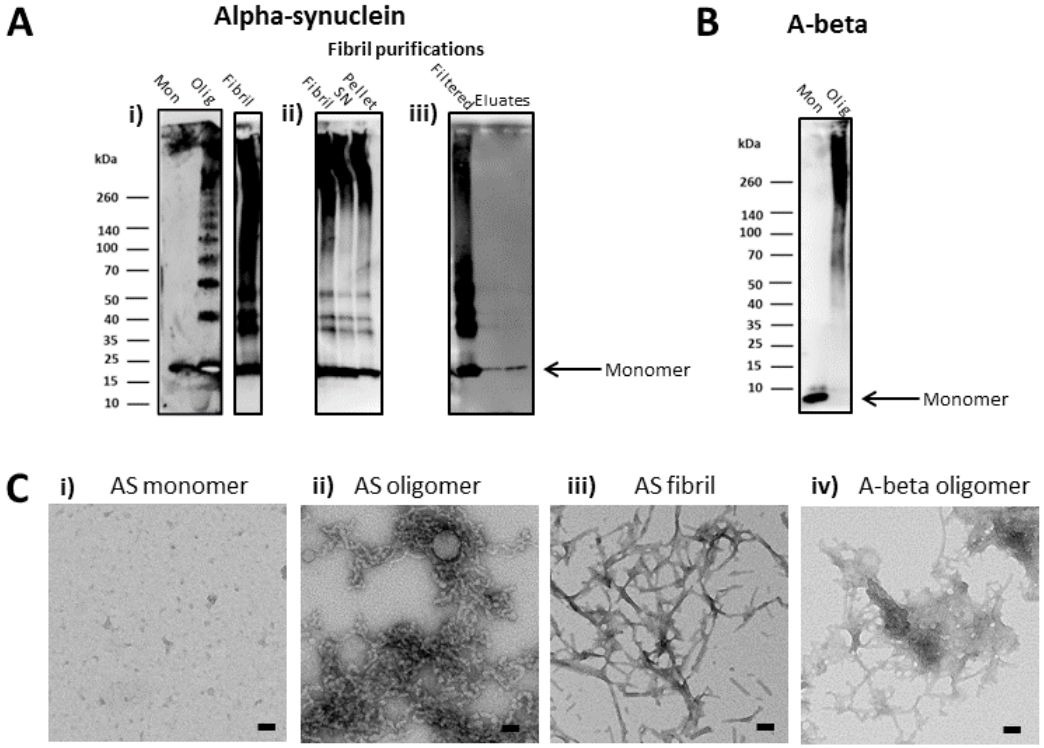

Figure 3.12. Analysis of *in vitro* formed oligomers and fibrils. A Western blot analysis of alpha-synuclein oligomers, alpha-synuclein fibrils and A-beta oligomers. **i)** Unmodified recombinant alpha-synuclein (monomer), alpha-synuclein oligomers produced by incubating recombinant protein with the aldehyde HNE for 18h and alpha-synuclein fibrils, produced by shaking recombinant alpha-synuclein at 1000 rpm at 37 °C for 5 days, were resolved by SDS-PAGE and visualised with syn211. **ii)** We attempted to purify the fibrils from contaminating monomer and oligomers by ultracentrifugation and resolved the original preparation (fibril), supernatant (SN) and pellet by SDS-PAGE and visualised with syn211. **iii)** A 100 kDa cut-off ultra-centrifugal unit (Millipore) was used for the purification of fibrils. Filtered fibrils and eluates were resolved by SDS-PAGE and visualised with syn211. Filtration did not purify the fibrils from contaminating monomers and oligomers (filtered) and only a small proportion of the contaminants were found in the eluates. **B** Recombinant A-beta and A-beta oligomers produced by incubating recombinant protein with the aldehyde HNE for 18h were resolved by SDS-PAGE and visualised with the 4G8 antibody. **C** Electron microscopy analysis of monomeric alpha-synuclein (**i**), HNE-induced alpha-synuclein oligomers (**ii**), alpha-synuclein fibrils (**iii**), and HNE-induced A-beta oligomers (**iv**) at high magnification. Scale bars: 50 nm. Electron microscopy was performed by Dr Errin Johnson (Dunn School of Pathology, University of Oxford).

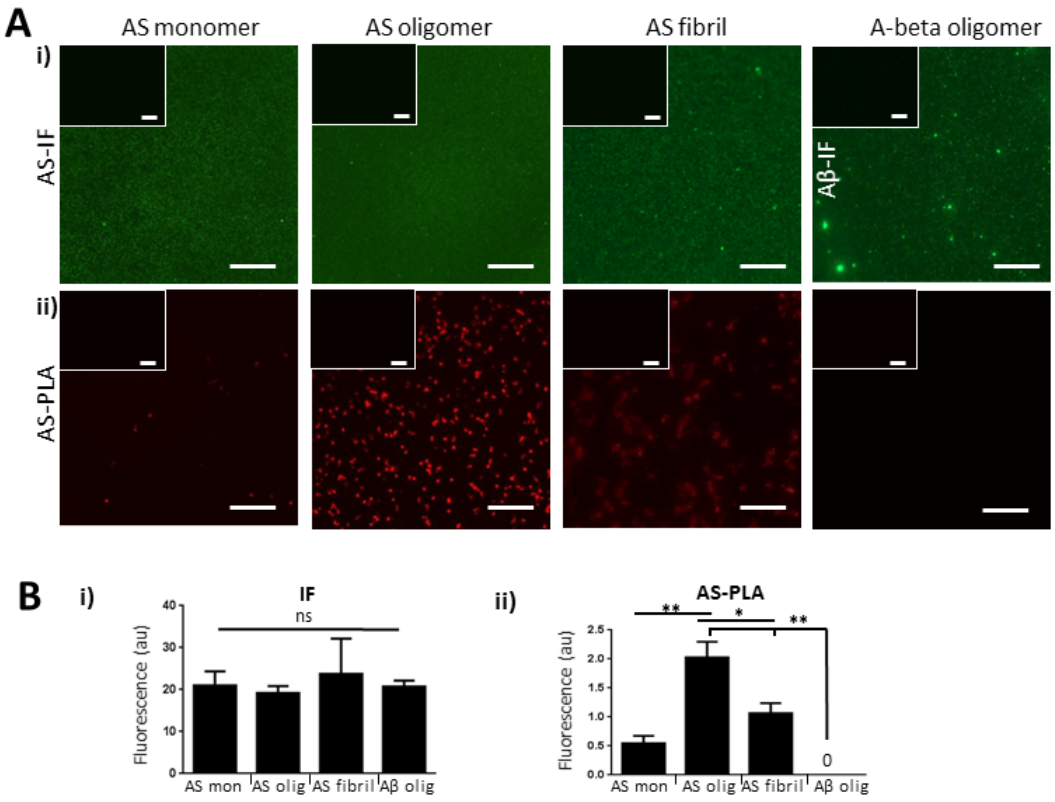

Figure 3.13. *In vitro* formed alpha-synuclein oligomers were specifically detected by AS-PLA. A i) Immunofluorescence (AS-IF or A-beta-IF) and **ii)** AS-PLA analysis of monomeric alpha-synuclein, HNE-induced alpha-synuclein oligomers, alpha-synuclein fibrils and HNE-induced A-beta oligomers. Representative images of 3 independent experiments are shown. Negative control images are shown inset of each image. Scale bars: 10 µm. **C** Analysis of **i)** IF and **ii)** AS-PLA signal. N=3. Error bars: +SEM. *=p<0.05, **=p<0.01. One-way ANOVA with Tukey's multiple comparisons test. AU: arbitrary units.

Spots of equally concentrated monomer, oligomer or fibril samples were placed onto poly-D-lysine coated coverslips and dried for 30 minutes at room temperature before fixing with 4% PFA and immunostaining for alpha-synuclein or A-beta, and AS-PLA. The immunofluorescence signal was similar between samples (Figure 3.13Ai+Bi), confirming the presence of the same amount of protein for each sample. AS-PLA signal was significantly greater in the alpha-synuclein oligomer samples compared with alpha-synuclein monomers or fibrils, confirming the specificity of AS-PLA for alpha-synuclein oligomers over other conformational species of alpha-synuclein (Figure 3.13Aii+Bii). No AS-PLA signal was observed in the A-beta sample, which demonstrates that AS-PLA is specific to alpha-synuclein and does not recognise oligomers formed of other proteins. As it was not possible to purify fibrils from contaminating monomers and oligomers using either ultracentrifugation or filtration, the presence of these contaminants may account for the residual signal in the fibril sample.

Finally, when either probe, the ligase or polymerase enzymes were omitted from their respective steps, no AS-PLA signal was observed in cells transfected with the FKBP-FRB constructs treated with rapamycin (Figure 3.14A) or on *in vitro* produced oligomers (Figure 3.14B). This demonstrates that AS-PLA signal observed in the presence of oligomers is not background signal arising as a result of non-specific recognition by the probes or ectopic priming of the amplification reaction.

3.2.5 What type of oligomer(s) does AS-PLA detect?

Next, I explored whether AS-PLA was detecting specific, conformationally distinct oligomer(s) using AS-PLA detection on PVDF blots. BiFC HEK293 cell lysates, an abundant source of alpha-synuclein oligomers, were resolved on non-denaturing PAGE or SDS-PAGE and HNE alpha-synuclein oligomeric preparations by SDS-PAGE before transfer to a PVDF membrane. Non-denaturing PAGE western blots of BiFC constructs demonstrated specificity of AS-PLA for high molecular weight bands (Figure 3.15Ai). When SDS-PAGE was used to resolve BiFC constructs, numerous bands were detected by AS- PLA. However, the species detected most strongly by AS-PLA was the monomer (Figure 3.15Aii), which was also the case for *in vitro* formed alpha-synuclein

oligomers resolved by SDS-PAGE (Figure 3.15B). Assuming monomer detection was a function of the molecular proximity due to the process of PAGE, BiFC lysates were subject to a limiting dilution on the rationale that if individual species of alpha-synuclein could be separated from one another at low concentrations, the monomer should not be detected (Figure 3.15C). None of the dilutions prevented the detection of alpha-synuclein monomers, suggesting that i) monomeric species are very abundant; ii) sufficient species separation may only occur at a concentration below the limit of detection of our assay.

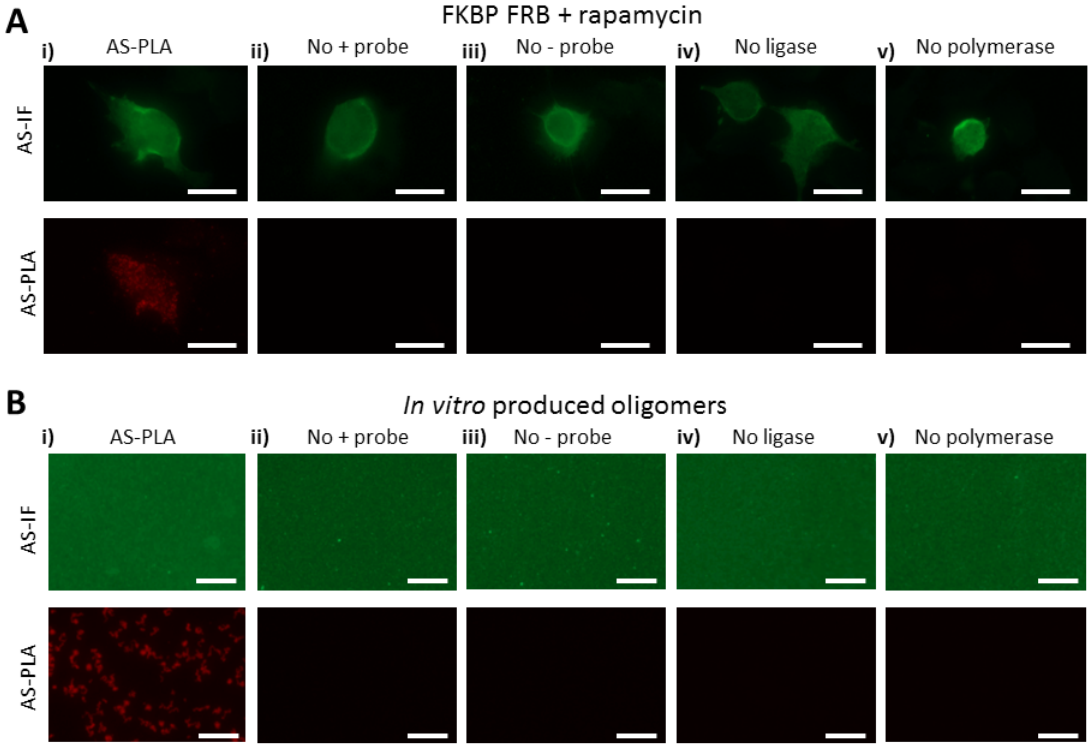

Figure 3.14. No AS-PLA signal was generated when either probe or the enzymes required for the ligation or amplification steps were omitted. FKBP-FRB transfected cells treated with rapamycin (**A**) or *in vitro* produced alpha-synuclein oligomers spotted onto coverslips (**B**) were stained with AS-PLA (**i**), or AS-PLA with either probe (**ii**+**iii**) or the ligase (**iv**) or polymerase (**v**) enzymes omitted at their respective steps. AS-PLA signal was not generated under these conditions, despite the presence of AS-IF signal, indicating the presence of alpha-synuclein. Scale bars: 10 µm. N=1.

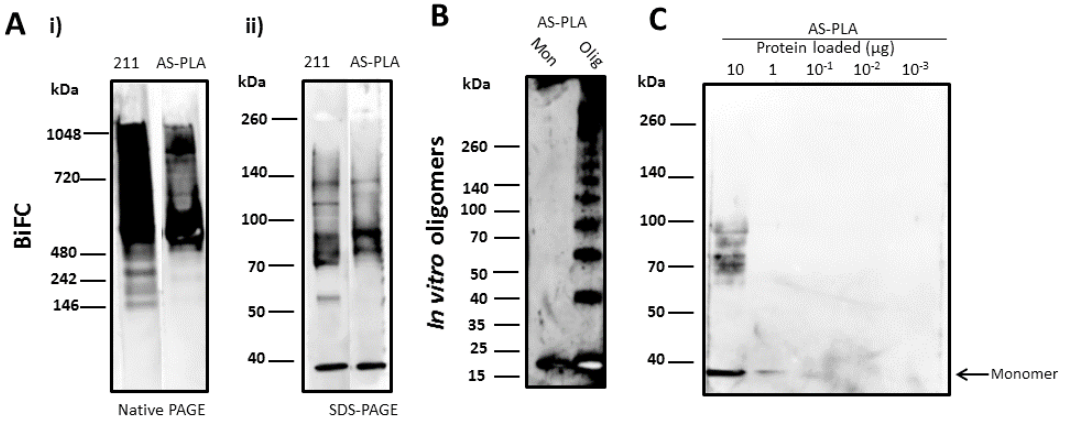

Figure 3.15. Investigating oligomeric species detected by AS-PLA using western blotting. **A** Lysates from HEK293 cells expressing alpha-synuclein BiFC constructs were ultracentrifuged and proteins were separated using non-denaturing PAGE (**i**) or non-reducing SDS-PAGE (**ii**) and western blotted onto a PVDF membrane, before probing with alpha-synuclein antibody 211 (211) or AS-PLA. N=3. **B** HNE-induced alpha-synuclein oligomers were separated by SDS-PAGE, transferred to PVDF membrane and probed with AS-PLA. AS-PLA detected monomers as well as oligomers in this preparation, most likely due to the proximity of molecules of the same size following PAGE. Note that the oligomer lane is overexposed. N=3. **C** To attempt to prevent the detection of the monomer, we titrated the amount of protein from BiFC lysates loaded on SDS-PAGE and probed with AS-PLA. Arrow indicating monomer is also true for Ai and B. N=1.

3.3 Discussion

This chapter has described the *in vitro* validation of AS-PLA, a novel technique for the specific detection of alpha-synuclein oligomers *in situ.* In three independent paradigms, I have shown that AS-PLA specifically detected alpha-synuclein oligomers and not monomers, fibrils or A-beta oligomers.

AS-PLA signal co-localised with fluorescence from alpha-synuclein BiFC constructs, which is indicative of the presence of alpha-synuclein oligomers. No AS-PLA signal was present in BE(2)M17 cells that endogenously express non-oligomeric alpha-synuclein, suggesting the specific detection of alpha-synuclein oligomers by AS-PLA. In the BiFC transfected HEK293 cells, there was not complete co-localisation between the BiFC fluorescence and AS-PLA signal. This could be for a number of reasons. Firstly, AS-PLA is designed to produce punctate signal that will inevitably not appear to co-localise fully with diffuse fluorescence, as BiFC produces. Secondly, it is likely that AS-PLA only detects a subset of the oligomeric species generated by the BiFC constructs. Finally, oligomers bound by AS-PLA probes of the same type (+/+ or -/-) will not generate signal as a + probe and a – probe must be in proximity to one another to allow the binding of connector oligonucleotides. Therefore, the observed AS-PLA signal can only represent a maximum of 50% of the interactions present.

Constructs for the inducible formation of alpha-synuclein oligomers were generated that consisted of alpha-synuclein fused to either FKBP or FRB. Long-arm primer PCRs were used to add restriction enzyme sites for sub-cloning 5’ or 3’ to each open reading frame and generated expression vector containing each protein alone (alpha-synuclein, FKBP or FRB) under the control of a CMV promoter as well as FKBP-a-syn and FRB-a-syn. Rapamycin induced oligomerisation of FKBP-a-syn and FRB-a-syn after 1 hour of treatment, and this was reflected in the significant increase in AS-PLA signal. However, at later time points it was found that even in the absence of rapamycin oligomerisation occurred, which was demonstrated to be due to the tendency of alpha-synuclein to aggregate when over-expressed. Although it has been previously reported that FKBP

induces the aggregation of alpha-synuclein (Gerard *et al.*, 2006), no such effect was observed in this experimental set-up by AS-PLA staining.

Finally, alpha-synuclein oligomers and fibrils were generated *in vitro* from recombinant, monomeric alpha-synuclein. Alpha-synuclein oligomers produced significantly more AS-PLA signal compared to alpha-synuclein fibrils or monomers. The process of drying and fixing protein solutions to coverslips may contribute to the formation of ectopic alpha-synuclein oligomers in the monomeric sample, and background AS-PLA signal, due to molecular crowding (Shtilerman *et al.*, 2002). Furthermore, residual signal in fibrils is most likely due to contaminating oligomers, which were not removed by ultracentrifugation or filtration, possibly due to dissociation of oligomers from fibrils during this process or poor efficiency of the purification techniques. Therefore, these experiments demonstrated that alpha-synuclein oligomers and not fibrils are the preferred supramolecular species detected by AS-PLA. A-beta oligomers were not detected by AS-PLA, demonstrating that the generation of AS-PLA signal is specific to alpha-synuclein oligomers and is not a general conformational reaction. This finding is in contrast to several other techniques described for the detection of alpha-synuclein oligomers, including the A11 antibody and single chain variable fragment antibodies that detect many kinds of oligomers, including A-beta oligomers (Kayed *et al.*, 2003, Zhang *et al.*, 2011). Furthermore, the FILA-1 antibody that has been used in an ELISA described as specific to alpha-synuclein oligomers also detects alpha-synuclein fibrils (Paleologou *et al.*, 2009).

The type of oligomeric species detected by AS-PLA was also investigated in this chapter. Despite detecting some differences in which species of oligomer were detected by AS-PLA compared to conventional antibody detection, the species of alpha-synuclein detected most strongly by AS-PLA was the monomer. This is not wholly unsurprising as PAGE is designed to bring proteins of the same size together and current reports of PLA western blot protocols aim to more sensitively detect one protein (Liu *et al.*, 2011), as opposed to the detection of protein-protein interactions. Therefore, western blotting was not the ideal method for such studies. Techniques such as size exclusion chromatography for the isolation of discrete populations of

oligomers will be helpful to allow the identification of the specific type(s) of oligomers detected by AS-PLA.

In conclusion, in this chapter I have shown that AS-PLA specifically detects alpha-synuclein oligomers.

4. Detection of alpha-synuclein oligomeric pathology with AS-PLA

4.1 Introduction

4.1.1 Current methods for the detection of alpha-synuclein pathology in PD patient tissue

Although alpha-synuclein oligomers are suspected to be the toxic agents in PD, the specific oligomeric species that are associated with disease have remained elusive. The vast majority of studies that uncover pathogenic effects of alpha-synuclein oligomers have utilised *in vitro* formed oligomers. It is not clear the extent to which these oligomers recapitulate the structure and properties of those found in diseased brain. In order to address these questions, we must first be able to specifically detect alpha-synuclein oligomers in patient tissue.

Previously, alpha-synuclein oligomers from patient tissue have been studied using techniques such as western blotting that provide no localisation information (Sharon *et al.*, 2003) or using histochemical immunodetection. However, alpha-synuclein oligomeric pathology cannot be specifically recognised using conventional alpha-synuclein immunohistochemistry (AS-IHC). Therefore, the identification of pathological structures stained by AS-IHC is limited to lesions associated with the late stage of disease such as Lewy neurites (LNs), Lewy bodies (LBs) or pale bodies (PBs) and less frequently dot-like structures in neuronal soma (Kuusisto *et al.*, 2003). An antibody specific to alpha-synuclein phosphorylated at Ser129 demonstrated the presence of grain-like 'Lewy dots' in the neuropil around LBs (Saito *et al.*, 2003), but it is more common to study alpha-synuclein pathology using an antibody against unmodified alpha-synuclein. Furthermore, in areas such as the cortex where alpha-synuclein is highly abundant at synaptic terminals, it is not possible to differentiate AS-IHC signal from pathological alpha-synuclein species from the physiological, synaptic staining of alpha-synuclein (Schulz-Schaeffer, 2010).

To overcome this limitation of traditional AS-IHC and to differentiate pathological forms of alpha-synuclein from normal, synapse-localised alpha-synuclein, slides can be pre-treated with proteinase K (PK). Non-pathological alpha-synuclein is sensitive to PK and only aggregated alpha-synuclein remains following incubation with PK. Tanji *et al* identified pre-synaptic aggregates in addition to extensive LN and LB pathology using this method (Tanji *et al.*, 2010). However, such aggregates did not precede LB formation and therefore are unlikely to represent early aggregated alpha-synuclein species associated with PD. For example, pre-synaptic aggregates were only present in the medulla and pons of Braak stage V and VI patients, despite heavy LB pathology being found in tissue from these regions in Braak stage II patients.

Using the PK paraffin embedded tissue blot (PK-PET blot), tissue is digested with PK for long periods (up to 8 hours) and more extensive pathology is revealed compared to the approach used by Tanji *et al* (2010). Heavy neuritic pathology, in addition to LBs, was revealed in the SNc of PD patients using the PK-PET blot (Neumann *et al.*, 2002), while neuritic pathology was identified in the striatum of PD patients with different subtypes of the disease (brainstem, limbic, or neocortical predominant; (Neumann *et al.*, 2004)). Small aggregates of alpha-synuclein shown to be localised to synapses were uncovered in the frontal and cingulate cortex of DLB patients and in the SNc of PD patients with the PK-PET blot (Kramer and Schulz-Schaeffer, 2007, Schulz-Schaeffer, 2010). Although earlier pathology is revealed with the PK-PET blot compared to traditional AS-IHC, the extremely proteinase K resistant species are likely to represent aggregates with high beta-sheet content that occur late in the misfolding process (Miake *et al.*, 2002). Furthermore, the extended digestion degrades the integrity of the tissue and therefore very poor neuroanatomical resolution remains for analysis.

The problem of differentiating pathological alpha-synuclein staining from physiological staining was further addressed with the development of the 5G4 antibody that was raised against amino acids 44-57 of alpha-synuclein (Kovacs *et al.*, 2012) and was shown to bind high molecular weight beta-sheet rich alpha-synuclein oligomers (Kovacs *et al.*, 2014). Although the 5G4 antibody did not detect physiological alpha-

synuclein and detected Lewy dots, LBs, LNs, as well as granular structures in soma, the antibody did not detect pathology more efficiently than an antibody against full-length alpha-synuclein (4D6) (Kovacs *et al.*, 2012) and did not identify previously unreported pathology by light microscopy (Braak *et al.*, 2007, Kovacs *et al.*, 2014).

Antibodies raised against nitrated/oxidised alpha-synuclein demonstrated the presence of synaptic alpha-synuclein pathology in the striatum of cases with DLB and PD, which had not previously been reported (Duda *et al.*, 2002). No other regions were studied and no further studies of pathology in human brain tissue using this antibody have since been reported.

Similarly, FILA-1, an antibody specific to aggregated alpha-synuclein used for ELISAs (Paleologou *et al.*, 2009), does not recognise LBs isolated from tissue or in tissue sections using AS-IHC (Lindersson *et al.*, 2004) but any other pathology it may detect has not been described.

The FILA-1 antibody is specific to alpha-synuclein aggregates, not to alpha-synuclein oligomers, while the antibodies targeting nitrated/oxidised alpha-synuclein can detect any conformational form of alpha-synuclein that has been nitrated or oxidised at a specific residue. Therefore, none of these studies has addressed alpha-synuclein oligomeric pathology. An antibody specific to alpha-synuclein oligomers, mAb38F, was shown to recognise LBs in PD and DLB tissue but no additional pathology was detected by this antibody in human tissue (Fagerqvist *et al.*, 2013).

To understand the contribution of alpha-synuclein oligomers to PD it is of utmost importance to study oligomeric pathology and its distribution at sequential stages of the disease in the human brain. In the previous chapter, I showed that AS-PLA specifically detects alpha-synuclein oligomers *in vitro.* Therefore, I wanted to investigate the alpha-synuclein oligomeric pathology in human brain tissue using AS-PLA.

4.1.2 Aims of the chapter

1. To optimise AS-PLA for staining human brain tissue.
2. To study alpha-synuclein oligomeric pathology in PD brain and in tissue from the *SNCA*-OVX model of PD.

4.2 Results

4.2.1 Optimisation of human tissue AS-PLA

In order to study alpha-synuclein oligomeric pathology in human brain tissue using AS-PLA, several adaptations to the protocol were required. Due to the high levels of autofluorescence in aged human brain and the advantages of brightfield microscopy for identifying neuroanatomical structures, brightfield detection was used for AS-PLA studies in tissue. Therefore, the detection oligonucleotide was tagged with horseradish peroxidase (HRP) as opposed to a fluorophore and detection was performed by incubation with a chromogenic substrate, in this case NovaRED (see Section 2.7.3). Further optimisation for brightfield AS-PLA was required due to these extra steps.

Formalin-fixed, paraffin-embedded tissue sections, in which epitopes may be masked by the process of fixing and embedding, were used. Therefore, the efficiency of formic acid or citrate buffer antigen retrieval to reveal the epitope of syn211, the antibody used to form the AS-PLA probes, in LBs was compared. In consecutive sections of basal ganglia from a PD patient, LBs were more strongly stained by AS-IHC following antigen retrieval using formic acid (Figure 4.1). However, no AS-PLA staining was present following formic acid treatment (Figure 4.2A). The potentially labile nature of the oligomeric species AS-PLA detects, particularly in human tissue, led to the less harsh citrate buffer retrieval being used in all further experiments. In addition, the concentration of the probes was increased and under these conditions very weak AS-PLA signal was observed (Figure 4.2B). In order to produce robust AS-PLA signal, the sections were incubated with the probes at 4°C overnight following the initial incubation for 1 hour at 37°C and the sections were incubated with the substrate for 20 minutes

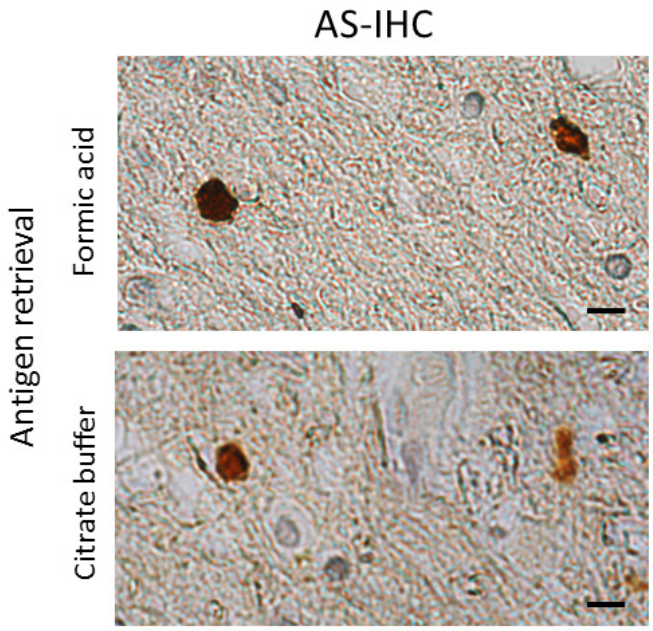

Figure 4.1. Testing antigen retrieval methods for uncovering the syn211 epitope. Consecutive sections of basal ganglia from a Parkinson's patient were stained with AS-IHC using syn211 as the primary antibody. We compared the strength of staining of LBs following antigen retrieval by incubation with formic acid (top panel) or heat-mediated retrieval in citrate buffer, pH 6 (bottom panel). Scale bars: 10 µm. N=1.

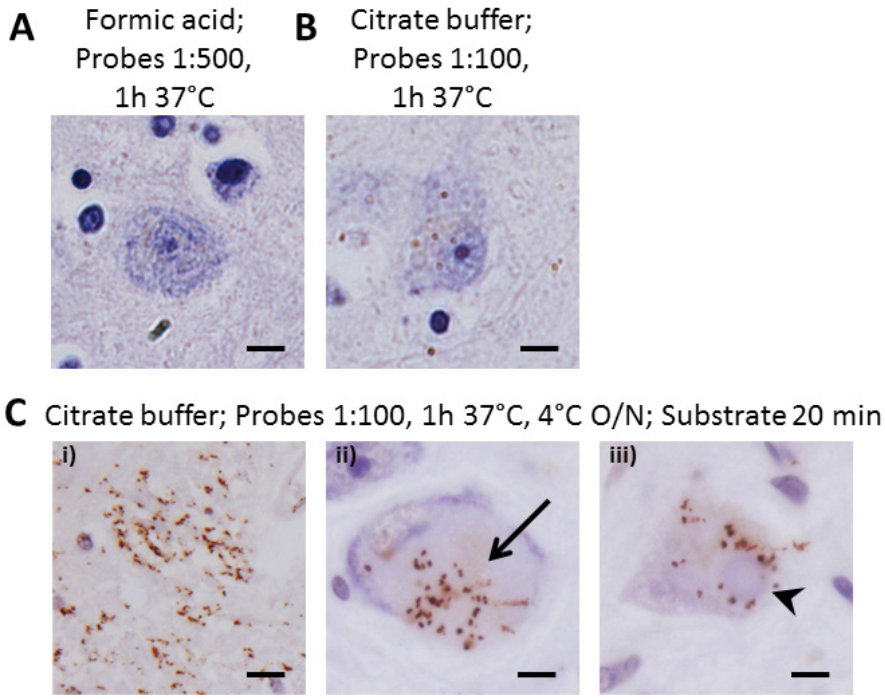

Figure 4.2. Optimising AS-PLA for brightfield staining of human brain tissue. **A** No AS-PLA signal was generated following formic acid antigen retrieval and probes used at a dilution of 1:500. **B** A small amount of weak AS-PLA signal was observed following heat-mediated antigen retrieval with citrate buffer and increasing the concentration of the probes to 1:100. **C** Robust AS-PLA signal was produced with the conditions as in (**B**), plus incubating the sections with the probes overnight at 4°C following the 1 hour 37°C incubation, and incubating with the substrate for 20 minutes. The signal produced included diffusely distributed signal in the intermediate reticular zone of the medulla (i) and staining of PBs (ii) and at the periphery of LBs (iii). Scale bars for A, B and Cii + iii: 10 µm. Scale bar for Ci: 20 µm.

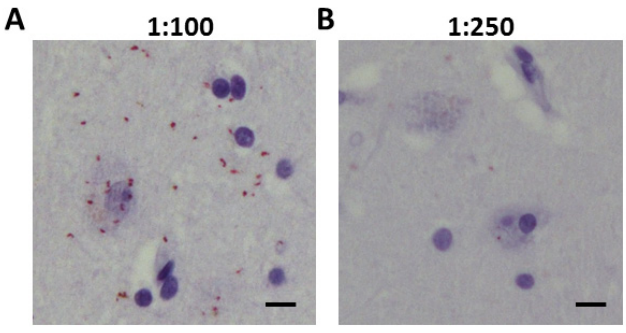

Figure 4.3. Titration of AS-PLA probe dilution. The concentration of the AS-PLA probes was reduced to remove background but the robust signal that was observed using a dilution of 1:100 (**A**) was not observed when the probes were diluted to 1:250 (**B**). Scale bars: 20 µm. N=1.

instead of 10 minutes. These conditions allowed the visualisation of alpha-synuclein oligomers diffusely distributed in the intermediate reticular zone of the medulla (Figure 4.2Ci), accumulated in a PB (Figure 4.2Cii, arrow) and surrounding a LB (Figure 4.2Ciii, arrowhead) in degenerating neurons of the SNc of a PD patient.

The concentration of the probes was titrated to ensure minimal background, but negligible AS-PLA signal was observed when the probes were used at a dilution of 1:250 compared to the abundant signal produced at 1:100 (Figure 4.3).

4.2.2 Early Parkinson's disease lesions are selectively recognised by AS-PLA

To examine alpha-synuclein oligomeric pathology and its relationship to LB pathology, post-mortem brain tissue from eight PD patients and eight age and sex-matched controls was stained using AS-PLA (Figure 4.4). Three neuroanatomical areas relevant to PD were chosen that, according to the Braak hypothesis, are progressively affected by alpha-synuclein pathology: medulla, midbrain and cingulate cortex (Braak *et al.*, 2003).

PBs and other early lesions in the brainstem displayed prominent AS-PLA staining (medulla and midbrain, Figure 4.5A + B, arrows). However, brainstem LBs, which are considered late-stage lesions, were only very exceptionally stained (Figure 4.5A + B, arrowheads). Lesions detected by AS-PLA were present in nuclei associated with PD pathology, and where pathology was also found using AS-IHC. These include the dorsal motor nucleus of the vagus (DMNV), intermediate reticular zone, raphe and reticular formation in the medulla; in the midbrain the reticular formation, raphe, periaqueductal grey and oculomotor nucleus were affected. Many lesions were also detected in the SNc (Figure 4.5B). Similarly to the DMNV, PBs and extrasomal LBs were strongly detected (arrows, Figure 4.5A + B), while intracellular LBs were unstained (arrowheads, Figure 4.5Aii, Bi+ii). Occasionally, a crown of AS-PLA stained oligomers surrounded LBs (arrowheads, Figure 4.5Av + Biii).

Most strikingly, AS-PLA revealed diffuse cytoplasmic staining in neurons that contained

Diagnosis	Sex	Age at death	Disease duration (years)	Braak stage	Dementia (age at onset)	Post-mortem interval (h)
C1	F	71				17
C2	M	77				48
C3	M	65				12
C4	F	78				23
C5	F	80				23
C6	F	84				11
C7	M	82				48
C8	M	90				12
P1	M	76	8	4	N	40
P2	F	80	13	4	80	10
P3	M	82	11	6	81	30
P4	F	78	19	6	74	22
P5	M	92	12	5	N	21
P6	M	78	10	5	N	11
P7	F	86	18	3	N	5
P8	F	73	6	3	N	43

Figure 4.4. Parkinson's patient and control case information. Clinical and neuropathological details of the 8 Parkinson's patients (P1 – P8) and the 8 age- and sex-matched controls (C1 – C8) used in the human oligomeric pathology study.

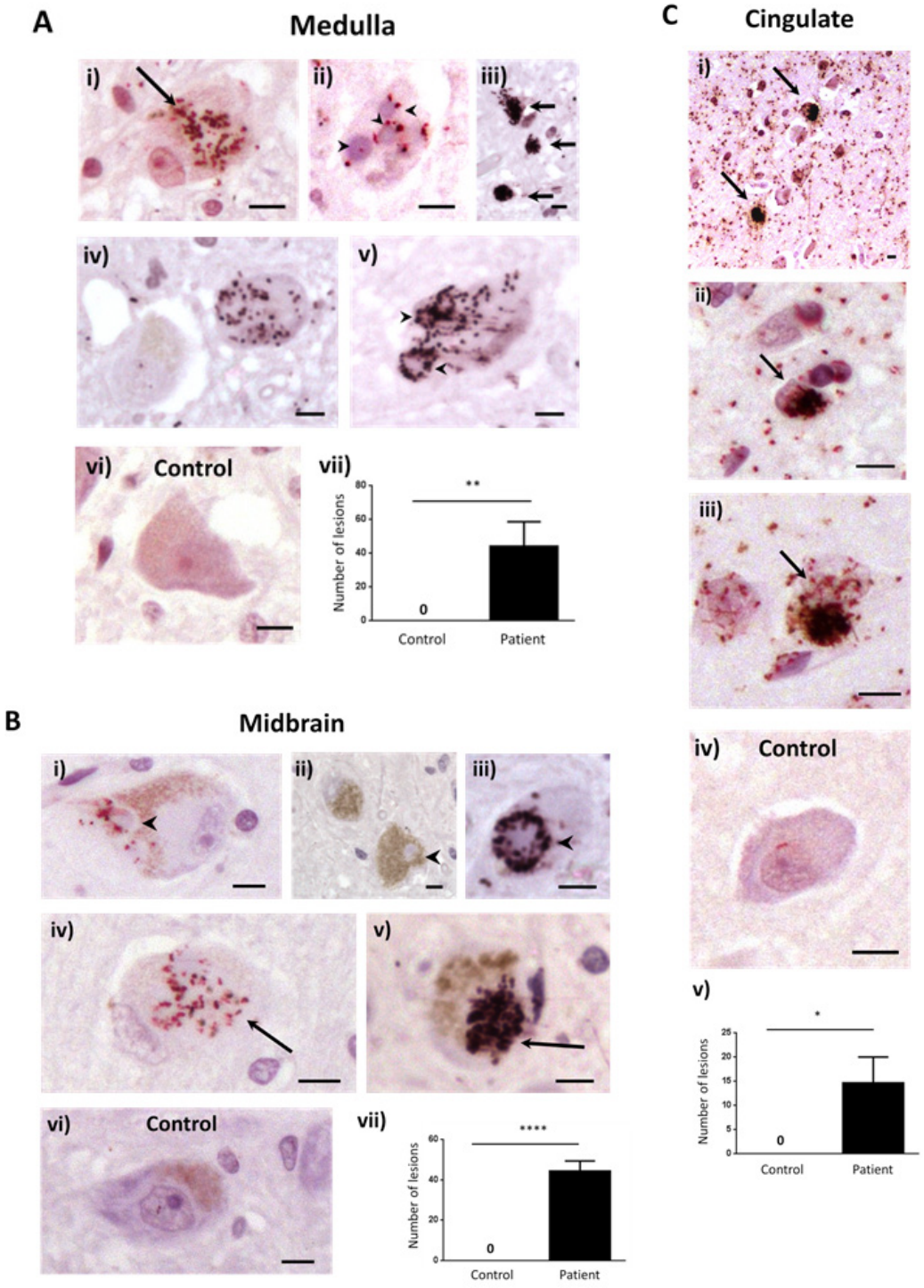

Figure 4.5. AS-PLA stained alpha-synuclein oligomers in early Parkinson's disease lesions. Tissue from 8 patients and 8 age and gender matched controls was stained with AS-PLA. In the medulla (**A**) and midbrain (**B**), AS-PLA selectively stained pale bodies and extrasomal Lewy bodies (arrows in A + B). If any staining was associated with LBs (arrowheads), it was at their periphery (**Av** + **Bi,iii**). We also observed staining in cells where no obvious PB or LB was present, suggesting even earlier aggregation centres were detected (**Aiv**). In the cingulate cortex (**C**), cortical LBs were detected (arrows, **Ci-iii**). No lesions were detected in control tissue (**Avi, Bvi** + **Civ**). In all regions studied, there were significantly more Parkinson's disease lesions detected in patients (**Avii, Bvii** + **Cv**). Scale bars: 10 μm. Error bars: +SEM. *=p<0.05;**=p<0.01; ****=p<0.0001. Student's *t* test.

neither PBs nor LBs (Figure 4.5Aiv). This suggests that AS-PLA is able to detect alpha-synuclein oligomerisation in cells very early in the aggregation process, even before the larger aggregates forming PBs appear. The majority of surviving neurons that lacked PBs or LBs did not have any AS-PLA staining (indicated in Figure 4.5Aiv adjacent to a neuron harbouring diffuse cytoplasmic AS oligomers), suggesting that alpha-synuclein self-interaction is not a physiological event occurring constitutively in all cells. In addition, no diffuse cytoplasmic AS-PLA signal was observed in controls, indicating that this type of staining is strictly pathological and may represent early aggregates that precede currently recognised pathology.

In contrast to the brainstem, cortical LBs in the cingulate cortex were strongly detected by AS-PLA (Figure 4.5C). Quantification of pathological lesions detected by AS-PLA in each region showed that no PD lesions were detected in tissue from control cases, confirming the association of these lesions with PD (Figure 4.5Avii, Bvii + Cv).

Currently, AS-IHC is the most widely used method for detection of PD pathology. In the brainstem, LBs were rarely stained by AS-PLA, in contrast to the widespread staining of LBs by AS-IHC. For example, a low magnification image of consecutive sections of the DMNV revealed extensive staining of LBs by AS-IHC (Figure 4.6A), whereas AS-PLA was much more selective, staining mainly PBs and extrasomal LBs, which are LBs localised outside the cell body (Figure 4.6B, arrows). Quantification of the number of lesions in the medulla and midbrain detected by both techniques supports this (Figure 4.7A + B). AS-PLA detected significantly more PBs than AS-IHC, suggesting AS-PLA more sensitively detects earlier lesions compared with AS-IHC. AS-IHC detected more lesions overall, suggesting the majority of the pathology is LBs, which is unsurprising as all patients were at least Braak stage III when the medulla and midbrain are already heavily affected.

Interestingly, in the cingulate cortex there was a strong correlation between the number of lesions detected by AS-PLA and AS-IHC ($p<0.001$), with a trend towards the detection of more lesions by AS-PLA compared to AS-IHC (Figure 4.7C), suggesting that not only are cortical LBs detected by both AS-PLA and AS-IHC, but that AS-PLA

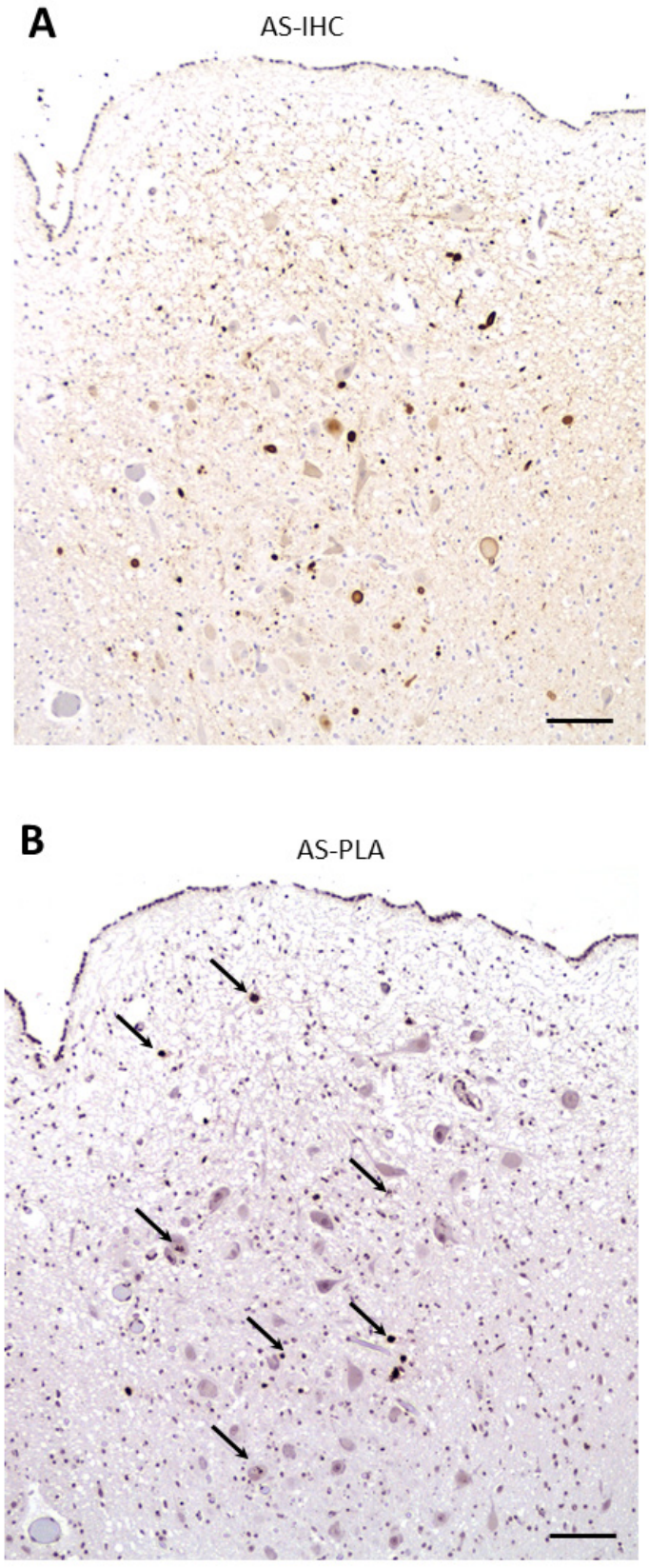

Figure 4.6. AS-PLA selectively detected early Parkinson's lesions, such as pale bodies, and not Lewy bodies. A low magnification image of the dorsal motor nucleus of the vagus from a Parkinson's patient reveals extensive LB pathology detected by AS-IHC (**A**), but the more selective detection of pale bodies and extrasomal LBs by AS-PLA (**B**, arrows). Scale bars: 50 µm.

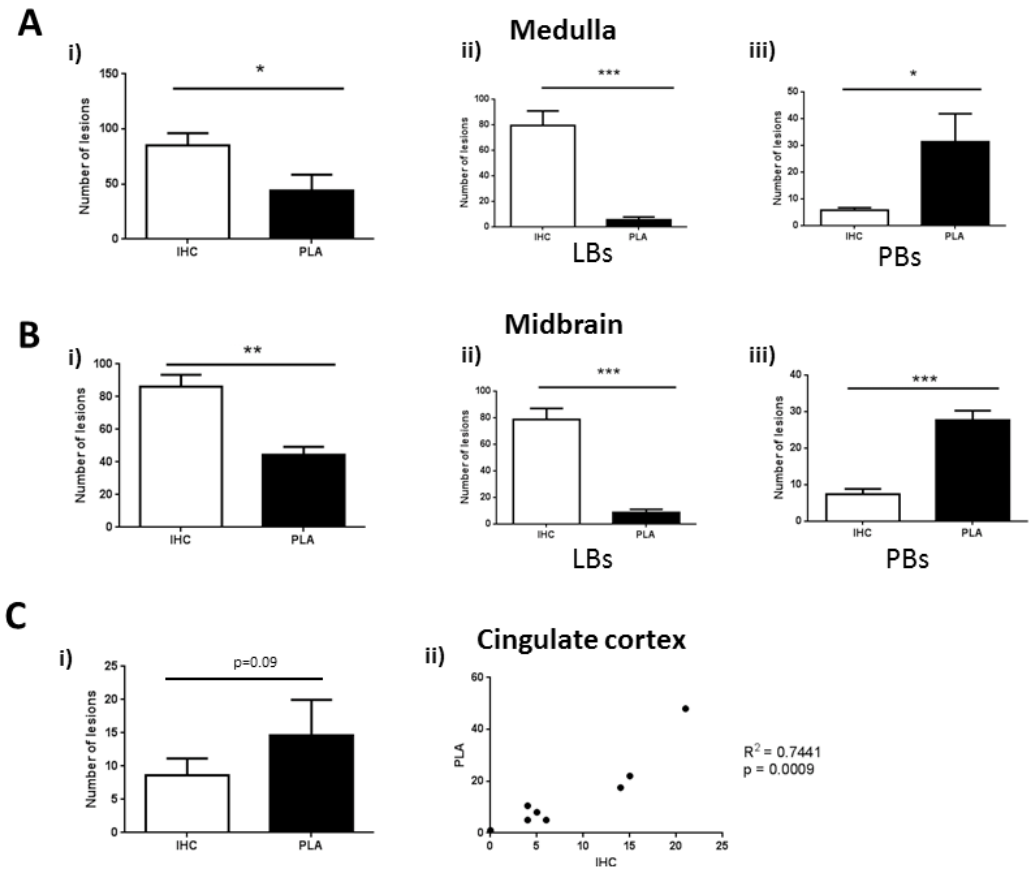

Figure 4.7. Early Parkinson's lesions were preferentially detected by AS-PLA. The total number of Parkinson's lesions detected by AS-PLA and AS-IHC were counted and compared in the medulla (**Ai**), midbrain (**Bi**) and cingulate cortex (**Ci**). The number of Lewy bodies or pale bodies stained using both techniques were compared in the medulla (**Aii+iii**) and midbrain (**Bii+iii**). In the cingulate cortex, Pearson's regression analysis revealed a correlation between the number of cortical Lewy bodies detected with AS-IHC and AS-PLA (**Cii**). *=p<0.05, **=p<0.01, ***=p<0.001. Student's *t*-test. N=8.

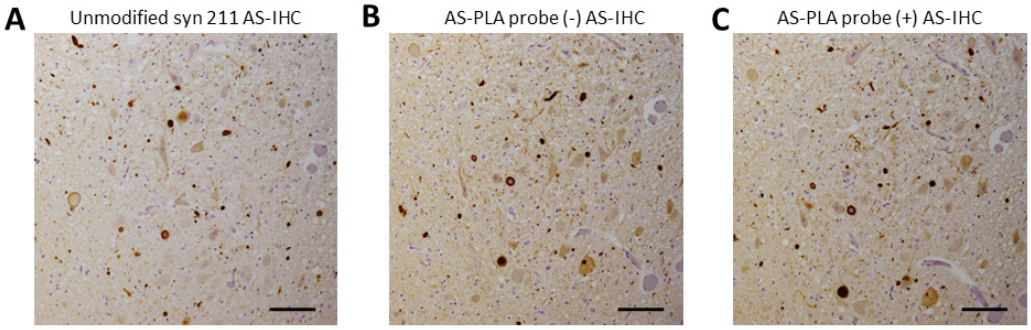

Figure 4.8. The conjugation process did not affect the recognition ability of syn211, used to produce the AS-PLA probes. Consecutive sections of medulla were stained with AS-IHC, using unmodified syn211 (**A**), or AS-PLA probe – (**B**) or + (**C**) as the primary antibody. Lewy bodies were strongly detected with all antibodies in the dorsal motor nucleus of the vagus of a Parkinson's patient. Scale bar: 100 µm. N=1.

displays more sensitivity for their detection.

The unmodified antibody and both AS-PLA probes strongly labelled brainstem LBs when used as a primary antibody for AS-IHC, demonstrating that the lack of brainstem LB staining by AS-PLA is not due to an inability of the antibody to access such structures nor due to ablation of antibody epitope recognition following its conjugation to oligonucleotides to produce the AS-PLA probes (Figure 4.8).

Next, it was investigated whether pathological lesions found in other neurodegenerative diseases were stained by AS-PLA. Cingulate cortex from patients with dementia with Lewy bodies (DLB), midbrain from multiple system atrophy (MSA) and progressive supranuclear palsy (PSP) cases, and hippocampus from Alzheimer's disease (AD) cases were stained. First it was confirmed that the selected regions were affected by pathological lesions of each disease using IHC (Figure 4.9A, B, C and D). Lesions from patients with DLB and MSA, known alpha-synucleinopathies, were stained by AS-PLA. In tissue from patients with DLB, cortical LBs were detected by AS-PLA (Figure 4.9A), similarly to LBs in the affected cortex of PD patients. In MSA cases, diseased glial cells harbouring glial cytoplasmic inclusions (GCIs) showed cytoplasmic labelling by AS-PLA at the periphery of GCIs similar to brainstem LBs in PD (arrows, Figure 4.9B). In contrast, tau inclusions in tissue from patients with PSP and tau neurofibrillary tangles and A-beta plaques from patients with AD were unstained (Figure 4.9C+D).

4.2.3 AS-PLA reveals previously unrecognised diffuse alpha-synuclein oligomeric pathology in the neuropil and white matter of specific anatomical nuclei

Further to the staining of early PD lesions, AS-PLA revealed a qualitatively distinct diffuse type of staining localised to specific neuroanatomical nuclei including areas usually mildly affected by classical PD pathology. This second type of AS-PLA staining was diffuse and located in the neuropil, clumping around neurons in the most severely affected areas, or less frequently in the white matter (Figure 4.11).

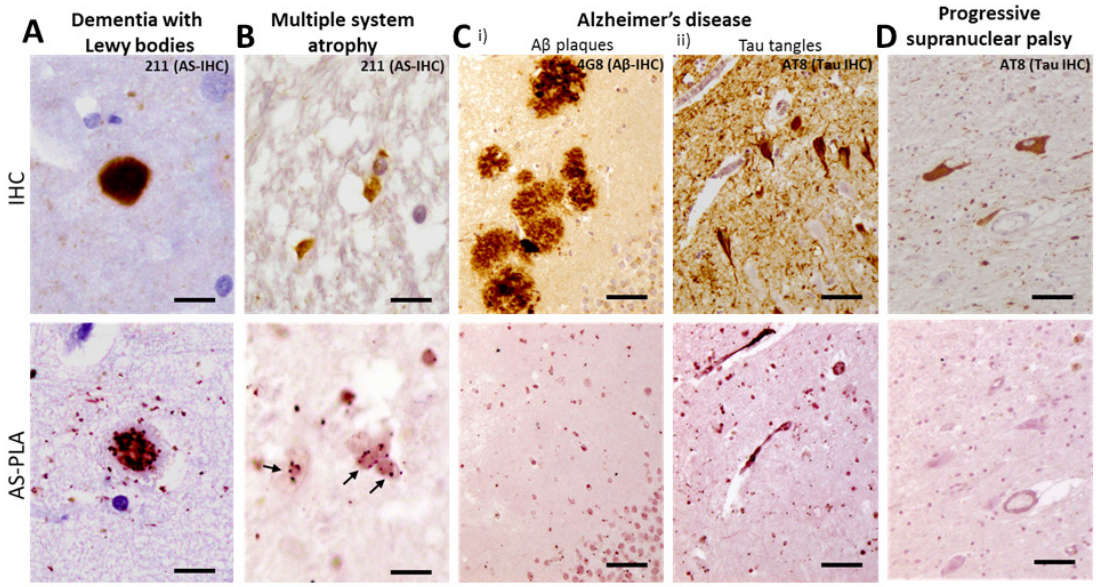

Figure 4.9. AS-PLA stained aggregates in dementia with Lewy bodies and multiple system atrophy but not Alzheimer's disease or progressive supranuclear palsy. Tissue from patients with dementia with Lewy bodies (**A**) and multiple system atrophy (**B**) was stained with AS-PLA and AS-IHC. Glial cytoplasmic inclusions stained on their periphery by AS-PLA in (**B**) are indicated by arrows. Alzheimer's disease tissue (**C**) was stained with 4G8 (**i**) for A-beta IHC or AT8 (**ii**) for tau IHC and AS-PLA. AT8 IHC was also used to stain progressive supranuclear palsy tissue (**D**). Scales bars: A+B – 12.5 µm, C+D - 50 µm. N=2.

In order to quantify the diffuse type of AS-PLA staining and evaluate its potential association with PD, the heaviness of diffuse AS-PLA staining was scored in blinded sections (Figure 4.10). PD patients specifically showed intense diffuse AS-PLA staining in the reticular formation (Figure 4.11Aii) and intermediate reticular zone (Figure 4.11Aiii) of the medulla, where the mean scores were 6.5- and 4.5-fold higher, respectively, than controls (Figure 4.11A + C), while in the cingulate cortex patients had a mean score 1.6-fold higher than controls (Figure 4.11B + E). Staining in the raphe in the medulla was 2.75-fold higher in patients on average, although this was not statistically significant (Figure 4.11C). In the midbrain, no region had a higher deposition of oligomers in patients compared to controls (Figure 4.11D). Several white matter tracts, including the corticospinal tract, the subcortical white matter of the cingulate gyrus and the corpus callosum showed a weak diffuse AS-PLA staining but not a pathological deposition of oligomers above the level of controls.

Next, diffuse AS-PLA staining was compared with AS-IHC staining in consecutive sections. The diffuse oligomeric pathology detected by AS-PLA did not correspond to any type of pathological staining that could be detected by AS-IHC including LBs and PBs (Figure 4.11A, adjacent panels). Furthermore, the diffuse neuropil oligomeric pathology did not correspond to physiological alpha-synuclein pre-synaptic staining (Figure 4.11B).

Western blot analysis of sequentially extracted alpha-synuclein from human brain tissue corroborated an accumulation of high molecular alpha-synuclein species in PD compared to controls, in keeping with the findings with AS-PLA (Figure 4.12). By western blot, it was demonstrated that an accumulation of a ~60 kDa oligomer and higher molecular species were present in the urea fraction, which contained aggregated proteins, in the midbrain and cingulate cortex of PD patients, while in the medulla only accumulation of the ~60 kDa oligomer was observed. The ~60 kDa oligomer also variably accumulated in the TBS soluble and Triton soluble fractions, which correspond to cytoplasmic and membrane-associated proteins, respectively, in the midbrain and medulla of PD patients.

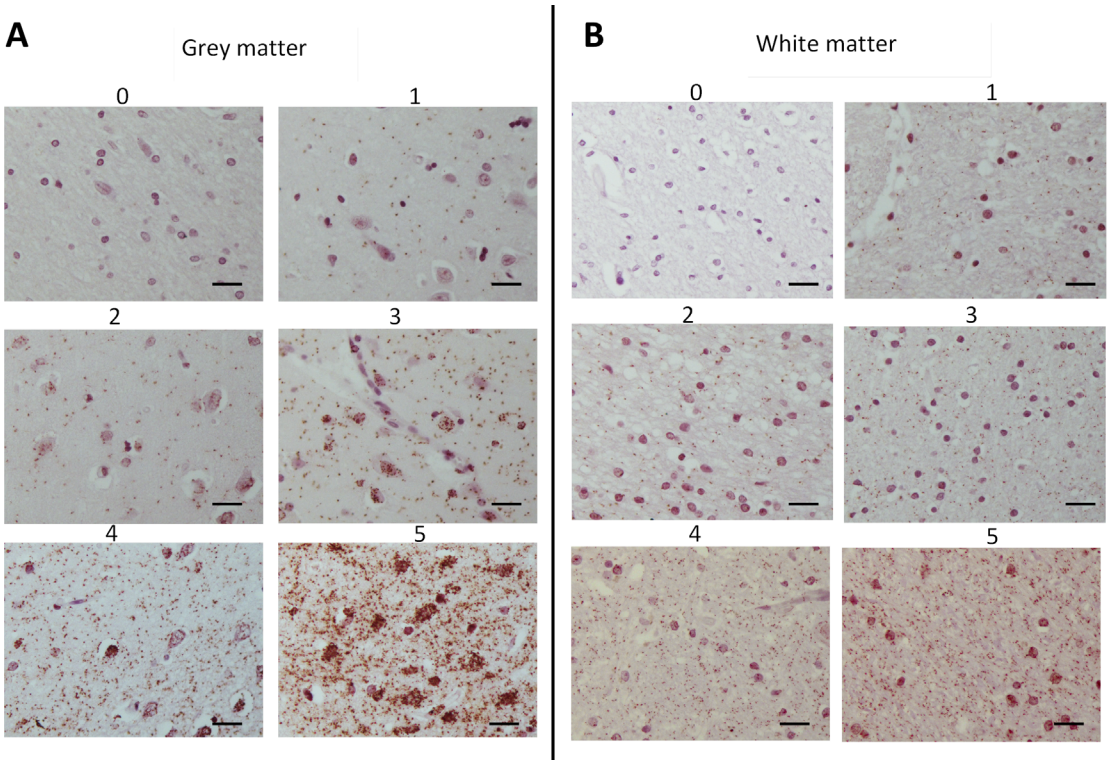

Figure 4.10. Scoring reference plates. Images were taken at 20x magnification that represented the spread of abundance of diffuse AS-PLA staining in grey (**A**) and white matter (**B**) and were assigned scores from 0 – 5, with a score of 5 indicating the presence of the strongest possible staining. The assessors used the plate when analyzing the slides to assign scores for the heaviness of diffuse AS-PLA staining to each area. Scale bars: 50 µm.

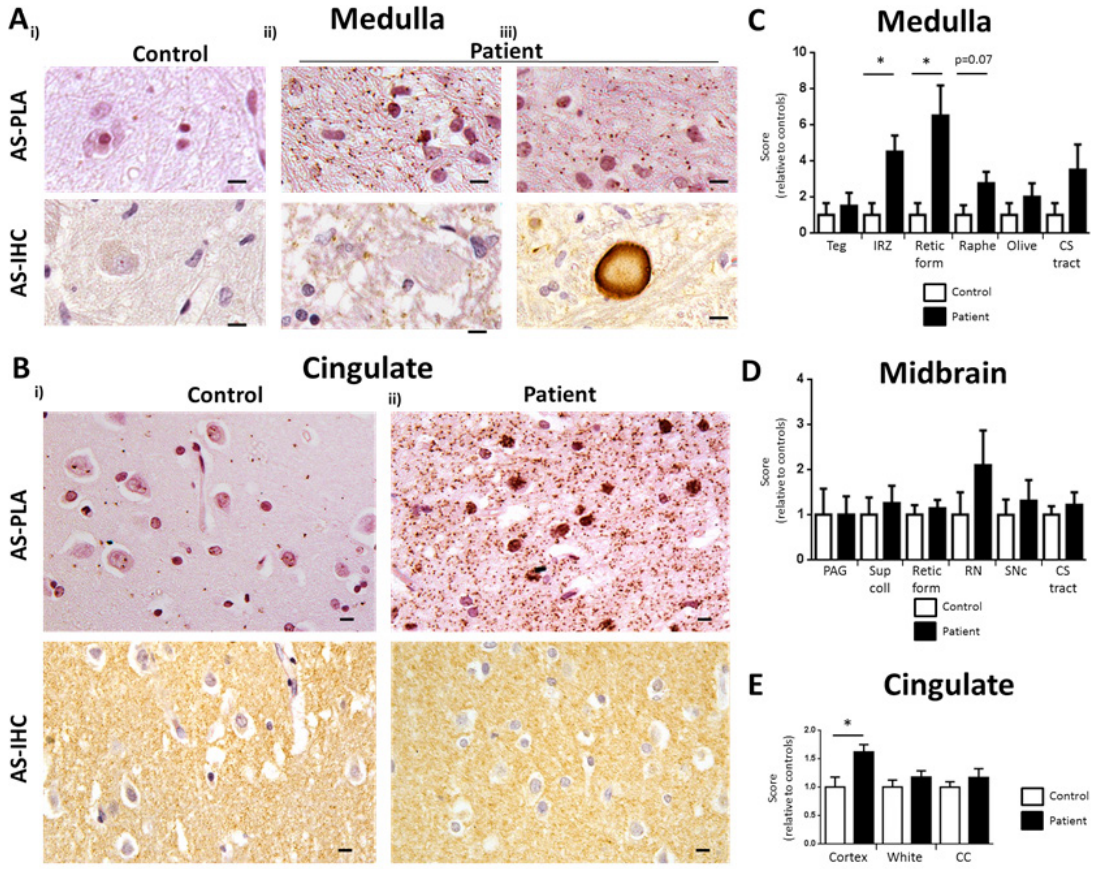

Figure 4.11. Previously unrecognised oligomeric pathology was revealed by AS-PLA. Striking diffuse AS-PLA staining was revealed in post-mortem brain sections. The heaviness of diffuse staining in blinded sections was scored semi-quantitatively by two independent assessors (RFR and Dr Javier Alegre-Abarrategui) against predefined standards. In the medulla, staining was most prominent in patients in the reticular formation (**Aii**), and intermediate reticular zone (IRZ, **Aiii**) in the patients, and contrasted with AS-IHC staining, where only pre-synaptic staining or Lewy bodies were stained (bottom panels). A significant difference between the heaviness of AS-PLA diffuse staining in patients and controls was scored in these regions (**C**). In the midbrain, there was no difference in the amount of staining in patients and controls (**D**). In the cingulate, strong staining was observed in the grey matter of patients (**B**) compared to the controls but no difference in AS-PLA signal was observed in the white matter and corpus callosum (**E**). Similar levels of AS-IHC synaptic staining were present in patients and controls (**B**). Scale bars: 10 μm. N=8. *=p<0.05 one-way ANOVA (Kruskal-Wallis) with Dunn's multiple comparisons test. Regions included in analyses in the medulla were the tegmentum (teg), intermediate reticular zone (IRZ), reticular formation (retic form), raphe, inferior olivary nucleus (olive) and corticospinal tract (CS tract). In the midbrain, the periaqueductal grey (PAG), superior colliculus (SC), reticular formation (retic form), red nucleus (RN), *substantia nigra pars compacta* (SNc) and corticospinal tract (CS tract) were analysed. In the cingulate gyrus, the cortex, subcortical white matter and corpus callosum (CC) were analysed.

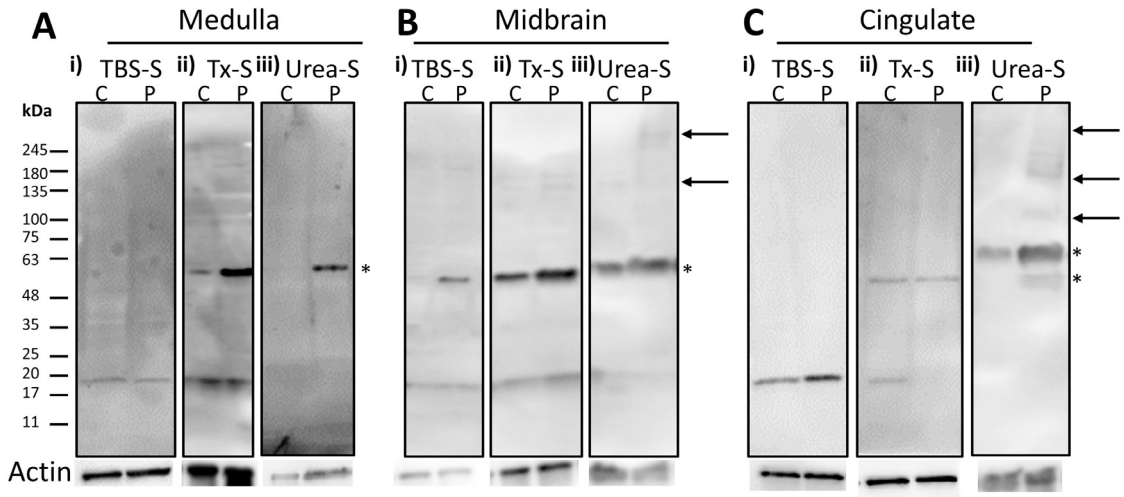

Figure 4.12. Oligomeric alpha-synuclein present in Parkinson's patients and controls was detected by western blot. Alpha-synuclein was sequentially extracted from human brain tissue, producing three fractions: TBS-S, containing cytoplasmic proteins, Tx-S, containing membrane-associated proteins and Urea-S, with aggregated proteins. The resulting lysates were resolved by SDS-PAGE and visualised by western blotting with the syn211 anti-alpha-synuclein antibody in the medulla (**A**), midbrain (**B**) and cingulate cortex (**C**). ~60 kDa oligomers (asterisks) and higher molecular species (arrows) accumulated in Parkinson's disease patient brain compared to controls. C: control, P: patient. N=3. Representative blots are shown.

4.2.4 The alpha-synuclein oligomeric species revealed by AS-PLA have a distinct intermediate sensitivity to proteinase K

To further understand the structural properties of the alpha-synuclein oligomeric species revealed by AS-PLA, their PK sensitivity was assessed. PK resistance is a property of highly aggregated proteins that usually display high beta-sheet content and is associated with amyloid-like misfolded proteins (Forloni, 1996, Neumann *et al.*, 2004). Sections of cingulate cortex tissue from patients and controls were treated with PK for 10 seconds, 1 minute or 2 minutes, as high levels of both cortical LBs and diffuse neuropil AS-PLA staining were found in this region. The PK sensitivity of the alpha-synuclein protein species detected by either AS-IHC or AS-PLA within cortical LBs of PD patients was studied first. As expected, a large proportion (~50%) of cortical LBs stained by AS-IHC showed PK resistance and were still present after harsh PK treatment (2 minutes, Figure 4.13Ai + B). Occasional dystrophic neurites were also stained by AS-IHC after 2 minutes PK treatment (Figure 4.13Ai). In contrast, the protein species stained by AS-PLA within cortical LBs were consistently more sensitive to PK treatment, and no staining was present after 2 minutes of PK digestion (Figure 4.13Aii), which quantification (Figure 4.13B) showed was significantly different from the response of AS-IHC stained cortical LBs to PK.

The PK sensitivity of the alpha-synuclein species detected by AS-PLA and AS-IHC in the neuropil was studied next. The diffuse alpha-synuclein oligomeric species stained by AS-PLA were moderately sensitive to PK treatment and an intermediate PK treatment (1 minute, Figure 4.13Aiii + C) abolished diffuse AS-PLA signal. Physiological AS-IHC pre-synaptic staining in both patients and controls was PK sensitive and removed after only 10 seconds' exposure to PK (Figure 4.13Aiv + C). This suggests that AS-PLA stained oligomers are in an early stage of aggregation due to their intermediate PK resistance (Figure 4.13D).

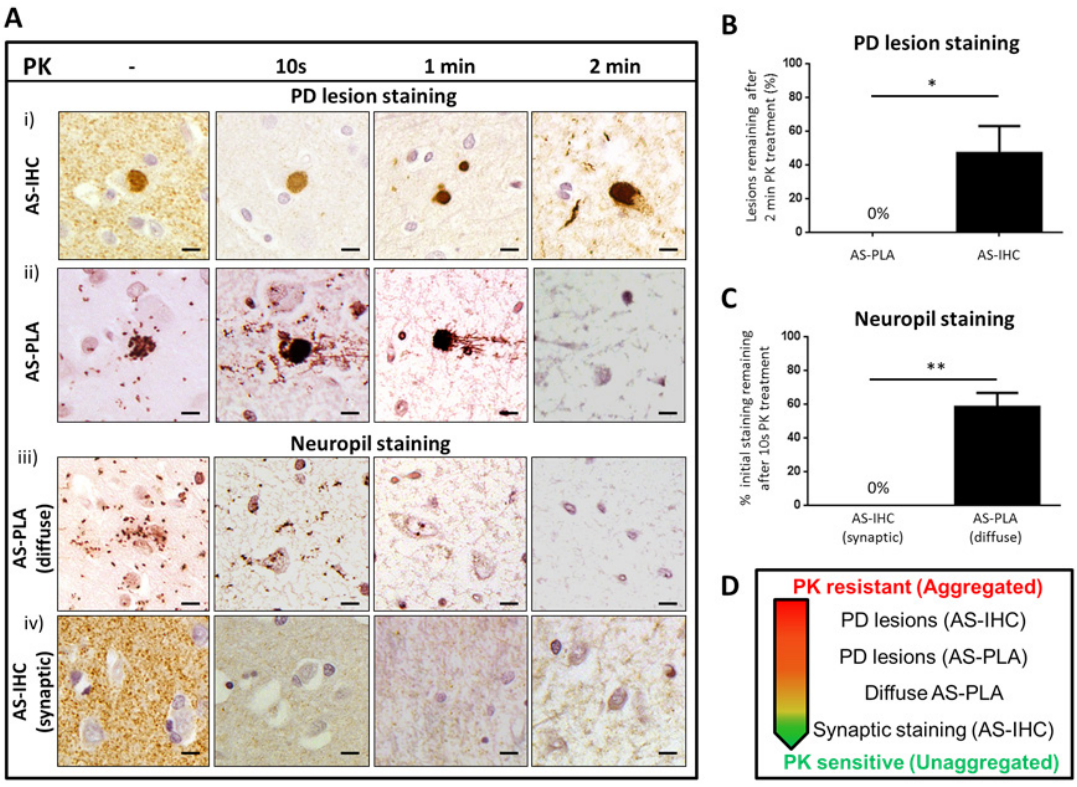

Figure 4.13. AS-PLA displayed a different profile of PK sensitivity to synaptic and pathological staining detected by AS-IHC. Tissue from the cingulate cortex of 3 patients and 3 controls was exposed to proteinase K for the indicated times and stained with AS-PLA or AS-IHC. Cortical LBs in patients were PK resistant and still remained after 2 minutes of PK treatment (**Ai + B**). In contrast, AS-PLA detection of cortical LBs was abolished after 2 minutes of PK treatment (**Aii + B**). AS-PLA diffuse staining was no longer present after 1 minute of PK treatment (**Aiii + C**). AS-IHC synaptic staining was removed after 10 seconds of PK treatment (**Aiv + C**). Therefore, oligomers detected by AS-PLA have a distinct intermediate resistance to PK (**D**). N=3. Student's *t* test. *=p<0.05, **=p<0.01. Scale bars: 10 μm.

4.2.5 Disease progression correlates of AS-PLA signal

In order to further delineate the relationship between the oligomeric species detected by AS-PLA and PD, analyses of the association of AS-PLA signal load and disease onset and progression were undertaken. There was no significant association between disease duration and either type of AS-PLA signal (Figure 4.14A). A correlation approaching significance ($p=0.057$) was found between the number of PD lesions detected by AS-PLA in the cingulate and age at onset of PD, while there was a significant association between diffuse signal and age at onset in the medulla (Figure 4.14B). However, the number of PD lesions detected by AS-PLA in the medulla and cingulate gyrus significantly correlated with the age at death (Figure 4.14C). Interestingly, there was a negative correlation between the diffuse signal and age at death in controls in the midbrain and a trend approaching significance in the cingulate gyrus. A positive correlation between age at death and AS-PLA diffuse signal was observed in the medulla of patients (Figure 4.14C).

The effect of age at death on AS-PLA signal in PD patients was not due to longer disease duration in the older cases nor to more advanced disease with age, as there was no correlation found between age at death and disease duration or Braak stage (Figure 4.14D).

The generation of AS-PLA signal is unlikely to be an artefact due to post-mortem interval as there was no correlation between either type of AS-PLA signal in any region with post-mortem interval (Figure 4.14E).

A **Disease duration**

i) PD lesions

	Medulla	Midbrain	Cingulate
Patients only	0.1211	0.0009	0.0119

ii) Diffuse

	Medulla	Midbrain	Cingulate
Patients only	0.01296	0.3471	0.1129

B **Age at onset**

i) PD lesions

	Medulla	Midbrain	Cingulate
Patients only	0.255	0.2779	0.4798 (p=0.057)

ii) Diffuse

	Medulla	Midbrain	Cingulate
Patients only	0.6029 (*)	-0.366	0.1554

C **Age at death**

i) PD lesions

	Medulla	Midbrain	Cingulate
Patients only	0.5301 (*)	0.2396	0.5973 (*)

ii) Diffuse

	Medulla	Midbrain	Cingulate
All cases	0.2421 (p=0.053)	-0.2577 (p=0.053)	-0.0002
Controls only	0.0802	-0.7227 (**)	-0.4829 (p=0.056)
Patients only	0.7703 (**)	-0.0145	0.4429

D

	Braak stage	Disease duration
Age	0.0285	0.1498
Age at onset	0.0001	0.1206

E **Post-mortem interval**

i) PD lesions

	Medulla	Midbrain	Cingulate
Post-mortem interval (h)	-0.08228	-0.01979	-0.0073

ii) Diffuse

	Medulla	Midbrain	Cingulate
Post-mortem interval (h)	-0.1191	0.0312	-0.0496

Figure 4.14. Regression analysis of AS-PLA staining and disease progression. Correlation between disease duration (**A**), age at onset (**B**) or age at death (**C**) and AS-PLA staining (number of PD lesions stained, **i**, or diffuse staining, **ii**), between age at onset or age at death and Braak stage or disease duration (**D**) and between post-mortem interval and AS-PLA staining (**E**, number of PD lesions stained, **i**, or diffuse staining, **ii**) was analysed using Pearson's correlation coefficient. The R^2 value is shown and statistical significance is shown in brackets by *=p<0.05, **=p<0.01, ***=p<0.001. N=8.

4.2.6 Pathological correlates of AS-PLA signal

According to the Braak hypothesis (Braak *et al.*, 2003), PD pathology proceeds caudo-rostrally, reaching the cortex at stage IV, following brainstem and limbic regions, while the neocortex is only affected at the late stages V and VI. AS-PLA can detect earlier pathology than AS-IHC and therefore whether AS-PLA signal load in brainstem and limbic nuclei was associated with the presence of PD pathology in the cortex or neocortex was studied. There was no difference in the levels of either type of AS-PLA signal in any region between patients with or without cortical or neocortical pathology (Figure 4.15A + B). AS-PLA stained PD lesions in the cingulate gyrus were present in patients reported to have no cortical pathology (Figure 4.15Aii), again suggesting that AS-PLA is superior at detecting early PD lesions compared to AS-IHC.

Many PD patients present neuropathologically with co-existent A-beta or tau pathology (Joachim *et al.*, 1987, Mastaglia *et al.*, 2003, Pletnikova *et al.*, 2005, Wills *et al.*, 2010). The functional consequences are far from being fully understood, although the load of amyloid-beta plaques and neurofibrillary tangles have been shown to correlate better with cognitive decline than cortical LB scores (Compta *et al.*, 2011). *In vitro,* tau and alpha-synuclein synergistically promote aggregation of each other (Giasson *et al.*, 2003). Therefore, the load of alpha-synuclein oligomers may be related to the levels of such pathology. However, no association was found between AS-PLA signal and the presence of A-beta or tau pathology (Figure 4.15C + D).

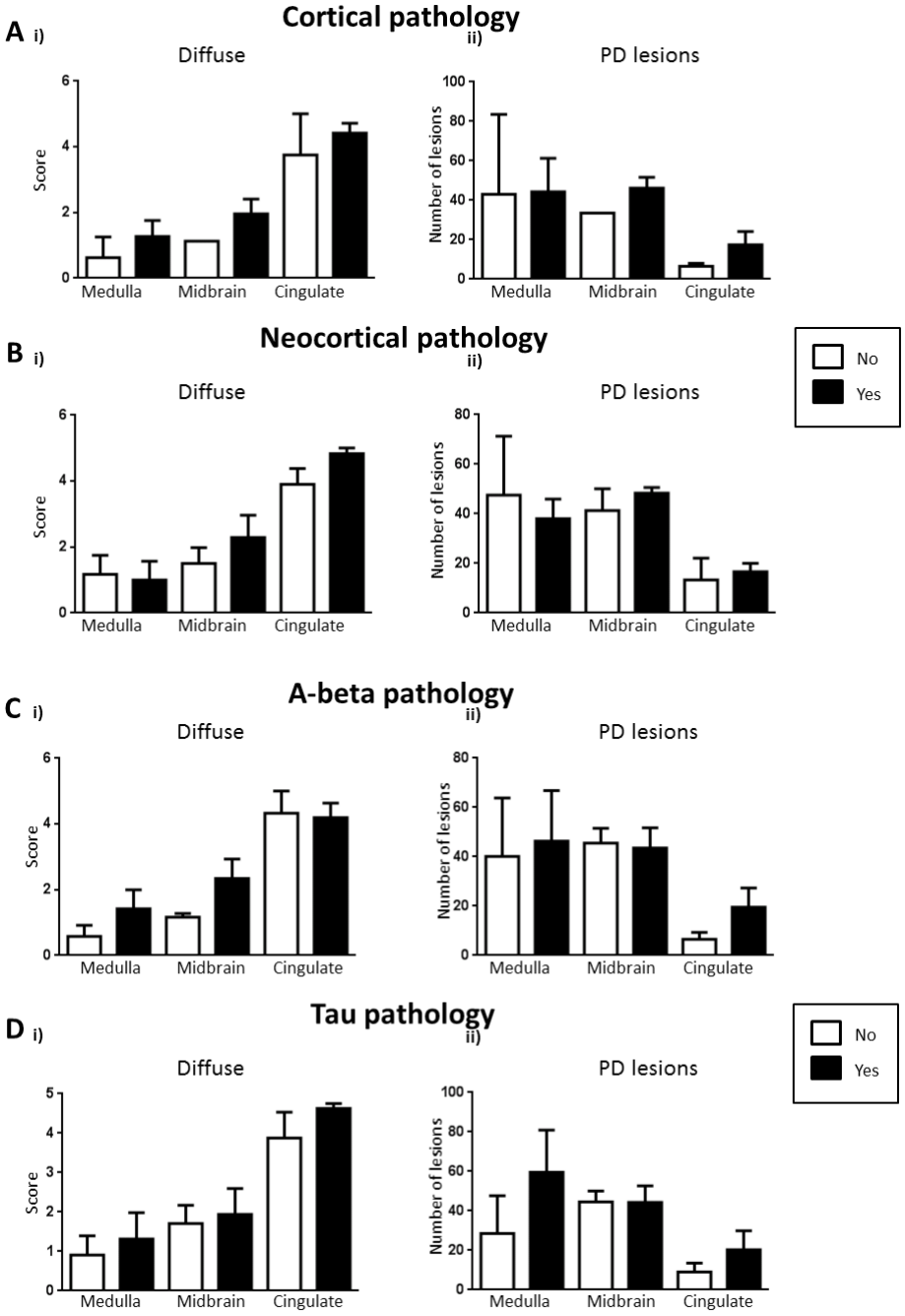

Figure 4.15. Pathological correlates of AS-PLA signal. The association between patients with (black bars) or without (white bars) cortical pathology (**A**), neocortical pathology (**B**), A-beta pathology (**C**) or tau pathology (**D**) and AS-PLA signal (number of PD lesions stained, **i**, or diffuse staining, **ii**) was analysed in 8 patients.

4.2.7 AS-PLA reveals early oligomeric pathology in the SNCA-OVX mouse model of PD

Our laboratory has generated a BAC transgenic mouse model of PD that over-expresses human alpha-synuclein at twice the level of endogenous mouse alpha-synuclein on an endogenous *SNCA* knock-out background (*SNCA*-OVX). These animals show early non-motor phenotypes, including gut abnormalities, and age-related nigral cell loss, motor deficits and dopamine transmission defects (Janezic *et al.*, 2013). These animals do not develop alpha-synuclein inclusions but alpha-synuclein oligomers are detected in the midbrain by native western blotting in animals as young as 3 months old (Janezic *et al.*, 2013).

In order to study the formation of alpha-synuclein oligomers in these animals *in situ,* AS-PLA signal in tissue from *SNCA*-OVX animals aged 3 and 24 months was compared with those expressing human alpha-synuclein at low to moderate levels (hWT; Figure 4.16). As a negative control *SNCA* knock-out mice (KO) were used. Using the scoring system developed to analyse AS-PLA staining of human tissue (Figure 4.10), five regions were analysed: *substantia nigra* (SN), pons, striatum, hippocampus and cortex. For each neuroanatomical region, the score assigned for diffuse AS-PLA signal was for the area of highest intensity staining that filled one whole field of view at 20x magnification.

Heavy accumulation of alpha-synuclein oligomers was observed in the SN of 24 month old *SNCA*-OVX animals (Figure 4.16Biii + iv). No AS-PLA staining above the background levels in KO animals was present in the hWT animals and scoring analysis revealed a significant increase in AS-PLA signal in the *SNCA*-OVX animals compared to both hWT and KO animals. In 3 month old animals, there was a trend towards more abundant AS-PLA in the SN of *SNCA*-OVX animals, although this was not significant (Figure 4.16A).

In the pons, there was a similar accumulation of oligomers with age but the increased oligomeric loads in the *SNCA*-OVX mice compared to the other genotypes at 24 months of age did not reach significance (Figured 4.17A). In the striatum (Figure

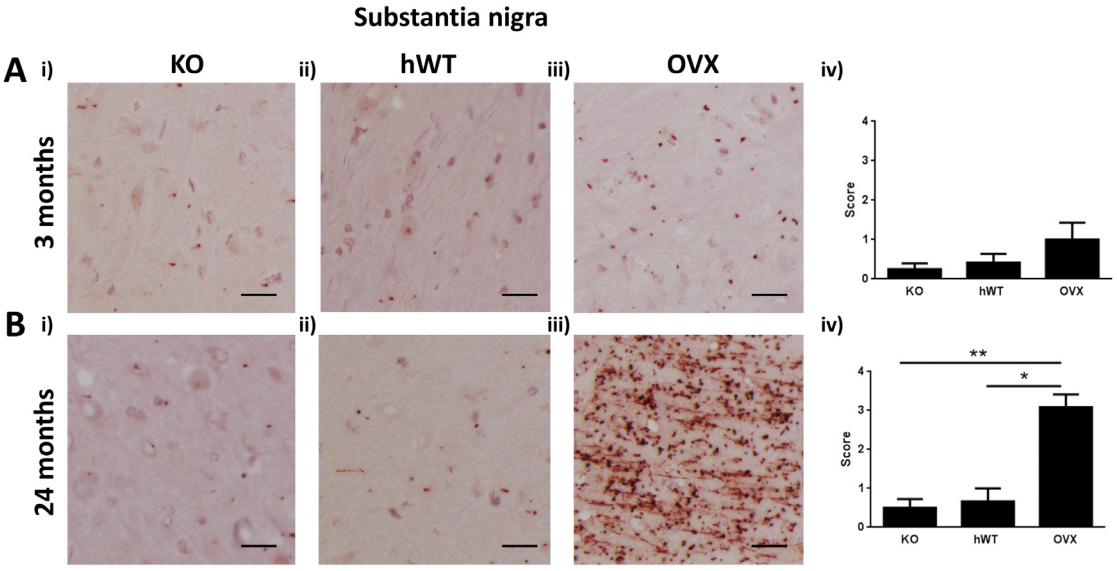

Figure 4.16. Age-dependent accumulation of alpha-synuclein oligomers in the *substantia nigra* of *SNCA*-OVX mice. 3 month old (**A**) and 24 month old (**B**) mice lacking alpha-synuclein (**i**, KO), expressing human alpha-synuclein at the same levels as human brain (**ii**, hWT) or over-expressing human alpha-synuclein at twice endogenous mouse levels, *SNCA*-OVX (**iii**, OVX) were stained with AS-PLA. The heaviness of AS-PLA diffuse staining in the SN was analysed semi-quantitatively (**iv**). N=3. One-way ANOVA (Kruskal-Wallis) with Dunn's multiple comparisons test. *=p<0.05, **=p<0.01. Scale bars: 20 µm.

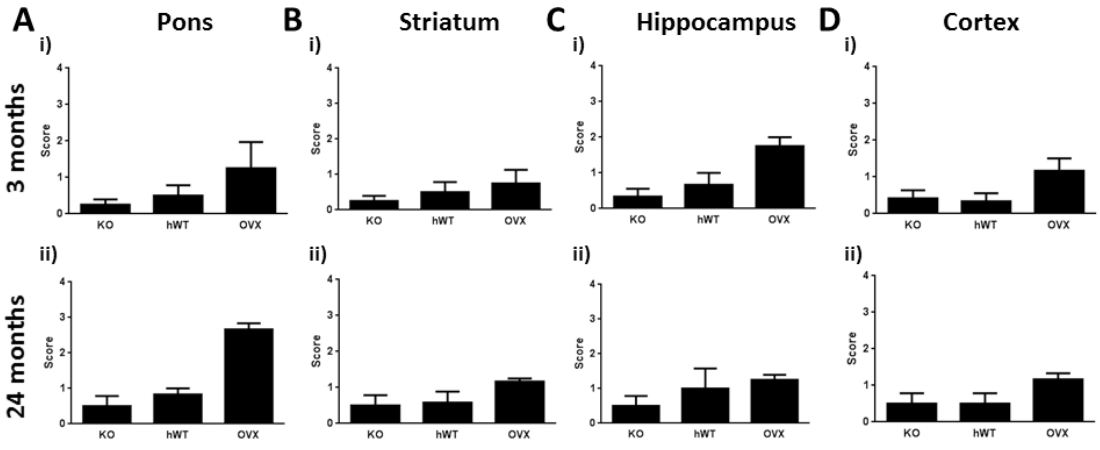

Figure 4.17. Further neuroanatomical analysis of AS-PLA staining in *SNCA*-OVX mice. The heaviness of AS-PLA diffuse staining in KO, ha-syn and OVX mice was analysed semi-quantitatively in the pons (**A**), striatum (**B**), hippocampus (**C**) and cortex (**D**) in 3 month old (**i**) and 24 month old (**ii**) animals. N=3. One-way ANOVA (Kruskal-Wallis) with Dunn's multiple comparisons test.

4.17B), hippocampus (Figure 4.17C) and cortex (Figure 4.17D) there were no significant differences between the genotypes at either age.

The region-specific, age-dependent accumulation of alpha-synuclein oligomers exclusively in the *SNCA*-OVX animals, which develop PD-like phenotypes, suggests AS-PLA has revealed pathologically related oligomers. Furthermore, previous unpublished work in our lab has shown that there is no change in alpha-synuclein expression with age in any of these animals, suggesting the difference in AS-PLA signal is not due to changes in alpha-synuclein expression and instead due to an increase in alpha-synuclein oligomers.

4.3 Discussion

In this chapter I have demonstrated that AS-PLA reveals early oligomeric pathology in PD patient tissue and provided the first direct evidence that alpha-synuclein self-interaction is a key pathological marker in diseased brain.

Following the optimisation of brightfield AS-PLA for human tissue, it was found that AS-PLA preferentially, and more sensitively compared to AS-IHC, detects early PD lesions such as PBs. Brainstem LBs were rarely stained, which is likely due to their composition of fibrillar alpha-synuclein: in the previous chapter I showed that AS-PLA specifically recognized alpha-synuclein oligomers over fibrils *in vitro*. Staining on the periphery of brainstem LBs was more frequent, which may represent the incorporation of oligomers from the cytoplasm into the fibrillar structure of LBs, a potential protective mechanism to sequester toxic species away from the cellular machinery (Bucciantini *et al.*, 2002, Muchowski, 2002, Soto and Estrada, 2008). Conversely, AS-PLA staining on the periphery of brainstem LBs could be oligomers disassociating from LBs as a dynamic equilibrium has been proposed to exist between fibrils in LBs and alpha-synuclein oligomers (Bosco *et al.*, 2011, Cremades *et al.*, 2012). The strong staining of cortical LBs, which do not have the classical core-halo structure of brainstem LBs and are believed to contain less compact aggregates (Kosaka, 1978, Katsuse *et al.*, 2003), and PBs suggests that AS-PLA detects oligomers in the *process* of being compacted

and not those that are already extensively fibrillar in structure as in brainstem LBs.

Cortical LBs in DLB were positively stained by AS-PLA similarly to PD, suggesting that PD and DLB belong to the same disease spectrum, as previously proposed (McKeith, 2000). While neurofibrillary tangles and amyloid plaques in AD and tau inclusions in PSP were negatively stained by AS-PLA, positive cytoplasmic staining around GCIs was found in MSA tissue. This suggests that similar protein species are formed in three alpha-synucleinopathies (PD, DLB and MSA), which warrants future investigation.

The association of alpha-synuclein self-interaction with pathogenesis is supported by the identification of extensive diffuse oligomeric pathology in specific neuroanatomical regions in patients using AS-PLA that had no AS-IHC counterpart in the form of PD lesions nor in physiological synaptic AS-IHC staining. This type of pathology was most abundant in patients in areas mildly affected by LB pathology, such as the intermediate reticular zone and the reticular formation of the medulla and the cingulate cortex. It is possible that the striking deposition of alpha-synuclein oligomers in the neuropil represents aberrant oligomerisation at the synapse or abnormal transport of pathological species along axons to the cell body. Dysfunction at synapses and altered axonal transport have been postulated to be some of the earliest pathological events in PD (Schulz-Schaeffer, 2010, Kim-Han *et al.*, 2011, Nakata *et al.*, 2012). Consistent with these pathological features, extensive diffuse AS-PLA signal was also found in patients in white matter tracts such as those in the medullary reticular formation.

Intriguingly, a small amount of AS-PLA-stained oligomers were also found in specific white matter tracts including the corticospinal tract, the subcortical white matter of the cingulate gyrus and the corpus callosum in some controls. The white matter tracts containing AS-PLA-stained alpha-synuclein oligomers in some controls are either composed of long projection axons, or are adjacent to or projecting to nuclei where striking accumulations of oligomers were found exclusively in patients, suggesting oligomer accumulation in white matter tracts may represent very early sub-clinical pathology.

Diffuse AS-PLA oligomeric pathology is likely to be a precursor to recognised neuritic and perikaryal pathology. Diffuse cytoplasmic alpha-synuclein oligomers were also detected by AS-PLA in neurons of otherwise normal appearance. Their detection is indicative of the capacity of AS-PLA to detect very early alpha-synuclein oligomerisation in neurons, even before the appearance of PBs or LBs. These accumulations may be related to punctate alpha-synuclein aggregates or perikaryal threads previously described (Arima *et al.*, 1998, Kuusisto *et al.*, 2003), which are hypothesised to progressively coalesce into PBs, in which alpha-synuclein and other proteins are further compacted to become LBs (Dale *et al.*, 1992, Gomez-Tortosa *et al.*, 2000, Kuusisto *et al.*, 2003, Kanazawa *et al.*, 2012).

The structural properties of the oligomeric species detected by AS-PLA were studied using PK digestion and they were demonstrated to display an intermediate PK sensitivity. This PK resistance profile suggests AS-PLA-stained oligomers are in a very early stage of aggregation and are clearly folded differently than physiological pre-synaptic alpha-synuclein, but have not yet acquired a highly compact structure resistant to prolonged digestion by PK**.**

There was no association between disease duration and AS-PLA signal. However, the disease duration is reported from the time the patient presents at clinic and therefore each patient is unlikely to have the start of the disease recorded at the same neuropathological stage of the disease.

The association between age at onset or age at death and diffuse signal in the medulla, as well as age at death and the number of PD lesions detected by AS-PLA in the medulla and cingulate gyrus, may reflect the increasing severity and rapidity of progression of the disease in old onset PD (Halliday *et al.*, 2011). Conversely, the negative correlation between the diffuse signal in midbrain of controls and their age at death may reflect an increased ability of those aged persons who do not develop PD to deal with accumulation of alpha-synuclein oligomers.

Finally, using AS-PLA, a region-specific, age-dependent accumulation of alpha-synuclein oligomers was revealed in *SNCA*-OVX mice. The abundant oligomeric pathology in the SN arises as the dopaminergic neurons in that area degenerate, resulting in a 30% decrease in the number of nigral neurons by 18 months of age (Janezic *et al.*, 2013). Although LBs do not develop in this model, signs of pathological protein accumulation *in situ* have been identified using AS-PLA. A further study analysing the accumulation of oligomers over the lifetime of these mice will help to unravel the relationship of alpha-synuclein oligomers to the degeneration observed in the SN and other phenotypes, such as the dopamine release deficit in the dorsal striatum (Janezic *et al.*, 2013). Furthermore, gene therapy approaches targeting alpha-synuclein that are being developed in our lab will help to address the question of oligomeric toxicity in this model.

Together, the results presented in this chapter show the detection of early oligomeric pathology in PD tissue and tissue from a PD model and demonstrate that AS-PLA is the ideal technique for the study of oligomeric pathology and the role of alpha-synuclein self-interaction in PD.

5. Screening for inhibitors of alpha-synuclein oligomerisation

5.1 Introduction

5.1.1 Alpha-synuclein oligomers as a therapeutic target for PD

Current treatments for PD only target the symptoms and do not prevent the progression of the disease, leaving a pressing need for disease-modifying therapies. The identification of pathological processes that occur in PD, particularly at the early stages of the disease, informs therapeutic targets. Alpha-synuclein oligomers have been shown to mediate neuronal toxicity in a variety of rodent and cellular model systems (Danzer *et al.*, 2007, Nasstrom *et al.*, 2011, Winner *et al.*, 2011) and are hypothesised to be responsible for the spread of PD pathology between neuroanatomically connected brain regions (Hansen *et al.*, 2011, Luk *et al.*, 2012, Masuda-Suzukake *et al.*, 2013). Therefore, they represent an ideal therapeutic target: preventing their formation may delay disease progression and perhaps even ameliorate neuronal health in areas already affected by pathology.

As previously discussed, alpha-synuclein oligomers are formed by the self-interaction of alpha-synuclein molecules. Therefore, preventing such interactions is an ideal strategy to inhibit the formation of alpha-synuclein oligomers. Molecules that can disrupt protein-protein interfaces are required for this approach.

5.1.2 Targeting alpha-synuclein oligomers

Peptides that target the interface between interacting proteins have previously been used to inhibit protein-protein interactions (Sillerud and Larson, 2005, Sandomenico *et al.*, 2009). Furthermore, specific peptide inhibitors of alpha-synuclein aggregation that centre on residues 69 – 72 have been identified (Bodles *et al.*, 2004, El-Agnaf *et al.*, 2004). However, peptides do not display pharmacokinetic properties, such as

blood brain barrier permeability, suitable for therapeutic candidates and they are not amenable to chemical modification to improve the strength of binding to the target and the specific activity, unlike small molecule compounds (Blazer and Neubig, 2009). An emerging class of small molecules is protein-protein interaction inhibitors (PPIs). Although protein interaction interfaces are large (750 – 1500 Å) and do not contain 'pockets' usually identified for small molecule targeting, it has been shown that there are 'hot-spots' on the interface that contribute a large proportion of the binding energy and therefore provide targets for small molecules (Bogan and Thorn, 1998). Several protein-protein interactions associated with cancer have been targeted with PPIs, including Bak/Bcl and Myc/Max (Arkin and Wells, 2004, Pagliaro *et al.*, 2004). PPIs tend to be rich in aromatic rings to produce bulky molecules that are able to disrupt the interface of a protein-protein interaction (Pagliaro *et al.*, 2004).

The structural features of known PPIs are similar to polyphenols such as curcumin, quercetin, (-)-epigallocatechine gallate (EGCG) and baicalein, all of which have been shown to inhibit alpha-synuclein aggregation. Curcumin can prevent the formation of both oligomers and fibrils (Pandey *et al.*, 2008, Ahmad and Lapidus, 2012, Herva *et al.*, 2014), while quercetin, baicalein and EGCG have been shown to inhibit the formation of fibrils and disaggregate pre-existing fibrils, resulting in the formation of stabilised intermediate oligomeric species (Zhu *et al.*, 2004, Bieschke *et al.*, 2010, Zhu *et al.*, 2013). Interestingly, the alpha-synuclein oligomers formed as a result of EGCG treatment were not toxic to mammalian cells in culture (Bieschke *et al.*, 2010), suggesting not all oligomeric conformers are associated with disease *per se*. Furthermore, in an independent study quercetin, baicalein and EGCG were shown to disaggregate and inhibit the formation of alpha-synuclein oligomers (Caruana *et al.*, 2011) suggesting the anti-aggregation effects of such compounds may be specific to particular oligomeric species.

Dopamine and its analogues have also been shown to inhibit the formation of, and disaggregate, alpha-synuclein fibrils by stabilising oligomeric and protofibrillar species (Conway *et al.*, 2001, Li *et al.*, 2004, Latawiec *et al.*, 2010). Indeed, dopamine is often used to produce oligomeric species of alpha-synuclein for analysis (Lee *et al.*, 2011)

and is therefore not a suitable molecule for consideration as a starting compound for the screen described in this chapter, which aims to identify inhibitors of alpha-synuclein oligomerisation.

5.1.3 Measuring alpha-synuclein oligomerisation

In order to identify compounds that can prevent alpha-synuclein oligomerisation, a read-out of the levels of alpha-synuclein self-interaction and alpha-synuclein oligomers is required. The majority of inhibitors of alpha-synuclein aggregation have been identified in experimental paradigms using aggregates produced from recombinant alpha-synuclein. Therefore, in these studies the inhibitors were examined in conditions of alpha-synuclein in isolation and not in the complex cellular milieu. To obtain findings in a more relevant context, a cellular system was chosen for the initial screen.

Bimolecular fluorescence complementation assays (BiFC, as described in Chapter 3) provide simple read-outs of protein-protein interactions (Shyu *et al.*, 2006). Non-fluorescent halves of GFP (or a fluorescent protein of choice) are fused to the protein(s) of interest and only upon their self-interaction can GFP be reconstituted and fluoresce. Therefore, fluorescence intensity provides an index of the levels of complex formation between the protein(s) of interest. BiFC has previously been used to screen for inhibitors of the interaction between Beclin1 and Bcl2, which is required for autophagy, for the suppression of influenza A virus replication (Dai *et al.*, 2013) and for inhibitors of HIV-1 viral protein R dimerisation (Zych *et al.*, 2013).

In Chapter 3, I demonstrated that alpha-synuclein BiFC constructs form oligomers, by western blotting and AS-PLA recognition. The alpha-synuclein BiFC assay will provide a fluorescent read-out of alpha-synuclein oligomerisation and hits will be compounds that decrease BiFC signal. Unlike the reversible luciferase protein complementation assay (Remy and Michnick, 2006), the formation of the full fluorescent protein in BiFC is irreversible. Therefore, in this chapter the aim is to identify compounds that prevent the *formation* of alpha-synuclein oligomers.

5.1.4 Aims of the chapter

1. To miniaturise and validate the alpha-synuclein BiFC assay for screening.

2. To screen for compounds that can prevent the formation of alpha-synuclein oligomers using the BiFC assay.

3. To investigate potential hits arising from the initial compound screen by dose response analysis.

5.2 Results

5.2.1 Miniaturisation and optimisation of the alpha-synuclein BiFC assay for screening

Alpha-synuclein BiFC was used as a read-out for alpha-synuclein oligomerisation, allowing fluorescence to be quantified as an index of the level of alpha-synuclein oligomers in cells. Using the constructs described in Chapter 3 and Figure 3.1, the assay was miniaturised for use in 96 well plates. To ensure consistency between wells, HEK293 cells were seeded and transfected at the same time. Two different transfection protocols (JAA and LF), which differed in how the transfection complexes and cells were plated (see section 2.17.2), and various cell densities were used and their transfection efficiencies were compared using fluorescence microscopy and fluorescence intensity quantification using ImageJ (Figure 5.1). The protocol JAA with 100,000 cells per well resulted in the highest fluorescence, and therefore transfected cells, after 48 hours, and continued to produce high levels of fluorescence at later time points (Figure 5.1Ai + B). Therefore, this transfection protocol and cell density were chosen for further experiments.

In order to allow unbiased quantification of BiFC fluorescence in live cells, a fluorescent plate reader (BioTek Synergy HT) was trialled in further experiments. However, the plate reader was unable to detect fluorescence in BiFC transfected HEK293 cells above background fluorescence in untransfected wells (Figure 5.2A). As a positive

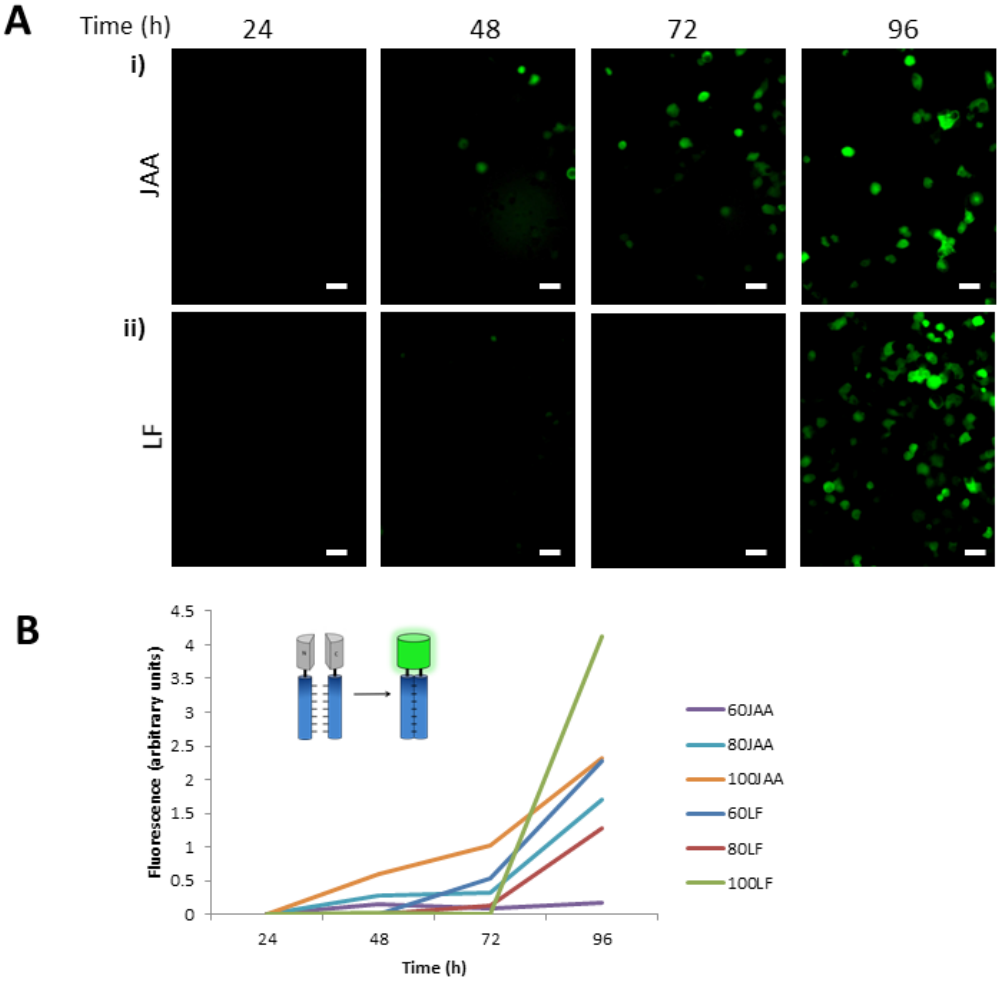

Figure 5.1. Miniaturisation of alpha-synuclein BiFC assay to 96 well plates. A) Two different transfection protocols (JAA, **i** and LF, **ii**) were used and their efficacy visualised using fluorescent microscopy. The cell density was 100,000 cells per well. Scale bars: 35 µm. **B)** Quantification of fluorescence intensity of wells transfected using each protocol with different cell densities, in number of cells x 10^3 followed by name of the transfection protocol JAA or LF. h: hours.

control, a plasmid, pHGCX, which expresses enhanced GFP (eGFP) under the control of a strong viral promoter was used. pHGCX produced sufficiently high levels of fluorescence at 72 and 96 hours following transfection that the plate reader could detect fluorescence above background levels (Figure 5.2A). Therefore, pHGCX was used for further attempts to optimise fluorescence analysis using the plate reader. Cell culture media displayed high levels of autofluorescence due to the presence of phenol red and flavin, which was reduced when the media was replaced with PBS while measuring fluorescence in the plate reader (Figure 5.2B). Reading the plate with the cells in PBS allowed the differentiation of untransfected cells and pHGCX transfected cells 48 hours after transfection (Figure 5.2B). However, the difference was still very small, especially given that eGFP was under the control of a strong promoter.

To address these issues, alpha-synuclein BiFC constructs with brighter fluorescent tags were sought. The BiFC constructs described thus far are tagged with split eGFP, which required the incubation of BiFC-transfected cells at 30 °C to allow reconstitution of the fluorophore. eGFP has been superseded in many applications by brighter fluorescent proteins, such as Venus. Venus is a variant of yellow fluorescent protein (YFP) containing the substitution F46L to produce a brighter fluorescent protein that matures more quickly than eGFP, can fold at 37°C (Nagai *et al.*, 2002) and has been adapted for BiFC (Shyu *et al.*, 2006). BiFC constructs tagged with split Venus were kindly provided by Professor Tiago Outeiro (University of Göttingen, Germany). For experiments with the Venus BiFC constructs (VN VC), cells were transfected and seeded at a density of 50,000 per well. The lower cell density was used as cells were grown at 37°C as opposed to 30°C, allowing more efficient recovery from transfection and faster growth rates.

The plate reader was still not able to differentiate between Venus BiFC transfected and untransfected HEK293 cells 48 hours after transfection (Figure 5.3A), similarly to the eGFP BiFC constructs. Therefore, the EVOS FL Auto automated fluorescent microscope (Life Technologies) was utilised to acquire one picture per well at 4x magnification and the number and intensity of transfected cells were quantified using Cell Profiler software (Carpenter *et al.*, 2006). No fluorescent cells were

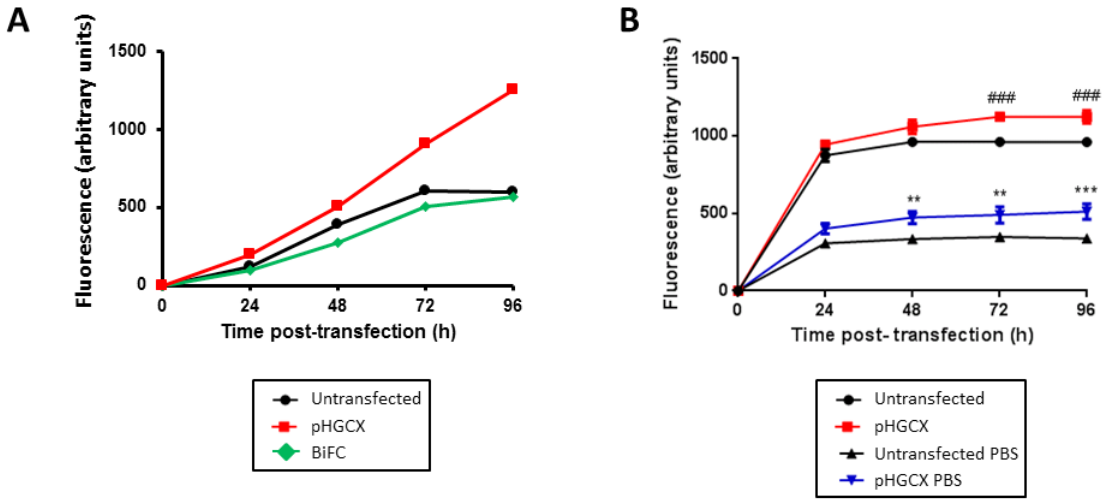

Figure 5.2. Optimisation of BiFC fluorescence measurements using a fluorescent plate reader. A) HEK293 cells were untransfected, co-transfected with BiFC constructs or transfected with a control plasmid, pHGCX, which expresses eGFP and fluorescence of live cells was read in a BioTEK Synergy HT plate reader. The BiFC constructs did not produce fluorescence above background autofluorescence in untransfected cells, so pHGCX was used in further optimisation experiments. N=1. **B)** Significantly more fluorescent signal was detected from pHGCX-transfected HEK293 cells compared to untransfected control cells (###: p<0.001) 72 and 96 hours post-transfection. When the media was replaced with PBS before the read, significantly more fluorescence was observed in transfected cells compared to untransfected at 48, 72 and 96 hours post-transfection. N=1, n=48. One-way ANOVA with Dunnett's post-hoc test. **=p<0.01, ***=p<0.001.

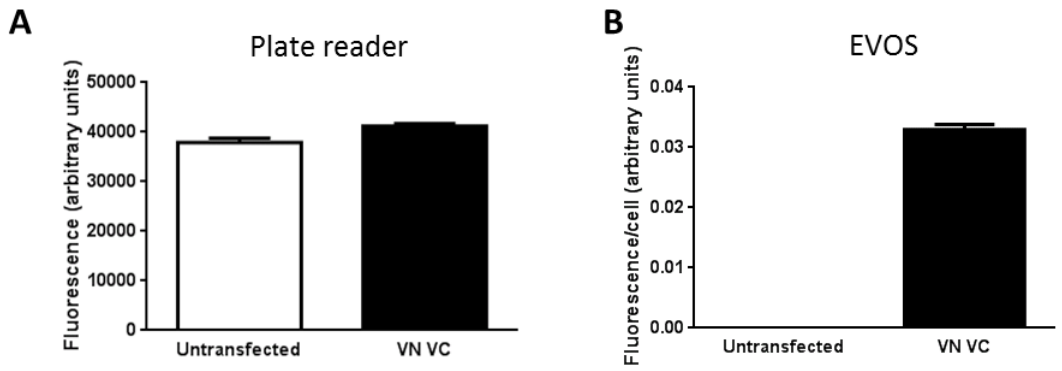

Figure 5.3. Comparison of BiFC fluorescence detection with a fluorescent plate reader and the EVOS automatic fluorescent microscope. Fluorescence levels in untransfected HEK293 cells and HEK293 cells transfected with Venus BiFC constructs (VN VC) in wells (n=48) from the same plate were analysed 48 hours following transfection using a fluorescent plate reader (**A**) or the EVOS automated fluorescent microscope (**B**). For the EVOS analysis, one image per well was acquired using the 4x objective and the number of fluorescent cells and their fluorescence intensity was analysed using Cell Profiler software. N=1, n=48.

identified in the untransfected wells, whereas fluorescent cells with a mean intensity of approximately 0.035 arbitrary units were identified in wells transfected with VN VC (Figure 5.3B). The EVOS microscope and Cell Profiler software were used for all subsequent analyses and the average fluorescence intensity per cell was used as the read-out to control for the variability in the number of transfected cells in each well.

5.2.2 BiFC assay consistency

To ensure that variability arising from the transfection process or BiFC complex formation efficiency did not influence the identification of hits, the fluorescence per cell was measured in at least three plates in three independent experiments. Data from two representative plates are shown in Figure 5.4 and demonstrate the consistency of fluorescence between wells when each is transfected with the same amount of DNA.

The compounds to be screened are dissolved in DMSO, and therefore it must be ensured that any effects observed in the screen are due to the compounds and not DMSO. Treating the cells with 0.1% or 0.5% DMSO does not affect the fluorescence levels (Figure 5.5) demonstrating that any effect observed in the screen will be due to the compound and not DMSO.

5.2.3 Identifying a suitable positive control

Curcumin is a polyphenol found in the spice turmeric that has previously been shown to inhibit the aggregation of alpha-synuclein at concentrations of 5 μM in cell culture (Pandey *et al.*, 2008) and 5 – 10 μM in pure preparations of protein (Ahmad and Lapidus, 2012). Therefore, curcumin was tested as a positive control to demonstrate that the assay was sufficiently sensitive to detect the inhibition of alpha-synuclein oligomerisation and the resultant decrease in BiFC fluorescence. Transfected HEK293 cells were treated with curcumin (1, 5, 10 or 20 μM) dissolved in DMSO. The maximal DMSO concentration the cells were exposed to was 0.1% for the 20 μM curcumin treatment. Therefore, DMSO (0.1%) was used as a control. Treatment with 10 or 20 μM curcumin resulted in reduced BiFC fluorescence (Figure 5.6A+B), but this was due to cell death, as shown by the fragmented cells observed by fluorescence microscopy

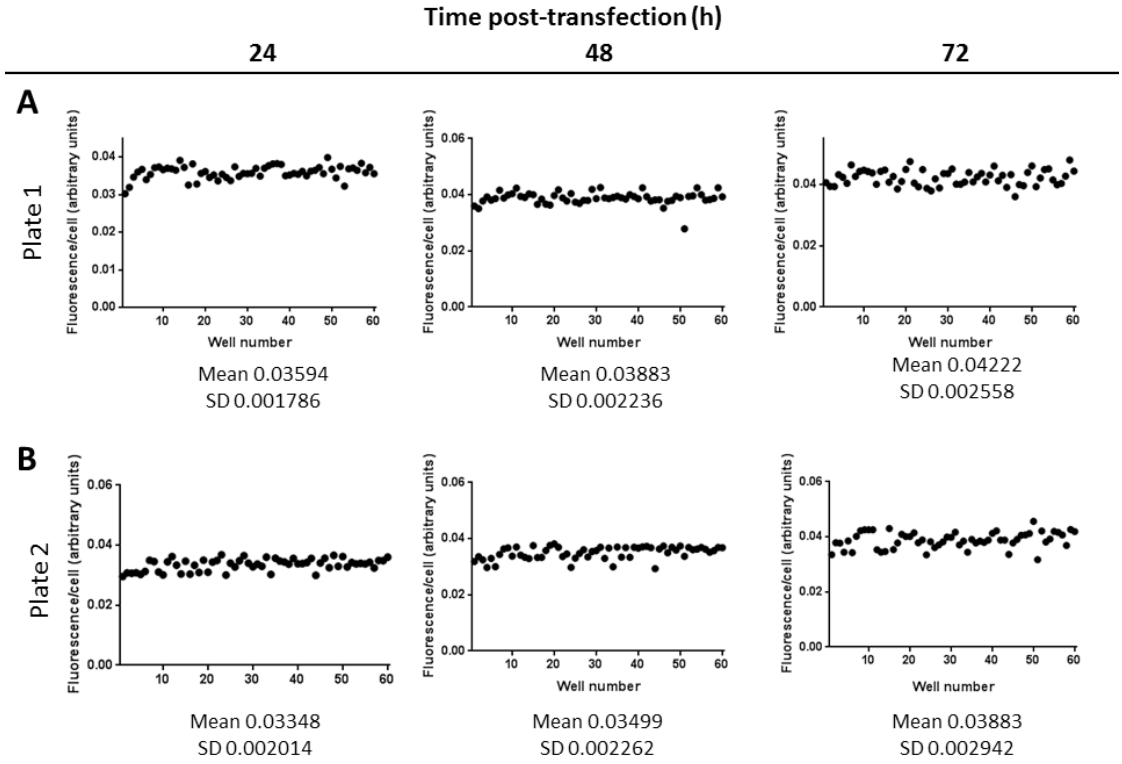

Figure 5.4. Consistency of fluorescent signal between wells and plates. HEK293 cells were co-transfected with BiFC constructs and fluorescence levels analysed using the EVOS automatic fluorescent microscope and Cell Profiler analysis every 24 hours (h) following transfection up to 72 hours. The fluorescence per cell for two representative plates (**A** & **B**) over the time course is shown, with the mean and standard deviation (SD) indicated underneath each graph, demonstrating consistency between plates. N=3.

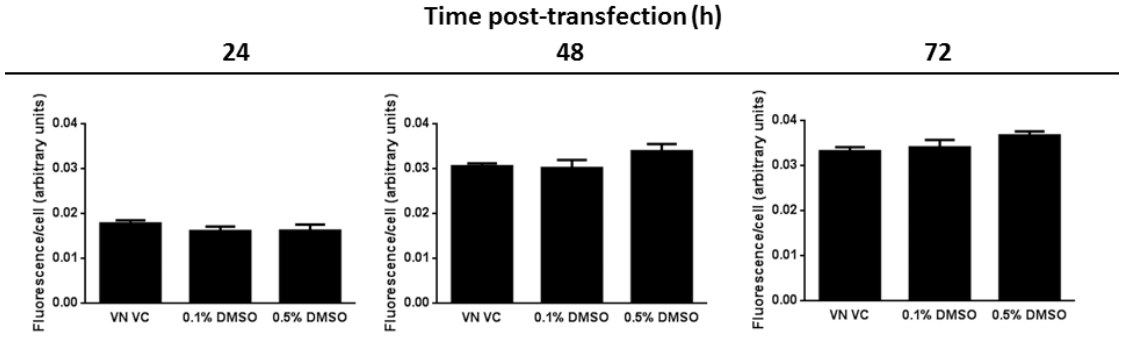

Figure 5.5. DMSO treatment did not affect BiFC fluorescence. HEK293 cells transfected with BiFC constructs were treated with 0.1% DMSO, 0.5% DMSO or untreated (VN VC). No difference was observed in the levels of fluorescence per cell at any time point after transfection: 24 hours, 48 hours or 72 hours (h). N=1, n=8.

(Figure 5.6A), which was consistent with previous observations (Jana *et al.*, 2004). A statistically significant reduction in fluorescence of approximately 40% was observed after 5 μM curcumin treatment for 24 hours. However, no decrease in fluorescence was observed with 5 μM treatment at subsequent time points. Previously, effects on the levels of alpha-synuclein aggregation in cells treated with 5 μM curcumin were observed after 48 hours (Pandey *et al.*, 2008). The difference between the results of this study and those of Pandey *et al* may be due to the differing cell lines used, as Pandey *et al* worked with the SH-SY5Y cell line, whereas HEK293 cells were used in this study. Furthermore, the read-out used by Pandey *et al* was the number of small inclusions (1 – 6 μm in diameter) present in SH-SY5Y cells over-expressing A53T alpha-synuclein tagged with DsRed2, which are likely to be much larger aggregates than the oligomeric species whose presence is indicated by BiFC fluorescence. However, these results demonstrate that curcumin is not a suitable positive control for this assay, as no sustained reduction in BiFC fluorescence is observed following curcumin treatment.

To obtain a positive control for the screen, an approach that did not involve the addition of compounds was explored. The desired reduction of BiFC fluorescence required for a positive control was achieved by transfecting an excess of one of the BiFC constructs (Figure 5.7). The same amount of DNA was transfected, but the ratio of the two constructs was adjusted to 29:1 or 99:1 (VN:VC), which resulted in fewer fluorescent complexes forming and therefore reduced fluorescence (Figure 5.7A). A significant reduction in fluorescence, which was more pronounced when the constructs were transfected at a ratio of 99:1, was sustained throughout the 72 hour analysis (Figure 5.7B). Although it would be ideal to have a compound that reduced BiFC fluorescence as a positive control, the main function of the positive control was to ensure that a decrease in BiFC fluorescence would be detected by the read-out system that had been developed. Therefore, the artificial induction of reduced BiFC fluorescence by transfecting cells with a 99:1 ratio of VN:VC was chosen as the positive control for the screen. Analysis of fluorescence levels 72 hours following transfection was also chosen as the ideal time point for analysis due to the higher levels of fluorescence than at earlier time points. All further results were obtained at this time point.

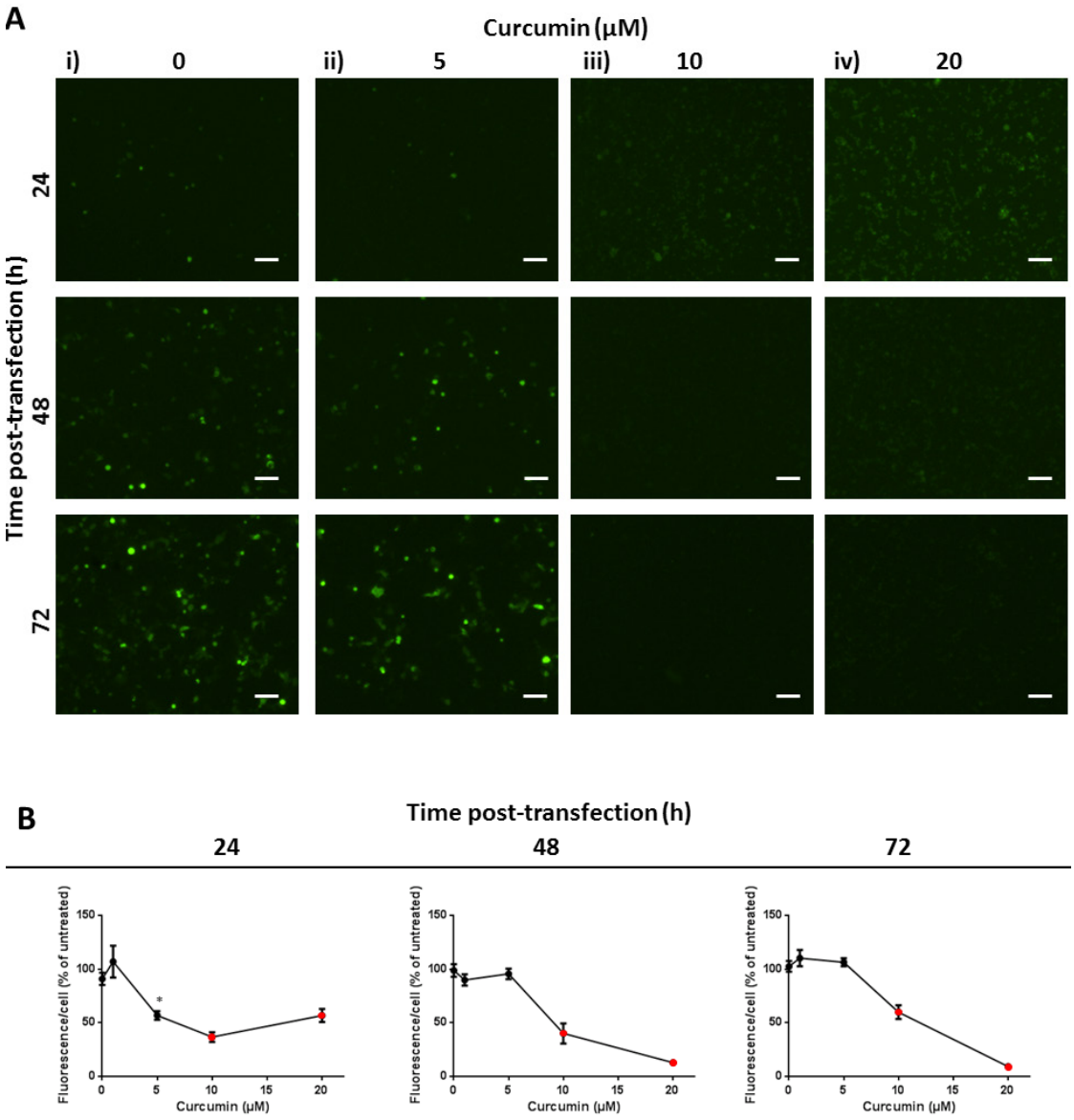

Figure 5.6. Curcumin did not reduce BiFC fluorescence at previously reported concentrations and is toxic at 10 μM and above. HEK293 cells co-transfected with BiFC constructs were treated with 0.1% DMSO or curcumin at concentrations of 1, 5, 10 or 20 μM for the indicated times. One image per well was acquired using the EVOS automated fluorescent microscope (**A**) and the levels of fluorescence intensity per cell were analysed using Cell Profiler software and normalised to the values for untreated HEK293 cells co-transfected with BiFC constructs (**B**). Red data points in **B** indicate that cell death was observed. At concentrations of 10 and 20 μM, curcumin induced cell death and fragmentation (**Aiii** + **iv**), accounting for the observed decrease in relative fluorescence at these concentrations (**B**). Treatment with 5μM curcumin resulted in a decrease in fluorescence after 24 hours' treatment but this was not sustained at later time points (**B**). Scale bars: 100 μm. N= 1, n=8. One-way ANOVA with Tukey's post-hoc test. *=$p<0.05$.

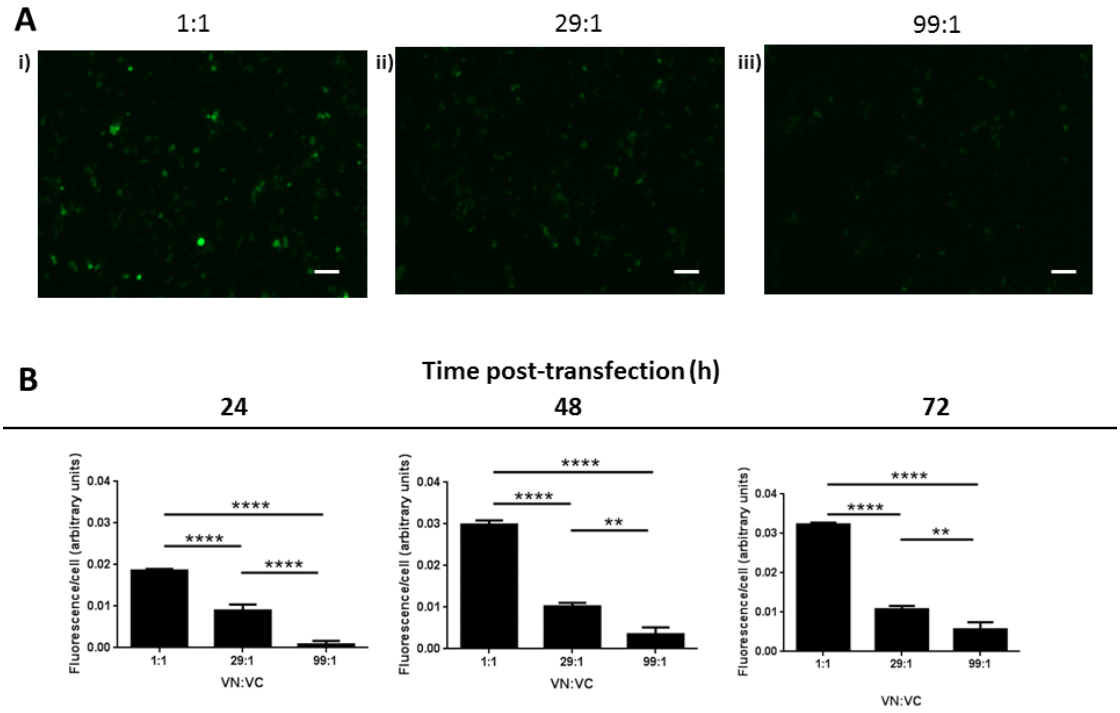

Figure 5.7. Altering the ratio of BiFC constructs transfected decreased BiFC fluorescence. HEK293 cells were co-transfected with Venus BiFC constructs (VN and VC) at various ratios of VN:VC and fluorescence was analysed using the EVOS automated fluorescent microscope (**A** VN:VC **i** – 1:1, **ii** – 29:1, **iii** – 99:1) and Cell Profiler software (**B**). A significant decrease in BiFC fluorescence was observed when cells were transfected with the constructs at a ratio of 29:1 or 99:1 compared to 1:1. Scale bars: 100 μm. N=1, n=24. One-way ANOVA with Dunnett's post-hoc test. **: $p<0.01$, ****:$p<0.001$.

5.2.4 Calculation of Z'-Factor

The Z' factor indicates the validity of an assay for screening purposes by defining the available signal window, which is equal to the separation between the negative and positive controls, taking into account the error associated with each (Zhang *et al.*, 1999). It is defined as:

$$Z' = 1 - \frac{3(\sigma_{-ve} + \sigma_{+ve})}{(\mu_{-ve} - \mu_{+ve})}$$

σ: standard deviation, μ: mean, -ve: negative control, +ve: positive control.

A Z' factor value >0.05 indicates a good assay, while a Z' factor value >0.06 indicates an ideal assay.

The positive control was HEK293 cells transfected with the BiFC constructs at a ratio of 99:1 (VN:VC, see Figure 5.7) treated with 0.1% DMSO, while the negative control was a transfection ratio of 1:1 (VN:VC), plus treatment with 0.1% DMSO, as will be used for the screen. Three plates, each with 30 wells of positive controls and 30 of negative controls, were analysed.

When fluorescence per cell was used as a read-out the variability within both controls resulted in insufficient separation of negative and positive controls, and a Z' factor of -0.972 (Figure 5.8A). In contrast to the data presented in Figure 5.7, there was not a significant difference in the fluorescence per cell between those transfected with VN:VC at a 1:1 ratio and 1:99 ratio (Figure 5.8Ai). As can be observed from the images of each experiment, the difference is accounted for by the altered distribution of fluorescent complexes (Figure 5.7Aiv). In Figure 5.7, the cells transfected with a 99:1 ratio of BiFC constructs were each fluorescing with lower levels of fluorescence compared to those transfected with a 1:1 ratio (Figure 5.7B), whereas in Figure 5.8 very few of the cells transfected with the 99:1 ratio fluoresced and those that did displayed intense fluorescence (Figure 5.8Aiv). The only difference in experimental procedure was treatment with 0.1% DMSO for the calculation of the Z' factor, but this

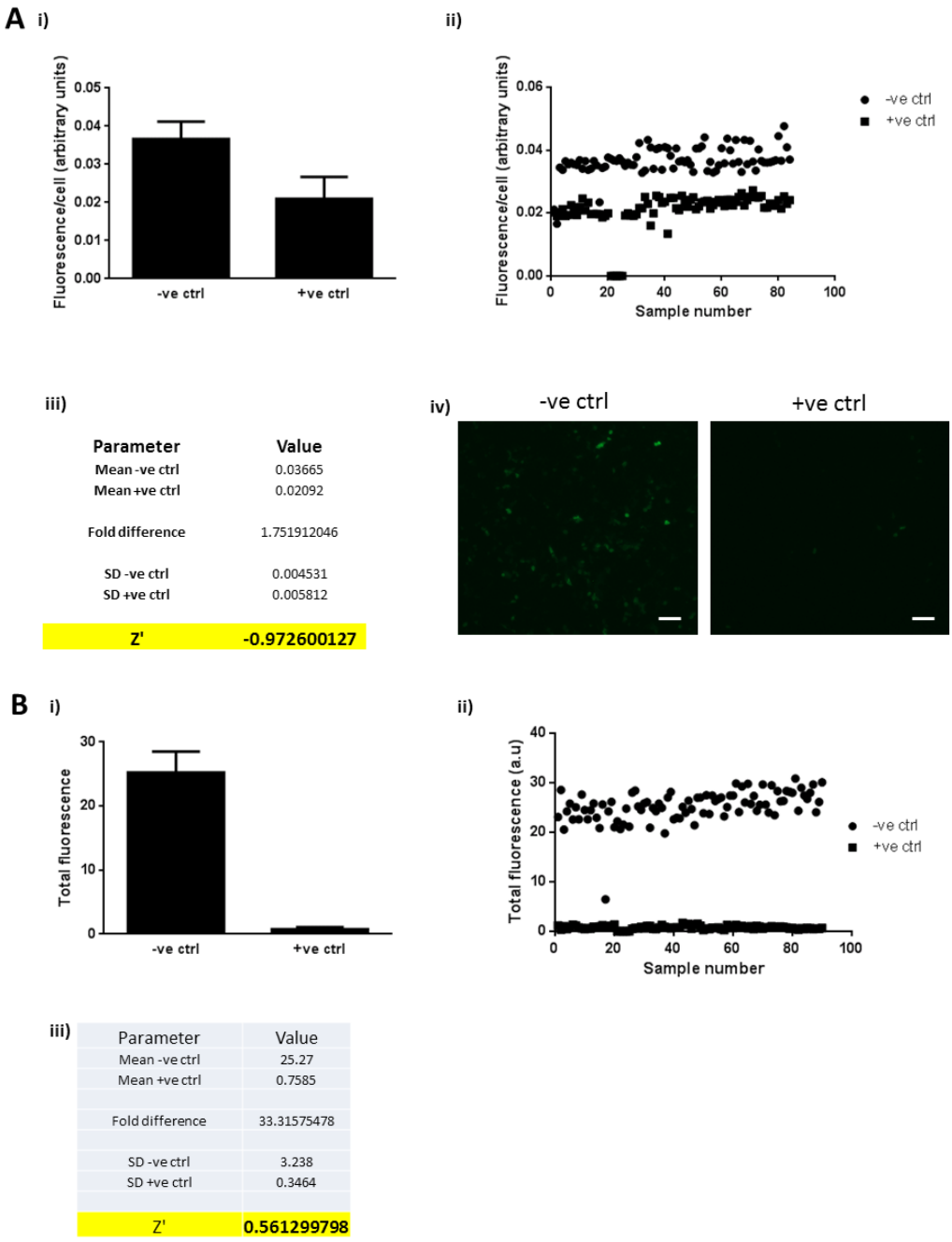

Figure 5.8. Z' factor calculation for the BiFC assay using fluorescence per cell and total fluorescence as read-outs. The Z' factor, which analyses the available signal window that is the separation between positive and negative controls, including their variation, was calculated to determine whether the BiFC assay was suitable for screening. For a negative control (-ve ctrl) BiFC co-transfected HEK293 cells were treated with 0.1% DMSO and the positive control (+ve ctrl) was HEK293 cells co-transfected with BiFC constructs at a ratio of 99:1 (VN:VC) treated with 0.1% DMSO. Analysis of fluorescence was performed using the EVOS automated fluorescent microscope and Cell Profiler software. **A) i)** Mean fluorescence per cell for both conditions. **ii)** Scatter plot of individual values. **iii)** Calculation of Z' factor. The value indicates fluorescence per cell does not provide adequate separation of positive and negative controls. This is due to fairly intense fluorescence of the few cells that display fluorescence in the positive control (**iv**). Scale bars: 100 µm. **B) i)** Total fluorescence per well for both conditions. **ii)** Scatter plot of individual values. **iii)** Calculation of Z' factor. The value indicates BiFC is an ideal screening assay when total fluorescence per well is used as a read-out. N=1, n=90.

is unlikely to account for the difference as an earlier experiment demonstrated that addition of 0.1% DMSO did not have an effect on the levels of BiFC fluorescence (Figure 5.5). It is not possible to control the distribution of the two constructs between cells and this may account for the differences between the initial experiments using the altered ratio of the two BiFC constructs and the Z' factor experiments.

When total fluorescence was analysed, a large separation between positive and negative controls was achieved that was combined with low variation, resulting in a Z' factor of 0.56 (Figure 5.8B).

The Z' factor analysis has demonstrated that the BiFC assay provides sufficient signal window to identify hits when total fluorescence is used as a read out.

5.2.5 In silico selection of screening compounds and primary screen analysis

In order to identify inhibitors of alpha-synuclein oligomerisation, small molecules with motifs similar to molecules known to disrupt protein-protein interactions were selected for screening. In collaboration with Dr Angela Russell (Departments of Chemistry and Pharmacology, University of Oxford), who has created an in-house compound library that consists of 25,000 drug-like small molecules, Dr Graham Wynne (Department of Chemistry, University of Oxford) selected 288 compounds that had PPI-like structures for screening from the library. The molecules covered targeted motifs and diverse drug-like molecules. Although hot-spot analysis is an ideal method to identify putative PPIs for a particular interaction, it requires structural information on the interaction. Currently, only low resolution structures of alpha-synuclein oligomers obtained using atomic force microscopy, nuclear magnetic resonance, Raman microscopy or Fourier transform infrared spectroscopy are available (Apetri *et al.*, 2006, Kim *et al.*, 2009, Celej *et al.*, 2012), which is insufficient for hot-spot analysis. A fingerprint based method was therefore chosen for the selection of the compounds for screening. The molecular fingerprints of 32 molecules that have previously been shown to inhibit a wide range of protein-protein interactions (Pagliaro *et al.*, 2004, Sperandio *et al.*, 2010, Ferrari, 2013) were generated using KNIME software (Mazanetz *et al.*, 2012).

Each fingerprint was compared to each of the 12,000 compounds selected from the compound library and a Tanimoto coefficient, a similarity score ranging from 0 to 1 where 1 is identical (Chen and Reynolds, 2002), was generated. For each PPI input query, the top 10 most similar library compounds were selected and following the removal of duplicates 288 compounds were selected for screening.

The compounds were received in three 96 well plates (compound plates 1 – 3) and all compounds from each plate were screened in the same experiment, i.e. three experiments, with 96 compounds screened per experiment, were required to screen all of the compounds. Each screening plate had 60 wells available, as the outside wells were excluded to avoid edge effects due to evaporation of media. The compounds were screened in triplicate at 20 μM, alongside untreated cells and 0.1 % DMSO controls. Therefore, six screening plates were used for each experiment, which allowed an untreated control, to which all results were normalised, and 0.1% DMSO control to be present on each plate.

Compound addition was undertaken concurrently with cell seeding and transfection to allow the identification of compounds that can prevent the formation of alpha-synuclein oligomers. Fluorescence levels were analysed 72 hours following compound addition using the EVOS microscope and Cell Profiler software.

Fluorescence per cell (Figure 5.9, 5.10 & 5.11 A-F) and total fluorescence (Figure 5.9, 5.10 & 5.11 G-L) Cell Profiler software read-outs were used to identify hits. Although only total fluorescence had a Z' factor high enough for an ideal assay, analysing both read-outs together will provide extra information. Furthermore, the positive control was an artificial model of reduction of BiFC fluorescence that relied on modifying the ratio of the two constructs. It was not possible to control the distribution of the two constructs and therefore the fluorescence per cell for the positive control in the Z' analysis was high. When screening for compounds, the ratio of the constructs was the same between wells and therefore both read-outs were used. Hits were defined as compounds that inhibited both BiFC fluorescence read-outs (fluorescence per cell *and* total fluorescence) with a mean inhibition of more than the arbitrarily selected cut-off

of 25%. The combination of both read-outs results in hits that affect both the levels of oligomerisation in individual cells (fluorescence per cell read-out) and the overall levels of oligomerisation in the cells in the well (total fluorescence read-out) i.e. how many cells contain oligomers, presuming similar transfection efficiencies and complex formation efficiency between wells. Compounds that reduced fluorescence by inducing cell death were identified by brightfield microscopy and are shown with red bars. Nine compounds, indicated with green bars, were identified as potential hits according to these criteria.

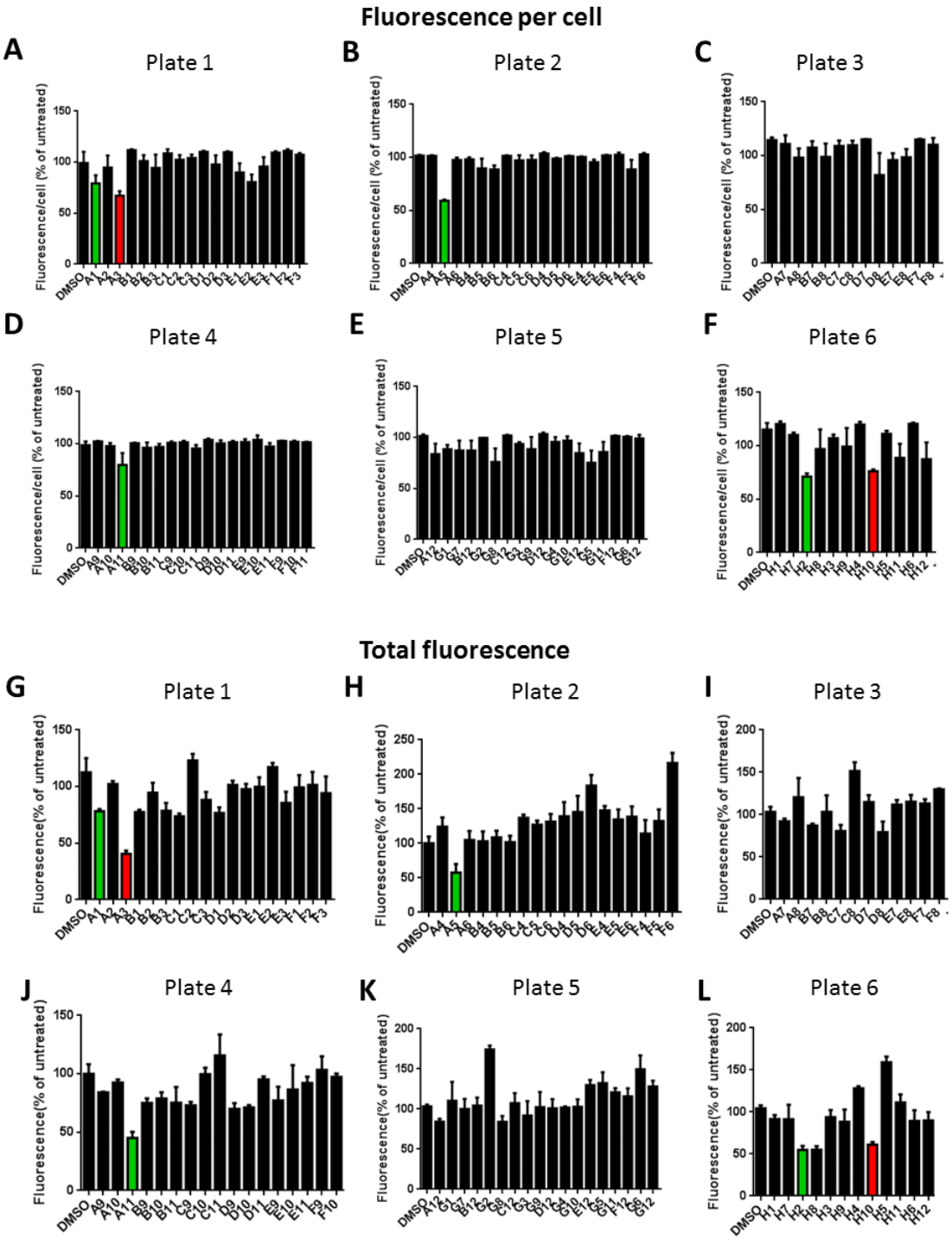

Figure 5.9. Screening compounds from Compound Plate 1. Compounds were screened in triplicate at 20 μM and added to BiFC co-transfected HEK293 cells at the time of transfection and cell plating. Six screening plates were used to screen all compounds from Compound Plate 1 in one experiment. Images were acquired following 72 hours of treatment using the EVOS automated fluorescent microscope using the 4x objective and Cell Profiler software analysis was used to determine fluorescence per cell (**A** – **F**) and total fluorescence (**G** – **L**). Compounds that induced cell death are shown with red bars, while those identified as hits have green bars. N=1, n=3.

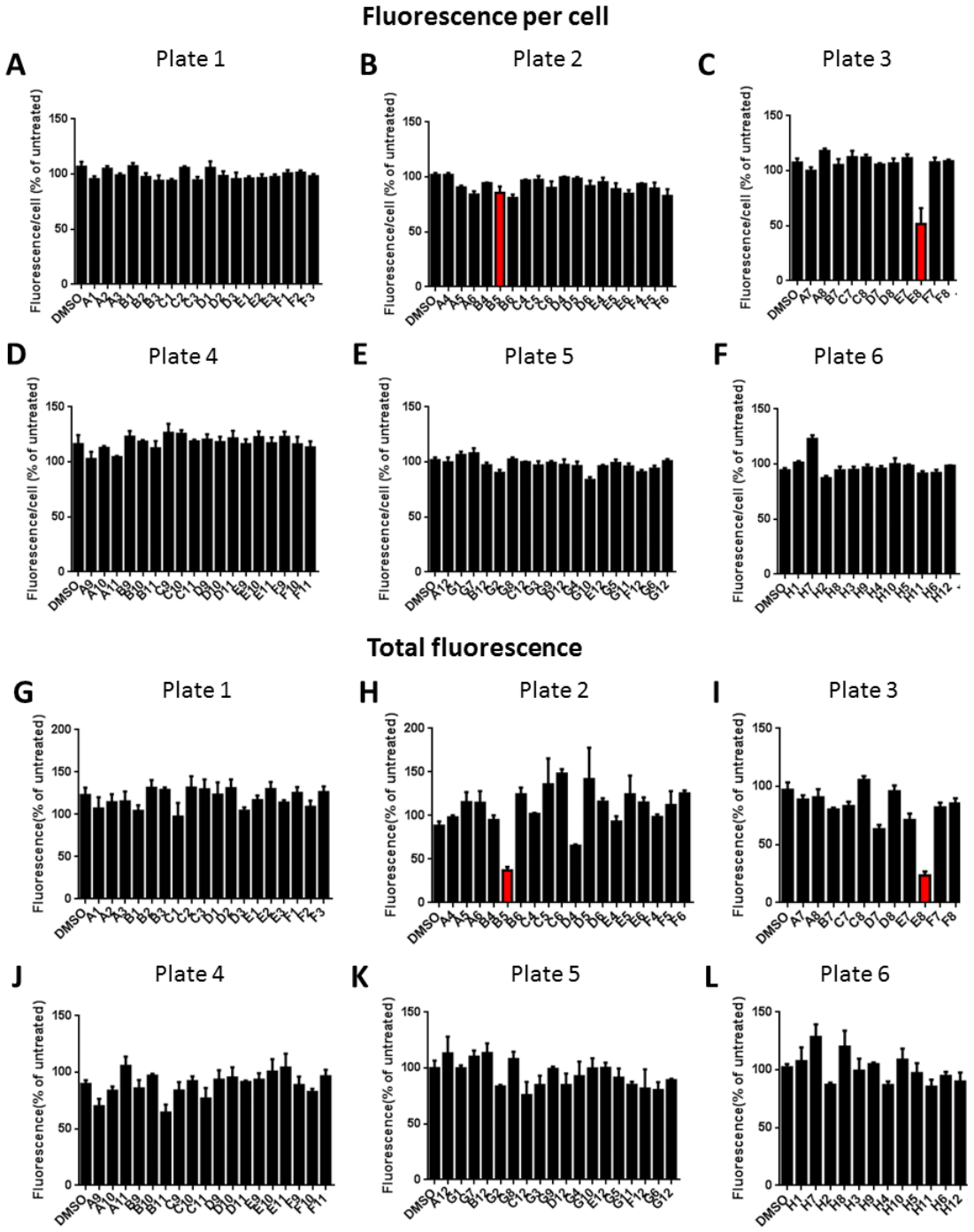

Figure 5.10. Screening compounds from Compound Plate 2. Compounds were screened in triplicate at 20 µM and added to BiFC co-transfected HEK293 cells at the time of transfection and seeding. Six screening plates were used to screen all compounds from Compound Plate 2 in one experiment. Images were acquired using the EVOS automated fluorescent microscope with the 4x objective following 72 hours of treatment and Cell Profiler analysis was used to determine fluorescence per cell (**A** – **F**) and total fluorescence (**G** – **L**). Compounds that induced cell death are shown with red bars, while those identified as hits have green bars. N=1, n=3.

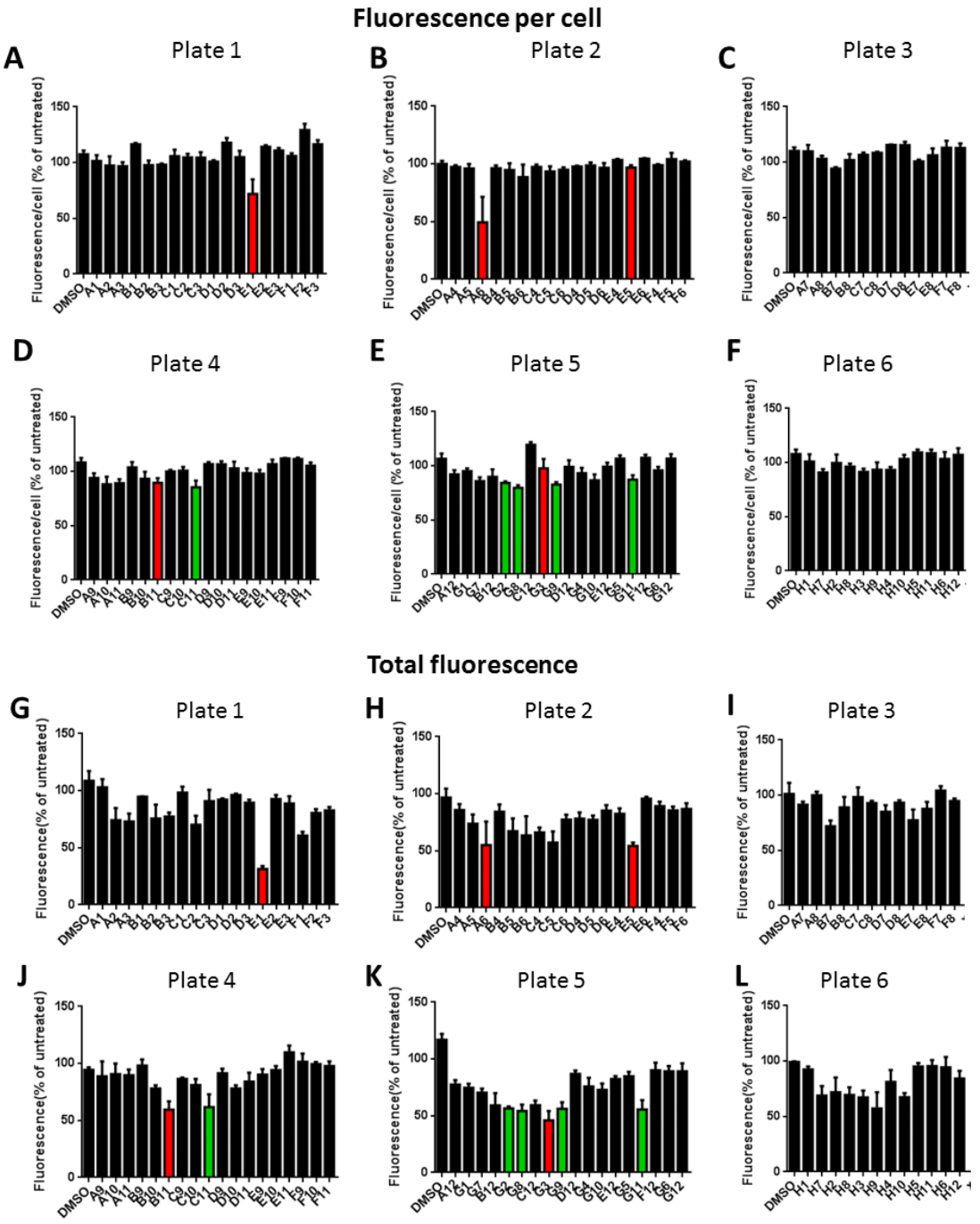

Figure 5.11. Screening compounds from Compound Plate 3. Compounds were screened in triplicate at 20 µM and added to BiFC co-transfected HEK293 cells at the time of transfection and seeding. Six screening plates were used to screen all compounds from Compound Plate 3 in one experiment. Images were acquired using the EVOS automated fluorescent microscope with the 4x objective following 72 hours of treatment and Cell Profiler analysis was used to determine fluorescence per cell (**A** – **F**) and total fluorescence (**G** – **L**). Compounds that induced cell death are shown with red bars, while those identified as hits have green bars. N=1, n=3.

5.2.6 Analysis of primary screen hits

The structures of the compounds identified as hits are shown in Figure 5.12, split into clusters according to the presence of particular functional groups (**A** – **E**). To further analyse these hits, dose response curves were generated for each compound (Figure 5.13). Fluorescence was assessed 72 hours following transfection and treatment with 1, 5, 20 or 50 μM of the compound or 0.1% DMSO.

A dose response curve for each compound was generated by utilising the curve fitting function in GraphPad Prism (Figure 5.13) and red data points were used to indicate concentrations of compounds that induced cell death, which was the case for treatment with 50 μM of A5 and 50 μM of A11 (Figure 5.13B+C). Compounds A1 and A5 from compound plate 1 showed inhibitory activity and had IC50 values of 15.12 μM and 5.64 μM, respectively (Figure 5.13A+B). No effect of the other compounds was observed.

The dose response curves of 2 compounds, A1 and A5, demonstrated that they are promising hits. Further analyses are required to demonstrate they are *bona fide* inhibitors of alpha-synuclein oligomerisation.

Sensitive content removed

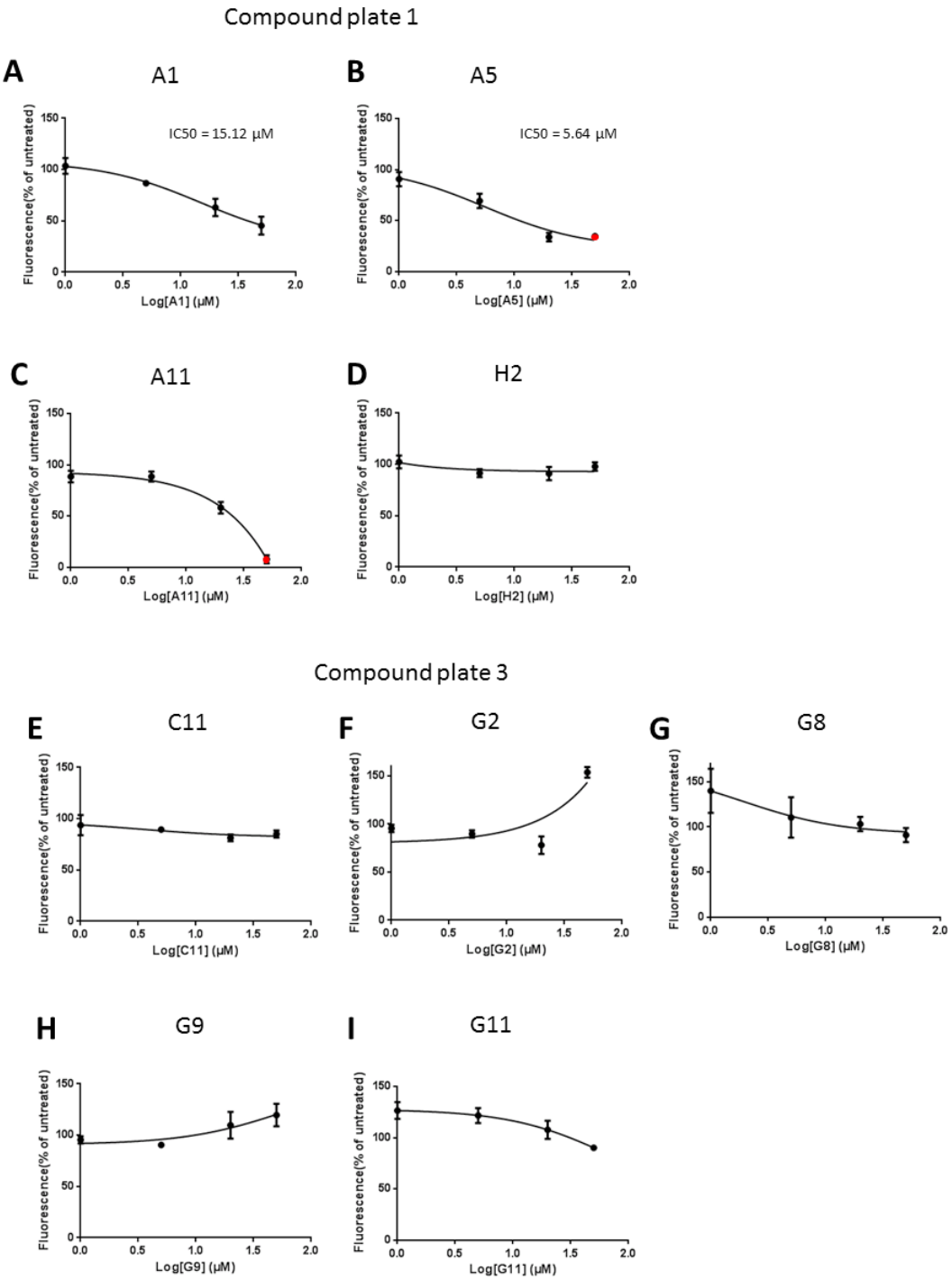

Figure 5.13. Dose response curves for compounds identified as hits in primary screen. HEK293 cells co-transfected with BiFC constructs were treated with 1, 5, 20 or 50 µM of each of the hits identified in the primary screen, or 0.1% DMSO. Total fluorescence was analysed after 72 hours of treatment using the EVOS automated fluorescent microscope and Cell Profiler. Concentrations that induced cell death are indicated as red data points (**B** + **C**). N=1, n=3.

5.3 Discussion

This chapter has described the use of an alpha-synuclein BiFC assay to screen for molecules that can prevent the formation of alpha-synuclein oligomers. The BiFC assay was shown to be consistent between wells and analysis of fluorescence using the EVOS automated fluorescent microscope and Cell Profiler software was demonstrated to detect changes in fluorescence with high sensitivity. The Z' factor analysis showed that analysing total BiFC fluorescence in each well provides the best assay signal window but BiFC fluorescence per cell was also analysed in the screen to ensure the detection of hits that have more subtle effects.

The initial screen identified nine molecules as hits (A1, A5, A11 and H2 from compound plate 1 and C11, G2, G8, G9 and G11 from compound plate 3) according to pre-defined criteria that took into account the total fluorescence and fluorescence per cell. All nine molecules were taken forward for dose response analysis and compounds A1 and A5 from compound plate 1 demonstrated a dose-dependent decrease in BiFC fluorescence.

It is crucial to ensure the dose-dependent effects of compounds A1 and A5 are not due to off-target interactions. Further experiments are required in order to ensure that the activity of the compounds is not fluorescence quenching or inhibition of transcription or translation, as opposed to inhibiting the formation of alpha-synuclein oligomers. To this end, HEK293 cells will be transfected with a construct expressing GFP (or preferably Venus) under the control of the same CMV promoter used in the BiFC constructs and will subsequently be treated with A1 and A5 at the same concentrations used for the dose response curve. AS-PLA will also be used to demonstrate that a decrease in oligomerisation, as opposed to fluorescence quenching, is induced by treatment with the compounds. If there is a decrease in fluorescence of the CMV-GFP construct, similar to that of the BiFC constructs, the compounds will be discarded as hits. Those that do not show such off-target effects will be modified to identify related compounds that may have more potent effects.

It will also be important to demonstrate that variation in transfection efficiency does not account for the effect of any compound on total BiFC fluorescence. Immunostaining for alpha-synuclein was attempted for all screening plates. However, very few cells remained in the wells after the numerous wash steps required for the protocol. Therefore, more gentle wash steps will be undertaken in future experiments to ensure the cells do not get washed from the plate. Assays for toxicity, such as detection of adenylate kinase in the media, will be undertaken to ensure reductions in fluorescence are not due to cell death.

The compounds identified in this screen may be inhibitors of the formation of alpha-synuclein oligomers. As PD is only diagnosed late in the disease process, it may be useful to identify molecules that can reverse aggregation or break apart oligomers that have already formed. For this purpose the use of a protein complementation assay (PCA) in which the interaction of the reporter protein halves is reversible would be required, such as a luciferase based PCA system (Remy and Michnick, 2006). A novel fluorescent PCA has been developed in which the two halves of *Deinococcus radiodurans* infrared fluorescent protein IFP1.4 can reversibly interact with each other allowing the study of the interaction dynamics of proteins tagged by the split IFP1.4 (Tchekanda *et al.*, 2014).

Finally, it is important to study untagged alpha-synuclein oligomers. Each half of Venus tagging alpha-synuclein is large – the N-terminal portion is 158 amino acids long, larger than the whole alpha-synuclein protein (140 amino acids), while the C-terminal is 80 amino acids long. Such large tags may influence the behaviour of the alpha-synuclein oligomers. A recently described protein-protein interaction assay utilises engineered beta-strands of GFP that are 22 amino acids long to tag the proteins of interest (Cabantous *et al.*, 2013). The shorter tags reduce effects of the tag on protein folding and interactions, although the constructs must be co-transfected with a third construct containing the remaining GFP sequence to allow fluorescence to develop. Alternatively, oligomerisation of endogenous alpha-synuclein could be induced using toxins such as malondialdehyde (Dalfo and Ferrer, 2008) or peroxynitrite (Souza *et al.*, 2000, Paxinou *et al.*, 2001). AS-PLA could then be used to measure changes in alpha-

synuclein oligomerisation as a result of treatment with the compounds identified in the screen. *In vivo,* the *SNCA*-OVX mouse model, which has widespread alpha-synuclein oligomers (Janezic *et al.*, 2013) and specific accumulation of oligomers in the SNc with aging (Chapter 4), will be used to test the compounds. It is anticipated that these approaches will result in the development of a compound that prevents, and possibly reverses, alpha-synuclein oligomerisation as a promising candidate for a novel therapy for PD.

6. Discussion

The aim of this thesis was to investigate the role of alpha-synuclein oligomers in PD by i) developing and validating a novel technique for the specific detection of alpha-synuclein oligomers, ii) studying oligomeric pathology in post-mortem PD brain tissue and iii) screening for molecules that can prevent the formation of alpha-synuclein oligomers.

6.1 Specific detection of alpha-synuclein oligomers in vitro and of oligomeric pathology in PD tissue

In recent years, the spotlight of attention on protein aggregates in neurodegenerative disease has turned from large inclusions, such as LBs, to smaller pre-fibrillar aggregates known as oligomers. The discovery that mutations in the gene encoding alpha-synuclein were sufficient to cause PD and that alpha-synuclein was a key component of LBs, coupled with the demonstration of pathogenic roles for A-beta oligomers in Alzheimer's disease, have led to an emerging field investigating alpha-synuclein oligomers and their relationship to PD. However, there has not yet been a systematic study of alpha-synuclein oligomeric pathology in post-mortem PD brain tissue, which limits our understanding of the localisation and effects of alpha-synuclein oligomers during the disease process. Furthermore, current techniques for the detection of alpha-synuclein oligomers have various limitations, including the non-exclusive detection of alpha-synuclein oligomers because oligomers formed of other proteins such as A-beta, or alpha-synuclein fibrils are also detected. The use of antibodies raised against *in vitro* formed alpha-synuclein oligomers may result in the detection of a limited complement of disease relevant species, because we do not yet understand whether oligomers formed *in vitro* are analogous to those found in diseased brain. In this thesis I have described the development of AS-PLA, which specifically detects alpha-synuclein oligomers and overcomes these limitations.

In Chapter 3, AS-PLA was validated through the use of three *in vitro* oligomerisation

systems. AS-PLA was demonstrated to specifically detect oligomeric, but not monomeric, forms of alpha-synuclein in two cellular oligomerisation paradigms. Using pure preparations of recombinant protein, this finding was confirmed and it was also demonstrated that fibrillar forms of alpha-synuclein were not detected by AS-PLA. Although it was not possible to discover the exact identity of the oligomer(s) detected by AS-PLA in the experiments undertaken in Chapter 3, our studies in Chapter 4 revealed that AS-PLA-detected oligomers displayed an intermediate proteinase K resistance, suggesting the detection of oligomer(s) with low beta-sheet content, likely to represent an oligomer in the early stages of aggregation. Further studies *in vitro* will be required to identify the oligomers detected by AS-PLA and understand their properties. A useful approach would be to separate alpha-synuclein oligomeric species by size from homogenised PD brain, or a preparation of *in vitro* formed oligomers, using size exclusion chromatography and probe each fraction immobilised on coverslips with AS-PLA. The pathological impact of the oligomeric fractions shown to be detected by AS-PLA could then be investigated by injection into non-transgenic animals. This approach has been utilised to demonstrate that a specific A-beta oligomer is responsible for memory impairment in a mouse model of AD (Lesne *et al.*, 2006).

It is likely, however, that multiple species of oligomer are detected by AS-PLA. The generation of AS-PLA signal depends on sufficient proximity of the epitope targeted by both AS-PLA probes on interacting monomers of alpha-synuclein, which in principle means that any supramolecular species consisting of at least a dimer could be detected. The constraint of proximity between the epitopes is defined by the length of the probe oligonucleotide. Although the sequence of the Duolink® probe oligonucleotides is propriety information and therefore it is not possible to know definitively the distance constraints for AS-PLA, the patent describes the same sequences as the original paper (Soderberg *et al.*, 2006). In this case, the distance constraints imposed would result in a maximum possible distance between epitopes of approximately 40 nm (Soderberg *et al.*, 2006). Using a simplified formula that assumes globular conformation of proteins, the minimum radius for a globular protein of alpha-synuclein's molecular weight would be approximately 1.6 nm (Erickson, 2009). The natively unfolded conformation of alpha-synuclein results in a larger Stokes radius

of 3.4 nm (Weinreb *et al.*, 1996), but 40 nm allows ample room for the detection of oligomers consisting of many molecules of alpha-synuclein. The varied range of oligomer sizes reported *in vitro* and isolated from patient tissue (Conway *et al.*, 2000, Lashuel *et al.*, 2002, Pountney *et al.*, 2004, Nasstrom *et al.*, 2011, Fauerbach *et al.*, 2012), which range from approximately 5 nm to between 30 and 50 nm, indicates that the distance constraints imposed by AS-PLA may allow for the detection of an excellent subset of disease-related species.

One of the advantages of PLA over other techniques for the detection of protein-protein interactions is its adaptability. Modifying the length of the probe oligonucleotide allows the variation of the conformational constraints for the detection of interaction. Therefore, in future studies, AS-PLA probes with variable probe oligonucleotide length could be used in tandem to elucidate the presence and role of a variety of oligomers. A panel of antibodies with epitopes targeting distinct regions of the protein may also be useful to investigate structural differences as the aggregation process proceeds.

The epitope of the antibody (syn211, Abcam) utilised for the AS-PLA probes localises to residues 121 – 125 of the C-terminal of alpha-synuclein (Giasson *et al.*, 2000). AS-PLA has detected significant oligomeric pathology in the brains of PD patients, although this will not include oligomers that are composed wholly of C-terminally truncated alpha-synuclein, in which only residues 1 – 110 or 1 – 120 are present (Li *et al.*, 2005). C-terminal truncation of alpha-synuclein has been shown to increase the propensity of the protein to fibrillise (Crowther *et al.*, 1998) and can seed the aggregation of full-length alpha-synuclein (Liu *et al.*, 2005, Ulusoy *et al.*, 2010). The proportion of alpha-synuclein in LBs that is truncated has been reported to be as high as 15% (Baba *et al.*, 1998). Further investigations using AS-PLA probes that target different domains of the protein could shed light on different aggregation pathways for C-terminally truncated forms of alpha-synuclein.

AS-PLA detected early PD lesions such as PBs more sensitively than AS-IHC, the routine technique used for pathological PD diagnosis. PBs can be difficult to identify with haematoxylin and eosin as they are non-eosinophilic and these data suggest

that some PBs evade detection by AS-IHC. AS-PLA will therefore allow PBs to be identified more easily, which will be particularly useful since they are enriched in cases at the early stage of the disease (Dale *et al.*, 1992). Interestingly, brainstem LBs were not detected by AS-PLA, similarly to the FILA-1 antibody that targets alpha-synuclein aggregates (Lindersson *et al.*, 2004). This is unsurprising as *in vitro* alpha-synuclein fibrils were not detected. However, the various combinations of AS-PLA probe oligonucleotide length and antibody could also be used to investigate whether different conformations of alpha-synuclein within LBs exist.

The diffuse AS-PLA staining revealed previously unrecognised oligomeric pathology in the form of widespread accumulation of alpha-synuclein oligomers in the neuropil and some white matter tracts, which was specifically localised to nuclei such as the medullary reticular formation and cingulate cortex in patients. This distribution has not previously been described, but most studies used western blotting for the detection of oligomers (Sharon *et al.*, 2003, Tong *et al.*, 2010), which cannot give any information on exact neuroanatomical localisation. The PK-PET blot has identified neuritic pathology in the SNc (Neumann *et al.*, 2002, Schulz-Schaeffer, 2010) and striatum of PD patients (Neumann *et al.*, 2004). AS-PLA did not identify significant accumulation of oligomeric pathology in the SNc of PD patients, which perhaps is unsurprising given it is likely to detect oligomers in a much earlier stage of aggregation compared to the PK-PET blot, which utilises a prolonged PK digestion to reveal aggregated species.

In addition to the pathology observed in patients, accumulations of small amounts of alpha-synuclein oligomers were present in some controls. Most studies have shown oligomers specifically accumulated in patients, but others have found the presence of oligomers in some controls by western blotting (Tong *et al.*, 2010). AS-PLA staining in controls was present in white matter tracts such as the corticospinal tract, the subcortical white matter of the cingulate gyrus and the corpus callosum, and I hypothesised that their presence may be pre-clinical signs, relating to aberrant alpha-synuclein oligomerisation in the axons following mis-localisation of alpha-synuclein from the synapse. PD pathology has rarely been reported in white matter, although Saito *et al* described the detection of intra-axonal alpha-synuclein pathology in limbic

subcortical white matter, including the white matter of the cingulate gyrus, using an antibody against phosphorylated alpha-synuclein (Saito *et al.*, 2003). Further studies are required to determine whether AS-PLA stained oligomers in the white matter are localised intra-axonally and whether some oligomers in the grey matter are localised to synapses. The question of synaptic accumulation will be particularly interesting to address in the striatum where the terminals of SNc dopaminergic neurons are found. Striatal accumulation of alpha-synuclein in PD, DLB and AD/DLB has been described by Duda *et al* using antibodies targeting oxidised/nitrated alpha-synuclein (Duda *et al.*, 2002). The presence of LBs, LNs and 'grain-like aggregates' were reported, although striatal pathology was lowest in tissue from PD patients compared to tissue from AD/DLB or DLB cases. It is possible that early-stage oligomers, as detected by AS-PLA, were not detected in this study and therefore AS-PLA may reveal more extensive pathology in the striatum of PD patient tissue.

The signal found in some controls also raises the possibility that AS-PLA detects the recently proposed physiological tetrameric form of alpha-synuclein (Bartels *et al.*, 2011, Wang *et al.*, 2011), although this is unlikely for a number of reasons. Firstly, AS-PLA signal was not present in BE(2)M17 cells nor in untransfected HEK293 cells, which were both shown to contain tetrameric physiological forms of alpha-synuclein (Bartels *et al.*, 2011); in our hands, BE(2)M17 cells expressed high levels of monomeric alpha-synuclein. Secondly, although alpha-synuclein is highly and widely expressed in the central nervous system (Jakes *et al.*, 1994, Iwai *et al.*, 1995), the low levels of alpha-synuclein oligomers detected by AS-PLA in controls had a restricted neuroanatomical distribution. Thirdly, the diffuse oligomers of both patient and controls share an intermediate sensitivity to PK, suggesting that they contain a proportion of beta-sheet content unlike tetrameric alpha-synuclein which is formed by alpha helices (Bartels *et al.*, 2011, Wang *et al.*, 2011).

However, it is not currently clear whether all oligomeric forms of alpha-synuclein are toxic. Although LBs are now thought to form as a protective mechanism against toxic oligomers, smaller 'sequestration' accumulations of alpha-synuclein may exist. For example, the formation *in vitro* of off-pathway oligomers that are non-toxic to cells in

culture has been described (Ehrnhoefer *et al.*, 2008, Zhou *et al.*, 2010). If this type of oligomer exists in PD patient brain tissue, it may be detected by AS-PLA. Perhaps the control cases are capable of producing non-toxic oligomers more efficiently than those who go on to develop PD. It is also possible that toxic off-pathway oligomers are detected by AS-PLA and the signal in controls relates to an oligomeric load that has not yet reached pathological levels.

To investigate these possibilities, further neuroanatomical regions need to be studied including the striatum, pre-frontal cortex, amygdala and hippocampus, using AS-PLA in further patients and controls, in order to build a picture of the progression of oligomeric pathology through the brain. Investigations in the *SNCA*-OVX mouse model may also provide insights into the relationship of oligomeric pathology and PD progression. In Chapter 4, I demonstrated the specific, age-dependent accumulation of AS-PLA stained oligomers in the SNc of 24 month old *SNCA*-OVX animals, which already had marked cell loss in this region. Therefore, it will be interesting to study these animals at earlier time points, including at 12 months of age, to elucidate whether this accumulation precedes neurodegeneration and whether pathological oligomeric changes are found in further regions. The detection of oligomers using AS-PLA in this model can provide a window into the early mechanisms of PD.

6.2 Targeting alpha-synuclein oligomers therapeutically

In Chapter 5, I described the primary screen for molecules that can prevent the formation of alpha-synuclein oligomers, which led to the identification of nine preliminary hits, two of which showed promise in dose response analysis and displayed IC50 values in the micromolar range. The next step will be to confirm the effects observed with fresh preparations of the compounds and ensure they are not off-target effects related to fluorescence quenching or transcriptional inhibition.

(Paragraph removed due to sensitive content).

Many studies are focusing on eliminating alpha-synuclein oligomers as a therapeutic strategy, including pharmaceutical companies. For example, Roche and Prothena are undertaking clinical phase I trials for PRX002, a monoclonal antibody against alpha-synuclein that has been shown to reduce C-terminal truncation of alpha-synuclein in animal models and partially rescued pathological and behavioural phenotypes, including the accumulation of alpha-synuclein (Games *et al.*, 2014). The double blind trial began in August 2014 and therefore clinical outcomes in PD patients have not yet been reported. Utilising antibodies that target oligomeric forms of alpha-synuclein for immunotherapy has also been trialled in animal models and has shown success in terms of reduction in alpha-synuclein oligomer levels and improvement in motor phenotypes in the transgenic Thy1-*SNCA*[A30P] model of PD (Lindstrom *et al.*, 2014). An alternative approach is to induce the production of anti-alpha-synuclein antibodies by vaccination. AFFiRiS have developed the PD01A vaccine (Schneeberger *et al.*, 2012), which has been shown to be safe and well-tolerated in a small study and half of those vaccinated produced neutralising anti-alpha-synuclein antibodies (Brachmann, 2014). Immunisation of two animal models of PD with a peptide that binds alpha-synuclein oligomers has recently been shown to induce the production of antibodies that recognise alpha-synuclein aggregates in the animals and leads to decreased accumulation of alpha-synuclein accompanied by an improvement in PD-like phenotypes (Mandler *et al.*, 2014).

However, small molecule approaches are useful as it is possible to easily modify the affinity of the molecule for the target and the outcomes of variable dosing are likely to be more predictable than with a vaccine. Neuropore Therapies have identified a small molecule, NPT200-11, that is thought to stabilise conformations of alpha-synuclein that are incapable of oligomerising and reduces alpha-synuclein pathology and motor phenotypes in mThy1-asyn transgenic mice (Reznichenko *et al.*, 2012). NPT200-11 can penetrate the blood brain barrier and has good oral bioavailability, and clinical phase I trials are due to begin this year.

The hits identified in the screen in Chapter 5 that can prevent the formation of alpha-synuclein oligomers will be taken forward to test in *SNCA*-OVX animals following further validation. Assays will also be undertaken to evaluate whether the hits can reverse, as well as prevent, alpha-synuclein oligomerisation. Such a property would be useful in a drug expected to be administered to PD patients who are initially diagnosed when extensive neurodegeneration and alpha-synuclein accumulation are already present.

In conclusion, the work presented here has demonstrated that the specific detection of alpha-synuclein oligomers in brain tissue using the novel technique developed in this thesis, AS-PLA, reveals early and previously unrecognised oligomeric pathology both in PD patients and in the *SNCA*-OVX mouse model of PD. Furthermore, the identification of compounds that can prevent the formation of alpha-synuclein oligomers *in vitro* could provide a functional link between the insights into the early mechanisms of PD provided by the detection of alpha-synuclein oligomers in post-mortem tissue using AS-PLA and a disease-modifying therapy for PD.

7. References

Abeliovich A, Schmitz Y, Farinas I, Choi-Lundberg D, Ho WH, Castillo PE, et al. Mice lacking alpha-synuclein display functional deficits in the nigrostriatal dopamine system. Neuron. 2000;25(1):239-52.

Ahmad B, Lapidus LJ. Curcumin prevents aggregation in alpha-synuclein by increasing reconfiguration rate. J Biol Chem. 2012;287(12):9193-9.

Ahn TB, Kim SY, Kim JY, Park SS, Lee DS, Min HJ, et al. alpha-Synuclein gene duplication is present in sporadic Parkinson disease. Neurology. 2008;70(1):43-9.

Alegre-Abarrategui J, Ansorge O, Esiri M, Wade-Martins R. LRRK2 is a component of granular alpha-synuclein pathology in the brainstem of Parkinson's disease. Neuropathol Appl Neurobiol. 2008;34(3):272-83.

Alvarez-Erviti L, Rodriguez-Oroz MC, Cooper JM, Caballero C, Ferrer I, Obeso JA, et al. Chaperone-mediated autophagy markers in Parkinson disease brains. Arch Neurol. 2010;67(12):1464-72.

Anglade P, Vyas S, Javoy-Agid F, Herrero MT, Michel PP, Marquez J, et al. Apoptosis and autophagy in nigral neurons of patients with Parkinson's disease. Histol Histopathol. 1997;12(1):25-31.

Anwar S, Peters O, Millership S, Ninkina N, Doig N, Connor-Robson N, et al. Functional alterations to the nigrostriatal system in mice lacking all three members of the synuclein family. J Neurosci. 2011;31(20):7264-74.

Apaydin H, Ahlskog JE, Parisi JE, Boeve BF, Dickson DW. Parkinson disease neuropathology: later-developing dementia and loss of the levodopa response. Arch Neurol. 2002;59(1):102-12.

Apetri MM, Maiti NC, Zagorski MG, Carey PR, Anderson VE. Secondary structure of alpha-synuclein oligomers: characterization by raman and atomic force microscopy. J Mol Biol. 2006;355(1):63-71.

Appel-Cresswell S, Vilarino-Guell C, Encarnacion M, Sherman H, Yu I, Shah B, et al. Alpha-synuclein p.H50Q, a novel pathogenic mutation for Parkinson's disease. Mov Disord. 2013;28(6):811-3.

Arima K, Hirai S, Sunohara N, Aoto K, Izumiyama Y, Ueda K, et al. Cellular co-localization of phosphorylated tau- and NACP/alpha-synuclein-epitopes in lewy bodies in sporadic Parkinson's disease and in dementia with Lewy bodies. Brain Res. 1999;843(1-2):53-61.

Arima K, Ueda K, Sunohara N, Hirai S, Izumiyama Y, Tonozuka-Uehara H, et al. Immunoelectron-microscopic demonstration of NACP/alpha-synuclein-epitopes on the filamentous component of Lewy bodies in Parkinson's disease and in dementia with Lewy bodies. Brain Res. 1998;808(1):93-100.

Arkin MR, Wells JA. Small-molecule inhibitors of protein-protein interactions: progressing towards the dream. Nature reviews Drug discovery. 2004;3(4):301-17.

Athanassiadou A, Voutsinas G, Psiouri L, Leroy E, Polymeropoulos MH, Ilias A, et al. Genetic analysis of families with Parkinson disease that carry the Ala53Thr mutation in the gene encoding alpha-synuclein. Am J Hum Genet. 1999;65(2):555-8.

Auluck PK, Chan HY, Trojanowski JQ, Lee VM, Bonini NM. Chaperone suppression of alpha-synuclein toxicity in a Drosophila model for Parkinson's disease. Science. 2002;295(5556):865-8.

Azeredo da Silveira S, Schneider BL, Cifuentes-Diaz C, Sage D, Abbas-Terki T, Iwatsubo T, et al. Phosphorylation Does Not Prompt, Nor Prevent, the Formation of -synuclein Toxic Species in a Rat Model of Parkinson's Disease. Human Molecular Genetics. 2008.

Baan B, Pardali E, ten Dijke P, van Dam H. In situ proximity ligation detection of c-Jun/AP-1 dimers reveals increased levels of c-Jun/Fra1 complexes in aggressive breast cancer cell lines in vitro and in vivo. Mol Cell Proteomics. 2010;9(9):1982-90.

Baba M, Nakajo S, Tu PH, Tomita T, Nakaya K, Lee VM, et al. Aggregation of alpha-synuclein in Lewy bodies of sporadic Parkinson's disease and dementia with Lewy bodies. Am J Pathol. 1998;152(4):879-84.

Bartels T, Choi JG, Selkoe DJ. alpha-Synuclein occurs physiologically as a helically folded tetramer that resists aggregation. Nature. 2011.

Bayer TA, Jakala P, Hartmann T, Havas L, McLean C, Culvenor JG, et al. Alpha-synuclein accumulates in Lewy bodies in Parkinson's disease and dementia with Lewy bodies but not in Alzheimer's disease beta-amyloid plaque cores. Neurosci Lett. 1999;266(3):213-6.

Beach TG, Adler CH, Lue L, Sue LI, Bachalakuri J, Henry-Watson J, et al. Unified staging system for Lewy body disorders: correlation with nigrostriatal degeneration, cognitive impairment and motor dysfunction. Acta Neuropathol. 2009;117(6):613-34.

Ben Gedalya T, Loeb V, Israeli E, Altschuler Y, Selkoe DJ, Sharon R. Alpha-synuclein and polyunsaturated fatty acids promote clathrin-mediated endocytosis and synaptic vesicle recycling. Traffic (Copenhagen, Denmark). 2009;10(2):218-34.

Bennett MC, Bishop JF, Leng Y, Chock PB, Chase TN, Mouradian MM. Degradation of alpha-synuclein by proteasome. J Biol Chem. 1999;274(48):33855-8.

Bertoncini CW, Jung YS, Fernandez CO, Hoyer W, Griesinger C, Jovin TM, et al. Release of long-range tertiary interactions potentiates aggregation of natively unstructured alpha-synuclein. Proc Natl Acad Sci U S A. 2005;102(5):1430-5.

Betarbet R, Sherer TB, MacKenzie G, Garcia-Osuna M, Panov AV, Greenamyre JT. Chronic systemic pesticide exposure reproduces features of Parkinson's disease. Nat Neurosci. 2000;3(12):1301-6.

Bidinosti M, Shimshek DR, Mollenhauer B, Marcellin D, Schweizer T, Lotz GP, et al. Novel one-step immunoassays to quantify alpha-synuclein: applications for biomarker development and high-throughput screening. J Biol Chem. 2012;287(40):33691-705.

Bieschke J, Russ J, Friedrich RP, Ehrnhoefer DE, Wobst H, Neugebauer K, et al. EGCG remodels mature alpha-synuclein and amyloid-beta fibrils and reduces cellular toxicity. Proc Natl Acad Sci U S A. 2010;107(17):7710-5.

Blasco MA, Serrano M, Fernandez-Capetillo O. Genomic instability in iPS: time for a break. EMBO J. 2011;30(6):991-3.

Blazer LL, Neubig RR. Small molecule protein-protein interaction inhibitors as CNS therapeutic agents: current progress and future hurdles. Neuropsychopharmacology. 2009;34(1):126-41.

Bodles AM, El-Agnaf OM, Greer B, Guthrie DJ, Irvine GB. Inhibition of fibril formation and toxicity of a fragment of alpha-synuclein by an N-methylated peptide analogue. Neurosci Lett. 2004;359(1-2):89-93.

Bogan AA, Thorn KS. Anatomy of hot spots in protein interfaces. J Mol Biol. 1998;280(1):1-9.

Bosco DA, Lavoie MJ, Petsko GA, Ringe D. Proteostasis and Movement Disorders: Parkinson's Disease and Amyotrophic Lateral Sclerosis. Cold Spring Harb Perspect Biol. 2011.

Braak H, de Vos RA, Bohl J, Del Tredici K. Gastric alpha-synuclein immunoreactive inclusions

in Meissner's and Auerbach's plexuses in cases staged for Parkinson's disease-related brain pathology. Neurosci Lett. 2006;396(1):67-72.

Braak H, Del Tredici K, Bratzke H, Hamm-Clement J, Sandmann-Keil D, Rub U. Staging of the intracerebral inclusion body pathology associated with idiopathic Parkinson's disease (preclinical and clinical stages). J Neurol. 2002;249 Suppl 3:III/1-5.

Braak H, Del Tredici K, Rub U, de Vos RA, Jansen Steur EN, Braak E. Staging of brain pathology related to sporadic Parkinson's disease. Neurobiol Aging. 2003;24(2):197-211.

Braak H, Sandmann-Keil D, Gai W, Braak E. Extensive axonal Lewy neurites in Parkinson's disease: a novel pathological feature revealed by alpha-synuclein immunocytochemistry. Neurosci Lett. 1999;265(1):67-9.

Braak H, Sastre M, Del Tredici K. Development of alpha-synuclein immunoreactive astrocytes in the forebrain parallels stages of intraneuronal pathology in sporadic Parkinson's disease. Acta Neuropathol. 2007;114(3):231-41.

Brachmann S. Successful Phase 1 Trial for Parkinson's Vaccine. 2014 August 7 2014 [cited 2015 20 February]; Available from: http://www.ipwatchdog.com/2014/08/07/successful-phase-1-trial-for-parkinsons-vaccine/id=50717/

Breit S, Schulz JB, Benabid AL. Deep brain stimulation. Cell Tissue Res. 2004;318(1):275-88.

Bucciantini M, Giannoni E, Chiti F, Baroni F, Formigli L, Zurdo J, et al. Inherent toxicity of aggregates implies a common mechanism for protein misfolding diseases. Nature. 2002;416(6880):507-11.

Burre J, Sharma M, Tsetsenis T, Buchman V, Etherton MR, Sudhof TC. Alpha-synuclein promotes SNARE-complex assembly in vivo and in vitro. Science. 2010;329(5999):1663-7.

Burre J, Vivona S, Diao J, Sharma M, Brunger AT, Sudhof TC. Properties of native brain alpha-synuclein. Nature. 2013;498(7453):E4-6; discussion E-7.

Cabantous S, Nguyen HB, Pedelacq JD, Koraichi F, Chaudhary A, Ganguly K, et al. A new protein-protein interaction sensor based on tripartite split-GFP association. Scientific reports. 2013;3:2854.

Cabin DE, Shimazu K, Murphy D, Cole NB, Gottschalk W, McIlwain KL, et al. Synaptic vesicle depletion correlates with attenuated synaptic responses to prolonged repetitive stimulation in mice lacking alpha-synuclein. J Neurosci. 2002;22(20):8797-807.

Cai J, Yang M, Poremsky E, Kidd S, Schneider JS, Iacovitti L. Dopaminergic neurons derived from human induced pluripotent stem cells survive and integrate into 6-OHDA-lesioned rats. Stem Cells Dev. 2010;19(7):1017-23.

Calne DB, Snow BJ, Lee C. Criteria for diagnosing Parkinson's disease. Ann Neurol. 1992;32 Suppl:S125-7.

Carmo-Goncalves P, Pinheiro AS, Romao L, Cortines J, Follmer C. UV-induced selective oxidation of Met5 to Met-sulfoxide leads to the formation of neurotoxic fibril-incompetent alpha-synuclein oligomers. Amyloid. 2014;21(3):163-74.

Carpenter AE, Jones TR, Lamprecht MR, Clarke C, Kang IH, Friman O, et al. CellProfiler: image analysis software for identifying and quantifying cell phenotypes. Genome biology. 2006;7(10):R100.

Caruana M, Hogen T, Levin J, Hillmer A, Giese A, Vassallo N. Inhibition and disaggregation of alpha-synuclein oligomers by natural polyphenolic compounds. FEBS Lett. 2011;585(8):1113-20.

Caughey B, Lansbury PT. Protofibrils, pores, fibrils, and neurodegeneration: separating the

responsible protein aggregates from the innocent bystanders. Annu Rev Neurosci. 2003;26:267-98.

Celej MS, Sarroukh R, Goormaghtigh E, Fidelio GD, Ruysschaert JM, Raussens V. Toxic prefibrillar alpha-synuclein amyloid oligomers adopt a distinctive antiparallel beta-sheet structure. Biochem J. 2012;443(3):719-26.

Chan SL, Angeles DC, Tan EK. Targeting leucine-rich repeat kinase 2 in Parkinson's disease. Expert Opin Ther Targets. 2013;17(12):1471-82.

Chandra S, Fornai F, Kwon HB, Yazdani U, Atasoy D, Liu X, et al. Double-knockout mice for alpha- and beta-synucleins: effect on synaptic functions. Proc Natl Acad Sci U S A. 2004;101(41):14966-71.

Chartier-Harlin MC, Kachergus J, Roumier C, Mouroux V, Douay X, Lincoln S, et al. Alpha-synuclein locus duplication as a cause of familial Parkinson's disease. Lancet. 2004;364(9440):1167-9.

Chen L, Jin J, Davis J, Zhou Y, Wang Y, Liu J, et al. Oligomeric alpha-synuclein inhibits tubulin polymerization. Biochem Biophys Res Commun. 2007;356(3):548-53.

Chen L, Periquet M, Wang X, Negro A, McLean PJ, Hyman BT, et al. Tyrosine and serine phosphorylation of alpha-synuclein have opposing effects on neurotoxicity and soluble oligomer formation. J Clin Invest. 2009;119(11):3257-65.

Chen L, Thiruchelvam MJ, Madura K, Richfield EK. Proteasome dysfunction in aged human alpha-synuclein transgenic mice. Neurobiol Dis. 2006;23(1):120-6.

Chen X, Reynolds CH. Performance of similarity measures in 2D fragment-based similarity searching: comparison of structural descriptors and similarity coefficients. Journal of chemical information and computer sciences. 2002;42(6):1407-14.

Chen X, Zaro JL, Shen WC. Fusion protein linkers: property, design and functionality. Advanced drug delivery reviews. 2013;65(10):1357-69.

Chiba-Falek O, Lopez GJ, Nussbaum RL. Levels of alpha-synuclein mRNA in sporadic Parkinson disease patients. Mov Disord. 2006;21(10):1703-8.

Chinta SJ, Mallajosyula JK, Rane A, Andersen JK. Mitochondrial alpha-synuclein accumulation impairs complex I function in dopaminergic neurons and results in increased mitophagy in vivo. Neuroscience Letters. 2010;486(3):235-9.

Choi BK, Choi MG, Kim JY, Yang Y, Lai Y, Kweon DH, et al. Large alpha-synuclein oligomers inhibit neuronal SNARE-mediated vesicle docking. Proc Natl Acad Sci U S A. 2013;110(10):4087-92.

Chu Y, Dodiya H, Aebischer P, Olanow CW, Kordower JH. Alterations in lysosomal and proteasomal markers in Parkinson's disease: relationship to alpha-synuclein inclusions. Neurobiol Dis. 2009;35(3):385-98.

Chu Y, Kordower JH. Age-associated increases of alpha-synuclein in monkeys and humans are associated with nigrostriatal dopamine depletion: Is this the target for Parkinson's disease? Neurobiol Dis. 2007;25(1):134-49.

Colla E, Jensen PH, Pletnikova O, Troncoso JC, Glabe C, Lee MK. Accumulation of Toxic alpha-Synuclein Oligomer within Endoplasmic Reticulum Occurs in alpha-Synucleinopathy In Vivo. J Neurosci. 2012;32(10):3301-5.

Colosimo C, Hughes AJ, Kilford L, Lees AJ. Lewy body cortical involvement may not always predict dementia in Parkinson's disease. J Neurol Neurosurg Psychiatry. 2003;74(7):852-6.

Compta Y, Parkkinen L, O'Sullivan SS, Vandrovcova J, Holton JL, Collins C, et al. Lewy- and

Alzheimer-type pathologies in Parkinson's disease dementia: which is more important? Brain. 2011;134(Pt 5):1493-505.

Conway KA, Lee SJ, Rochet JC, Ding TT, Harper JD, Williamson RE, et al. Accelerated oligomerization by Parkinson's disease linked alpha-synuclein mutants. Ann N Y Acad Sci. 2000;920:42-5.

Conway KA, Rochet JC, Bieganski RM, Lansbury PT, Jr. Kinetic stabilization of the alpha-synuclein protofibril by a dopamine-alpha-synuclein adduct. Science. 2001;294(5545):1346-9.

Cookson MR, Hardy J, Lewis PA. Genetic neuropathology of Parkinson's disease. International journal of clinical and experimental pathology. 2008;1(3):217-31.

Cremades N, Cohen SI, Deas E, Abramov AY, Chen AY, Orte A, et al. Direct observation of the interconversion of normal and toxic forms of alpha-synuclein. Cell. 2012;149(5):1048-59.

Crowther RA, Jakes R, Spillantini MG, Goedert M. Synthetic filaments assembled from C-terminally truncated alpha-synuclein. FEBS Lett. 1998;436(3):309-12.

Culvenor JG, McLean CA, Cutt S, Campbell BC, Maher F, Jakala P, et al. Non-Abeta component of Alzheimer's disease amyloid (NAC) revisited. NAC and alpha-synuclein are not associated with Abeta amyloid. Am J Pathol. 1999;155(4):1173-81.

Cummings JL. Intellectual impairment in Parkinson's disease: clinical, pathologic, and biochemical correlates. J Geriatr Psychiatry Neurol. 1988;1(1):24-36.

Czlapinski JL, Schelle MW, Miller LW, Laughlin ST, Kohler JJ, Cornish VW, et al. Conditional glycosylation in eukaryotic cells using a biocompatible chemical inducer of dimerization. J Am Chem Soc. 2008;130(40):13186-7.

D'Costa DF, Sheehan LJ, Phillips PA, Moore-Smith B. The levodopa test in Parkinson's disease. Age and ageing. 1995;24(3):210-2.

Dachsel JC, Lincoln SJ, Gonzalez J, Ross OA, Dickson DW, Farrer MJ. The ups and downs of alpha-synuclein mRNA expression. Mov Disord. 2007;22(2):293-5.

Dai JP, Zhao XF, Zeng J, Wan QY, Yang JC, Li WZ, et al. Drug screening for autophagy inhibitors based on the dissociation of Beclin1-Bcl2 complex using BiFC technique and mechanism of eugenol on anti-influenza A virus activity. PLoS One. 2013;8(4):e61026.

Dale GE, Probst A, Luthert P, Martin J, Anderton BH, Leigh PN. Relationships between Lewy bodies and pale bodies in Parkinson's disease. Acta Neuropathol. 1992;83(5):525-9.

Dalfo E, Ferrer I. Early alpha-synuclein lipoxidation in neocortex in Lewy body diseases. Neurobiol Aging. 2008;29(3):408-17.

Danzer KM, Haasen D, Karow AR, Moussaud S, Habeck M, Giese A, et al. Different species of alpha-synuclein oligomers induce calcium influx and seeding. J Neurosci. 2007;27(34):9220-32.

Davidson WS, Jonas A, Clayton DF, George JM. Stabilization of alpha-synuclein secondary structure upon binding to synthetic membranes. J Biol Chem. 1998;273(16):9443-9.

de Rijk MC, Tzourio C, Breteler MM, Dartigues JF, Amaducci L, Lopez-Pousa S, et al. Prevalence of parkinsonism and Parkinson's disease in Europe: the EUROPARKINSON Collaborative Study. European Community Concerted Action on the Epidemiology of Parkinson's disease. J Neurol Neurosurg Psychiatry. 1997;62(1):10-5.

Dehay B, Martinez-Vicente M, Caldwell GA, Caldwell KA, Yue Z, Cookson MR, et al. Lysosomal impairment in Parkinson's disease. Mov Disord. 2013;28(6):725-32.

Dehay B, Martinez-Vicente M, Ramirez A, Perier C, Klein C, Vila M, et al. Lysosomal dysfunction in Parkinson disease: ATP13A2 gets into the groove. Autophagy. 2012;8(9):1389-91.

Del Tredici K, Rub U, De Vos RA, Bohl JR, Braak H. Where does parkinson disease pathology begin in the brain? J Neuropathol Exp Neurol. 2002;61(5):413-26.

Dettmer U, Newman AJ, Luth ES, Bartels T, Selkoe D. In vivo cross-linking reveals principally oligomeric forms of alpha-synuclein and beta-synuclein in neurons and non-neural cells. J Biol Chem. 2013;288(9):6371-85.

Devi L, Raghavendran V, Prabhu BM, Avadhani NG, Anandatheerthavarada HK. Mitochondrial import and accumulation of alpha-synuclein impair complex I in human dopaminergic neuronal cultures and Parkinson disease brain. J Biol Chem. 2008;283(14):9089-100.

Di Monte DA. The environment and Parkinson's disease: is the nigrostriatal system preferentially targeted by neurotoxins? Lancet Neurol. 2003;2(9):531-8.

Di Monte DA, Lavasani M, Manning-Bog AB. Environmental factors in Parkinson's disease. Neurotoxicology. 2002;23(4-5):487-502.

Diao J, Burre J, Vivona S, Cipriano DJ, Sharma M, Kyoung M, et al. Native alpha-synuclein induces clustering of synaptic-vesicle mimics via binding to phospholipids and synaptobrevin-2/VAMP2. eLife. 2013;2:e00592.

Dickson DW, Fujishiro H, DelleDonne A, Menke J, Ahmed Z, Klos KJ, et al. Evidence that incidental Lewy body disease is pre-symptomatic Parkinson's disease. Acta Neuropathol. 2008;115(4):437-44.

Dickson DW, Fujishiro H, Orr C, DelleDonne A, Josephs KA, Frigerio R, et al. Neuropathology of non-motor features of Parkinson disease. Parkinsonism Relat Disord. 2009;15 Suppl 3:S1-5.

Dickson DW, Uchikado H, Fujishiro H, Tsuboi Y. Evidence in favor of Braak staging of Parkinson's disease. Mov Disord. 2010;25 Suppl 1:S78-82.

Dimant H, Kalia SK, Kalia LV, Zhu LN, Kibuuka L, Ebrahimi-Fakhari D, et al. Direct detection of alpha synuclein oligomers in vivo. Acta neuropathologica communications. 2013;1(1):6.

Do CB, Tung JY, Dorfman E, Kiefer AK, Drabant EM, Francke U, et al. Web-based genome-wide association study identifies two novel loci and a substantial genetic component for Parkinson's disease. PLoS Genet. 2011;7(6):e1002141.

Duda JE, Giasson BI, Chen Q, Gur TL, Hurtig HI, Stern MB, et al. Widespread nitration of pathological inclusions in neurodegenerative synucleinopathies. Am J Pathol. 2000;157(5):1439-45.

Duda JE, Giasson BI, Mabon ME, Lee VM, Trojanowski JQ. Novel antibodies to synuclein show abundant striatal pathology in Lewy body diseases. Ann Neurol. 2002;52(2):205-10.

Ebrahimi-Fakhari D, Cantuti-Castelvetri I, Fan Z, Rockenstein E, Masliah E, Hyman BT, et al. Distinct Roles In Vivo for the Ubiquitin-Proteasome System and the Autophagy-Lysosomal Pathway in the Degradation of {alpha}-Synuclein. J Neurosci. 2011;31(41):14508-20.

Edwards TL, Scott WK, Almonte C, Burt A, Powell EH, Beecham GW, et al. Genome-wide association study confirms SNPs in SNCA and the MAPT region as common risk factors for Parkinson disease. Ann Hum Genet. 2010;74(2):97-109.

Ehrnhoefer DE, Bieschke J, Boeddrich A, Herbst M, Masino L, Lurz R, et al. EGCG redirects amyloidogenic polypeptides into unstructured, off-pathway oligomers. Nature structural & molecular biology. 2008;15(6):558-66.

El-Agnaf OM, Paleologou KE, Greer B, Abogrein AM, King JE, Salem SA, et al. A strategy for designing inhibitors of alpha-synuclein aggregation and toxicity as a novel treatment for Parkinson's disease and related disorders. FASEB J. 2004;18(11):1315-7.

El-Agnaf OM, Salem SA, Paleologou KE, Curran MD, Gibson MJ, Court JA, et al. Detection

of oligomeric forms of alpha-synuclein protein in human plasma as a potential biomarker for Parkinson's disease. FASEB J. 2006;20(3):419-25.

Elia AE, Petrucci S, Fasano A, Guidi M, Valbonesi S, Bernardini L, et al. Alpha-synuclein gene duplication: marked intrafamilial variability in two novel pedigrees. Mov Disord. 2013;28(6):813-7.

Emmanouilidou E, Stefanis L, Vekrellis K. Cell-produced alpha-synuclein oligomers are targeted to, and impair, the 26S proteasome. Neurobiol Aging. 2010;31(6):953-68.

Erickson HP. Size and shape of protein molecules at the nanometer level determined by sedimentation, gel filtration, and electron microscopy. Biological procedures online. 2009;11:32-51.

Esteban-Martin S, Silvestre-Ryan J, Bertoncini CW, Salvatella X. Identification of Fibril-Like Tertiary Contacts in Soluble Monomeric alpha-Synuclein. Biophys J. 2013;105(5):1192-8.

Fagerqvist T, Lindstrom V, Nordstrom E, Lord A, Tucker SM, Su X, et al. Monoclonal antibodies selective for alpha-synuclein oligomers/protofibrils recognize brain pathology in Lewy body disorders and alpha-synuclein transgenic mice with the disease-causing A30P mutation. J Neurochem. 2013;126(1):131-44.

Fagerqvist T, Nasstrom T, Ihse E, Lindstrom V, Sahlin C, Fangmark Tucker SM, et al. Off-pathway alpha-synuclein oligomers seem to alter alpha-synuclein turnover in a cell model but lack seeding capability in vivo. Amyloid. 2013.

Fares MB, Ait-Bouziad N, Dikiy I, Mbefo MK, Jovicic A, Kiely A, et al. The novel Parkinson's disease linked mutation G51D attenuates in vitro aggregation and membrane binding of alpha-synuclein, and enhances its secretion and nuclear localization in cells. Hum Mol Genet. 2014;23(17):4491-509.

Farrer M, Kachergus J, Forno L, Lincoln S, Wang DS, Hulihan M, et al. Comparison of kindreds with parkinsonism and alpha-synuclein genomic multiplications. Ann Neurol. 2004;55(2):174-9.

Farrer M, Maraganore DM, Lockhart P, Singleton A, Lesnick TG, de Andrade M, et al. alpha-Synuclein gene haplotypes are associated with Parkinson's disease. Hum Mol Genet. 2001;10(17):1847-51.

Fauerbach JA, Yushchenko DA, Shahmoradian SH, Chiu W, Jovin TM, Jares-Erijman EA. Supramolecular Non-Amyloid Intermediates in the Early Stages of alpha-Synuclein Aggregation. Biophys J. 2012;102(5):1127-36.

Fauvet B, Mbefo MK, Fares MB, Desobry C, Michael S, Ardah MT, et al. Alpha-synuclein in the central nervous system and from erythrocytes, mammalian cells and E. coli exists predominantly as a disordered monomer. J Biol Chem. 2012.

Fearnley JM, Lees AJ. Ageing and Parkinson's disease: substantia nigra regional selectivity. Brain. 1991;114 (Pt 5):2283-301.

Ferrari S, Pellati, F., Costi, M.P. Protein-Protein Interaction Inhibitors: Case Studies on Small Molecules and Natural Compounds. In: Mangani S, editor. Disruption of Protein-Protein Interfaces: Springer Berlin Heidelberg; 2013. p. pp31-60.

Forloni G. Neurotoxicity of beta-amyloid and prion peptides. Curr Opin Neurol. 1996;9(6):492-500.

Fortin DL. Lipid Rafts Mediate the Synaptic Localization of -Synuclein. Journal of Neuroscience. 2004;24(30):6715-23.

Fredenburg RA, Rospigliosi C, Meray RK, Kessler JC, Lashuel HA, Eliezer D, et al. The impact of the E46K mutation on the properties of alpha-synuclein in its monomeric and oligomeric states. Biochemistry. 2007;46(24):7107-18.

Freed CR, Greene PE, Breeze RE, Tsai WY, DuMouchel W, Kao R, et al. Transplantation of embryonic dopamine neurons for severe Parkinson's disease. N Engl J Med. 2001;344(10):710-9.

Friedman LG, Lachenmayer ML, Wang J, He L, Poulose SM, Komatsu M, et al. Disrupted autophagy leads to dopaminergic axon and dendrite degeneration and promotes presynaptic accumulation of alpha-synuclein and LRRK2 in the brain. J Neurosci. 2012;32(22):7585-93.

Frigerio R, Fujishiro H, Ahn TB, Josephs KA, Maraganore DM, DelleDonne A, et al. Incidental Lewy body disease: do some cases represent a preclinical stage of dementia with Lewy bodies? Neurobiol Aging. 2011;32(5):857-63.

Fuchs J, Tichopad A, Golub Y, Munz M, Schweitzer KJ, Wolf B, et al. Genetic variability in the SNCA gene influences alpha-synuclein levels in the blood and brain. FASEB J. 2008;22(5):1327-34.

Fujimi K, Sasaki K, Noda K, Wakisaka Y, Tanizaki Y, Matsui Y, et al. Clinicopathological outline of dementia with Lewy bodies applying the revised criteria: the Hisayama study. Brain Pathol. 2008;18(3):317-25.

Fujiwara H, Hasegawa M, Dohmae N, Kawashima A, Masliah E, Goldberg MS, et al. alpha-Synuclein is phosphorylated in synucleinopathy lesions. Nat Cell Biol. 2002;4(2):160-4.

Galloway PG, Grundke-Iqbal I, Iqbal K, Perry G. Lewy bodies contain epitopes both shared and distinct from Alzheimer neurofibrillary tangles. J Neuropathol Exp Neurol. 1988;47(6):654-63.

Galvin JE, Uryu K, Lee VM, Trojanowski JQ. Axon pathology in Parkinson's disease and Lewy body dementia hippocampus contains alpha-, beta-, and gamma-synuclein. Proc Natl Acad Sci U S A. 1999;96(23):13450-5.

Games D, Valera E, Spencer B, Rockenstein E, Mante M, Adame A, et al. Reducing C-terminal-truncated alpha-synuclein by immunotherapy attenuates neurodegeneration and propagation in Parkinson's disease-like models. J Neurosci. 2014;34(28):9441-54.

Geng X, Lou H, Wang J, Li L, Swanson AL, Sun M, et al. alpha-Synuclein binds the K(ATP) channel at insulin-secretory granules and inhibits insulin secretion. Am J Physiol Endocrinol Metab. 2011;300(2):E276-86.

George JM, Jin H, Woods WS, Clayton DF. Characterization of a novel protein regulated during the critical period for song learning in the zebra finch. Neuron. 1995;15(2):361-72.

Gerard M, Debyser Z, Desender L, Kahle PJ, Baert J, Baekelandt V, et al. The aggregation of alpha-synuclein is stimulated by FK506 binding proteins as shown by fluorescence correlation spectroscopy. FASEB J. 2006;20(3):524-6.

Ghosh D, Mondal M, Mohite GM, Singh PK, Ranjan P, Anoop A, et al. The Parkinson's disease-associated H50Q mutation accelerates alpha-Synuclein aggregation in vitro. Biochemistry. 2013;52(40):6925-7.

Giasson BI, Duda JE, Murray IV, Chen Q, Souza JM, Hurtig HI, et al. Oxidative damage linked to neurodegeneration by selective alpha-synuclein nitration in synucleinopathy lesions. Science. 2000;290(5493):985-9.

Giasson BI, Duda JE, Quinn SM, Zhang B, Trojanowski JQ, Lee VM. Neuronal alpha-synucleinopathy with severe movement disorder in mice expressing A53T human alpha-synuclein. Neuron. 2002;34(4):521-33.

Giasson BI, Forman MS, Higuchi M, Golbe LI, Graves CL, Kotzbauer PT, et al. Initiation and synergistic fibrillization of tau and alpha-synuclein. Science. 2003;300(5619):636-40.

Giasson BI, Jakes R, Goedert M, Duda JE, Leight S, Trojanowski JQ, et al. A panel of epitope-specific antibodies detects protein domains distributed throughout human alpha-synuclein in

Lewy bodies of Parkinson's disease. J Neurosci Res. 2000;59(4):528-33.

Giasson BI, Murray IV, Trojanowski JQ, Lee VM. A hydrophobic stretch of 12 amino acid residues in the middle of alpha-synuclein is essential for filament assembly. J Biol Chem. 2001;276(4):2380-6.

Gibb WR, Scott T, Lees AJ. Neuronal inclusions of Parkinson's disease. Mov Disord. 1991;6(1):2-11.

Giehm L, Svergun DI, Otzen DE, Vestergaard B. Low-resolution structure of a vesicle disrupting α-synuclein oligomer that accumulates during fibrillation. Proc Natl Acad Sci U S A. 2011;108(8):3246-51.

Gilks WP, Abou-Sleiman PM, Gandhi S, Jain S, Singleton A, Lees AJ, et al. A common LRRK2 mutation in idiopathic Parkinson's disease. Lancet. 2005;365(9457):415-6.

Gill SS, Patel NK, Hotton GR, O'Sullivan K, McCarter R, Bunnage M, et al. Direct brain infusion of glial cell line-derived neurotrophic factor in Parkinson disease. Nat Med. 2003;9(5):589-95.

Goker-Alpan O, Schiffmann R, LaMarca ME, Nussbaum RL, McInerney-Leo A, Sidransky E. Parkinsonism among Gaucher disease carriers. J Med Genet. 2004;41(12):937-40.

Goldman SM, Tanner CM, Oakes D, Bhudhikanok GS, Gupta A, Langston JW. Head injury and Parkinson's disease risk in twins. Ann Neurol. 2006;60(1):65-72.

Gomez-Tortosa E, Newell K, Irizarry MC, Sanders JL, Hyman BT. alpha-Synuclein immunoreactivity in dementia with Lewy bodies: morphological staging and comparison with ubiquitin immunostaining. Acta Neuropathol. 2000;99(4):352-7.

Gorell JM, Johnson CC, Rybicki BA, Peterson EL, Kortsha GX, Brown GG, et al. Occupational exposures to metals as risk factors for Parkinson's disease. Neurology. 1997;48(3):650-8.

Gosavi N, Lee HJ, Lee JS, Patel S, Lee SJ. Golgi fragmentation occurs in the cells with prefibrillar alpha-synuclein aggregates and precedes the formation of fibrillar inclusion. J Biol Chem. 2002;277(50):48984-92.

Gruber S, Arumugam P, Katou Y, Kuglitsch D, Helmhart W, Shirahige K, et al. Evidence that loading of cohesin onto chromosomes involves opening of its SMC hinge. Cell. 2006;127(3):523-37.

Guardia-Laguarta C, Area-Gomez E, Rub C, Liu Y, Magrane J, Becker D, et al. alpha-Synuclein Is Localized to Mitochondria-Associated ER Membranes. J Neurosci. 2014;34(1):249-59.

Gullberg M, Gustafsdottir SM, Schallmeiner E, Jarvius J, Bjarnegard M, Betsholtz C, et al. Cytokine detection by antibody-based proximity ligation. Proc Natl Acad Sci U S A. 2004;101(22):8420-4.

Halliday GM, Holton JL, Revesz T, Dickson DW. Neuropathology underlying clinical variability in patients with synucleinopathies. Acta Neuropathol. 2011;122(2):187-204.

Hansen C, Angot E, Bergstrom AL, Steiner JA, Pieri L, Paul G, et al. alpha-Synuclein propagates from mouse brain to grafted dopaminergic neurons and seeds aggregation in cultured human cells. J Clin Invest. 2011;121(2):715-25.

Hargus G, Cooper O, Deleidi M, Levy A, Lee K, Marlow E, et al. Differentiated Parkinson patient-derived induced pluripotent stem cells grow in the adult rodent brain and reduce motor asymmetry in Parkinsonian rats. Proc Natl Acad Sci U S A. 2010;107(36):15921-6.

Harris MA, Shen H, Marion SA, Tsui JK, Teschke K. Head injuries and Parkinson's disease in a case-control study. Occupational and environmental medicine. 2013;70(12):839-44.

Healy DG, Falchi M, O'Sullivan SS, Bonifati V, Durr A, Bressman S, et al. Phenotype, genotype,

and worldwide genetic penetrance of LRRK2-associated Parkinson's disease: a case-control study. Lancet Neurol. 2008;7(7):583-90.

Herva ME, Zibaee S, Fraser G, Barker RA, Goedert M, Spillantini MG. Anti-amyloid compounds inhibit alpha-synuclein aggregation induced by protein misfolding cyclic amplification (PMCA). J Biol Chem. 2014;289(17):11897-905.

Hilton D, Stephens M, Kirk L, Edwards P, Potter R, Zajicek J, et al. Accumulation of alpha-synuclein in the bowel of patients in the pre-clinical phase of Parkinson's disease. Acta Neuropathol. 2013.

Hindle JV. Ageing, neurodegeneration and Parkinson's disease. Age and ageing. 2010;39(2):156-61.

Hochfeld WE, Lee S, Rubinsztein DC. Therapeutic induction of autophagy to modulate neurodegenerative disease progression. Acta Pharmacol Sin. 2013;34(5):600-4.

Hughes AJ, Daniel SE, Ben-Shlomo Y, Lees AJ. The accuracy of diagnosis of parkinsonian syndromes in a specialist movement disorder service. Brain. 2002;125(Pt 4):861-70.

Ibanez P, Bonnet AM, Debarges B, Lohmann E, Tison F, Pollak P, et al. Causal relation between alpha-synuclein gene duplication and familial Parkinson's disease. Lancet. 2004;364(9440):1169-71.

Iwai A, Masliah E, Yoshimoto M, Ge N, Flanagan L, de Silva HA, et al. The precursor protein of non-A beta component of Alzheimer's disease amyloid is a presynaptic protein of the central nervous system. Neuron. 1995;14(2):467-75.

Jakes R, Spillantini MG, Goedert M. Identification of two distinct synucleins from human brain. FEBS Lett. 1994;345(1):27-32.

Jaleel M, Nichols RJ, Deak M, Campbell DG, Gillardon F, Knebel A, et al. LRRK2 phosphorylates moesin at threonine-558: characterization of how Parkinson's disease mutants affect kinase activity. Biochem J. 2007;405(2):307-17.

Jana NR, Dikshit P, Goswami A, Nukina N. Inhibition of proteasomal function by curcumin induces apoptosis through mitochondrial pathway. J Biol Chem. 2004;279(12):11680-5.

Janezic S, Threlfell S, Dodson PD, Dowie MJ, Taylor TN, Potgieter D, et al. Deficits in dopaminergic transmission precede neuron loss and dysfunction in a new Parkinson model. Proc Natl Acad Sci U S A. 2013.

Jankovic J. An update on the treatment of Parkinson's disease. The Mount Sinai journal of medicine, New York. 2006;73(4):682-9.

Jensen PH, Hager H, Nielsen MS, Hojrup P, Gliemann J, Jakes R. alpha-synuclein binds to Tau and stimulates the protein kinase A-catalyzed tau phosphorylation of serine residues 262 and 356. J Biol Chem. 1999;274(36):25481-9.

Joachim CL, Morris JH, Kosik KS, Selkoe DJ. Tau antisera recognize neurofibrillary tangles in a range of neurodegenerative disorders. Ann Neurol. 1987;22(4):514-20.

Kahle PJ, Neumann M, Ozmen L, Muller V, Jacobsen H, Schindzielorz A, et al. Subcellular localization of wild-type and Parkinson's disease-associated mutant alpha -synuclein in human and transgenic mouse brain. J Neurosci. 2000;20(17):6365-73.

Kahle PJ, Neumann M, Ozmen L, Muller V, Odoy S, Okamoto N, et al. Selective insolubility of alpha-synuclein in human Lewy body diseases is recapitulated in a transgenic mouse model. Am J Pathol. 2001;159(6):2215-25.

Kalaitzakis ME, Graeber MB, Gentleman SM, Pearce RK. Controversies over the staging of alpha-synuclein pathology in Parkinson's disease. Acta Neuropathol. 2008;116(1):125-8; author

reply 9-31.

Kalaitzakis ME, Graeber MB, Gentleman SM, Pearce RK. The dorsal motor nucleus of the vagus is not an obligatory trigger site of Parkinson's disease: a critical analysis of alpha-synuclein staging. Neuropathol Appl Neurobiol. 2008;34(3):284-95.

Kamali-Moghaddam M, Pettersson FE, Wu D, Englund H, Darmanis S, Lord A, et al. Sensitive detection of Abeta protofibrils by proximity ligation--relevance for Alzheimer's disease. BMC Neurosci. 2010;11:124.

Kamp F, Exner N, Lutz AK, Wender N, Hegermann J, Brunner B, et al. Inhibition of mitochondrial fusion by alpha-synuclein is rescued by PINK1, Parkin and DJ-1. EMBO J. 2010;29(20):3571-89.

Kanazawa T, Adachi E, Orimo S, Nakamura A, Mizusawa H, Uchihara T. Pale neurites, premature alpha-synuclein aggregates with centripetal extension from axon collaterals. Brain Pathol. 2012;22(1):67-78.

Kanazawa T, Uchihara T, Takahashi A, Nakamura A, Orimo S, Mizusawa H. Three-layered structure shared between Lewy bodies and lewy neurites-three-dimensional reconstruction of triple-labeled sections. Brain Pathol. 2008;18(3):415-22.

Kara E, Kiely AP, Proukakis C, Giffin N, Love S, Hehir J, et al. A 6.4 Mb duplication of the alpha-synuclein locus causing frontotemporal dementia and Parkinsonism: phenotype-genotype correlations. JAMA neurology. 2014;71(9):1162-71.

Karpinar DP, Balija MB, Kugler S, Opazo F, Rezaei-Ghaleh N, Wender N, et al. Pre-fibrillar alpha-synuclein variants with impaired beta-structure increase neurotoxicity in Parkinson's disease models. EMBO J. 2009;28(20):3256-68.

Katsuse O, Iseki E, Marui W, Kosaka K. Developmental stages of cortical Lewy bodies and their relation to axonal transport blockage in brains of patients with dementia with Lewy bodies. J Neurol Sci. 2003;211(1-2):29-35.

Kayed R, Head E, Thompson JL, McIntire TM, Milton SC, Cotman CW, et al. Common structure of soluble amyloid oligomers implies common mechanism of pathogenesis. Science. 2003;300(5618):486-9.

Keane PC, Kurzawa M, Blain PG, Morris CM. Mitochondrial dysfunction in Parkinson's disease. Parkinsons Dis. 2011;2011:716871.

Kefalopoulou Z, Politis M, Piccini P, Mencacci N, Bhatia K, Jahanshahi M, et al. Long-term clinical outcome of fetal cell transplantation for Parkinson disease: two case reports. JAMA neurology. 2014;71(1):83-7.

Ki CS, Stavrou EF, Davanos N, Lee WY, Chung EJ, Kim JY, et al. The Ala53Thr mutation in the alpha-synuclein gene in a Korean family with Parkinson disease. Clinical genetics. 2007;71(5):471-3.

Kim-Han JS, Antenor-Dorsey JA, O'Malley KL. The Parkinsonian Mimetic, MPP+, Specifically Impairs Mitochondrial Transport in Dopamine Axons. J Neurosci. 2011;31(19):7212-21.

Kim HY, Cho MK, Kumar A, Maier E, Siebenhaar C, Becker S, et al. Structural properties of pore-forming oligomers of alpha-synuclein. J Am Chem Soc. 2009;131(47):17482-9.

Kingsbury AE, Bandopadhyay R, Silveira-Moriyama L, Ayling H, Kallis C, Sterlacci W, et al. Brain stem pathology in Parkinson's disease: an evaluation of the Braak staging model. Mov Disord. 2010;25(15):2508-15.

Kingsbury AE, Daniel SE, Sangha H, Eisen S, Lees AJ, Foster OJ. Alteration in alpha-synuclein mRNA expression in Parkinson's disease. Mov Disord. 2004;19(2):162-70.

Kirik D, Georgievska B, Bjorklund A. Localized striatal delivery of GDNF as a treatment for Parkinson disease. Nat Neurosci. 2004;7(2):105-10.

Klein C, Westenberger A. Genetics of Parkinson's disease. Cold Spring Harbor perspectives in medicine. 2012;2(1):a008888.

Klucken J, Outeiro TF, Nguyen P, McLean PJ, Hyman BT. Detection of novel intracellular alpha-synuclein oligomeric species by fluorescence lifetime imaging. FASEB J. 2006;20(12):2050-7.

Konig P, Krasteva G, Tag C, Konig IR, Arens C, Kummer W. FRET-CLSM and double-labeling indirect immunofluorescence to detect close association of proteins in tissue sections. Laboratory investigation; a journal of technical methods and pathology. 2006;86(8):853-64.

Kordower JH, Chu Y, Hauser RA, Freeman TB, Olanow CW. Lewy body-like pathology in long-term embryonic nigral transplants in Parkinson's disease. Nat Med. 2008;14(5):504-6.

Kosaka K. Lewy bodies in cerebral cortex, report of three cases. Acta Neuropathol. 1978;42(2):127-34.

Kovacs GG, Breydo L, Green R, Kis V, Puska G, Lorincz P, et al. Intracellular processing of disease-associated alpha-synuclein in the human brain suggests prion-like cell-to-cell spread. Neurobiol Dis. 2014;69C:76-92.

Kovacs GG, Wagner U, Dumont B, Pikkarainen M, Osman AA, Streichenberger N, et al. An antibody with high reactivity for disease-associated alpha-synuclein reveals extensive brain pathology. Acta Neuropathol. 2012.

Kramer ML, Schulz-Schaeffer WJ. Presynaptic alpha-synuclein aggregates, not Lewy bodies, cause neurodegeneration in dementia with Lewy bodies. J Neurosci. 2007;27(6):1405-10.

Krishnan S, Chi EY, Wood SJ, Kendrick BS, Li C, Garzon-Rodriguez W, et al. Oxidative dimer formation is the critical rate-limiting step for Parkinson's disease alpha-synuclein fibrillogenesis. Biochemistry. 2003;42(3):829-37.

Kruger R, Kuhn W, Muller T, Woitalla D, Graeber M, Kosel S, et al. Ala30Pro mutation in the gene encoding alpha-synuclein in Parkinson's disease. Nat Genet. 1998;18(2):106-8.

Kuusisto E, Parkkinen L, Alafuzoff I. Morphogenesis of Lewy bodies: dissimilar incorporation of alpha-synuclein, ubiquitin, and p62. J Neuropathol Exp Neurol. 2003;62(12):1241-53.

Lang AE, Gill S, Patel NK, Lozano A, Nutt JG, Penn R, et al. Randomized controlled trial of intraputamenal glial cell line-derived neurotrophic factor infusion in Parkinson disease. Ann Neurol. 2006;59(3):459-66.

Langston JW, Ballard P, Tetrud JW, Irwin I. Chronic Parkinsonism in humans due to a product of meperidine-analog synthesis. Science. 1983;219(4587):979-80.

Lashuel HA, Hartley D, Petre BM, Walz T, Lansbury PT, Jr. Neurodegenerative disease: amyloid pores from pathogenic mutations. Nature. 2002;418(6895):291.

Latawiec D, Herrera F, Bek A, Losasso V, Candotti M, Benetti F, et al. Modulation of alpha-synuclein aggregation by dopamine analogs. PLoS One. 2010;5(2):e9234.

Lavedan C. The synuclein family. Genome Res. 1998;8(9):871-80.

Lazaro DF, Rodrigues EF, Langohr R, Shahpasandzadeh H, Ribeiro T, Guerreiro P, et al. Systematic comparison of the effects of alpha-synuclein mutations on its oligomerization and aggregation. PLoS Genet. 2014;10(11):e1004741.

Lee HJ, Baek SM, Ho DH, Suk JE, Cho ED, Lee SJ. Dopamine promotes formation and secretion of non-fibrillar alpha-synuclein oligomers. Experimental & molecular medicine. 2011;43(4):216-22.

Leong SL, Pham CL, Galatis D, Fodero-Tavoletti MT, Perez K, Hill AF, et al. Formation of dopamine-mediated alpha-synuclein-soluble oligomers requires methionine oxidation. Free Radic Biol Med. 2009;46(10):1328-37.

Lesage S, Anheim M, Letournel F, Bousset L, Honore A, Rozas N, et al. G51D alpha-synuclein mutation causes a novel parkinsonian-pyramidal syndrome. Ann Neurol. 2013;73(4):459-71.

Lesne S, Koh MT, Kotilinek L, Kayed R, Glabe CG, Yang A, et al. A specific amyloid-beta protein assembly in the brain impairs memory. Nature. 2006;440(7082):352-7.

Leverenz JB, Hamilton R, Tsuang DW, Schantz A, Vavrek D, Larson EB, et al. Empiric refinement of the pathologic assessment of Lewy-related pathology in the dementia patient. Brain Pathol. 2008;18(2):220-4.

Leverenz JB, Umar I, Wang Q, Montine TJ, McMillan PJ, Tsuang DW, et al. Proteomic identification of novel proteins in cortical lewy bodies. Brain Pathol. 2007;17(2):139-45.

Lewy FH. Paralysis agitans. I Pathologische Anatomie. Handbuch der Neurologie III. Berlin: Springer; 1912. p. 920-33.

Li J, Zhu M, Manning-Bog AB, Di Monte DA, Fink AL. Dopamine and L-dopa disaggregate amyloid fibrils: implications for Parkinson's and Alzheimer's disease. FASEB J. 2004;18(9):962-4.

Li JY, Englund E, Holton JL, Soulet D, Hagell P, Lees AJ, et al. Lewy bodies in grafted neurons in subjects with Parkinson's disease suggest host-to-graft disease propagation. Nat Med. 2008;14(5):501-3.

Li W, West N, Colla E, Pletnikova O, Troncoso JC, Marsh L, et al. Aggregation promoting C-terminal truncation of alpha-synuclein is a normal cellular process and is enhanced by the familial Parkinson's disease-linked mutations. Proc Natl Acad Sci U S A. 2005;102(6):2162-7.

Li WW, Yang R, Guo JC, Ren HM, Zha XL, Cheng JS, et al. Localization of alpha-synuclein to mitochondria within midbrain of mice. Neuroreport. 2007;18(15):1543-6.

Lindersson E, Beedholm R, Hojrup P, Moos T, Gai W, Hendil KB, et al. Proteasomal inhibition by alpha-synuclein filaments and oligomers. J Biol Chem. 2004;279(13):12924-34.

Lindstrom V, Fagerqvist T, Nordstrom E, Eriksson F, Lord A, Tucker S, et al. Immunotherapy targeting alpha-synuclein protofibrils reduced pathology in (Thy-1)-h[A30P] alpha-synuclein mice. Neurobiol Dis. 2014;69:134-43.

Lindvall O, Sawle G, Widner H, Rothwell JC, Bjorklund A, Brooks D, et al. Evidence for long-term survival and function of dopaminergic grafts in progressive Parkinson's disease. Ann Neurol. 1994;35(2):172-80.

Liou HH, Tsai MC, Chen CJ, Jeng JS, Chang YC, Chen SY, et al. Environmental risk factors and Parkinson's disease: a case-control study in Taiwan. Neurology. 1997;48(6):1583-8.

Liu CW, Giasson BI, Lewis KA, Lee VM, Demartino GN, Thomas PJ. A precipitating role for truncated alpha-synuclein and the proteasome in alpha-synuclein aggregation: implications for pathogenesis of Parkinson disease. J Biol Chem. 2005;280(24):22670-8.

Liu G, Zhang C, Yin J, Li X, Cheng F, Li Y, et al. alpha-Synuclein is differentially expressed in mitochondria from different rat brain regions and dose-dependently down-regulates complex I activity. Neurosci Lett. 2009;454(3):187-92.

Liu Y, Gu J, Hagner-McWhirter A, Sathiyanarayanan P, Gullberg M, Soderberg O, et al. Western blotting via proximity ligation for high performance protein analysis. Mol Cell Proteomics. 2011;10(11):O111 011031.

Logroscino G, Gao X, Chen H, Wing A, Ascherio A. Dietary iron intake and risk of Parkinson's

disease. Am J Epidemiol. 2008;168(12):1381-8.

Lowe J, Blanchard A, Morrell K, Lennox G, Reynolds L, Billett M, et al. Ubiquitin is a common factor in intermediate filament inclusion bodies of diverse type in man, including those of Parkinson's disease, Pick's disease, and Alzheimer's disease, as well as Rosenthal fibres in cerebellar astrocytomas, cytoplasmic bodies in muscle, and mallory bodies in alcoholic liver disease. J Pathol. 1988;155(1):9-15.

Luik RM, Wang B, Prakriya M, Wu MM, Lewis RS. Oligomerization of STIM1 couples ER calcium depletion to CRAC channel activation. Nature. 2008;454(7203):538-42.

Luk KC, Kehm V, Carroll J, Zhang B, O'Brien P, Trojanowski JQ, et al. Pathological alpha-synuclein transmission initiates Parkinson-like neurodegeneration in nontransgenic mice. Science. 2012;338(6109):949-53.

Luk KC, Song C, O'Brien P, Stieber A, Branch JR, Brunden KR, et al. Exogenous alpha-synuclein fibrils seed the formation of Lewy body-like intracellular inclusions in cultured cells. Proc Natl Acad Sci U S A. 2009;106(47):20051-6.

Luth ES, Bartels T, Dettmer U, Kim NC, Selkoe DJ. Purification of alpha-Synuclein from Human Brain Reveals an Instability of Endogenous Multimers as the Protein Approaches Purity. Biochemistry. 2015;54(2):279-92.

Mandler M, Valera E, Rockenstein E, Weninger H, Patrick C, Adame A, et al. Next-generation active immunization approach for synucleinopathies: implications for Parkinson's disease clinical trials. Acta Neuropathol. 2014;127(6):861-79.

Manning-Bog AB, McCormack AL, Li J, Uversky VN, Fink AL, Di Monte DA. The herbicide paraquat causes up-regulation and aggregation of alpha-synuclein in mice: paraquat and alpha-synuclein. J Biol Chem. 2002;277(3):1641-4.

Maraganore DM, de Andrade M, Elbaz A, Farrer MJ, Ioannidis JP, Kruger R, et al. Collaborative analysis of alpha-synuclein gene promoter variability and Parkinson disease. JAMA. 2006;296(6):661-70.

Markesbery WR, Jicha GA, Liu H, Schmitt FA. Lewy body pathology in normal elderly subjects. J Neuropathol Exp Neurol. 2009;68(7):816-22.

Maroteaux L, Campanelli JT, Scheller RH. Synuclein: a neuron-specific protein localized to the nucleus and presynaptic nerve terminal. J Neurosci. 1988;8(8):2804-15.

Mastaglia FL, Johnsen RD, Byrnes ML, Kakulas BA. Prevalence of amyloid-beta deposition in the cerebral cortex in Parkinson's disease. Mov Disord. 2003;18(1):81-6.

Masuda-Suzukake M, Nonaka T, Hosokawa M, Oikawa T, Arai T, Akiyama H, et al. Prion-like spreading of pathological alpha-synuclein in brain. Brain. 2013;136(Pt 4):1128-38.

Mata IF, Yearout D, Alvarez V, Coto E, de Mena L, Ribacoba R, et al. Replication of MAPT and SNCA, but not PARK16-18, as susceptibility genes for Parkinson's disease. Mov Disord. 2011;26(5):819-23.

Mazanetz MP, Marmon RJ, Reisser CB, Morao I. Drug discovery applications for KNIME: an open source data mining platform. Current topics in medicinal chemistry. 2012;12(18):1965-79.

Mazzulli JR, Xu YH, Sun Y, Knight AL, McLean PJ, Caldwell GA, et al. Gaucher Disease Glucocerebrosidase and alpha-Synuclein Form a Bidirectional Pathogenic Loop in Synucleinopathies. Cell. 2011;146(1):37-52.

McCoy MK, Cookson MR. DJ-1 regulation of mitochondrial function and autophagy through oxidative stress. Autophagy. 2011;7(5):531-2.

McKeith IG. Spectrum of Parkinson's disease, Parkinson's dementia, and Lewy body dementia.

Neurologic clinics. 2000;18(4):865-902.

McKeith IG, Dickson DW, Lowe J, Emre M, O'Brien JT, Feldman H, et al. Diagnosis and management of dementia with Lewy bodies: third report of the DLB Consortium. Neurology. 2005;65(12):1863-72.

McLean PJ, Kawamata H, Shariff S, Hewett J, Sharma N, Ueda K, et al. TorsinA and heat shock proteins act as molecular chaperones: suppression of alpha-synuclein aggregation. J Neurochem. 2002;83(4):846-54.

McNaught KS, Belizaire R, Isacson O, Jenner P, Olanow CW. Altered proteasomal function in sporadic Parkinson's disease. Exp Neurol. 2003;179(1):38-46.

McNaught KS, Perl DP, Brownell AL, Olanow CW. Systemic exposure to proteasome inhibitors causes a progressive model of Parkinson's disease. Ann Neurol. 2004;56(1):149-62.

McNaught KS, Shashidharan P, Perl DP, Jenner P, Olanow CW. Aggresome-related biogenesis of Lewy bodies. Eur J Neurosci. 2002;16(11):2136-48.

Meissner WG. When does Parkinson's disease begin? From prodromal disease to motor signs. Rev Neurol (Paris). 2012;168(11):809-14.

Mencacci NE, Isaias IU, Reich MM, Ganos C, Plagnol V, Polke JM, et al. Parkinson's disease in GTP cyclohydrolase 1 mutation carriers. Brain. 2014;137(Pt 9):2480-92.

Mendez I, Vinuela A, Astradsson A, Mukhida K, Hallett P, Robertson H, et al. Dopamine neurons implanted into people with Parkinson's disease survive without pathology for 14 years. Nat Med. 2008;14(5):507-9.

Miake H, Mizusawa H, Iwatsubo T, Hasegawa M. Biochemical characterization of the core structure of alpha-synuclein filaments. J Biol Chem. 2002;277(21):19213-9.

Miller DW, Hague SM, Clarimon J, Baptista M, Gwinn-Hardy K, Cookson MR, et al. Alpha-synuclein in blood and brain from familial Parkinson disease with SNCA locus triplication. Neurology. 2004;62(10):1835-8.

Mizuno N, Varkey J, Kegulian NC, Hegde BG, Cheng N, Langen R, et al. Remodeling of lipid vesicles into cylindrical micelles by alpha-synuclein in an extended alpha-helical conformation. J Biol Chem. 2012;287(35):29301-11.

Mu L, Sobotka S, Chen J, Su H, Sanders I, Adler CH, et al. Alpha-synuclein pathology and axonal degeneration of the peripheral motor nerves innervating pharyngeal muscles in Parkinson disease. J Neuropathol Exp Neurol. 2013;72(2):119-29.

Muchowski PJ. Protein misfolding, amyloid formation, and neurodegeneration: a critical role for molecular chaperones? Neuron. 2002;35(1):9-12.

Munishkina LA, Fink AL, Uversky VN. Accelerated fibrillation of alpha-synuclein induced by the combined action of macromolecular crowding and factors inducing partial folding. Curr Alzheimer Res. 2009;6(3):252-60.

Murphy DD, Rueter SM, Trojanowski JQ, Lee VM. Synucleins are developmentally expressed, and alpha-synuclein regulates the size of the presynaptic vesicular pool in primary hippocampal neurons. J Neurosci. 2000;20(9):3214-20.

Muthuswamy SK, Gilman M, Brugge JS. Controlled dimerization of ErbB receptors provides evidence for differential signaling by homo- and heterodimers. Mol Cell Biol. 1999;19(10):6845-57.

Nagai T, Ibata K, Park ES, Kubota M, Mikoshiba K, Miyawaki A. A variant of yellow fluorescent protein with fast and efficient maturation for cell-biological applications. Nat Biotechnol. 2002;20(1):87-90.

Nakamura K, Nemani VM, Azarbal F, Skibinski G, Levy JM, Egami K, et al. Direct membrane association drives mitochondrial fission by the Parkinson disease-associated protein alpha-synuclein. J Biol Chem. 2011;286(23):20710-26.

Nakaso K, Tajima N, Ito S, Teraoka M, Yamashita A, Horikoshi Y, et al. Dopamine-mediated oxidation of methionine 127 in alpha-synuclein causes cytotoxicity and oligomerization of alpha-synuclein. PLoS One. 2013;8(2):e55068.

Nakata Y, Yasuda T, Fukaya M, Yamamori S, Itakura M, Nihira T, et al. Accumulation of alpha-synuclein triggered by presynaptic dysfunction. J Neurosci. 2012;32(48):17186-96.

Nalls MA, Pankratz N, Lill CM, Do CB, Hernandez DG, Saad M, et al. Large-scale meta-analysis of genome-wide association data identifies six new risk loci for Parkinson's disease. Nat Genet. 2014;46(9):989-93.

Narayanan V, Guo Y, Scarlata S. Fluorescence studies suggest a role for alpha-synuclein in the phosphatidylinositol lipid signaling pathway. Biochemistry. 2005;44(2):462-70.

Nasstrom T, Fagerqvist T, Barbu M, Karlsson M, Nikolajeff F, Kasrayan A, et al. The lipid peroxidation products 4-oxo-2-nonenal and 4-hydroxy-2-nonenal promote the formation of alpha-synuclein oligomers with distinct biochemical, morphological, and functional properties. Free Radic Biol Med. 2011;50(3):428-37.

Neudorfer O, Giladi N, Elstein D, Abrahamov A, Turezkite T, Aghai E, et al. Occurrence of Parkinson's syndrome in type I Gaucher disease. QJM : monthly journal of the Association of Physicians. 1996;89(9):691-4.

Neumann M, Kahle PJ, Giasson BI, Ozmen L, Borroni E, Spooren W, et al. Misfolded proteinase K-resistant hyperphosphorylated alpha-synuclein in aged transgenic mice with locomotor deterioration and in human alpha-synucleinopathies. J Clin Invest. 2002;110(10):1429-39.

Neumann M, Muller V, Kretzschmar HA, Haass C, Kahle PJ. Regional distribution of proteinase K-resistant alpha-synuclein correlates with Lewy body disease stage. J Neuropathol Exp Neurol. 2004;63(12):1225-35.

Neystat M, Lynch T, Przedborski S, Kholodilov N, Rzhetskaya M, Burke RE. Alpha-synuclein expression in substantia nigra and cortex in Parkinson's disease. Mov Disord. 1999;14(3):417-22.

Nichols WC, Pankratz N, Hernandez D, Paisan-Ruiz C, Jain S, Halter CA, et al. Genetic screening for a single common LRRK2 mutation in familial Parkinson's disease. Lancet. 2005;365(9457):410-2.

Nishioka K, Hayashi S, Farrer MJ, Singleton AB, Yoshino H, Imai H, et al. Clinical heterogeneity of alpha-synuclein gene duplication in Parkinson's disease. Ann Neurol. 2006;59(2):298-309.

Nordengrahn A, Gustafsdottir SM, Ebert K, Reid SM, King DP, Ferris NP, et al. Evaluation of a novel proximity ligation assay for the sensitive and rapid detection of foot-and-mouth disease virus. Vet Microbiol. 2008;127(3-4):227-36.

Norris EH, Giasson BI, Ischiropoulos H, Lee VM. Effects of oxidative and nitrative challenges on alpha-synuclein fibrillogenesis involve distinct mechanisms of protein modifications. J Biol Chem. 2003;278(29):27230-40.

Olanow CW, Goetz CG, Kordower JH, Stoessl AJ, Sossi V, Brin MF, et al. A double-blind controlled trial of bilateral fetal nigral transplantation in Parkinson's disease. Ann Neurol. 2003;54(3):403-14.

Orimo S, Uchihara T, Nakamura A, Mori F, Kakita A, Wakabayashi K, et al. Axonal alpha-synuclein aggregates herald centripetal degeneration of cardiac sympathetic nerve in Parkinson's disease. Brain. 2008;131(Pt 3):642-50.

Ostrerova N, Petrucelli L, Farrer M, Mehta N, Choi P, Hardy J, et al. alpha-Synuclein shares physical and functional homology with 14-3-3 proteins. J Neurosci. 1999;19(14):5782-91.

Outeiro TF, Putcha P, Tetzlaff JE, Spoelgen R, Koker M, Carvalho F, et al. Formation of toxic oligomeric alpha-synuclein species in living cells. PLoS One. 2008;3(4):e1867.

Pagliaro L, Felding J, Audouze K, Nielsen SJ, Terry RB, Krog-Jensen C, et al. Emerging classes of protein-protein interaction inhibitors and new tools for their development. Curr Opin Chem Biol. 2004;8(4):442-9.

Paik SR, Shin HJ, Lee JH. Metal-catalyzed oxidation of alpha-synuclein in the presence of Copper(II) and hydrogen peroxide. Arch Biochem Biophys. 2000;378(2):269-77.

Paleologou KE, Kragh CL, Mann DM, Salem SA, Al-Shami R, Allsop D, et al. Detection of elevated levels of soluble alpha-synuclein oligomers in post-mortem brain extracts from patients with dementia with Lewy bodies. Brain. 2009;132(Pt 4):1093-101.

Pals P, Lincoln S, Manning J, Heckman M, Skipper L, Hulihan M, et al. alpha-Synuclein promoter confers susceptibility to Parkinson's disease. Ann Neurol. 2004;56(4):591-5.

Pandey N, Strider J, Nolan WC, Yan SX, Galvin JE. Curcumin inhibits aggregation of alpha-synuclein. Acta Neuropathol. 2008;115(4):479-89.

Parkkinen L, Pirttila T, Alafuzoff I. Applicability of current staging/categorization of alpha-synuclein pathology and their clinical relevance. Acta Neuropathol. 2008;115(4):399-407.

Parkkinen L, Pirttila T, Tervahauta M, Alafuzoff I. Widespread and abundant alpha-synuclein pathology in a neurologically unimpaired subject. Neuropathology. 2005;25(4):304-14.

Patel NK, Gill SS. GDNF delivery for Parkinson's disease. Acta neurochirurgica Supplement. 2007;97(Pt 2):135-54.

Paxinou E, Chen Q, Weisse M, Giasson BI, Norris EH, Rueter SM, et al. Induction of alpha-synuclein aggregation by intracellular nitrative insult. J Neurosci. 2001;21(20):8053-61.

Payton JE, Perrin RJ, Clayton DF, George JM. Protein-protein interactions of alpha-synuclein in brain homogenates and transfected cells. Brain research Molecular brain research. 2001;95(1-2):138-45.

Periquet M, Fulga T, Myllykangas L, Schlossmacher MG, Feany MB. Aggregated alpha-synuclein mediates dopaminergic neurotoxicity in vivo. J Neurosci. 2007;27(12):3338-46.

Pletnikova O, West N, Lee MK, Rudow GL, Skolasky RL, Dawson TM, et al. Abeta deposition is associated with enhanced cortical alpha-synuclein lesions in Lewy body diseases. Neurobiol Aging. 2005;26(8):1183-92.

Politis M, Wu K, Loane C, Quinn NP, Brooks DJ, Rehncrona S, et al. Serotonergic neurons mediate dyskinesia side effects in Parkinson's patients with neural transplants. Science translational medicine. 2010;2(38):38ra46.

Polymeropoulos MH, Lavedan C, Leroy E, Ide SE, Dehejia A, Dutra A, et al. Mutation in the alpha-synuclein gene identified in families with Parkinson's disease. Science. 1997;276(5321):2045-7.

Porcari R, Proukakis C, Waudby CA, Bolognesi B, Mangione PP, Paton JF, et al. The H50Q Mutation Induces a 10-fold Decrease in the Solubility of alpha-Synuclein. J Biol Chem. 2015;290(4):2395-404.

Pountney DL, Lowe R, Quilty M, Vickers JC, Voelcker NH, Gai WP. Annular alpha-synuclein species from purified multiple system atrophy inclusions. J Neurochem. 2004;90(2):502-12.

Prots I, Veber V, Brey S, Campioni S, Buder K, Riek R, et al. alpha-Synuclein oligomers impair

neuronal microtubule-kinesin interplay. J Biol Chem. 2013;288(30):21742-54.

Proukakis C, Dudzik CG, Brier T, MacKay DS, Cooper JM, Millhauser GL, et al. A novel alpha-synuclein missense mutation in Parkinson disease. Neurology. 2013;80(11):1062-4.

Puschmann A, Ross OA, Vilarino-Guell C, Lincoln SJ, Kachergus JM, Cobb SA, et al. A Swedish family with de novo alpha-synuclein A53T mutation: evidence for early cortical dysfunction. Parkinsonism Relat Disord. 2009;15(9):627-32.

Rascol O, Brooks DJ, Korczyn AD, De Deyn PP, Clarke CE, Lang AE. A five-year study of the incidence of dyskinesia in patients with early Parkinson's disease who were treated with ropinirole or levodopa. N Engl J Med. 2000;342(20):1484-91.

Recchia A, Debetto P, Negro A, Guidolin D, Skaper SD, Giusti P. Alpha-synuclein and Parkinson's disease. FASEB J. 2004;18(6):617-26.

Redmond DE, Jr., Bjugstad KB, Teng YD, Ourednik V, Ourednik J, Wakeman DR, et al. Behavioral improvement in a primate Parkinson's model is associated with multiple homeostatic effects of human neural stem cells. Proc Natl Acad Sci U S A. 2007;104(29):12175-80.

Remy I, Campbell-Valois FX, Michnick SW. Detection of protein-protein interactions using a simple survival protein-fragment complementation assay based on the enzyme dihydrofolate reductase. Nature protocols. 2007;2(9):2120-5.

Remy I, Michnick SW. A highly sensitive protein-protein interaction assay based on Gaussia luciferase. Nat Methods. 2006;3(12):977-9.

Rey NL, Petit GH, Bousset L, Melki R, Brundin P. Transfer of human alpha-synuclein from the olfactory bulb to interconnected brain regions in mice. Acta Neuropathol. 2013.

Reznichenko L, Cheng Q, Mante M, Saisan PA, Rockenstein EM, Overk C, et al. Novel heteroaromatic organic compound normalized calcium abnormalities in α-synuclein transgenic Parkinson's Disease-like mice model. Society for Neuroscience. New Orleans; 2012.

Robertson DC, Schmidt O, Ninkina N, Jones PA, Sharkey J, Buchman VL. Developmental loss and resistance to MPTP toxicity of dopaminergic neurones in substantia nigra pars compacta of gamma-synuclein, alpha-synuclein and double alpha/gamma-synuclein null mutant mice. J Neurochem. 2004;89(5):1126-36.

Rockenstein E, Hansen LA, Mallory M, Trojanowski JQ, Galasko D, Masliah E. Altered expression of the synuclein family mRNA in Lewy body and Alzheimer's disease. Brain Res. 2001;914(1-2):48-56.

Rodrigues e Silva AM, Geldsetzer F, Holdorff B, Kielhorn FW, Balzer-Geldsetzer M, Oertel WH, et al. Who was the man who discovered the "Lewy bodies"? Mov Disord. 2010;25(12):1765-73.

Rohn TT. Targeting alpha-synuclein for the treatment of Parkinson's disease. CNS Neurol Disord Drug Targets. 2012;11(2):174-9.

Roostaee A, Beaudoin S, Staskevicius A, Roucou X. Aggregation and neurotoxicity of recombinant alpha-synuclein aggregates initiated by dimerization. Mol Neurodegener. 2013;8:5.

Roy S, Wolman L. Ultrastructural observations in Parkinsonism. J Pathol. 1969;99(1):39-44.

Saito Y, Kawashima A, Ruberu NN, Fujiwara H, Koyama S, Sawabe M, et al. Accumulation of phosphorylated alpha-synuclein in aging human brain. J Neuropathol Exp Neurol. 2003;62(6):644-54.

Samii A, Nutt JG, Ransom BR. Parkinson's disease. Lancet. 2004;363(9423):1783-93.

Sandomenico A, Monti SM, Sabatella M, De Capua A, Tornatore L, Doti N, et al. Protein-protein interactions: a simple strategy to identify binding sites and peptide antagonists. Chemical

biology & drug design. 2009;73(5):483-93.

Satake W, Nakabayashi Y, Mizuta I, Hirota Y, Ito C, Kubo M, et al. Genome-wide association study identifies common variants at four loci as genetic risk factors for Parkinson's disease. Nat Genet. 2009;41(12):1303-7.

Scarffe LA, Stevens DA, Dawson VL, Dawson TM. Parkin and PINK1: much more than mitophagy. Trends Neurosci. 2014;37(6):315-24.

Schlingemann J, Leijon M, Yacoub A, Schlingemann H, Zohari S, Matyi-Toth A, et al. Novel means of viral antigen identification: improved detection of avian influenza viruses by proximity ligation. J Virol Methods. 2010;163(1):116-22.

Schneeberger A, Mandler M, Mattner F, Schmidt W. Vaccination for Parkinson's disease. Parkinsonism Relat Disord. 2012;18 Suppl 1:S11-3.

Schulz-Schaeffer WJ. The synaptic pathology of alpha-synuclein aggregation in dementia with Lewy bodies, Parkinson's disease and Parkinson's disease dementia. Acta Neuropathol. 2010;120(2):131-43.

Shannon KM, Keshavarzian A, Dodiya HB, Jakate S, Kordower JH. Is alpha-synuclein in the colon a biomarker for premotor Parkinson's disease? Evidence from 3 cases. Mov Disord. 2012;27(6):716-9.

Sharon R, Bar-Joseph I, Frosch MP, Walsh DM, Hamilton JA, Selkoe DJ. The formation of highly soluble oligomers of alpha-synuclein is regulated by fatty acids and enhanced in Parkinson's disease. Neuron. 2003;37(4):583-95.

Sharon R, Bar-Joseph I, Mirick GE, Serhan CN, Selkoe DJ. Altered fatty acid composition of dopaminergic neurons expressing alpha-synuclein and human brains with alpha-synucleinopathies. J Biol Chem. 2003;278(50):49874-81.

Sharon R, Goldberg MS, Bar-Josef I, Betensky RA, Shen J, Selkoe DJ. alpha-Synuclein occurs in lipid-rich high molecular weight complexes, binds fatty acids, and shows homology to the fatty acid-binding proteins. Proc Natl Acad Sci U S A. 2001;98(16):9110-5.

Shtilerman MD, Ding TT, Lansbury PT, Jr. Molecular crowding accelerates fibrillization of alpha-synuclein: could an increase in the cytoplasmic protein concentration induce Parkinson's disease? Biochemistry. 2002;41(12):3855-60.

Shults CW. Lewy bodies. Proc Natl Acad Sci U S A. 2006;103(6):1661-8.

Shyu J, Liu H, Deng X, Hu C-D. Identification of new fluorescent protein fragments for bimolecular fluorescence complementation analysis under physiological conditions. Biotechniques. 2006;40(1):61-6.

Sillerud LO, Larson RS. Design and structure of peptide and peptidomimetic antagonists of protein-protein interaction. Curr Protein Pept Sci. 2005;6(2):151-69.

Simon-Sanchez J, Schulte C, Bras JM, Sharma M, Gibbs JR, Berg D, et al. Genome-wide association study reveals genetic risk underlying Parkinson's disease. Nat Genet. 2009;41(12):1308-12.

Singleton AB, Farrer M, Johnson J, Singleton A, Hague S, Kachergus J, et al. alpha-Synuclein locus triplication causes Parkinson's disease. Science. 2003;302(5646):841.

Slevin JT, Gerhardt GA, Smith CD, Gash DM, Kryscio R, Young B. Improvement of bilateral motor functions in patients with Parkinson disease through the unilateral intraputaminal infusion of glial cell line-derived neurotrophic factor. Journal of neurosurgery. 2005;102(2):216-22.

Snyder H, Mensah K, Theisler C, Lee J, Matouschek A, Wolozin B. Aggregated and monomeric alpha-synuclein bind to the S6' proteasomal protein and inhibit proteasomal function. J Biol

Chem. 2003;278(14):11753-9.

Soderberg O, Gullberg M, Jarvius M, Ridderstrale K, Leuchowius KJ, Jarvius J, et al. Direct observation of individual endogenous protein complexes in situ by proximity ligation. Nat Methods. 2006;3(12):995-1000.

Soto C, Estrada LD. Protein misfolding and neurodegeneration. Arch Neurol. 2008;65(2):184-9.

Sousa VL, Bellani S, Giannandrea M, Yousuf M, Valtorta F, Meldolesi J, et al. {alpha}-synuclein and its A30P mutant affect actin cytoskeletal structure and dynamics. Mol Biol Cell. 2009;20(16):3725-39.

Souza JM, Giasson BI, Chen Q, Lee VM, Ischiropoulos H. Dityrosine cross-linking promotes formation of stable alpha -synuclein polymers. Implication of nitrative and oxidative stress in the pathogenesis of neurodegenerative synucleinopathies. J Biol Chem. 2000;275(24):18344-9.

Sperandio O, Reynes CH, Camproux AC, Villoutreix BO. Rationalizing the chemical space of protein-protein interaction inhibitors. Drug discovery today. 2010;15(5-6):220-9.

Spillantini MG, Crowther RA, Jakes R, Hasegawa M, Goedert M. alpha-Synuclein in filamentous inclusions of Lewy bodies from Parkinson's disease and dementia with lewy bodies. Proc Natl Acad Sci U S A. 1998;95(11):6469-73.

Spillantini MG, Goedert M. The alpha-synucleinopathies: Parkinson's disease, dementia with Lewy bodies, and multiple system atrophy. Ann N Y Acad Sci. 2000;920:16-27.

Spillantini MG, Schmidt ML, Lee VM, Trojanowski JQ, Jakes R, Goedert M. Alpha-synuclein in Lewy bodies. Nature. 1997;388(6645):839-40.

Tanji K, Mori F, Mimura J, Itoh K, Kakita A, Takahashi H, et al. Proteinase K-resistant alpha-synuclein is deposited in presynapses in human Lewy body disease and A53T alpha-synuclein transgenic mice. Acta Neuropathol. 2010;120(2):145-54.

Tanner CM, Kamel F, Ross GW, Hoppin JA, Goldman SM, Korell M, et al. Rotenone, paraquat, and Parkinson's disease. Environ Health Perspect. 2011;119(6):866-72.

Tavoosidana G, Ronquist G, Darmanis S, Yan J, Carlsson L, Wu D, et al. Multiple recognition assay reveals prostasomes as promising plasma biomarkers for prostate cancer. Proc Natl Acad Sci U S A. 2011;108(21):8809-14.

Tayebi N, Walker J, Stubblefield B, Orvisky E, LaMarca ME, Wong K, et al. Gaucher disease with parkinsonian manifestations: does glucocerebrosidase deficiency contribute to a vulnerability to parkinsonism? Molecular genetics and metabolism. 2003;79(2):104-9.

Tchekanda E, Sivanesan D, Michnick SW. An infrared reporter to detect spatiotemporal dynamics of protein-protein interactions. Nat Methods. 2014;11(6):641-4.

Tetzlaff JE, Putcha P, Outeiro TF, Ivanov A, Berezovska O, Hyman BT, et al. CHIP targets toxic alpha-Synuclein oligomers for degradation. J Biol Chem. 2008;283(26):17962-8.

Tofaris GK, Razzaq A, Ghetti B, Lilley KS, Spillantini MG. Ubiquitination of alpha-synuclein in Lewy bodies is a pathological event not associated with impairment of proteasome function. J Biol Chem. 2003;278(45):44405-11.

Tokuda T, Qureshi MM, Ardah MT, Varghese S, Shehab SA, Kasai T, et al. Detection of elevated levels of alpha-synuclein oligomers in CSF from patients with Parkinson disease. Neurology. 2010;75(20):1766-72.

Tong J, Wong H, Guttman M, Ang LC, Forno LS, Shimadzu M, et al. Brain alpha-synuclein accumulation in multiple system atrophy, Parkinson's disease and progressive supranuclear palsy: a comparative investigation. Brain. 2010;133(Pt 1):172-88.

Ueda K, Fukushima H, Masliah E, Xia Y, Iwai A, Yoshimoto M, et al. Molecular cloning of cDNA encoding an unrecognized component of amyloid in Alzheimer disease. Proc Natl Acad Sci U S A. 1993;90(23):11282-6.

Ulmer TS, Bax A, Cole NB, Nussbaum RL. Structure and dynamics of micelle-bound human alpha-synuclein. J Biol Chem. 2005;280(10):9595-603.

Ulusoy A, Febbraro F, Jensen PH, Kirik D, Romero-Ramos M. Co-expression of C-terminal truncated alpha-synuclein enhances full-length alpha-synuclein-induced pathology. Eur J Neurosci. 2010;32(3):409-22.

Uversky VN. Alpha-synuclein misfolding and neurodegenerative diseases. Curr Protein Pept Sci. 2008;9(5):507-40.

Uversky VN, Eliezer D. Biophysics of Parkinson's disease: structure and aggregation of alpha-synuclein. Curr Protein Pept Sci. 2009;10(5):483-99.

Uversky VN, Li J, Fink AL. Evidence for a partially folded intermediate in alpha-synuclein fibril formation. J Biol Chem. 2001;276(14):10737-44.

Uversky VN, Li J, Souillac P, Millett IS, Doniach S, Jakes R, et al. Biophysical properties of the synucleins and their propensities to fibrillate: inhibition of alpha-synuclein assembly by beta- and gamma-synucleins. J Biol Chem. 2002;277(14):11970-8.

Vilar M, Chou HT, Luhrs T, Maji SK, Riek-Loher D, Verel R, et al. The fold of alpha-synuclein fibrils. Proc Natl Acad Sci U S A. 2008;105(25):8637-42.

Vogiatzi T, Xilouri M, Vekrellis K, Stefanis L. Wild type alpha-synuclein is degraded by chaperone-mediated autophagy and macroautophagy in neuronal cells. J Biol Chem. 2008;283(35):23542-56.

Volles MJ, Lansbury PT, Jr. Zeroing in on the pathogenic form of alpha-synuclein and its mechanism of neurotoxicity in Parkinson's disease. Biochemistry. 2003;42(26):7871-8.

Volpicelli-Daley LA, Luk KC, Lee VM. Addition of exogenous alpha-synuclein preformed fibrils to primary neuronal cultures to seed recruitment of endogenous alpha-synuclein to Lewy body and Lewy neurite-like aggregates. Nature protocols. 2014;9(9):2135-46.

Wakabayashi K, Matsumoto K, Takayama K, Yoshimoto M, Takahashi H. NACP, a presynaptic protein, immunoreactivity in Lewy bodies in Parkinson's disease. Neurosci Lett. 1997;239(1):45-8.

Wang N, Gibbons CH, Lafo J, Freeman R. alpha-Synuclein in cutaneous autonomic nerves. Neurology. 2013.

Wang W, Perovic I, Chittuluru J, Kaganovich A, Nguyen LT, Liao J, et al. A soluble alpha-synuclein construct forms a dynamic tetramer. Proc Natl Acad Sci U S A. 2011;108(43):17797-802.

Webb JL, Ravikumar B, Atkins J, Skepper JN, Rubinsztein DC. Alpha-Synuclein is degraded by both autophagy and the proteasome. J Biol Chem. 2003;278(27):25009-13.

Weinreb PH, Zhen W, Poon AW, Conway KA, Lansbury PT, Jr. NACP, a protein implicated in Alzheimer's disease and learning, is natively unfolded. Biochemistry. 1996;35(43):13709-15.

Welander H, Bontha SV, Nasstrom T, Karlsson M, Nikolajeff F, Danzer K, et al. Gelsolin co-occurs with Lewy bodies in vivo and accelerates alpha-synuclein aggregation in vitro. Biochem Biophys Res Commun. 2011;412(1):32-8.

Wernig M, Zhao JP, Pruszak J, Hedlund E, Fu D, Soldner F, et al. Neurons derived from reprogrammed fibroblasts functionally integrate into the fetal brain and improve symptoms of rats with Parkinson's disease. Proc Natl Acad Sci U S A. 2008;105(15):5856-61.

West AB, Moore DJ, Biskup S, Bugayenko A, Smith WW, Ross CA, et al. Parkinson's disease-associated mutations in leucine-rich repeat kinase 2 augment kinase activity. Proc Natl Acad Sci U S A. 2005;102(46):16842-7.

West AB, Moore DJ, Choi C, Andrabi SA, Li X, Dikeman D, et al. Parkinson's disease-associated mutations in LRRK2 link enhanced GTP-binding and kinase activities to neuronal toxicity. Hum Mol Genet. 2007;16(2):223-32.

Wills J, Jones J, Haggerty T, Duka V, Joyce JN, Sidhu A. Elevated tauopathy and alpha-synuclein pathology in postmortem Parkinson's disease brains with and without dementia. Exp Neurol. 2010;225(1):210-8.

Winner B, Jappelli R, Maji SK, Desplats PA, Boyer L, Aigner S, et al. In vivo demonstration that alpha-synuclein oligomers are toxic. Proc Natl Acad Sci U S A. 2011;108(10):4194-9.

Winslow AR, Chen CW, Corrochano S, Acevedo-Arozena A, Gordon DE, Peden AA, et al. alpha-Synuclein impairs macroautophagy: implications for Parkinson's disease. J Cell Biol. 2010;190(6):1023-37.

Wittig I, Schagger H. Advantages and limitations of clear-native PAGE. Proteomics. 2005;5(17):4338-46.

Wolters E. Non-motor extranigral signs and symptoms in Parkinson's disease. Parkinsonism Relat Disord. 2009;15 Suppl 3:S6-12.

Xia Q, Liao L, Cheng D, Duong DM, Gearing M, Lah JJ, et al. Proteomic identification of novel proteins associated with Lewy bodies. Front Biosci. 2008;13:3850-6.

Yamashita T, Kawai H, Tian F, Ohta Y, Abe K. Tumorigenic development of induced pluripotent stem cells in ischemic mouse brain. Cell transplantation. 2011;20(6):883-91.

Yamin G, Uversky VN, Fink AL. Nitration inhibits fibrillation of human alpha-synuclein in vitro by formation of soluble oligomers. FEBS Lett. 2003;542(1-3):147-52.

Yavich L, Tanila H, Vepsalainen S, Jakala P. Role of alpha-synuclein in presynaptic dopamine recruitment. J Neurosci. 2004;24(49):11165-70.

Yoshiike Y, Minai R, Matsuo Y, Chen YR, Kimura T, Takashima A. Amyloid oligomer conformation in a group of natively folded proteins. PLoS One. 2008;3(9):e3235.

Yung HW, Charnock-Jones DS, Burton GJ. Regulation of AKT phosphorylation at Ser473 and Thr308 by endoplasmic reticulum stress modulates substrate specificity in a severity dependent manner. PLoS One. 2011;6(3):e17894.

Zaccai J, Brayne C, McKeith I, Matthews F, Ince PG. Patterns and stages of alpha-synucleinopathy: Relevance in a population-based cohort. Neurology. 2008;70(13):1042-8.

Zarranz JJ, Alegre J, Gomez-Esteban JC, Lezcano E, Ros R, Ampuero I, et al. The new mutation, E46K, of alpha-synuclein causes Parkinson and Lewy body dementia. Ann Neurol. 2004;55(2):164-73.

Zesiewicz TA, Sullivan KL, Arnulf I, Chaudhuri KR, Morgan JC, Gronseth GS, et al. Practice Parameter: treatment of nonmotor symptoms of Parkinson disease: report of the Quality Standards Subcommittee of the American Academy of Neurology. Neurology. 2010;74(11):924-31.

Zhang JH, Chung TD, Oldenburg KR. A Simple Statistical Parameter for Use in Evaluation and Validation of High Throughput Screening Assays. J Biomol Screen. 1999;4(2):67-73.

Zhang NY, Tang Z, Liu CW. alpha-Synuclein protofibrils inhibit 26 S proteasome-mediated protein degradation: understanding the cytotoxicity of protein protofibrils in neurodegenerative disease pathogenesis. J Biol Chem. 2008;283(29):20288-98.

Zhang X, Sun XX, Xue D, Liu DG, Hu XY, Zhao M, et al. Conformation-dependent scFv antibodies specifically recognize the oligomers assembled from various amyloids and show colocalization of amyloid fibrils with oligomers in patients with amyloidoses. Biochim Biophys Acta. 2011;1814(12):1703-12.

Zhou W, Long C, Reaney SH, Di Monte DA, Fink AL, Uversky VN. Methionine oxidation stabilizes non-toxic oligomers of alpha-synuclein through strengthening the auto-inhibitory intra-molecular long-range interactions. Biochim Biophys Acta. 2010;1802(3):322-30.

Zhu M, Han S, Fink AL. Oxidized quercetin inhibits alpha-synuclein fibrillization. Biochim Biophys Acta. 2013;1830(4):2872-81.

Zhu M, Rajamani S, Kaylor J, Han S, Zhou F, Fink AL. The flavonoid baicalein inhibits fibrillation of alpha-synuclein and disaggregates existing fibrils. J Biol Chem. 2004;279(26):26846-57.

Zimprich A, Biskup S, Leitner P, Lichtner P, Farrer M, Lincoln S, et al. Mutations in LRRK2 cause autosomal-dominant parkinsonism with pleomorphic pathology. Neuron. 2004;44(4):601-7.

Zimprich A, Muller-Myhsok B, Farrer M, Leitner P, Sharma M, Hulihan M, et al. The PARK8 locus in autosomal dominant parkinsonism: confirmation of linkage and further delineation of the disease-containing interval. Am J Hum Genet. 2004;74(1):11-9.

Zych C, Domling A, Ayyavoo V. Development of a robust cell-based high-throughput screening assay to identify targets of HIV-1 viral protein R dimerization. Drug design, development and therapy. 2013;7:403-12.